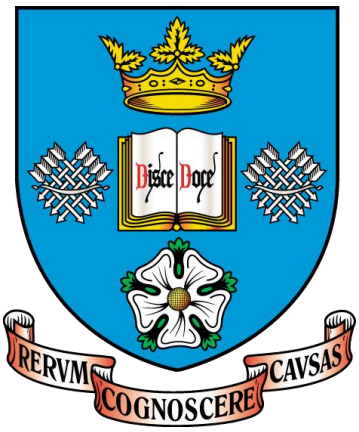

Technical, Economic and Environmental Assessment of Energy Generation using Bioenergy with Carbon Capture, Utilisation and Storage.

By:

Oluchi Eziuche Emenike

A thesis submitted in fulfilment of the requirements for the degree of Doctor of Philosophy.

The University of Sheffield

Energy 2050

Department of Mechanical Engineering

Faculty of Engineering

April 2021

Declaration

I, the author, confirm that the work submitted is my own work, except where work that has formed part of jointly authored publications has been included. The contribution of the candidate and the other authors to this work has been explicitly indicated below. I confirm that appropriate credit has been given within the thesis where reference has been made to the work of others. I am aware of the University's Guidance on the Use of Unfair Means (www.sheffield.ac.uk/ssid/unfair-means). This work has not been previously presented for an award at this, or any other, university.

Publications and Presentations

Some of the work presented in Chapter 3 of this thesis appears in the following publication:

1. Michailos, S., **Emenike, O.,** Ingham, D., Hughes, K. J., & Pourkashanian, M. (2019). Methane production via syngas fermentation within the bio-CCS concept: A techno-economic assessment. Biochemical Engineering Journal, 150, 107290. https://doi.org/https://doi.org/10.1016/j.bej.2019.107290

Some of the work presented in Chapter 4 of this thesis appears in the following publication and presentation:

2. **Emenike, O.,** Michailos, S., Finney, K. N., Hughes, K. J., Ingham, D., & Pourkashanian, M. (2020). Initial techno-economic screening of BECCS technologies in power generation for a range of biomass feedstock. Sustainable Energy Technologies and Assessments, 40, 100743. https://doi.org/10.1016/j.seta.2020.100743
3. **Emenike, O.,** Michailos, S., Hughes, K. J., & Pourkashanian, M. (2020). Initial techno-economic screening of BECCS technologies in power generation for a range of biomass feedstock. Poster presentation in the 28th European Biomass Conference and Exhibition (EUBCE 2020). July 2020.

Some of the work presented in Chapter 5 of this thesis appears in the following publication:

4. **Emenike, O.,** Michailos, S., Hughes, K. J., Ingham, D., & Pourkashanian, M. (2021). Techno-economic and environmental assessment of BECCS in fuel generation for FT-fuel, bioSNG and OMEx. Sustainable Energy & Fuels https://doi.org/10.1039/D1SE00123J

The contributions from the co-author Michailos, S. has not appeared in this thesis. The other authors Ingham, D., Finney, K. N, Hughes, K.J. and Pourkashanian, M., were supervisors who have acted in an advisory role.

Acknowledgements

Over the course of this programme, I received a lot of assistance and guidance. I would like to thank Dr Stavros Michailos for his invaluable help in guiding the direction of my project and providing technical advice. I would also like to thank Prof. Derek Ingham and Dr Kevin Hughes for always taking their time to read my drafts and provide corrections, as well as the constant support and guidance. I would like to acknowledge Prof. Mohammed Pourkashanian for giving me the opportunity to take on this project. I would also like to acknowledge my colleagues from the process modelling group within the Energy2050 group for their technical advice.

Furthermore, I would like to thank my entire support group for their emotional support over the past four years. I would like to particularly thank my parents, Engr. Emenike and Dr Blessing Onyegeme-Okerenta for sponsoring this programme in addition to their unending love and advice. Also, I would like to thank my siblings, Chigozie, Tochi and Ugochi and my friends in Sheffield and Nigeria for motivating and supporting me. I would also like to thank the members of the now defunct Planet Shakers E-group for providing a listening ear and encouraging me.

Finally, I would like to thank the Almighty God for without whom all this would have been impossible.

Abstract

Bioenergy with Carbon Capture and Storage is a promising negative emissions technology to mitigate climate change across different sectors. This thesis explores the application potential of this technology in energy generation by evaluating the technical, economic and environmental performance to present detailed information for the literature. This will help stakeholders including researchers, policymakers and the public make informed choices on the best route to decarbonisation. In power generation, the performance of different types of biomass, coupled with different CO_2 abatement technologies, has been evaluated. The performance of each case has been thoroughly assessed against technical, economic and environmental parameters, then benchmarked against natural gas in power generation. An analysis to determine the effect on carbon pricing as an economic tool has been explored as well as a sensitivity analysis to identify the most significant factors influencing the production of electricity. In fuel generation, the production of Fischer-Tropsch fuels, synthetic natural gas and oxymethylene ethers via biomass gasification without carbon capture and storage and with carbon capture and storage has been assessed. After modelling and simulation in Aspen Plus to determine the mass and energy balances, an economic model has been developed in Microsoft Excel to estimate the capital costs, operating costs, levelised costs of energy and minimum selling prices; and the greenhouse gas emission factors have been estimated to investigate the environmental effect. Then, fuel generation via electrochemical conversion and CO_2 utilisation has been considered. The electrofuel production routes have focused on storing renewable energy in fuels. The gasification step has been replaced with an electrolyser to produce H_2 in addition to the CO_2 captured from different sources to produce the same fuels. The environmental assessment compared different CO_2 sources on the mitigation potential of each electrofuel production route. In conclusion, energy generation via bioenergy with CCS cannot currently compete with energy generation using fossil fuels mainly due to the higher levelised costs of energy but with the use of carbon pricing in the range of £48/tCO_2 and £146/tCO_2, such that these plants are rewarded for each tonne of CO_2 removed and the fossil-fuel plants are penalised, fossil-fuel energy generation could be phased out faster to achieve decarbonisation. Also, these routes show promising mitigation potential with the ability to remove up to 1.52 Mt of CO_2 per year from the atmosphere. With electrofuel production, there is more work to be done to attain feasibility and this is mainly due to the cost of electricity which is the major

expense in the economics; also, CO_2 storage needs to be coupled with CO_2 utilisation to increase the chances of achieving negative emissions.

TABLE OF CONTENTS

LIST OF FIGURES

LIST OF TABLES

NOMENCLATURE

A_o	preexponential constant (s^{-1})
C_f	estimated fixed capital cost (£)
E_a	activation energy (kJ/mol)
f_l	Lang factor
G	Gibbs energy (J)
H	enthalpy (J)
k	reaction constant
n	reaction order
R	universal gas constant (0.008314 kJ/mol.K)
S	entropy (J/K)
T	temperature (K)
H	energy efficiency
η_c	carbon conversion efficiency
ΔG	change in Gibbs energy (J)

ABBREVIATIONS

ASPEN	Advanced System for Process Engineering
ASU	Air Separation Unit
BECCS	Bioenergy with Carbon Capture and Storage
BioSNG	Bio-synthetic Natural Gas
BFB	Bubbling Fluidised Bed
BGL	British Gas/Lurgi
CAPEX	Capital Expenditure
CCS	Carbon Capture and Storage
CCUS	Carbon Capture, Utilisation and Storage
CDU	Carbon Dioxide Utilisation
CEPCI	Chemical Engineering Plant Cost Index
CFB	Circulating Fluidised Bed
CGE	Cold Gas Efficiency
DAC	Direct Air Capture
DACCS	Direct Air Carbon, Capture and Storage
DCFROR	Discounted Cash Flow Rate of Return
DFB	Dual Fluidised Bed
DOE	Department of Energy
DoF	Degree of Freedom
EO	Equation-Oriented

EFG	Entrained Flow Gasifier
ESP	Electrostatic Precipitator
FCF	Fixed Charge Factor
FTS	Fischer-Tropsch Synthesis
GE	General Electric
GHG	Greenhouse Gases
IECM	Integrated Environment Control Model
IGCC	Integrated Gasification Combined Cycle
LCOE	Levelised Cost of Energy
LCOF	Levelised Cost of Fuel
MEA	Monoethanolamine
MSP	Minimum Selling Price
NET	Negative Emission Technology
NETL	National Energy Technology Laboratory
NGCC	Natural Gas Combined Cycle
OME	Oxymethylene Ethers
OPEX	Operating Expenditure
PCC	Post Combustion Capture
RES	Renewable Energy Sources
RWGS	Reverse Water Gas Shift
SM	Sequential Modular
SNG	Synthetic Natural Gas

TGA	Thermogravimetric Analysis
VDU	Vacuum Distillation Unit
WGS	Water Gas Shift

1 Introduction

This chapter gives a detailed insight into the background of the topic of this thesis. It explains the motivation for the topic and describes the aim and objectives to be achieved.

1.1 Background

As of 2018, 81% of the world's energy supply was from fossil fuels with coal accounting for 26.9% of this amount while biofuels and waste accounted for 9.3% of the world's supply [1]. Since 1973, energy consumption has risen by 200% and energy demand is expected to rise by 30% in the next 23 years due to the growing global economy and an increasing population [2]. An increasing population and a demand for better standards of living are inextricably linked and overall, the solution for better standards of living is dependent on energy. This summarises the significance of energy to humans.

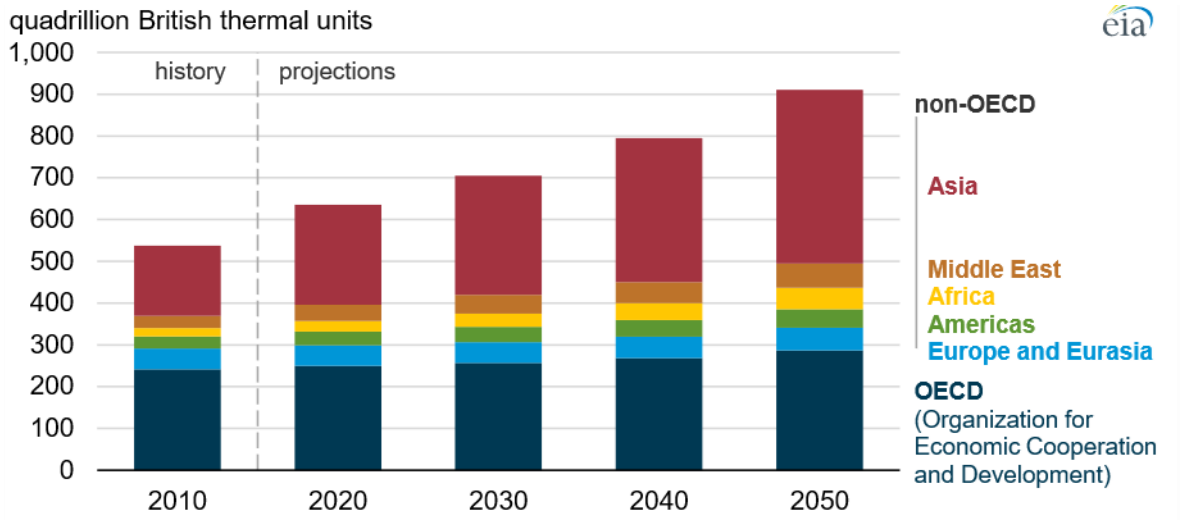

Figure 1.1: Global primary energy consumption by region (2010-2050) [3].

There is no doubt that energy has played an important role in civilisation; however, in the quest for rapid economic growth and to improve the quality of life, energy related innovations have resulted in significant environmental degradation [4]. The spike in energy usage during the industrial revolution points to the bridge between energy and the development of a country. During this period, the prevalent energy source was coal [5]. As many countries move towards development, energy is fundamental and the challenge of meeting the energy demand whilst protecting the environment remains. Figure 1.1 highlights how the global primary energy consumption is projected to increase by 50% between 2018

and 2050 [3]. This increase in demand is mainly driven by regions experiencing strong economic growth especially Asia as shown in Figure 1.2.

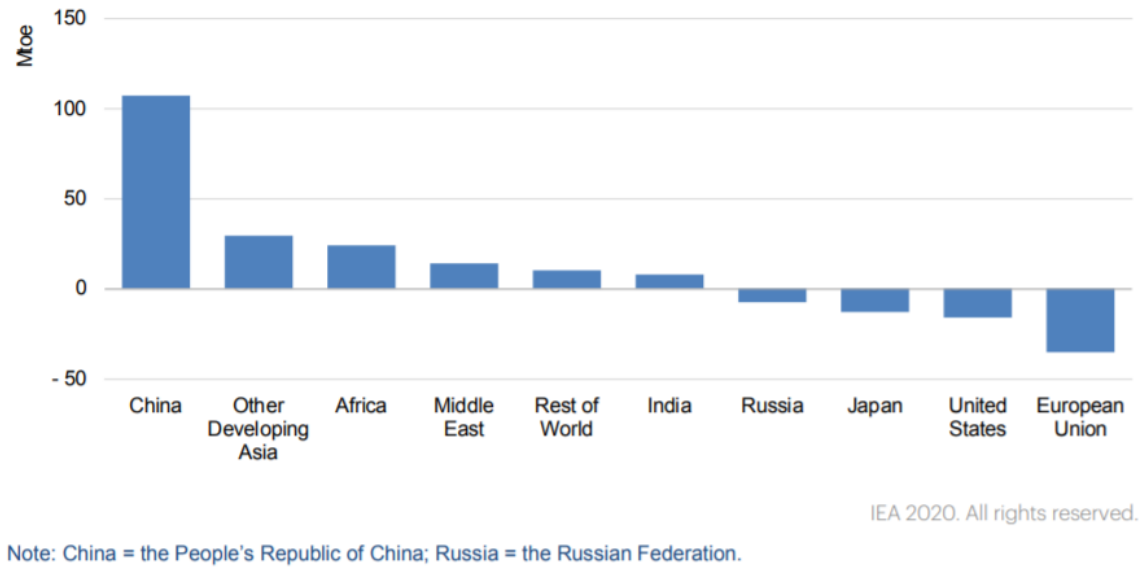

Figure 1.2: Change in primary energy demand by region, 2018-19 [6].

Fossil fuels have been burnt for energy production in over many years. The three major fossil fuels which account for more than 80% of the world's energy supply are coal, oil and natural gas. Fossil fuels are primarily carbon stores and when burnt, gases are released into the atmosphere. The most important gas of concern, that is released by fossil fuels is CO_2 due to its effect on global temperatures. CO_2 is an important aspect of photosynthesis but the rate at which CO_2 is absorbed from the atmosphere does not equal the rate at which it is being released to the atmosphere, thus resulting in an accumulation of CO_2 in the Earth's protective layer [7].

The concentration of greenhouse gases (GHG) with carbon dioxide (CO_2) being the primary GHG present in the atmosphere is evidence of the impact of burning fossil fuels. In the UK alone, industrial and commercial activities account for 46% of the CO_2 emissions [8]. The environment is the main victim of this activity. Figure 1.3 shows the trend of global CO_2 emissions by sector between 1990 and 2018. This figure has increased by 83.3% from 7,622 Mt in 1990 to 13,978 Mt in 2018 and the energy production and usage accounts for majority of global CO_2 emissions accounting for 73.2% of the 2016 figure [9].

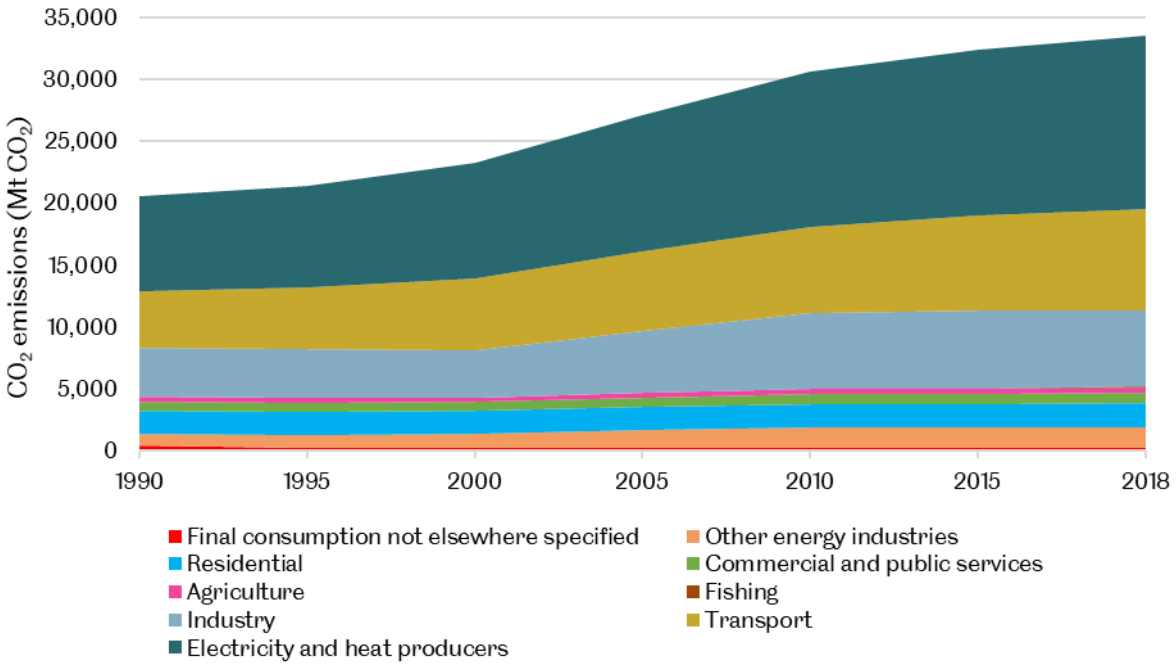

Figure 1.3: Global CO_2 emissions by sector, 1990-2018 [10].

The Kyoto Protocol, effective since 2005, was introduced as a means for countries to take responsibility towards reducing these concentrations; the bulk of this responsibility falls on developed countries due to their contribution during the industrial revolution [11]. As the economy of developing countries grows, the pattern of energy use during the industrial revolution is being reproduced and this demand is met by coal [12,13]. Jakob and Steckel [13] argue that for GHG emissions to be reduced significantly, in order to ensure sustainability of the environment, developing countries need to mandatorily contribute to the solutions as opposed to the voluntary contribution status conferred by the Paris Agreement in 2015.

In the UK, the electricity supplied by fossil fuels decreased from 77% in 1990 to 56% in 2016 [14]. Also, the UK CO_2 emissions have decreased since 1990 by 41% [15] and the main driver of this change is a cleaner electricity mix based on natural gas and renewables instead coal; other drivers are the reduction in industrial fuel consumption, reduction in electricity use and an increase in energy efficiency [15,16]. Figure 1.4 shows the UK electricity generation by source since 1990. The contribution of coal and oil to electricity generation have significantly decreased by over 96%, the portion of nuclear has decreased by 15%, while the portion from natural gas, renewables, waste and have increased. The contribution of natural gas has increased significantly to 26 times the 1990 figure. By sector, the electricity and heat producers sector and the transport sector, contribute over 50% of CO_2 emissions with the transport sector contributing 34% of total emissions in 2018 [10]. With the electricity and

heat producers' sector, emissions have reduced by 63% from the 1990 figure, however, in the transport sector, it has increased by 5% since the 1990 figure, thus indicating the need to focus on decarbonising the transport sector.

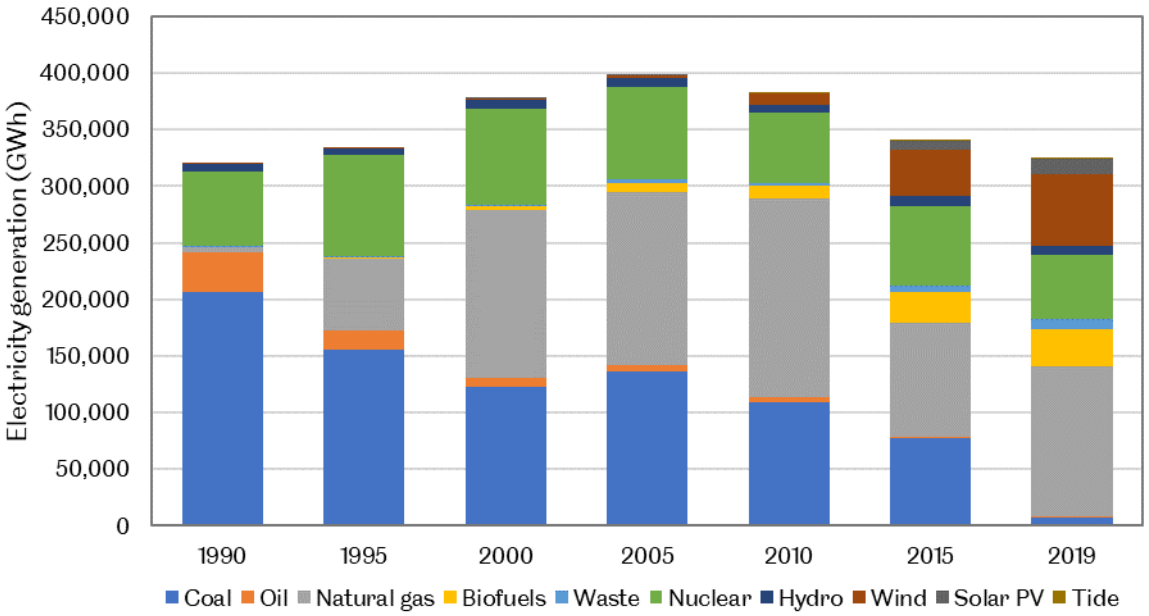

Figure 1.4: UK electricity generation by source, 1990-2019 [10].

While the dependence on fossil fuels has decreased in developed countries, this is not the case globally. In the journey towards creating a sustainable environment, there is the need to provide solutions that can be adopted worldwide. There is no panacea that can be applied worldwide owing to the differences in countries ranging from technical to environmental and social issues, but it is possible to have different options that can be refined to meet the needs of any nation. There are different CO_2 emission reduction strategies including carbon capture and storage (CCS), carbon dioxide utilisation (CDU) and switching to renewable energy sources (RES).

Renewable energy sources replacing fossil fuels include hydroelectric energy, wind power, solar power, geothermal power and biomass. Biofuels are a renewable alternative to fossil fuels and the raw material for biofuels is biomass, but biofuels have not been a favourable choice due to the cost. However, as biofuels become competitive with gasoline and diesel from fossil fuels due to tax exemptions on biofuels and the increase in fossil fuel prices, the demand for biofuels is expected to increase [17]. Biomass is the oldest source of fuel; wood has been used as fuel since the time of Neanderthals. In this thesis, biomass is a source of

interest because it is present around the world and it is similar to coal and hence the fundamental knowledge of the technology for its processing is readily available.

1.2 CO_2 Emission Reduction

There are different methods that have been employed to reduce CO_2 emissions globally, some of which have been mentioned in the previous section. These emission reduction methods include:

- Carbon capture, utilisation and storage (CCUS),
- Reducing the carbon intensity by using low carbon fuels,
- Deploying renewable energy sources,
- Improving energy efficiency and promoting energy conservation,
- Negative emission technologies - DACCS, afforestation, BECCS.

1.2.1 Carbon capture, utilisation and storage

Carbon capture and storage (CCS), as the name implies, involves capturing CO_2 and storing CO_2 to reduce the amount of CO_2 released to the atmosphere. The steps involved are CO_2 capture, transport and storage. CO_2 capture technologies include separation with chemical or physical solvents (absorption), separation with membrane, separation with solid sorbents (adsorption) and cryogenic separation [18].

The three main CO_2 capture systems are post-combustion capture, pre-combustion capture and oxy-fuel combustion capture. These capture technologies are shown in Figure 1.5. Post-combustion capture involves the capture of CO_2 from flue gas after combustion. This technology can be easily retrofitted to existing plants and it is a mature and proven technology [19]. However, the process has a large parasitic load and involves separating low concentrations of CO_2 from large amounts of nitrogen which increases the energy penalty and increases the cost of the capture unit [20]. Pre-combustion capture involves capturing CO_2 before combustion by subjecting the solid fuel to gasification in order to derive syngas, which undergoes cleaning to remove CO_2 before the downstream process. This technology is a fully developed technology [20] and works well for high CO_2 concentration and pressure; it also has a lower energy penalty than the post-combustion capture and higher capital and operating costs.

In oxy-fuel combustion, the fuel is burned with nearly pure oxygen instead of air resulting in a flue gas containing CO_2 and steam. The flue gas stream can be easily dehydrated leaving a pure stream of CO_2 for storage [21]. This technology reduces NOx from combustion due to combustion with oxygen [22].

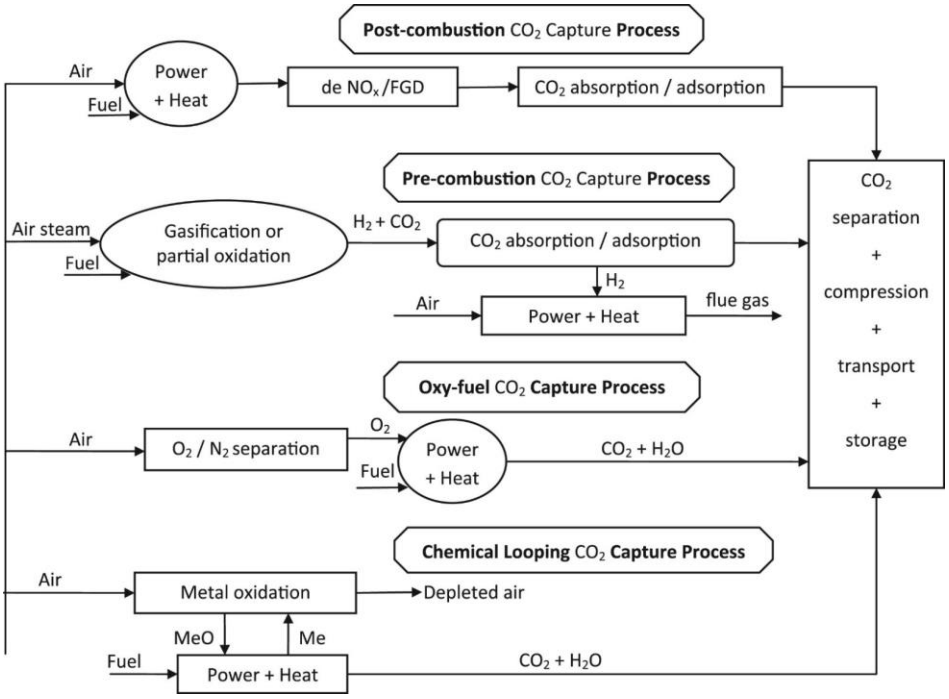

Figure 1.5: CO_2 capture technologies [20].

However, it requires an energy intensive air separation unit to produce oxygen which increases the energy penalty even without CCS and significantly increases the cost [20]. Chemical looping combustion involves the use of a metal oxide as an oxygen carrier in place of pure oxygen as in oxy-fuel combustion. During the combustion process, the metal oxide undergoes reduction to a metal while the fuel is oxidised to CO_2 and steam. In a separate stage, the metal is oxidised and recycled to the process. Like in oxy-fuel combustion, steam can be easily condensed out of the flue gas stream leaving a pure CO_2 stream. This technology does not require the energy intensive air separation unit; however, it is immature due to no large scale experience [20].

CO_2 transport is the stage that links CO_2 capture and storage. CO_2 can be transported in gas, liquid, or solid state and is transported commercially using tanks, pipelines and ships. CO_2 transported in the gas phase occupies a large volume and requires large storage facilities unless it is compressed to reduce its volume while transportation in a solid state requires much more energy for solidification than the other phases and is not cost-effective [18,20]. Transportation using pipelines is the most viable and common option for transporting CO_2. It

also has the highest level of maturity [18]. This option requires compressing gaseous CO_2 to pressures over 80 bar to prevent two-phase flow and increase the density making It easier and cost-effective to transport. In considering CO_2 transport options, the design, environment, safety and risk aspects need to be considered,

CO_2 storage is the last stage of CCS and this involves storing CO_2 for over 10,000 years [23] without contact with the atmosphere. Common CO_2 storage options are geological storage, ocean storage and mineral carbonation. In geological storage, CO_2 is injected into deep underground porous rock formations both onshore and offshore. After it is injected, it is retained by physical trappings. Geological storage options include: depleted oil and gas reservoirs, use in enhanced oil recovery, deep saline formations and use in enhanced coal bed methane recovery [18]. CO_2 can also be stored by injecting into the deep ocean at depths greater than 3000 m, where CO_2 is denser than sea water. By reacting with the ocean, it forms carbonate and bicarbonate ions and isolates the CO_2 from the atmosphere for centuries. This dissolved CO_2 eventually becomes part of the global carbon cycle [18]. The option of ocean storage is the most controversial option due to local risks and environmental concerns [20]. In mineral carbonation, CO_2 is reacted with metal oxides and converted to solid inorganic carbonates, thereby fixing CO_2 in these carbonates. The solid carbonates can be either reused in construction or disposed in depleted mines. While this option is the safest storage option, it is currently the most expensive form of storage [18,20].

Instead of storing captured CO_2, it could be utilised as a key raw material in production processes. This is referred to as carbon dioxide utilisation. The captured CO_2 is a pure stream (>99%) and a useful feedstock in various industries such as plastic production, carbonating drinks and synthetic fuel production.

1.2.2 Renewable energy

Renewable energy refers to energy from limitless sources that are continually replenished naturally [24]. The major renewable energy sources are biomass, hydropower, geothermal, wind, solar and tide. Most renewable energy sources originate from solar energy either as primary sources (direct solar energy) or secondary sources (biomass, wind and hydropower).

Direct solar energy is harvested from the sun using technologies such as photovoltaic (PV) cells, solar collectors, solar concentrators, solar chimneys and solar ponds. Biomass refers to

any fuel derived from plants [25] and it stores chemical energy from the sun when it is produced from plants via photosynthesis. It can be converted to energy via a number of ways similar to the conversion of coal, such as direct combustion; thermochemical conversion, chemical conversion and biological conversion to fuels [26]. Wind is as a result of the sun heating the earth's surface unevenly [27]. Energy from the wind is used to generate electricity using wind turbines which could be onshore or offshore [25]. Hydropower relies on the water cycle where the sun heats up water on land and in the ocean leading to evaporation, condensation and precipitation. Hydroelectric power generation uses hydro turbines to generate electricity and is dependent on water falling and losing elevation [28] .

Geothermal energy originates from heat trapped within the earth's crust. This energy is renewable because heat is constantly produced inside the earth [25]. This heat is used in heating buildings using heat pumps and in electricity generation using turbines. Tidal energy originates from the moon's gravitational pull causing tidal flows. These tidal flows are harnessed to generate electricity using hydro turbines like in hydroelectric generation [29,30].

1.2.3 Negative emission technologies

Negative emission technologies (NETs) have been identified as tools to play a meaningful role in keeping the increase in the global temperatures to below 2 °C (in comparison to pre-industrial levels) as set by the Paris Agreement [31]. These NETs such as afforestation and reforestation, land management, bioenergy with carbon capture and storage (BECCS), enhanced weathering, direct air carbon capture and storage (DACCS), ocean fertilisation and carbon capture and storage (explained in sub-section 1.2.1), could ease the difficulty of achieving net zero CO_2 emissions by 2050 [31].

Afforestation involves creating a new forest by planting new trees on land where trees have not previously been planted while reforestation involves planting more trees in a forest where the number of trees has been decreasing [32]. In both cases, the process absorbs CO_2 from the atmosphere as it is required for plant growth. Storing carbon in soils is another way to remove CO_2 from the atmosphere with little energy demand and costs. Carbon is stored in soils via the lifecycle of a plant. When a plant dies and the soil is protected from microbial activity, the breakdown and release of carbon compounds is prevented enabling the soil to store carbon [33]. Better land management by modifying agricultural practice can increase the amount of carbon stored in soils.

Bioenergy with carbon capture and storage involves coupling bioenergy generation which CCS. The growth of biomass involves the absorption of CO_2 from the atmosphere and instead of being returned upon combustion, it is captured and stored thereby removing CO_2 from the atmosphere. Direct air capture and storage involves using a system to remove CO_2 from the atmosphere by selectively separating it from air [31].

Weathering is a natural process in which rock is naturally decomposed by physical and chemical processes including rainwater, human activity and extreme temperatures. When rocks containing carbonate minerals are dissolved in rainwater which is slightly acidic, CO_2 from the atmosphere is drawn into the solution. The dissolved calcium and bicarbonate ions eventually travel via groundwater to rivers and seas where the carbon is stored in dissolved form. This process takes place over millions of years acting as a carbon sink. Enhanced weathering artificially speeds up this process using methods such as spreading finely ground carbonate or silicate minerals over large warm and humid land areas thereby increasing the amount of CO_2 removed from the atmosphere [31,34,35]. Ocean fertilisation involves deliberately adding nutrients to the upper ocean water so that planktonic algae and other microscopic plants absorb CO_2 and convert it to organic matter. This subsequently leads to sequestration in the deep ocean [31,35].

Globally, BECCS has a large technical potential and can result in negative emissions of up to 10 $GtCO_2e\ yr^{-1}$ if deployed [36]; with a carbon value of €50/tonne, the economic potential is 3.5 $GtCO_2e\ yr^{-1}$ using biomass integrated gasification combined cycle by 2050. In comparison to other NETs, DACCS has a mitigation potential of 0.5 - 5 $GtCO_2\ yr^{-1}$ in 2050 [35], however this technology is very expensive and energy intensive with the costs at $100 - $300 per ton of CO_2 as more plants are built. The total mitigation potential of afforestation, reduced deforestation and forest management could range from 1.9 - 5.5 $GtCO_2\ yr^{-1}$ by 2040 with a carbon value of less than $20/tonne [37]; another projection [38] gives the mitigation potential of tropical reforestation at 0.078 - 1.84 $GtCO_2\ yr^{-1}$ at $5 - $100 per tonne of CO_2 respectively in 2050.

1.3 Climate Change Laws and Policies

According to the Intergovernmental Panel on Climate Change (IPCC), greenhouse gas emissions need to be halved by 2050 relative to 1990 levels in order to keep global warming below 2 °C [39] and this burden of reducing emissions falls on developed countries. This

section highlights some of the policies in the EU and the UK that have been adopted to fight climate change.

A database by the Grantham Research Institute on Climate Change and the Environment [40] reports that there are over 2000 climate laws and policies across the globe. The European Union currently has 11 policies and 40 laws on climate change. The EU 2030 climate & energy framework that passed in 2014 aims to cut GHG emissions by at least 40% from 1990 levels, to increase its renewable energy share by at least 27% and to improve energy efficiency by at least 27% by 2030 [41]. The EU energy security strategy [42] that passed in 2014 is connected to the 2030 climate & energy framework and this strategy aims to reduce the EU's dependence on energy imports and protect itself from energy supply disruptions; it targets reducing the reliance on imports by 24% from 2012 levels [43]. The most recent policy that passed in November 2020 is a strategy to harness the potential of offshore renewable energy [44] and make it a core component of Europe's energy system by 2050.

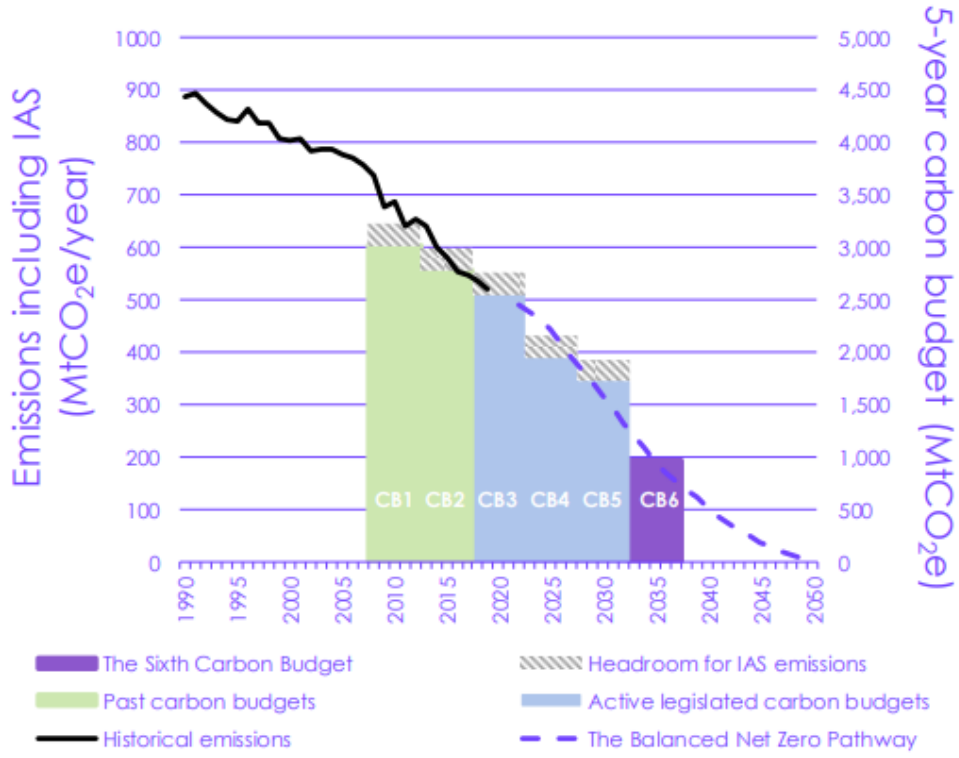

Figure 1.6: UK carbon budgets including IAS (international aviation and shipping)[45].

In the United Kingdom, the Climate Change Act of 2008 provides a long-term framework to help the UK transition to a low carbon economy. This law established legally binding targets to achieve net zero GHG emissions by 2050 [46]. The Act provides a system for carbon budgeting to cap emissions over 5-year periods to help keep the UK on track for the 2050

target and established the Committee on Climate Change (CCC), an independent, statutory body to advise the UK government on emission targets and report progress to the UK Parliament. There are now six carbon budgets covering 2008 - 2037 and a 78% reduction relative to 1990 levels is expected by 2035 [45]. Figure 1.6 shows the targets of the carbon budgets since 2008. The first three carbon budgets were set in 2009 and the fourth one was set in 2011. The first budget (2008 - 2012) limited GHG emissions to 3,018 $MtCO_2e$ and this target was met with emissions being 2,982 $MtCO_2e$, a 23.6% reduction relative to 1990 levels [47]. The second budget (2013 - 2017) set a cap of 2,782 $MtCO_2e$ and this target was also met with emissions in that period being 2,398 $MtCO_2e$, a 40% reduction relative to 1990 levels and 14% below the cap [48]. The third budget (2018 - 2022) has a target of 2,544 $MtCO_2e$ and this target is likely to be met partly due to the effect of the covid-19 pandemic [49].The fourth carbon budget (2023 - 2027) was set at 1,950 $MtCO_2e$, with a 50% reduction by 2025. The fifth carbon budget (2028 - 2032) set in 2016, limits GHG emissions to 1,765 $MtCO_2e$ corresponding to a 57% reduction. The Climate Change Act also grants powers to use emissions trading schemes (ETS) through secondary legislation leading to the introduction of the Carbon Reduction Commitment Energy Efficiency Scheme [50].

The Renewables Obligation [51] was introduced as a way to support large-scale generation of renewable electricity. With this mechanism, generators are issued a Renewable Obligation Certificate (ROC) for each MWh of electricity generated using renewable energy sources. However, this scheme closed to all new generating capacity in March 2017 [52] and the Contracts for Difference (CfD) scheme introduced by the 2013 Energy Act [53] replaced this, to support low-carbon electricity generation. The CfD scheme reduces the risks faced by low carbon electricity generators by fixing the prices and ensures investment in eligible technology; the fixed price is called the strike price. If the market price of electricity is lower than the strike price, the CfD pays the generators a top-up and if the market price of electricity is higher than the strike price, the generator is obligated to pay the difference price [54]. The Renewables Transport Fuel Obligation (RTFO) [55], like the RO, issues Renewable Transport Fuel Certificates (RTFC) to transport fuels supplied from renewable energy sources in order to support the UK's government policy to reduce GHG emissions from vehicles and drive the supply of renewable fuels.

These are some of the policies and laws enacted in the United Kingdom to support reducing GHG emissions and mitigating climate change. The different laws and policies passed by different countries can be found on the Grantham Research Institute database [40].

1.4 Research Interest

In recent years, there has been an increased interest in using negative emission technologies to reduce CO_2 emissions. In this area, bioenergy with carbon capture, utilisation and storage is of special interest to the researcher.

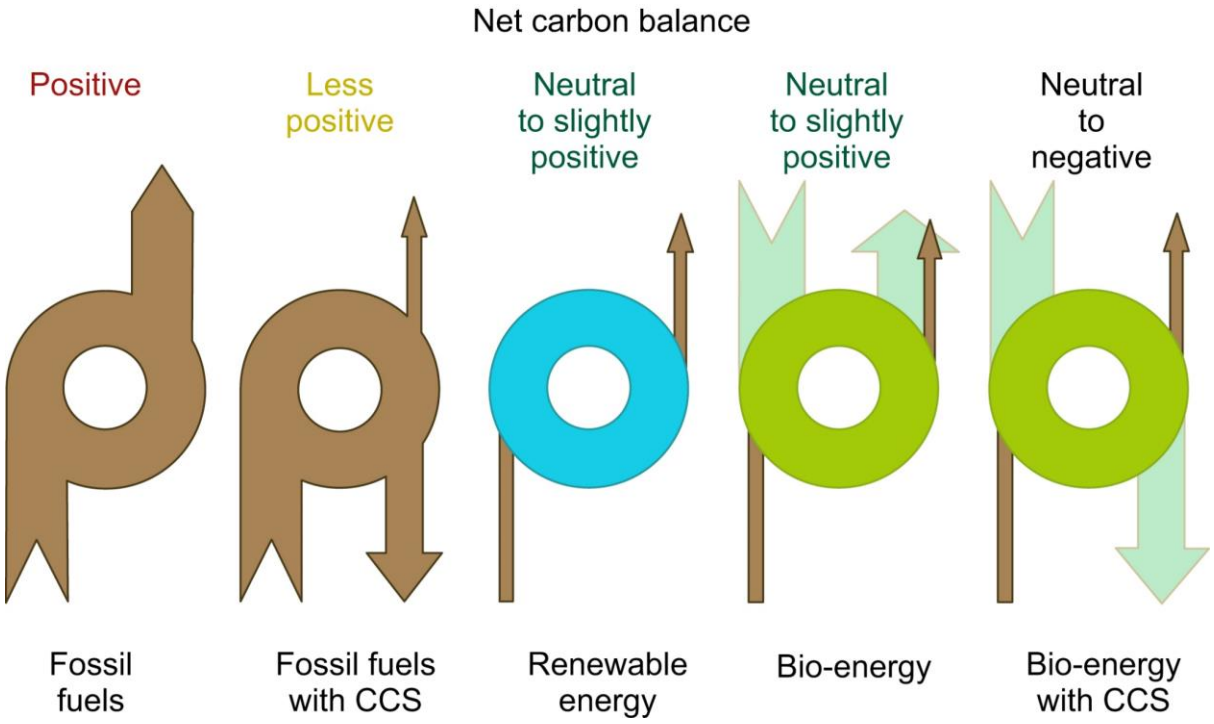

Figure 1.7: Carbon balance in the atmosphere using different techniques [56].

Bioenergy with carbon capture and storage (BECCS) is a technique that combines the production of bioenergy with carbon capture and storage as a means of reducing the accumulation of CO_2 in the atmosphere. Overall, this is a negative emission strategy because while bioenergy production is a neutral emission strategy (the amount of CO_2 released during its lifetime equates to the amount needed for its growth), capturing CO_2 during the production process further reduces the amount of CO_2 during the net lifetime of the biomass [56]. The effect of different techniques on the carbon balance in the atmosphere is shown in Figure 1.7 [56]. From this figure, it is evident that BECCS is the option to make the most significant impact in the journey towards meeting climate targets of keeping the increase in the global temperatures below 2 °C above the pre-industrial average [57].

BECCS is an important technology due to its mitigation potential and the technical status is currently in demonstration [31]. The topic of BECCS is a complex one with potential research areas to fully develop the concept and it is currently being researched to fully understand its

different applications and apply it to GHG emissions across different countries and sectors. As a result, BECCS as a climate change mitigation tool is the theme of this research and this thesis focuses on the application of BECCS in the energy sector, which is responsible for a significant amount of GHG emissions. Also, this research considers the role of carbon dioxide utilisation in CO_2 emissions reduction due to the growing interest in understanding the potential of CCU in reducing greenhouse gas emissions.

1.4.1 Current challenges and suggestions

The major barrier to the deployment of BECCS involves the costs, which are higher than that of fossil-based technologies, limited literature on the subject and lack of BECCS projects to analyse [58]. In order to make BECCS an attractive option and replace fossil-based technologies in the future, certain changes need to be implemented. Some of the suggested changes include:

- A more detailed and wider range of information being available on the application of BECCS in different sectors [59].
- Making the downstream application of syngas from biomass gasification highly competitive. Biomass gasification is a significant part of fuel generation as it produces syngas, a precursor for biofuel production. Currently, gasoline and olefin production via gasification of bio-oil from biomass pyrolysis, is not competitive when compared to the market prices [60].
- Developing and implementing government policies in support of BECCS such as, creating subsidies for biofuel production via a negative carbon emission route.
- Lowering the capital costs of biomass gasification by process intensification, cheaper and effective air separation unit where oxygen is the gasifying agent and improved agricultural practices for low and stable feedstock costs [61].

1.5 Research Aim and Objectives

The main aim of this project is to contribute significant and detailed information to the literature on the application of BECCS. Due to the limited information currently available in the open literature, this research aims to fill the gap in the energy generation sector by holistically evaluating the technical, economic and environmental performance of a range of bioenergy routes without CCS and with CCS; an approach which to the knowledge of the author has not previously been applied in the literature. Again, while most assessments are

either a techno-economic assessment or a lifecycle analysis, this research combines both to render a well-rounded view, make the information more easily accessible and influence the decision-making process. This thesis will develop and assess different BECCS combinations in energy generation to assess the negative emissions potential, the feasibility of deployment, the barriers to be overcome and the opportunities to be maximised. This thesis is divided into three main parts. The first part of the thesis covers power generation and the last two parts cover fuel generation. The objectives of this thesis include the following:

- Comparatively assess the different types of biomass in power generation coupled with different CCS technologies.
- Investigate different fuel production routes via biomass gasification.
- Investigate the potential of CO_2 utilisation in fuel generation.
- Quantify the technical performance of each technology in terms of energy efficiency and yield.
- Discover the effects of incorporating CCS with bioenergy on the production performance.
- Explore the mitigation potential and carbon savings of each energy generation route.
- Determine the feasibility of each energy generation route.
- Evaluate the critical parameters hindering the levelised cost of producing energy.
- Assess the current competitiveness of bioenergy with conventional fossil-fuels.
- Use financial analysis tools to highlight possible incentive schemes to be considered in policymaking.

1.6 Outline of Thesis

This thesis is organised in 7 chapters and the outline of each chapter is described as follows:

Chapter 1 is the introductory chapter which explains the background of the thesis and motivation for the research.

Chapter 2 describes the different concepts associated with the subject of the research and reviews the literature on the topic.

Chapter 3 is the methodology chapter which explains the modelling and simulation approach and techniques applied in the thesis.

Chapter 4 presents the assessment of three different types of biomass in post-combustion, oxyfuel combustion and pre-combustion carbon capture.

Chapter 5 presents the assessment of Fischer-Tropsch fuels, Synthetic Natural Gas (SNG) and Oxymethylene Ethers (OMEx) synthesis via gasification without CCS and with CCS.

Chapter 6 presents the assessment of the synthesis of same fuels from Chapter 5 via electrolysis and CO_2 utilisation.

Chapter 7 is the conclusion chapter which summarises the results and the importance of the work presented in this thesis and provides recommendations for future research.

2 Literature Review

2.1 Bioenergy

Bioenergy refers to energy from biomass. Biomass is described as a renewable and sustainable energy source from organic materials; this includes plants and animals [62,63]. Bioenergy feedstocks comes from four main categories and this depends on the origin of the biomass. These four categories are:

- Energy crops – lignocellulosic crops grown specifically for energy production such as Miscanthus.
- Forestry residues – generally but not limited to residues (barks and small branches) from forestry operations and wood processing industries.
- Agricultural residues – materials leftover from crop harvesting and processing e.g., bagasse, oil palm husks and straw.
- Biogenic wastes – waste from different sectors but not including agricultural or forestry residues e.g. municipal solid waste (MSW), livestock manure, sewage sludge and waste cooking oil [64].

Biomass can be likened to coal in terms of basic elemental composition, but these fuels are different from each other. Biomass has a higher volatile matter content, higher ash content, higher acidic content and lower sulphur and nitrogen content while coal has a higher calorific value and lower carbon to oxygen (C: O) ratio [65,66]. Biomass with calcium (Ca), potassium (K) rich and silicon (Si) lean ash are more reactive than fossil fuel ash and sinter between 900 °C and 1000 °C while biomass with Ca, K lean and Si rich ash sinter between 700 °C and 900 °C [67].

With respect to the formation of each fuel, coal formation requires millions of years of carbon sequestration from dead vegetation while biomass formation requires a shorter time of a few months to years of carbon sequestration (depending on the type of biomass) rendering biomass an infinite source.

In 2017, biomass accounted for 9.5% (55.6 EJ) of the world total primary energy supply [68]. In the journey towards a sustainable future, it is necessary that this figure increases to create a reliable energy mix. Bioenergy is not a new concept and has been in existence since the discovery of fire. In developing countries, biomass in the form of wood and waste is used for lighting, cooking and heating. This is referred to as traditional biomass. In 2017, traditional

biomass accounted for approximately 86% of the biomass supply [69]. The remainder went towards modern bioenergy. Modern bioenergy is biomass used in generating electricity, producing transport fuels, or producing heat and power. Modern bioenergy dates to the early 1900s when Rudolf Diesel designed his diesel engine to run on peanut oil [70]. Then, Henry Ford designed his Model T car to run on alcohol [71,72]. However, the reduced price of crude oil caused a reduction in the use of biofuels. During the second war, demand for biofuels increased due to an increased demand for alternative fuels. During that period, fuel from potatoes and grains were explored [70] and in the 1970s, bioethanol was mass produced from sugarcane and corn in Brazil and the United States [73]. These biofuels, derived from food crops such as sugarcane and corn, are classified as first-generation biofuels. While these biofuels contribute to climate change mitigation, the impact on biodiversity is negative [74]. Second generation biofuels derived from lignocellulosic biomass and waste lessens the impact on biodiversity and addresses the 'food vs fuel' dilemma but the issue of land use remains. Third generation biofuels derived from photosynthetic microorganisms (algae) result in higher yields with lower feedstock and land use, but this is still at the research stage.

2.1.1 Biomass conversion routes

Biomass is converted to biofuels via several routes. These routes are biochemical or thermochemical. A summary of biomass conversion routes is illustrated in Figure 2.1.

Combustion of biomass involves the exothermic oxidation of biomass at high temperatures (700 °C – 1400 °C) in the presence of excess oxygen/air to produce gases and heat. The heat can be extracted from the flue gases to generate electricity in a conventional power plant or heat and power in a cogeneration plant.

Gasification involves partial oxidation of biomass at temperatures in the range 800 °C to 1800 °C to convert the biomass into synthetic gas (syngas), consisting of mainly (hydrogen) H_2 and (carbon monoxide) CO, which has a higher volumetric heating value than the biomass due to the removal of the inert components such as nitrogen [75,76]. Other constituents of syngas are methane (CH_4) and carbon dioxide (CO_2). The ratio of these constituents present in syngas depends mainly on the type of biomass and the operating conditions. Syngas from this process can be used directly in heat and power generation but syngas is also a precursor for many products including synthetic natural gas (SNG), methanol, hydrogen and gasoline.

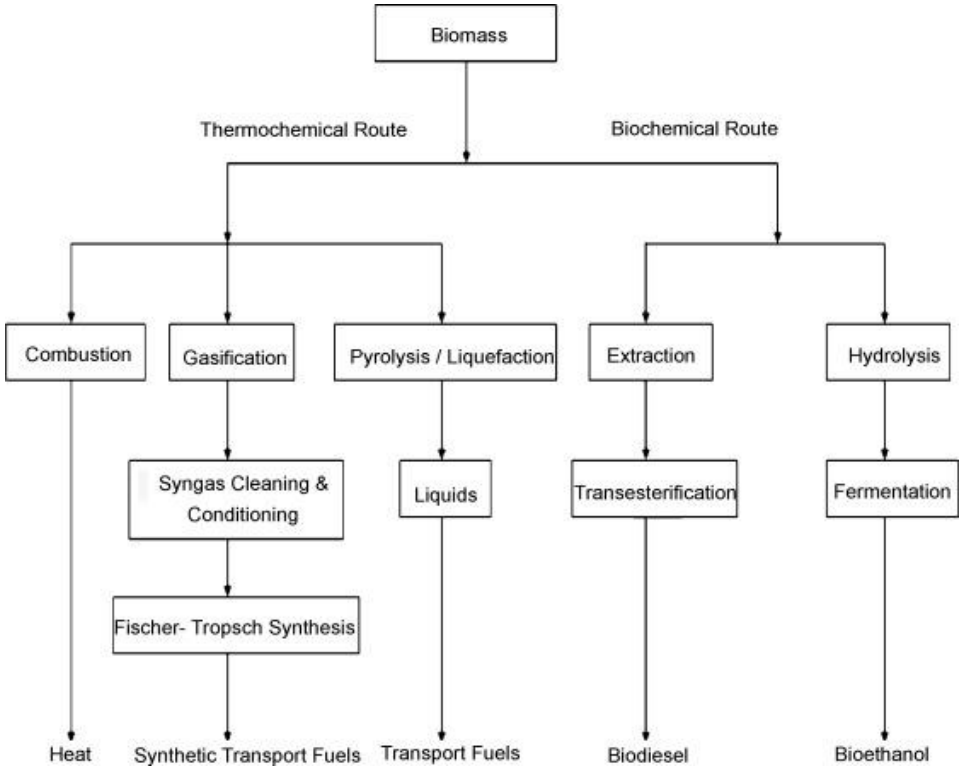

Figure 2.1: Illustration of the biomass conversion route [77].

Pyrolysis of biomass is the decomposition of biomass at temperatures in the range 300 °C to 600 °C [62] in the absence of any oxidant. Depending on the rate of pyrolysis, the main products of biomass pyrolysis are bio-oil and charcoal. Faster heating rates favour bio-oil production while slower heating rates favour char production.

In the biochemical conversion of biomass, microorganisms such as bacteria and enzymes are used to breakdown biomass into gaseous or liquid fuels in the absence of oxygen.

While bioenergy is a promising concept, there are certain factors hindering deployment on a commercial scale.

2.1.2 Environmental factors

Bioenergy is a controversial topic when considering emissions. While there are claims that biomass is carbon neutral, there are counterclaims that the emissions from bioenergy production is worse than that of fossil fuels. In theory, biomass, as a renewable energy source, is considered CO_2 neutral based on its lifecycle (CO_2 released = CO_2 absorbed) but some researchers argue against this label. Biomass combustion releases CO_2 more rapidly than biomass regeneration absorbs from the biosphere, hence in the short to medium term,

CO_2 present in the atmosphere increases. However, in the long term, emission reductions is achieved as biomass is regenerated [78]. Most importantly, the lifecycle emissions associated with biomass use negates the zero-carbon label. Lifecycle emissions arise from the cultivation, harvesting, processing and transportation of biomass. One argument against biomass carbon neutrality explains that large-scale production of biomass for bioenergy causes depletion of soil fertility and thus requiring fertilisation. Subsequently, fertilisation increases N_2O emissions which is a greenhouse gas, thus defeating the idea of carbon neutrality [79]. Another argument added that while describing all biomass as carbon neutral is incorrect and misleading, responsible sourced biomass, such as easily decomposable forest residues which reduce emissions from the beginning of its use and biomass produced on plantations that do not cause significant carbon stock losses, can earn this carbon neutral label [78]. Essentially, bioenergy production can adversely impact some environmental factors such as water quantity and quality due to high water consumption and nutrient pollution of groundwater; greenhouse gas emissions in the form of N_2O from fertiliser use and CO_2 from land conversion to first generation crops; and loss of biodiversity due to increasing temperatures. The degree of adversity is highly dependent on the type of biomass produced, the land location and the management practices [80] hereby summarising that these effects can be limited by making the right choices along the biomass production and supply chain [81] to render biomass carbon neutral.

2.1.3 Socio-economic and political factors

There is no doubt to the social and economic implications of deploying bioenergy in any region. The extent of the benefits varies between different regions and countries. Socio-economic impact studies are commonly performed to evaluate the implications of effecting decisions on a local, regional and/or national level. The indices measured include income, employment, health, energy usage and the local economy. A study on installing biogas plants on a domestic level in Pakistan [82] showed that this option could reduce energy expenses and cut down the risks of respiratory and cardiovascular ailments. Another study on the benefits of a local development bioenergy strategy in Finland [83] summarised that such a project could generate up to €12,000,000 in annual income impacts and increase employment. Also, an assessment on the effect of sugarcane ethanol production in Brazil [84] estimated that expanding production could increase the national GDP by 2.6 billion USD and employment by 53 000 fte (full-time equivalent). These are a few of the studies that have completed on the benefits of bioenergy.

There are social and economic impacts and concerns associated with bioenergy projects. Local bioenergy investments are important especially in regions with rural locations experiencing a depopulation. The major social implications are an increased standard of living and social cohesion and stability. The introduction of bioenergy production which is an income-generating source to a local area generates employment (direct, indirect and induced) and helps to stabilise the population. A sensitivity analysis on biofuel agroforestry systems showed that the income levels of smallholder farmers could potential increase by up to 60% [85] while a case study in Lieska, Finland showed a bio-oil production system could cause positive changes in the net migration by slowing population losses [86]. On a national level, a broad geographical distribution of bioenergy and a diversity of feedstock is advantageous to any nation due to the security of supply this creates. Also, the energy independence the nation endures because their energy supply is not subject to erratic and fluctuating prices of energy products which historically is a possibility. On the macro level, this creates room for economic growth through an increase in GDP, as in Brinkman et al. [84] and biomass exports. The benefits vary from developing to developed countries. Developed countries focus on modern bioenergy systems which are efficient, so the benefits enjoyed centre around the contribution to energy security and environmental benefits while in developing countries, the focus is on traditional biomass which is used inefficiently and in air polluting ways. In developing countries, the benefits will centre on health, job creation and economic growth.

In conclusion, the benefits of deploying bioenergy are the potential for increased employment, regional development and economic growth via development of a strong export industry [87]. However, there are socio-economic issues that should not be neglected. The main issue is the competition with demand for food and land. Globally, the area available for agriculture is restricted and with biomass cultivation expanding, there is an increased competition for land. This is the bane of the food vs land argument and the progression from first generation biomass to second generation. There is the possibility that biomass cultivation could displace food production resulting in land use changes which could be critical to climate change and biodiversity [88].

Notwithstanding, the most determining factor in the success and sustainability of bioenergy deployment is the policies – local, regional, national and global. These policies or the absence of these policies could either make or break a bioenergy development strategy. Ideally, these policies will assist in minimising the issues and maximising the benefits.

2.2 Bioenergy with Carbon Capture and Storage

Carbon capture and storage (CCS) is not a new term and has been in operation since the 1970s [89]. It is a climate change technology which captures CO_2 at the source, compresses it, transports it and injects it into a geological storage. This way, CO_2 is prevented from being released to the atmosphere. However, this technology was initially developed for fossil fuels. Hence, while greenhouse gas emissions to the atmosphere are reduced, net emissions are still positive. Also, this technology, although in commercial operation, has not been employed on a global scale to experience the benefits. As at June 2020 [90], there are only 21 CCS facilities in operation. Combining bioenergy with carbon capture and storage (BECCS) has come up as concept designed to achieve negative emissions, meet global warming targets and limit the effect of greenhouse gases on the climate [91]. The concept of BECCS is based on the use of bioenergy (a renewable energy source) in energy generation and preventing the release of CO_2 emissions from the process that would otherwise have been released to the atmosphere for biomass regeneration by applying CCS technology. This results in net negative CO_2 emissions as CO_2 is removed from the atmosphere. Based on scenario modelling exercises, BECCS deployment could remove up to 16 $GtCO_2$/yr in 2100 [39]. While this technology shows a lot of potential, deployment has been slow as the wide-scale deployment of CCS is integral to its success [91].

2.3 CO_2 Utilisation

Carbon capture, utilisation and storage (CCUS) has been identified as a means of reducing emissions and could be the key to decarbonising hard-to-decarbonise industrial sectors such as the cement, iron and steel sectors [92]. CCUS involves capturing CO_2 captured from processes producing pure streams of CO_2 such as natural gas processing and ammonia production, then compressing and transporting CO_2 for use and storage. Where CO_2 is captured for use only, it is termed carbon capture and utilisation (CCU) [93]. CO_2 is the major greenhouse gas responsible for global warming and efforts to mitigate the effect of greenhouse gas emissions are focused on CO_2 removal from the atmosphere such as CCS technology.

The global CO_2 market demand in 2019 was $7.66 billion and this value is expected to reach $10 billion by 2027 [94]. CO_2 is a valuable feedstock for creating products and services such as fuels, building materials and chemicals [95]. Using waste CO_2 from processes as a

feedstock contributes to achieving a CO_2 circular economy and reducing the dependence on fossil fuels [96,97]. Also, CO_2 from biomass or the air could play a major role in achieving a net zero carbon economy [95].

CCU technologies covers various sectors. It includes polymer processing in chemicals production, concrete curing in CO_2 mineralisation, synthetic fuels - methane, methanol, diesel etc. in CO_2-to-fuels, enhanced commodity production such as boosting urea yield, beverage carbonation in the food and drink industry and industrial applications such metal working [59]. This shows that there is a market for CO_2 utilisation and by increasing this market size and demand, CO_2 emissions to the atmosphere could be reduced. Alberici et al. [59] assessed the potential of CO_2 utilisation in the UK and summarised that there is limited evidence on the commercial potential of CCU with many CCU technologies still in early development. Also, many of the technologies capture CO_2 for a short time before re-releasing it. This summary drives the opinion that combining CO_2 utilisation with storage is the pathway required to improve the effectiveness of CO_2 utilisation in mitigating climate change and research and development on CCU technologies is necessary to expand the evidence on the potential of CCU in a CO_2 economy.

The CO_2-to-fuels sector relies on hydrogen production and is heavily dependent on energy [95]. CO_2 is a stable compound, consequently, breaking down this molecule during conversion in highly endothermic reactions requires a lot of energy. To supply the required energy, renewable energy such solar, wind, wave, hydropower and geothermal energy are good considerations [98]. Hydrogen (H_2) and CO_2 are the precursors for synthetic fuels and hydrogen can be produced through several means including gasification, fermentation and electrolysis [99]. Electrolysis involves splitting a water molecule into its constituent elements - H_2 and O_2 - when an electric current is supplied to an electrolyser. For a renewable perspective, excess renewable electricity is used resulting in reduced emissions over the lifetime the produced H_2. This electrochemical route produces a pure stream of hydrogen. The thermochemical route (gasification) involves subjecting coal or biomass to high-temperatures and limited oxygen in a gasifier. The resulting product is syngas which is a mix of hydrogen and carbon monoxide. The syngas produced requires cleaning and conditioning to get a pure hydrogen stream. Further reactions such as the water-gas shift reaction could be required in the conditioning stage to increase the hydrogen content. This route results in CO_2 emissions from the carbon content in coal or biomass. However, it is reduced when biomass is used, as biomass is a renewable fuel.

CO_2-to-fuels acts as a form of electricity storage where electrical energy is converted to chemical form in fuels. The electricity source varies and it could be excess electricity because of the intermittent nature of renewable energy (solar, wind, hydropower) which cannot be controlled to match energy demand, electricity from dedicated renewable energy plants, or electricity from a clean grid. With an increasing demand for electricity storage in the case of excess electricity, storing in fuels is one of the ways to tackle this problem.

2.4 Fuel Generation

Biomass use in power generation is straightforward as biomass is combusted and the heat from combustion drives a steam cycle to produce electricity. In fuel generation, there are many routes dependent on the resulting fuel. These fuels include diesel, gasoline, dimethyl ether (DME), methane, methanol and oxymethylene ethers (OMEx). This thesis focuses on three fuel production routes, fuels which are central to the transport sector - FT-fuel (diesel and gasoline), methane and OMEx. In particular, Fischer-Tropsch synthesis fuel (FT-fuel) is chosen because it is an alternative for the most common liquid fuels in transportation – gasoline and diesel. BioSNG is chosen as the alternative for the most common gaseous fuel – natural gas and OMEx is chosen because it is a relatively novel biofuel which is derived from methanol and it has shown potential in diesel engines; one of which is its ability to serve as an almost carbon-neutral component when 24% (wt) is blended with diesel [100]. The common precursor in fuel generation is the use of syngas which is produced by gasification and this is discussed in the next section.

2.4.1 Gasification

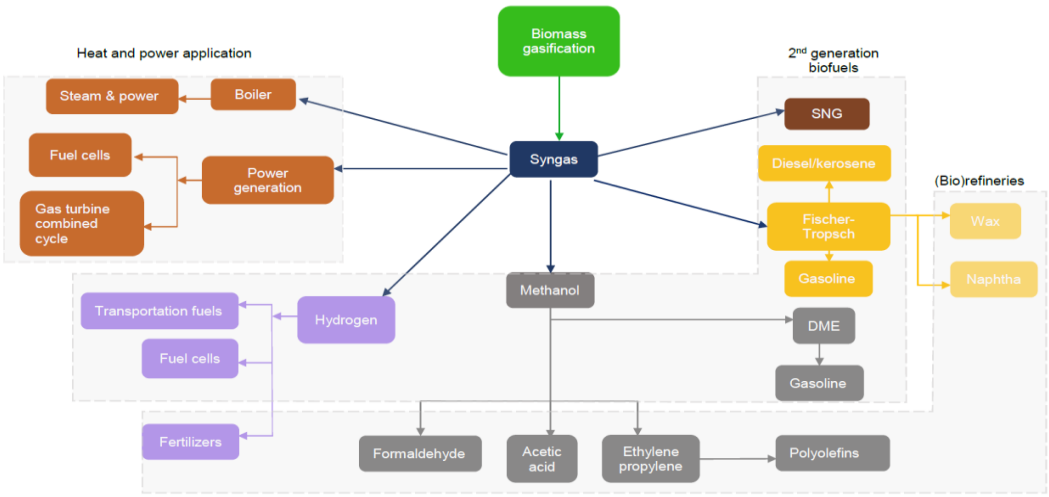

Figure 2.2: Schematic of syngas applications.

Biomass gasification involves the conversion of biomass into fuel gas by partial oxidation with either air, oxygen (O_2), steam (H_2O), carbon dioxide (CO_2) or a combination of the gasifying agents. The syngas from this process is a precursor for several applications and Figure 2.2 illustrates the wide range of use of syngas.

One of the main applications of syngas from biomass is in the production of biofuels, an environmental substitute for conventional fossil fuels in the economy. A simple route to biofuel production from syngas is by conditioning and upgrading syngas from biomass gasification.

The gasification process occurs in a gasifier and it involves several steps which can be split into zones in the gasifier. Depending on the type of gasifier, all the steps could either occur in one unit or in two units as in the case of an indirect gasifier [101–104]. The steps in the process are briefly explained as follows:

i. Drying: This step involves reducing the moisture content of the biomass feed for later reactions. The water removed from this stage is in the form of steam and depends on the operating parameters and this could take part in the gasification reactions in later steps.
ii. Pyrolysis: In this stage, the biomass feed is thermally decomposed in the absence of an oxidising agent. This results in the breaking down of large hydrocarbon molecules to simpler molecules which are released as volatile matter and tar vapour. The heavier components of the biomass that remains is referred to as char. At lower temperatures, the tar vapour condenses to form liquid tar.
iii. Oxidation: The volatile matter released during pyrolysis and some of the char undergo oxidation with limited oxygen present in the gasifying media supplied to the gasifier. The products formed include carbon dioxide (CO_2), carbon monoxide (CO) and H_2O. Due to this being an exothermic reaction, heat is also released for the gasification stage. The reactions at this stage are as follows [76]:

$$C + 0.5O_2 \rightarrow CO \qquad -111 \text{ kJ/mol} \qquad (2.1)$$

$$CO + 0.5O_2 \rightarrow CO_2 \qquad -283 \text{ kJ/mol} \qquad (2.2)$$

$$C + O_2 \rightarrow CO_2 \qquad -394 \text{ kJ/mol} \qquad (2.3)$$

$$H_2 + 0.5O_2 \rightarrow H_2O \qquad -242 \text{ kJ/mol} \qquad (2.4)$$

$$CH_4 + 2O_2 \rightarrow CO_2 + 2H_2O \quad \text{-803 kJ/mol} \quad (2.5)$$

iv. Gasification: The remaining char reacts with steam and CO_2 to form CO and H_2 following the equations as follows:

Hydrogasification

$$C + 2H_2 \leftrightarrow CH_4 \quad \text{-75 kJ/mol} \quad (2.6)$$

Boudouard reaction

$$C + CO_2 \leftrightarrow 2CO \quad \text{+172 kJ/mol} \quad (2.7)$$

Water-gas reaction

$$C + H_2O \leftrightarrow CO + H_2 \quad \text{+131 kJ/mol} \quad (2.8)$$

Steam methane reforming reaction

$$CH_4 + H_2O \leftrightarrow CO + 3H_2 \quad \text{+206 kJ/mol} \quad (2.9)$$

Other reactions take place during gasification which affect the final product composition and these include [76]:

Methanation reactions

$$2CO + 2H_2 \rightarrow CH_4 + CO_2 \quad \text{-247 kJ/mol} \quad (2.10)$$

$$CO + 3H_2 \rightarrow CH_4 + H_2O \quad \text{-206 kJ/mol} \quad (2.11)$$

$$CO_2 + 4H_2 \rightarrow CH_4 + 2H_2O \quad \text{-165 kJ/mol} \quad (2.12)$$

Water-gas shift reaction

$$CO + H_2O \leftrightarrow CO_2 + H_2 \quad \text{-41 kJ/mol} \quad (2.13)$$

Other steam methane reforming reaction

$$CH_4 + 0.5O_2 \leftrightarrow CO + 2H_2 \quad \text{-36 kJ/mol} \quad (2.14)$$

2.4.2 Gasifiers

The gasification process occurs in equipment referred to as gasifiers. Gasifiers can be classified based on the heating mode, gas – solid contact method and flow pattern between

the gas and biomass [105]. Based on the gas – solid contact method, gasifiers can be classified as follows:

i. Fixed or moving bed,
ii. Fluidised bed,
iii. Entrained-flow bed.

2.4.2.1 Fixed or Moving - Bed Gasifiers

In the fixed bed gasifier, the biomass is supported on a grate and it is fed in from the top of the gasifier and moves downwards continuously through the drying, pyrolysis, oxidation and gasification zones. The method by which the oxidant is fed into the gasifier determines the type of fixed bed gasifier. There are three main types of fixed bed gasifiers: updraft, downdraft and crossdraft gasifiers. Fixed bed gasifiers operate at moderate pressures between 25 atm and 30 atm and could operate in two different modes. One mode is the dry-ash mode where the char is reacted with excess steam to moderate the temperature to below the ash-slagging temperature; an example of this is the Lurgi Dry Ash gasifier [104]. The other mode is the slagging mode where less steam is employed to achieve a much higher temperature in the combustion zone, such that ash is melted and slag is produced; an example is the British Gas/Lurgi (BGL) gasifier [104].

a. Updraft gasifier

In the updraft gasifier, the oxidant is fed in from the bottom of the gasifier, thus creating a counter current flow between the gas and solids with the syngas leaving near the top of the gasifier. A schematic of the updraft gasifier and its temperature profile is given in Figure 2.3. This type of gasifier is suitable for biomass with high ash content up to 25% and high moisture content up to 60%. However, tar production in this gasifier is high but due to the good internal heat exchange, because of the counter-current operating mode, a high cold-gas efficiency is achieved and the gases exit at a low temperature [104,106,107].

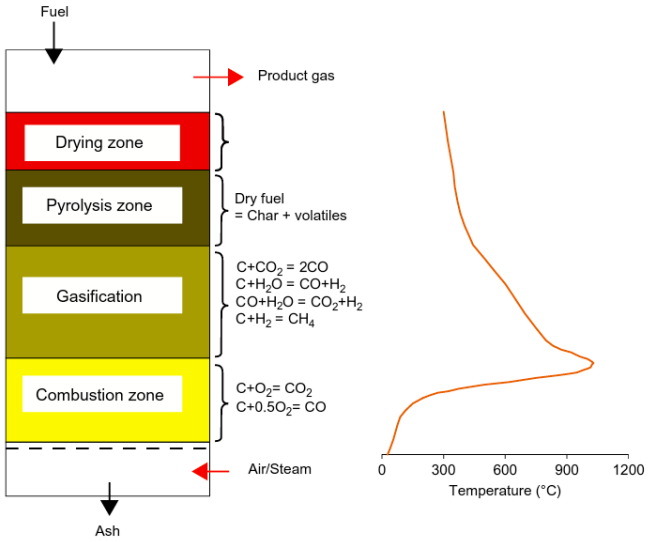

Figure 2.3: Schematic of an updraft gasifier and a typical temperature profile [106].

b. Downdraft gasifier

In the downdraft gasifier, the oxidant is fed in at a certain height below the top of the gasifier, thus creating a co-current flow between the gas and solids with the syngas leaving near the bottom of the gasifier. A schematic of the downdraft gasifier and its temperature profile is illustrated in Figure 2.4. The downdraft gasifier solves the problem of tar entrainment in the syngas that occurs in an updraft gasifier. The syngas passes through the hot bed ash at the bottom of the gasifier. The conditions in the hot bed of ash promotes tar cracking, thus leading to a syngas with low tar. However, this type of gasifier cannot operate on different feedstock and due to lack of internal heat exchange, the efficiency is lower with a syngas of lower heating value.

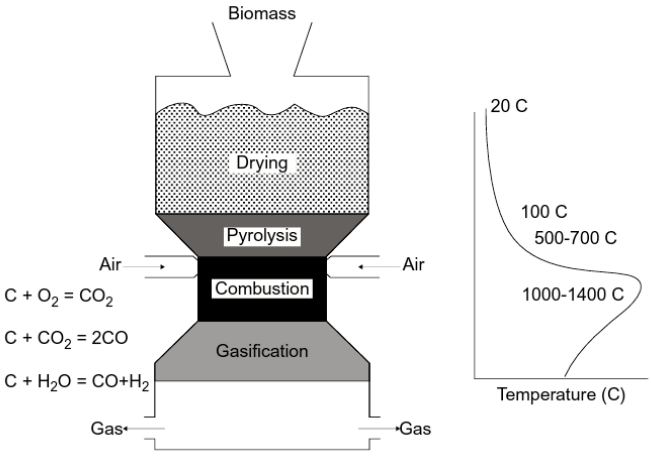

Figure 2.4: Schematic of a downdraft gasifier and a typical temperature profile [106].

2.4.2.2 Fluidised Bed Gasifiers

Some of the problems encountered in fixed bed gasifiers include the difficulty to achieve and maintain a uniform temperature distribution and its poor mixing. Fluidised bed gasifiers, on the other hand, are capable of perfect mixing and maintaining a uniform temperature which reduces the risk of fuel agglomeration. This gasifier consists of inert bed materials (granular solids) which are kept in a fluidised state by the action of the gasifying medium. Fuel is introduced from the top or side of the reactor while the oxidant is introduced through the bottom of the reactor at a sufficient velocity to maintain fluidisation. To support the suspension of biomass particles, small particles, usually less than 6 mm in diameter, are used. Fluidised beds are operated at moderately high temperatures (1000 °C) to ensure high carbon conversion rates up to 95% and tar decomposition. Due to the perfect solid-gas mixing and thermal inertia, the quality of biomass is irrelevant (fixed bed gasifiers are affected by the biomass quality). The disadvantage of this type of reactor is the issue of char entrainment in the syngas. To fix this problem, the syngas goes through a cyclone to recover bed material. There are two main types of fluidised bed gasifiers: bubbling and circulating; a schematic of a circulating gasifier is shown in Figure 2.5. While the circulating fluidised bed (CFB) has a longer gas residence time than the bubbling fluidised bed (BFB), temperature gradients tend to occur in the direction of the solid flow and hence its heat exchange mechanism is less efficient than that of the BFB [104–106].

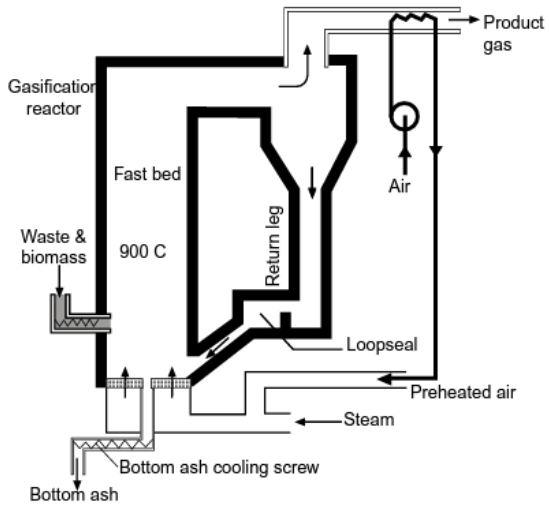

Figure 2.5: Schematic of a circulating fluidised bed [106].

2.4.2.3 Entrained gasifier

This type of gasifier is commonly found in large scale operations. The biomass and oxidant are fed co-currently and these travel through the reactor and they act like a plug flow reactor. Conditions in the gasifier are such that the residence time of the biomass particles in the reactor is short, carbon conversion is up 99.5% and the syngas contains very little or even no tar. These conditions include high temperatures of up to 1600 °C, high pressure up to 80 bar and finely reduced biomass below 75 µm. Temperatures within this type of gasifier are uniform, however when compared to other gasifiers, cold gas efficiency is low.

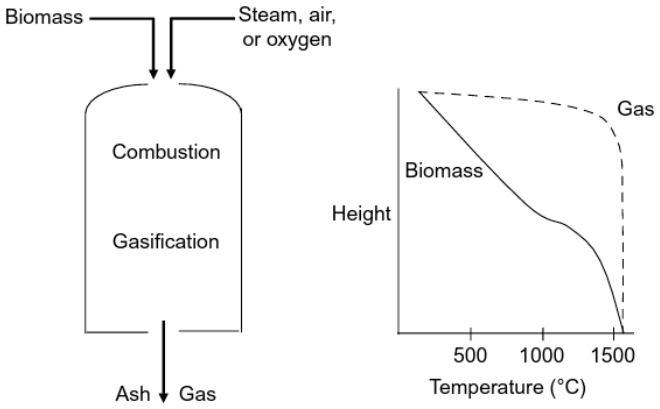

Figure 2.6: Schematic of an entrained gasifier and a typical temperature profile [106].

Entrained gasifiers operate in a slagging mode where the operating temperature is above the ash melting temperature in order to produce inert slag [76,104,106]. A schematic of the entrained gasifier is presented in Figure 2.6.

2.4.3 Fischer-Tropsch Synthesis

Fischer-Tropsch (FT) synthesis is a chemical process where liquid fuel is produced from carbon feedstock. This process was developed in 1925 by Franz Fischer and Hans Tropsch in Germany [108]. In the FT reaction, CO and H_2 in syngas are reacted over a catalyst via the reaction:

$$(2n+1)H_2 + nCO \rightarrow C_nH_{(2n+2)} + nH_2O \quad (2.15)$$

The reaction produces a mixture of hydrocarbons of varying molecular weights. A range of hydrocarbons can be obtained depending on the operating conditions such as the temperature and type of catalyst. The FT reaction occurs at a pressure of 20 - 40 bar. A

lower temperature range (200 – 250 °C) favours wax formation and produces more diesel than gasoline. For lower molecular weight olefins and more gasoline, a higher temperature range (300 – 350 °C) is preferred [109]. Generally, the catalysts are iron or cobalt based. Iron catalysts can be used in both temperature ranges, but it is generally used in the higher temperature.

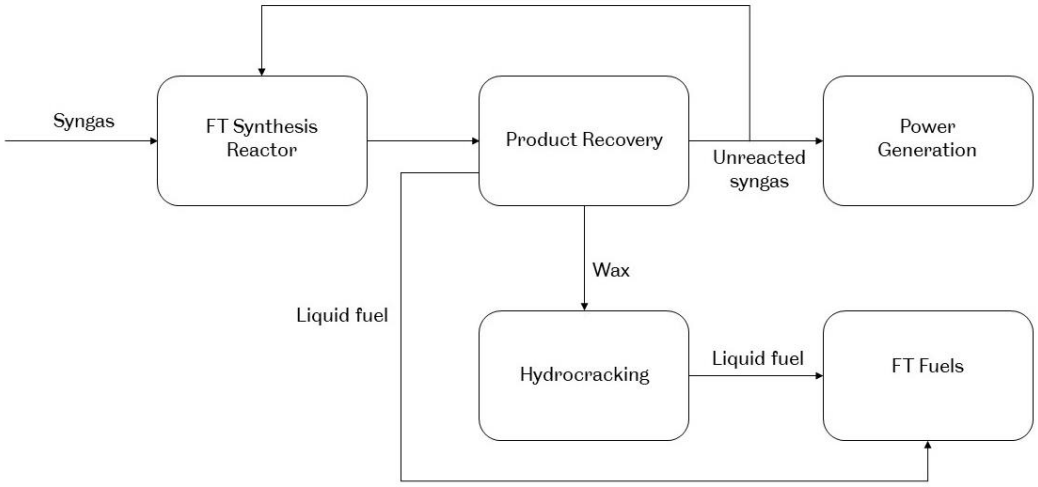

Figure 2.7: Block flow diagram of FT synthesis from syngas.

Also, iron catalysts have an inherent WGS activity which increases the H_2/CO ratio in syngas reducing the need for a WGS reactor in syngas cleaning and conditioning. Cobalt based catalysts are preferred in the lower temperature as methane formation occurs at higher temperatures with cobalt catalysts. While cobalt catalysts are more expensive than iron catalysts, the price is offset by lower operating costs and have longer lifetimes than iron catalysts due to lower coke deposition rates when compared to iron catalysts. However, with cobalt catalysts, the inlet H_2/CO ratio needs to be just above 2 [110] requiring a WGS reactor in syngas cleaning and conditioning where the syngas ratio from the gasifier is below this figure. Both catalysts could be poisoned by sulphur, so it is essential that the syngas going into the FT reactor has very low sulphur content [109–111]. A simplified block flow diagram of FT synthesis from syngas is illustrated in Figure 2.7.

The FT reactor is highly exothermic hence heat removal and temperature control are important factors in the reactor design [112]. The fluidised bed reactor is employed in high temperature FT synthesis and the technology was adapted from petroleum distillate cracking [109] . This technology in circulating mode (Synthol reactor) was initially used by Sasol and it has since been replaced by the fixed mode (Sasol Advanced Synthol reactor)

[112]. The fixed bed reactor is used for low temperature FT synthesis but most of these reactors are now being replaced by the slurry bed reactor due to better temperature control and higher conversion [113].

Since the 1920s, the FT synthesis has been commercially used to produce liquid transportation fuels from coal or natural gas [114]. The most common ones are the South African SASOL coal-to-liquid (CTL) technology and the Shell gas-to-liquid (GTL) technology [115]. The use of biomass in FT synthesis has since been researched and a commercial scale plant producing 15,000 tons of biofuel per annum was established by CHOREN. However, it requires producing a large volume of 100,000 tons for profitability [116].

2.4.4 Methanation

The methanation process discovered by Sabatier and Senderens in 1902 involves the production of methane (CH_4) by hydrogenation of CO and CO_2 by the reactions seen in Eqns. 2.11 and 2.12 in sub-section 2.4.1.

Methane created by this process is referred to as synthetic natural gas (SNG). The equilibrium of both reactions is influenced by temperature and pressure. Where both reactions are occurring in the same reactor, the water-gas shift reaction (Eqn. 2.13) also takes place. High pressures favour the production of methane while high temperatures limit the production of methane. These reactions are performed over catalysts. In terms of catalysts, ruthenium catalysts display the most activity and is the most desirable at low temperatures. However, it is expensive and not used commercially. Based on the activity order in Mills and Steffgen [117], nickel is highly selective towards methane and also has a high activity. Nickel catalyst is commonly used in methanation commercially owing to its relatively low price [118]. As with FT synthesis, sulphur removal is also essential to protect the catalyst [119,120].

Methanation can occur in fixed bed reactors, fluidised bed reactors and three-phase reactors. The methanation reactors are also exothermic so temperature control is an important factor. With the fixed bed reactors, it could be either adiabatic operation or near isothermal operation. However, the adiabatic fixed bed reactor is the most mature of all the reactor types [118]. Also, more than one reactor arranged in series are required improve CO conversion. Depending on the configuration, gas recycling is required to optimise methane yield. An example is the Topsøe Recycle Energy-efficient Methanation Process (TREMP™)

where three adiabatic fixed bed reactors are arranged in series with interstage cooling and recycling after the first reactor [121].

The UK has commissioned a commercial bioSNG plant using up to 175,000 tonnes of bio-resources, including unrecyclable wood and refuse-derived fuel (RDF)[122]. The Swedish GoBiGas project which produced 20 MW of bioSNG demonstrated good results but plans to move to large-scale production were terminated [123].

2.4.5 Oxymethylene Dimethyl Ethers Synthesis

Oxymethylene ethers (OMEx) synthesis, is an emerging technology and interest into this has increased over the past decade [124]. Oxymethylene ethers (OME) are diesel fuels substitutes or additives [125] with molecular formula $H_3CO(CH_2O)_nCH_3$ where n = 1 - 8. In order to reduce smoke and exhaust emissions from conventional diesel fuel combustion in engines, focus was placed on oxygenated compounds such as methanol which can achieve this [125]. OME can be used in diesel engines or added to conventional diesel with slight modifications to the fuel system [126] and interest in OME has increased over the past decade [124,127–131]. While OME_1 studies as fuel is more common, interest in higher OMEs (OME_3 – OME_5) are being considered due to their behaviour in diesel engines [132]. In this thesis, the mix of OME_3 – OME_5 is going to be referred to as OMEx.

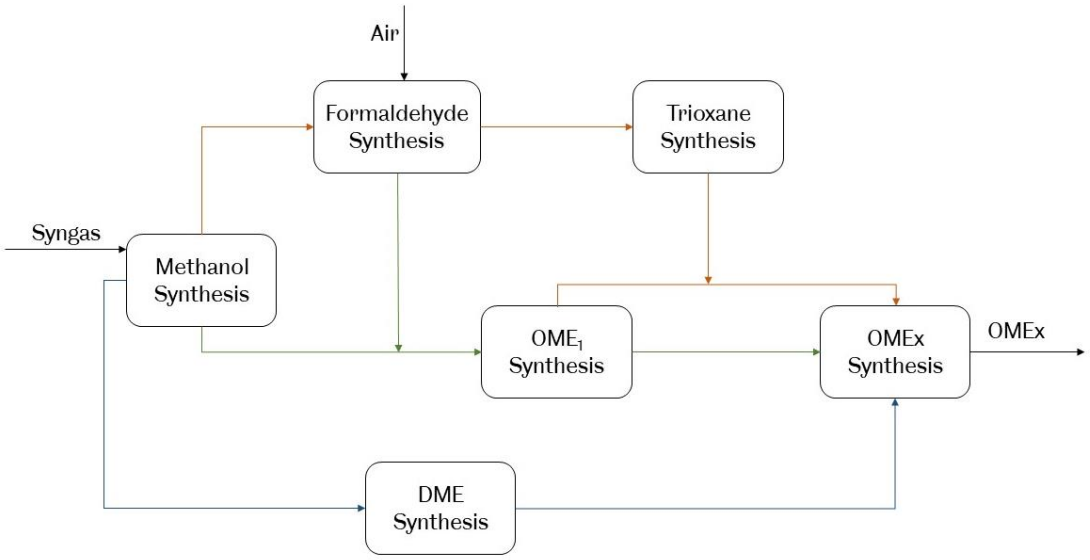

Figure 2.8: Block flow diagram of OMEx synthesis routes.

OMEx synthesis requires methanol as a raw material. The main precursor for OMEx is methanol which can be produced from syngas. While methanol itself is a useful fuel, its low

flammability makes it unsuitable in compression engines and its high toxicity increases operating expenditure [133]. OMEx can be synthesized from methanol (MeOH) via different routes involving dimethyl ether (DME), trioxane, methylal (OME_1) and formaldehyde (FA). The routes are displayed in Figure 2.8.

Depending on the route taken, there are different reactions involved. OMEx is synthesized according to the reactions [126,134–136]:

$$CH_3OH + \frac{1}{2}O_2 \rightarrow CH_2O + H_2O \quad (2.16)$$

$$CH_3OH \rightarrow CH_2O + H_2 \quad (2.17)$$

$$3CH_2O \leftrightarrow (CH_2O)_3 \quad (2.18)$$

$$2CH_3OH + CH_2O \leftrightarrow OME_1 + H_2O \quad (2.19)$$

$$2CH_3OH + nCH_2O \leftrightarrow OME_n + H_2O\ (n > 1) \quad (2.20)$$

$$CH_2O + H_2O \leftrightarrow MG_1 \quad (2.21)$$

$$CH_2O + MG_n \leftrightarrow MG_{n+1} \quad (2.22)$$

$$CH_3OH + CH_2O \leftrightarrow HF_1 \quad (2.23)$$

$$CH_2O + HF_n \leftrightarrow HF_{n+1}(n > 1) \quad (2.24)$$

$$CH_3OH + HF_n \leftrightarrow OME_n + H_2O \quad (2.25)$$

$$MG_n + CH_3OH \leftrightarrow HF_n + H_2O \quad (2.26)$$

$$OME_1 + CH_2O \leftrightarrow OME_2 \quad (2.27)$$

$$OME_n + CH_2O \leftrightarrow OME_{n+1} \quad (2.28)$$

Hemi-formals (HF_n) and polyoxymethylene glycols (MG_n) are intermediate monomers and polymers formed during the process. In the non-aqueous route, OMEx is synthesized from trioxane and methylal via Eqns. 2.18, 2.27 and 2.28. In the aqueous route, it is synthesized from directly methanol and formaldehyde via Eqns. 2.19 and 2.20.

OMEx synthesis is an acid-catalysed reaction employing both homogenous and heterogenous catalysts. Homogenous sulphuric acid is used in trioxane formation from aqueous formaldehyde while an acidic heterogeneous catalyst is used in methylal formation from formaldehyde and methanol [134]. Baranowski et al. [126] investigated the different catalysts and states in patents and scientific literature that have been used in OMEx synthesis.

2.5 Techno-Economic Assessments

Techno-economic assessments provide information to support the deployment of technologies and identify topics for improvement. This section reviews the literature of techno-economic assessments available on biomass power production, biofuels production and power-to-x production routes relevant to this thesis. This assists in identifying the gaps existing in literature and build upon the existing works for the purpose of this thesis.

2.5.1 Power Generation

Current BECCS research is focused on exploring different BECCS technologies, highlighting the mitigation potential and identifying drivers to create favourable policies for the large-scale deployment of BECCS. In the past, BECCS research has focused mainly on comparing biomass performance to coal performance, co-firing and biomass with a specific carbon capture technology. In biomass-based power generation, there are limited techno-economic assessments considering CCS with most of these being very recent. Chattopadhyay and Ghosh [137] performed a study on biomass-based combined power and cooling plant suitable for rural application. The 50 kWe capacity was based on an Indian village with 200 houses. The model combined a gasifier and a combustor where biomass in the form of sawdust was sent to a gasifier to produce syngas for combustion. Electricity was stored in a lithium-ion

battery while heat was stored in a Hitech salt-based phase change material. The price of electricity based on this model was 0.08 USD/kWh and 0.06 USD/kWh with 50% capital subsidy. While this study considered policy impacts, it did not include the effect on the environment as well as consider CCS. Valencia and Walter [138] assessed BECCS systems in a typical Brazilian sugarcane mill. The sugarcane mill was integrated with a combined heat and power unit. The cogeneration plant was designed to operate as a cogeneration unit in the harvest season and as a power-plant in the off-season. Also, a post-combustion carbon capture unit using MEA was coupled to the plant for both CO_2 from combustion and fermentation. For a milling capacity in the range of 2 - 8 Mt/yr, the investment cost per surplus electricity was in the range of 1099 - 1874 €/MWh with the cost reducing as the milling capacity increased. Also, the cost of CO_2 captured presented in this work was in the range of 45 - 80 €/tCO_2.

Bhave et al. [139] screened and assessed a range of bioenergy with CCS technologies involving combustion, gasification, as well as biomass co-firing with coal. This assessment also included coupling with post-combustion, oxyfuel combustion and pre-combustion CO_2 capture. Based on certain assessment criteria including a technical readiness level analysis, the initial 28 BECCS technology combinations was reduced to 8 focusing on biomass and co-firing (biomass and coal blend) with post combustion amine scrubbing, IGCC, oxyfuel combustion, chemical-looping combustion and post-combustion carbonate looping. This comprehensive assessment concluded that co-firing options had the lowest LCOEs due to cheap coal prices; biomass power plants with oxyfuel combustion and post-combustion capture with amine had low efficiencies and high LCOEs; biomass IGCC power plants, biomass chemical-looping power plants and co-fired carbonate looping plants had higher efficiencies and moderate LCOEs. Also, between 2010 and 2050, the cost of CO_2 captured for the technology combinations was in the range of 100 - 190 £/tCO_2 while the cost of CO_2 avoided was in the range of 60 - 90 £/tCO_2. Another comparative assessment by Al-Qayim et al. [140] compared the performance of white wood pellets and coal in electricity generation with both oxyfuel combustion and post-combustion carbon capture. Based on a 650 MW power plant, this study concluded that using white wood pellets in power generation with CCS could remove up to 3 million tonnes of CO_2 from the atmosphere yearly. However, this results in a 150% increase in LCOE when compared to coal and a reduced plant efficiency.

A study by Catalanotti et al. [141] assessed a range of combustion based power generation technologies with and without using coal, natural gas and a biomass blend (75% coal and 25%

biomass). In this paper, the authors highlighted the carbon negative potential of biomass-IGCC with CCS as concluded by Meerman et al. [142]. Catalanotti et al. [141] further identified the present knowledge gap as to how biomass-IGCC with CCS compares to other CO_2 abatement technologies and pointed out the need to perform consistent analyses of different technologies in order to make the right choices. However, there is no information available as to how capturing carbon in biomass-IGCC compares to capturing carbon post biomass combustion as well as the use of oxy-fuel capture in biomass combustion. Bui et al. [143] focused on enhancing the performance of a BECCS system by investigating the fuel properties, using high performance solvents and heat recovery in post-combustion capture. The recurring points in all the research are the high cost and the lack of economic policies as the major barriers to commercial deployment. Zhang et al. [144] assessed the scale at which bioenergy combustion plants and bioenergy combustion with combined heat and power plants can be deployed using both primary and secondary (waste-derived) biomass. This paper highlighted the important role of secondary biomass sources in increasing negative emissions potential and how improving BECCS power efficiency could reduce the cost of the system. On policy instruments, Cabral et al. [145] proposed the decarbonisation of multiple sectors by generating negative emission credits from BECCS plants in the power sector and auctioning them to a hard-to-decarbonise sector such as the industrial sector; following this approach, an economy could be quickly decarbonised.

2.5.2 Biofuel Generation

Most of the existing literature related to BECCS deals with the power generation sector [143,144,146–149]. Some of the literature considers the addition of CCS in fuel production, albeit without much information on the environmental impact and the required policy framework necessary for the biofuel routes to be competitive with fossil fuels. Tagomori et al. [150] performed a techno-economic assessment of FT-diesel production from eucalyptus and pine residues with the CCS case increasing production costs by 1%. Song et al. [151] carried out an assessment on four different agriculture residues to produce methane and the addition of CCS increased the production cost in the range of 3% - 4%. Michailos et al. [152] investigated the feasibility of coupling CCS with syngas biomethanation and concluded that the addition of CCS increases the production costs by approximately 17%. Del Álamo et al. [153] studied the techno-economic feasibility of adding CCS to FTS and bioSNG and estimated that production costs increase by 10% and 14%, respectively. Table 2.1 summarises

the results of some of the techno-economic assessments on the three production routes available in the literature.

Table 2.1: Summary of literature review on biofuels (*indicates prices with CCS).

Cost Year	Feedstock	Input	Technology	Biofuel	Production cost	Reference
2015	Eucalyptus residue	179.6 t/h	Entrained Gasification + FTS	FT-fuel	£26.12/GJ *£26.47/GJ	[150]
	Pine residue	177.4 t/h			£25.09/GJ *£25.38/GJ	
2014	Wood chips	2016 dt/d	Entrained Gasification + FTS	FT-fuel	£14.88/GJ	[154]
			CFB gasification + FTS		£14.42/GJ	
2007	Corn	2000 dt/d	Entrained Gasification + FTS	FT-fuel	£2.13/gal	[155]
2014	Woody biomass	20 MW (fuel output)	DFB gasification + Methanation	BioSNG	£115/MWh	[156]
2017	Virgin biomass	6.25 dt/h	DFB gasification + syngas fermentation	BioSNG	£73.81/MWh *£86.09/MWh	[152]
2011	Rice straw	600 t/d	DFB gasification + Methanation	BioSNG	£0.204/m^3 *£0.210/m^3	[151]
	Wheat straw				£0.167/m^3 *£0.173/m^3	
	Corn stalk				£0.157/m^3 *£0.163/m^3	
	Cotton				£0.149/m^3 *£0.1540/m^3	
2010	Imported woody biomass	500 MW	DFG gasification + Methanation	BioSNG	£10.47/GJ *£11.40/GJ	[157]
2016	Whole tree woodchips	500 t/d	DFB gasification + OMEx synthesis	OME_{1-8}	£1.42/L	[135]
	Forest residue				£1.24/L	
	Wheat straw				£1.22/L	
2013	Methanol at $300/t	1 Mio. t/y (fuel output)	OMEx synthesis	OME_{3-5}	£393.2/t	[134]

2.5.3 Power-to-X

Previous research on electrofuels has focused on the production of DME, methanol and FT-fuels [158] with current studies reviewing the information available. Adnan and Kibria [159] evaluated three Power-to-Methanol routes identifying technical and economic drivers to be improved upon and enable these routes compete with the conventional methanol from natural gas route. The three routes were - one step synthesis where CO_2 is converted directly to methanol in a CO_2 electrolyser; two step synthesis where hydrogen is produced from electrolysis then reacted with CO_2 in a methanol reactor; and three step synthesis where hydrogen in produced from water electrolysis, CO is produced from CO_2 electrolysis, then both H_2 and CO are combined in a methanol reactor. The levelised cost of methanol via these routes at $860 - $1585 per ton of methanol was 2 - 4 times higher than the current market price. Also, a cradle-to-gate lifecycle assessment indicated than an emission factor of less than 0.13 $kgCO_2$/kWh for the routes is required to offer climate benefits over the conventional route while using electricity from wind and nuclear power would result in negative emissions with a potential of 170,000 - 195,000 ton of CO_2 per year. This comparative analysis is the only work that considers the environmental impact alongside the techno-economics producing methanol using electricity.

König et al. [158] completed a techno-economic study on storing fluctuating renewable energy in FT-fuels. A Power-to-Liquid plant was modelled in Aspen Plus for this study. Electricity was supplied by a wind farm and a H_2 feed of 30 t/h resulted in 56.3 t/h of FT-fuels with a Power-to-Liquid efficiency of 44.6%. The net fuel production cost was in the range of $12.41 - $21.35 per GGE of FT-fuel for a wind power plant with a full load fraction of 47%. From the sensitivity analysis, full load fractions between 70% and 90% caused the net production cost to drop to a range of $5.48 - $8.03 per GGE of FT-fuels. Gorre et al. [160] published a study on the production costs of power-to-methane for 2030 and 2050. This study stated that the production cost of methane was particularly dependent on the electricity price and full load hours of the electricity supply. With optimised system configurations and expected developments, SNG production from power could be viable by 2030 and with electricity costs of 20 - 30 €/MWh. The authors concluded that Power-to-Gas as an option for long-term and large-scale seasonal storage of renewable energy is suitable.

Brynolf et al. [161] reviewed the production costs of electrofuels (methane, methanol, DME, diesel and gasoline) in the transport sector. This study focused on the reviewing the steps with the greatest uncertainty and largest impacts and compared productions costs of

different fuels in a coherent way. This work provided an update on the production costs in the range of 200 – 280 $€_{2015}$/MWh_{fuel} and 2030 projected production cost in the range of 160 – 210 $€_{2030}$/MWh_{fuel}. Also, Dieterich et al. [162] reviewed power-to-liquid production routes of methanol, DME and FT-fuels. This review provided an overview of the technologies and current developments for the three production routes. The authors noted that more advances have been made on the methanol and FT-fuels end with operating commercial plants and plans for industrial sized plants while there was not much interest in power-to-DME with this production route being in an earlier development stage. A conceptual design and techno-economic assessment [163] on power-to-DME estimated a minimum selling price €75.62/GJ. In most of these papers on the assessment of the techno-economics of electrofuel production, the environmental impact of each choice is not assessed, thereby not quantifying the mitigation potential of each route. However, a few lifecycle assessments have been carried out separately on Power-to-X production routes [164,165] in order to examine the environmental impact of electrofuels.

2.6 Summary

This chapter has presented an outline of the literature associated with the research topic of this thesis. This outline helps in understanding the background of the processes considered in Chapters 4, 5 and 6; it covers bioenergy, bioenergy with carbon capture and storage, CO_2 utilisation, gasification, fuel synthesis and techno-economic assessments.

A review of the literature has mainly identified the lack of comprehensive information on the application of BECCS technologies in energy generation and this thesis aims to fill this gap. This thesis seeks to substantially contribute to the existing literature on the application of BECCS in energy generation and provide very useful information for further research & development as well as influence policy makers concerning decarbonising an economy.

Applying the concept of BECCS to existing power generation and fuel generation technologies covers a wide range. Hence there is no one solution or template for all. Each route needs to be investigated with great care in order to realise the great opportunities and weaknesses in the production process. Also, BECCS has been identified as a negative emission tool, hence it is essential that the cradle-to-grave lifecycle of the production routes associated with BECCS indeed have the potential to remove CO_2 from the atmosphere. The next chapter presents the techniques and approach that are used in obtaining data and information to complete this research.

3 Methodology

This research is performed using process modelling, simulations, economic modelling and using data that is available in the open literature. Various flowsheet models are developed and simulated. The main techniques applied are sensitivity studies, energy analyses, economic assessments and environmental assessments to provide detailed information for this research. This chapter explains the methods and tools used to complete this research.

3.1 Process Modelling

Modelling a process is advantageous because it relays the effects of changing parameters on a process. A process model is a set of equations that involves the properties of the system being influenced by the process. In addition, process modelling involves associating these properties with each other using the appropriate governing equations under one or more assumptions. In process simulations, the process models created can be solved to find the values of the unknown system properties in the imitation of a real-world process [166]. These solutions provide much important information on the behaviour of real-world processes. From the modelling and simulations, the performance of the process can be predicted and this leads to process optimisation and ultimately resulting in the development of a very good, efficient and working plant.

Process modelling and simulation is useful for the prediction, estimation and optimisation by creating alternative process configurations, performing mass and energy balances and sizing and costing equipment.

As with any other computational work, the accuracy is dependent on the inputs into a model as 'garbage in = garbage out' [167], hence inconsistencies are due to oversimplifications, incorrect physical properties and inadequate data and information input into the model.

3.2 Modelling Tools

There are various process modelling and simulation tools available, including ASPEN (Advanced System for Process Engineering) developed by MIT, gPROMS, ChemCAD, UniSim and PRO/II. Ideally, process modelling and simulation tools should realistically perform operations to yield accurate results. The tools should be customisable for different modes of operation, user-friendly and consume little time and space during the computation.

3.2.1 ASPEN

ASPEN is a next-generation process simulator that is used across many industries today. It is capable of simulating large complex processes and even those involving non-ideal components. ASPEN can be used to design, operate and maintain complex manufacturing environments due to its reliability and accuracy. The ASPEN products cover three main areas – process engineering, manufacturing and supply chain and asset performance management [168]. In this thesis, the focus is on the process engineering products which are generally referred to as the Aspen suite henceforth. The Aspen suite is a software package that can perform both steady state and dynamic mode operations. It has the option of using either the sequential modular (SM) technique or equation-oriented (EO) technique in solving the simulations. Also, in the Aspen suite, there are integrated tools for better process analysis and design; these tools include energy management, costing, equipment design and safety analysis. The Aspen suite helps to create timesaving workflows as the basic unit operation models for chemicals, electrolytes, polymers and solids have been predefined with a range of proven physical properties from which one can choose from. The unit operation models can be combined to build a process flow diagram, the models can also be customised to meet the needs of the user and demands of the process in Excel and Fortran (this is the programming language the software is written in), thus making this package diverse and suitable for this research.

3.2.1.1 Why the Aspen suite?

There are a variety of process modelling and simulation tools as described earlier. Each tool offers advantages depending on the desired outcome or scope of the work to be completed. The Aspen suite has been selected for this research due to the wide range of tools it offers which are relevant to this work. It can be used in both steady state and dynamic modelling offering more options to the user and it also allows the option of either the sequential modular modelling or the equation-oriented modelling unlike gPROMS. While gPROMS can also be used in both steady state and dynamic modelling, it only uses the equation-oriented solving technique [169]. Overall, when the Aspen suite is compared to other modelling and simulation tools, it offers more benefits due to its integrated platform for energy analyses, equipment costing and equipment design which saves time when performing simulation as is required for this work. There is no need to export worksheets to other platforms and it is very user-friendly. Also, the Aspen Tech technical support provided is very helpful, including the examples and manuals included in the programme to get one started on modelling

different processes across the chemical engineering sector. Finally, another important element of the Aspen suite is that it can handle solids modelling, which is an important requirement for this research dealing with biomass.

Aspen Plus, the chemical industry's leading process simulation software, is a part of the Aspen suite and in Aspen Plus, simulations are commonly carried out using the SM technique. When compared to Aspen HYSYS (another process simulation software in the Aspen suite), both software packages are very similar with and should be chosen based on the application. Aspen HYSYS is optimised mainly for the petrochemical industry. Also, while Aspen HYSYS is more suitable for acid gas cleaning problems, due to the already defined gas cleaning packages, Aspen Plus is more suited to handle solids and non-ideal components, such as biomass. All of the work performed in this thesis is modelled in Aspen with the exception of the techno-economic assessment of biomass power generation with CCS which is completed with IECM which is discussed in the next section.

3.2.2 Integrated Environmental Control Model

The Integrated Environmental Control Model (IECM) software was developed by Carnegie Mellon University as a part of the US Department of Energy project in the mid-1980's and since then it has expanded into an important simulation model [170]. The IECM was developed as tool for calculating the performance, costs and emissions of a fossil-fuel power plant [171] hence, providing the preliminary economic, technical and environmental results of a power plant. It offers different power plant configurations with a range of gas cleaning equipment widely used.

The IECM is highly appropriate for the work on techno-economic assessment power generation because it was built to perform cost and performance analyses of combustion plants that can be coupled with a range of CO_2 capture technologies as is the scope of this thesis. The reliability of the IECM has been demonstrated in previous techno-economic studies on power plants [140,141,172–175]. In this thesis, the IECM version 11.2 is used and most of the default assumptions in the IECM were retained. As it is beyond the scope of this work to validate the IECM model, documentation on the methodology and framework of the IECM can be found on the IECM website [176].

3.3 Model and Simulation Development

There are certain steps to be taken to ensure that process simulation yields reliable results. A summary of the model and simulation development is depicted in Figure 3.1.

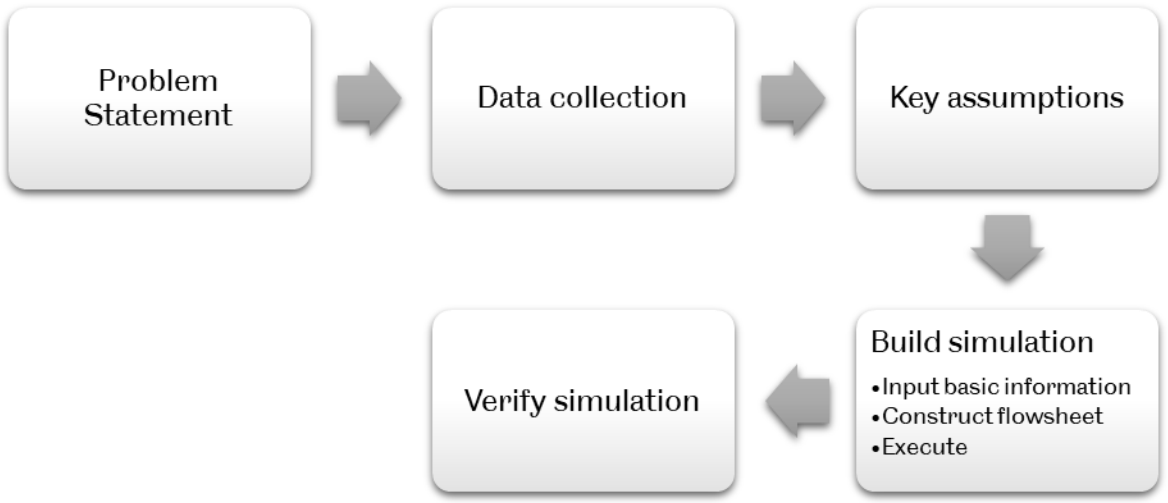

Figure 3.1: Flowchart of the modelling and simulation development

The first step is the problem statement. The problem definition sets the objectives and assists in conceptualising the model. The second step is collecting the data and deciding the key assumptions. This step should be detailed to ensure that the input to the model is reliable. This involves considering the thermodynamics and kinetics, listing the sub processes and providing the operating conditions. A degree of freedom (DoF) analysis is performed to determine the unknown variables and the governing independent equations. The DoF is essential because this analysis aids in the making of reasonable assumptions. Valid assumptions are required to reduce the number of sub processes and make the simulation possible. Nonetheless, the fewer assumptions made, the more detailed is the simulation. The next step involves building the simulation following three critical steps – inputting the basic information (selecting chemical components and property package), constructing the flowsheet and executing the simulation [177].

Aspen Plus has a user guide to assist the selection of the property package and this is dependent on the type of process being built. The property package is a group of techniques and models to compute the thermodynamic and transport properties in a process. Each

package leads to different material and energy balances when modelling some processes [178]. The flowsheet is constructed by selecting unit model operations and connecting the material and energy streams. In the execution stage, design specifications are added and the simulation is run until it has converged. After running the simulation, the simulation model needs to be verified and this is mostly achieved by comparing the numerical predictions to the experimental data [179]. Experiments are important to simulations because this assists to validate and calibrate the model. However, process models are for estimation, prediction, calibration and optimisation [180], hence the fewer assumptions employed results in a better model for estimation purposes. Rigorous and complex models have many sub processes and only a few assumptions [181].

3.4 Thermodynamics and Thermodynamic Modelling

The gasification process, as explained in sub-section 2.4.1, takes place at temperatures in the range 800 ºC – 1800 ºC [76]. The temperature of the process can be presented as a temperature profile across the reactor as there are different temperatures within the reactor. This temperature profile varies from reactor to reactor as it is dependent on several factors, including gasifier type and feedstock characteristics.

The conversion of biomass to syngas is controlled by the reaction kinetics and the thermodynamic equilibrium of the reactions involved. Some of the reactions involved in the process are reversible and depend on the reaction rate, temperature, pressure and concentration of the reactants and products, the reactions could proceed both ways to achieve equilibrium according to Le Chatelier's principle. From the basics of thermodynamics and kinetics, the rate constant and equilibrium constant are temperature dependent. Understanding the limits of each principle on a reaction can aid in accurately predicting the product composition.

The gasification process is a combination of the exothermic and endothermic processes and hence the operating temperature is critical to the process as it influences the final gas composition. Taking the Boudouard reaction in Eqn. (2.7) as an example, under standard conditions the forward reaction is an endothermic reaction and the equilibrium constant is 1 at a temperature of about 700 °C. According to Le Chatelier's principle, increasing the temperature above this value would shift the equilibrium to the right and hence more CO is produced. For the water gas shift reaction in Eqn. (2.13), under standard conditions and up to approximately 827 °C [182], the production of CO_2 and H_2 would be favoured and above

this temperature then the equilibrium shifts to the left-hand side of the reaction. Due to the complex reaction thermodynamics and its limitations on the system, it is essential to model the system for optimal plant design.

The thermodynamic equilibrium model builds a process based on the equilibrium state. When a system attains equilibrium, the composition of the outlet stream is at its most stable state and maximum conversion has occurred. The equilibrium model is independent of the gasifier design and time. General assumptions that have been employed when building such models include:

- Zero-dimensional reactor,
- No heat losses,
- Perfect mixing and hence a uniform temperature throughout the reactor,
- Fast reaction rates and long residence times to reach equilibrium,
- Reaction pathways and intermediates formed are neglected,
- Tar formation is ignored.

There are two general methods for the equilibrium model which are the stoichiometric and non-stoichiometric methods. In the stoichiometric method, a reaction mechanism involving all the chemical reactions and species needs to be defined [101]. Using the equilibrium equations for the chemical reactions to derive the equilibrium constants, the composition of the product gas can be calculated at equilibrium. The non-stoichiometric method only requires the elemental composition of the fuel to be specified (that is basically information from the ultimate analysis). This method is based on minimising the Gibbs free energy (the Gibbs free energy of the system approaches a minimum as the system approaches equilibrium). Both models are essentially equivalent (where the reaction mechanism is complete and the reaction rate coefficients are correct) as explained by Jarugthammachote and Dutta [183] and the models can predict the influence of the operating parameters on the process, such as the effect of the pressure and temperature.

Li et al. [184] and Jand et al. [185] used the equilibrium model to simulate biomass gasification and concluded that the equilibrium model was not suitable to accurately predict the situation in an actual gasifier. The deviations from a real model were attributed to the presence of non-equilibrium factors. Thermodynamic equilibrium in the gasification process may not be achieved due to the relatively low temperature range of the syngas outlet which is in the range 750 °C to 1000 °C [186]. Jand et al. [185] explained that the failure of the

equilibrium model to accurately predict the results is due to its failure to account for the two-stage nature of the gasification process. The overall thermochemical conversion of the biomass consists of the fast devolatilization of the biomass particles and then the conversion of methane and char which is much slower. The second stage, which is the slower conversion, is non-equilibrium and this results in deviations found when using the equilibrium models. Jand et al. [185] suggested improving the application of the equilibrium model by accounting for the non-equilibrium factors. This leads to an improved model and this is referred to as the pseudo-equilibrium model.

The pseudo-equilibrium model supports the equilibrium model with empirical relations or correction parameters. Gómez-Barea et al. [187] proposed a pseudo-equilibrium model to predict the gas composition from biomass gasifiers. This model estimates the conversion of tars, char and methane based on simple kinetic models and this is incorporated into the equilibrium model to reduce the deviations, but the application of this model is limited to high process temperatures and/or the presence of a catalyst in the bed otherwise equilibrium of the WGSR is not achieved. Jand et al. [185] used temperature dependent correction parameters in the elemental balance equations to account for carbon conversion, methane from devolatilization and methane conversion by steam reforming.

Another approach that is employed to improve the equilibrium models is the quasi-temperature approach. This approach was introduced by Gumz [188] and it involves evaluating the equilibrium of the reactions at lower temperatures than those that occur in the actual process.

The equilibrium model is not a sufficient tool to design a biomass gasification process; however, it is useful for first estimates and determining the thermodynamic limits of the system [101,189]. Also, the improved models, although being more accurate than the original equilibrium models, their predictive capability is reduced due to the dependence on the empirical parameters available from the experiments. Consequently, the pseudo-equilibrium models cannot be applied to all systems. Although the methane composition in the syngas can be predicted, the difficulty of predicting the tar and the chars content remains. In conclusion, there is a need for more advanced models that can handle tars and char while being flexible to accommodate all systems.

3.5 Kinetics and Kinetic Modelling

The kinetics of a process determines how fast the reactions occur in a reactor and the dimensions of the reactor to ensure a completion of reaction [106]. Kinetic models of biomass gasification attempt to explain the mechanism of the conversion process from biomass to the syngas and it relies on rate expressions derived from experiments. A schematic of the reaction sequence of biomass gasification is represented in Figure 3.2.

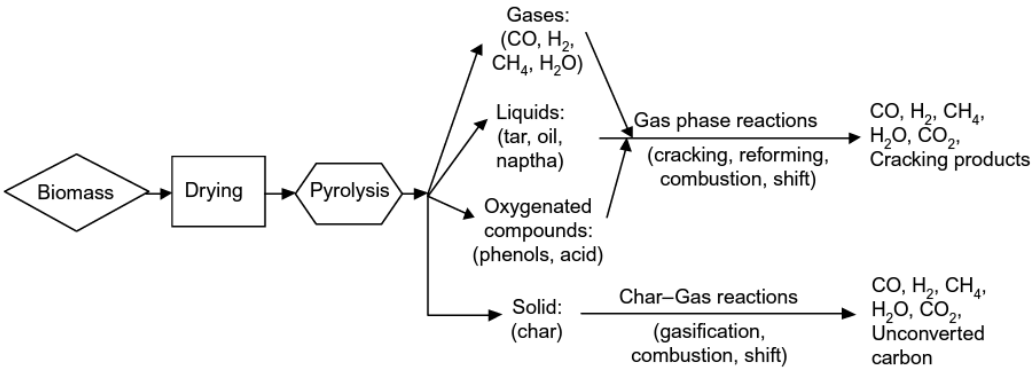

Figure 3.2: Schematic of the reaction sequence of biomass gasification [106].

The reaction rate constants, k, of all the reactions in pyrolysis are independent of the concentration of the reactions but they are dependent on the temperature and are expressed by the Arrhenius form as follows:

$$k = A_0 \exp\left(\frac{-E_a}{RT}\right) \tag{3.1}$$

where 'A_0' is the preexponential factor (s^{-1}), 'R' is the universal gas constant (0.008314 kJ/mol.K) and 'E_a' is the activation energy (kJ/mol) of the reaction [106].

Pyrolysis takes place at low temperatures between 350 °C and 800 °C for coal and 300 °C and 600 °C for biomass. The rate of devolatilization (pyrolysis) influences the subsequent steps in the gasification process; it is dependent on the heating rate, particle size, gasification rate, water-gas reaction, temperature of reaction and the partial pressure of steam [76]. The heating rate influences how the devolatilization occurs but at high temperatures, devolatilization of small particles is independent of the heating rate [190]. Slow heating translates to pyrolysis and gasification occurring consecutively, thus ensuring a high concentration of volatiles while fast heating translates to pyrolysis and gasification ensuing

simultaneously and hence a high concentration of volatiles is not sustained. The smaller the particle, the shorter the residence time and therefore finely reduced feedstock used in the entrained flow gasifiers have very short residence times. The product distribution from devolatilization varies with temperature changes and the speed of heating up. Bingyan et al. [191] showed that with increasing temperature, gas productivity from pyrolysis increased until a temperature of 800 °C was reached while char productivity decreased; also, tar productivity reached its peak value at a temperature of 500 °C. This same report showed that the time to complete pyrolysis decreased linearly with increasing temperature and the overall products from this are CO, CO_2, CH_4, H_2O, H_2, char and tar.

Hejazi et al. [192] described the pyrolysis as a two-step process and this is illustrated in Figure 3.3. The first step is the primary pyrolysis to gas, tar and char and the second step is the tar cracking.

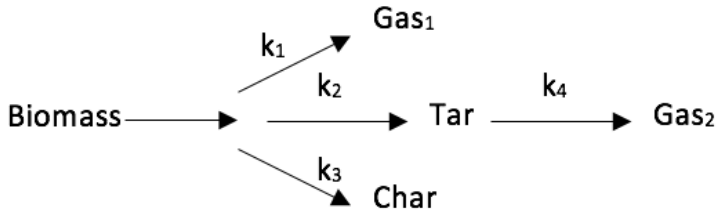

Figure 3.3: Schematic of the two-step pyrolysis process [192].

The kinetic parameters, as determined by thermogravimetric analysis (TGA) for the reaction, differ based on the type of biomass used. The kinetic parameters for components in the gas, tar and char phases can be found in Wurzenberger et al. [193] for primary pyrolysis and Boroson et al. [194] for secondary pyrolysis.

In the next step, which is the volatiles combustion, the products from the pyrolysis step react with the surrounding oxidant. The extent to which the oxidant is used up is dependent on the amount of volatiles produced from pyrolysis. The high volatile content ensures gasification rather than combustion in the given environment.

The last and most important step considered in the kinetic studies is char gasification. The heterogeneous reactions with carbon are the slowest gasification reactions, thus these govern the overall conversion rate.

The dominant reaction depends on the type of oxidant used [106]. In steam gasification, the water-gas reaction is the dominant reaction while in an air or oxygen gasifier, the dominant reaction is the Boudouard reaction.

The reactivity of char is affected by the pyrolysis conditions. Char produced at temperatures above 1000 °C is less reactive than that produced at 700 °C and this is due to the number of active sites being reduced by the high temperatures [106] and the reactivity is also reduced when the residence time at peak pyrolysis temperature is longer. The presence of inorganic materials in biomass can also affect the char reactivity. Basu [106] mentions that potassium and sodium increase the char yield by catalysing volatile matter polymerisation but at the same time solid materials are produced which are deposited on the char pores and thereby reducing the number of active sites. Dupont et al. [195] discuss the catalytic effect of potassium on the gasification of chars as well the inhibitor effect of silicon.

Generally, for gasification to occur, the oxidant needs to be transferred to the surface and the pores of the char which are the reaction sites. This could be kinetically controlled or diffusion controlled depending on the temperature. Below 900 °C (low temperatures), the rate-controlling factor is the chemical kinetics as at these temperatures it is the slowest when compared to pore diffusion and mass transfer. Above 900 °C (medium temperatures), the reaction rate is limited by pore diffusion and at high temperatures it is limited by the bulk surface diffusion and above 900 °C, char conversion is represented by the shrinking core model [76,196].

Kinetic modelling of biomass gasification has been investigated over recent years but due to its complexity, there is no simple kinetic model, such as the thermodynamic equilibrium model. Unlike the equilibrium model, the kinetic model is dependent on the gasifier design and explores the intricate system of kinetic reactions. It considers the hydrodynamics, mass and heat balances to estimate the composition of the syngas more accurately even with varying operating conditions and temperature profiles along the reactor. There are several models that describe the kinetics of the gasification reactions in reactors and the assumptions made in the kinetic models are similar.

Kaushal et al. [190], Wang and Kinoshita [196] and Radmanesh et al. [197] developed different kinetic models for biomass gasification. The assumptions common in these models are as follows:

- one-dimensional, isothermal reactor,
- existence of two phases – bubble and emulsion – that transfer mass between each other,
- constant voidage in the emulsion phase,
- instant devolatilization of the biomass particles.

These models have been used to evaluate the gasifier performance and summarise the effect of different operating conditions on the gasification process [196]. The temperature is a major operating parameter because it influences the equilibrium constants, the reaction rate constants and the residence time. Using a higher pressure results in higher reaction rates and longer residence times while lowering the yields of H_2 and CO but increasing the yields of carbon and methane due to the equilibrium shift. Increasing the equivalence ratio means increasing the oxygen available to the reactants; the CO_2 content increases while the C, H_2 and CO contents decrease. For the particle size, decreasing the particle size is equivalent to an increased char surface area and hence increased surface reaction rate and a shorter residence time.

3.6 Gasification in Aspen Plus

Aspen Plus, a tool for process simulations, has been applied by researchers to model the biomass gasification process [179–181,198]. This tool can be used to perform mass and energy balances, economic and environmental evaluations on process designs for process control and optimisation.

In Aspen Plus, the gasification process can either be equilibrium modelled or kinetic modelled. The complexity of the reaction prevents the simulation of the gasification process as a single unit operation model in Aspen Plus. The process is simulated using various reactor models. The most common models applied are the RGibbs, RYield and RStoic reactor models. The RGibbs model is a reactor that models single-phase or multi-phase and chemical equilibria. It determines the product composition by minimising the Gibbs free energy after parameters, such as temperature and pressure or pressure and enthalpy, have been specified [199]. When a heat stream is linked to the block, only the pressure needs to be specified; the reaction kinetics and stoichiometry are not required. The RYield models a reactor where the yield of each component or correlations are available; reaction kinetics and stoichiometry are also not required when using this model. The RStoic models a reactor where the reaction stoichiometry is known [200]. This model requires the extent of

conversion to be specified. Other reactor models are the RPlug and the RCSTR commonly used in detailed kinetic modelling. Both reactors model rate-based reactions, hence the reaction kinetics of any process are required when using these models. The RCSTR models a continuous-stirred tank reactor denoting that the reactor outlet has the same properties as the contents of the reactor. In addition, it models the equilibrium reactions simultaneously and either the heat duty or the temperature is required to compute the other. The RPlug models a plug flow reactor with the option of a cooling stream which could be co-current or counter current [201]. Generally, the RStoic simulates biomass drying, the RYield simulates pyrolysis, the RGibbs simulates the oxidation and gasification reactions, the RCSTR and the RPlug simulate gasification reactions.

The non-stoichiometric thermodynamic equilibrium model by minimizing the Gibbs free energy is the concept of the RGibbs model. The Gibbs free energy is the energy associated with a thermodynamic system that can be used to do work at constant temperature and pressure. At a single point, the Gibbs energy (G) of a system is represented by the equation:

$$G = H - TS \tag{3.2}$$

where 'H' is the enthalpy, 'T' is the temperature and 'S' is the entropy of the system. During a process at constant temperature energy changes:

$$\Delta G = \Delta H - T\Delta S \tag{3.3}$$

A spontaneous reaction favours the formation of products under given conditions while a non-spontaneous reaction does not favour the formation of products. The value of 'ΔG' indicates the spontaneity of a reaction. The 'ΔG' of a system less than 0 indicates a spontaneous reaction while the 'ΔG' of system greater than 0 indicates a non-spontaneous reaction. When 'ΔG' is 0, the system is in equilibrium and the Gibbs free energy is minimised.

Some researchers [202–204], have developed models to handle gasification of different biomass sources - rice husk, tyre, food waste, municipal solid waste (MSW) and poultry waste. These models have employed an overall equilibrium approach while neglecting the hydrodynamic conditions. Either two-unit operation models or three-unit operation models were used to simulate the process. In the two-unit model, drying and pyrolysis were coupled in the RYield and gasification-combustion were simulated in the RGibbs. The models did not consider tar and char yields; methane was the only hydrocarbon present; reaction kinetics

were excluded; and the products of pyrolysis were calculated based on a mass basis where the amount of volatiles released was equal to the amount of volatiles as specified by the proximate analysis. Consequently, these models deviated significantly from the actual process, thus resulting in an underestimated methane content and overestimated hydrogen content in the syngas.

The RGibbs reactor in Aspen Plus has the option to restrict equilibrium by specifying the temperature approach of individual reactions or the entire system, specifying a percentage of a feed component that is inert, fixing the extents of reaction or by fixing the moles of any of the products. The products of a reaction are calculated at a different temperature than the set temperature of the reactor, the temperature approach is the difference between these temperatures.

Doherty et al. [181] and Gagliano et al. [202] developed gasification models based on the restricted equilibrium approach. While Gagliano et al. [202] modelled the gasifier using three unit operation models, Doherty et al. [181] used one unit operation model. The hydrogasification, steam methane reforming and the water-gas shift were the reactions limited to at most 290 °C below the reactor temperature. Modelling gasification as one unit, as opposed to decoupling into stages, is more realistic because in a single gasifier, all the reactions are not necessarily stepwise and occur in one unit hence the reactions could be simultaneous and independent of each other. The idea of specifying the temperature approach is plausible when the temperature in the reactor varies along its height as in a fixed bed gasifier. However, in a fluidised bed reactor, the temperature is uniform, thus defeating the effect of freezing the thermodynamic equilibrium of specific reactions at a temperature different from that of the reactor. Also, specifying the temperature approach for only three reactions out of the ten reactions mentioned in the article is not sufficient as the components of the syngas possess the same enthalpy.

These models can predict the influence of the operating parameters on the gasifying process over a wide range of working conditions but lack the ability to provide highly accurate results due to the limitations in the thermodynamics in the gasifier, hence rendering the models only suitable for preliminary studies. For accurate results, better models that consider the kinetics of the gasification reactions and include the gasifier design should be implemented.

Several authors [180,198,203,204], have developed semi-empirical models to improve the prediction capability in Aspen Plus. These models go several steps further from the overall

equilibrium approach by introducing char gasification and tar cracking reaction kinetics that are written in an external Fortran code; these codes are coupled to the RCSTR or RPlug reactors. While the RGibbs reactor is used in these models, it is only used to simulate volatile combustion. Temperature dependent pyrolysis correlations are also written in Fortran and coupled to the RYield reactor for sensible distributions of the pyrolysis products. Char consideration is another addition to improve the models; although char consists of carbon, hydrogen and oxygen, most models assume char to be purely carbon and ash. Also, hydrodynamic parameters are involved in these models to simulate the gasifier design.

These semi-empirical models reduce the deviation from real results and provide more information as to how a gasifier operates. Major issues with these models are the lack of representation of the tar species formed in the gasifier. In Pauls et al. [204], only four tar compounds were accounted for in the model while in Abdelouahed et al. [203] ten tar species were listed but these were lumped into four species – benzene, toluene, phenol and naphthalene due to lack of kinetic data.

3.7 Modelling Approach

In the process modelling of biomass gasification, moving from equilibrium modelling to kinetic modelling increases the complexity of an already complex system and limits the usage for each model. Hence there is no standard kinetic model that can be applied to all plants; each model must be customised to suit each plant. For assessments which are preliminary studies, as concluded from the literature, applying the equilibrium-based model is a good way to approach modelling plants.

3.7.1 Dual fluidised gasifier model

In this sub-section, an indirect gasifier in the form of a dual fluidised bed gasifier is modelled and validated. A schematic of this gasifier is seen in Figure 3.4. The dual fluidised bed (DFB) gasifier has been used in several projects pertaining to biofuel production from biomass gasification (Goteborg, Gussing, Varnamo, MILENA etc).

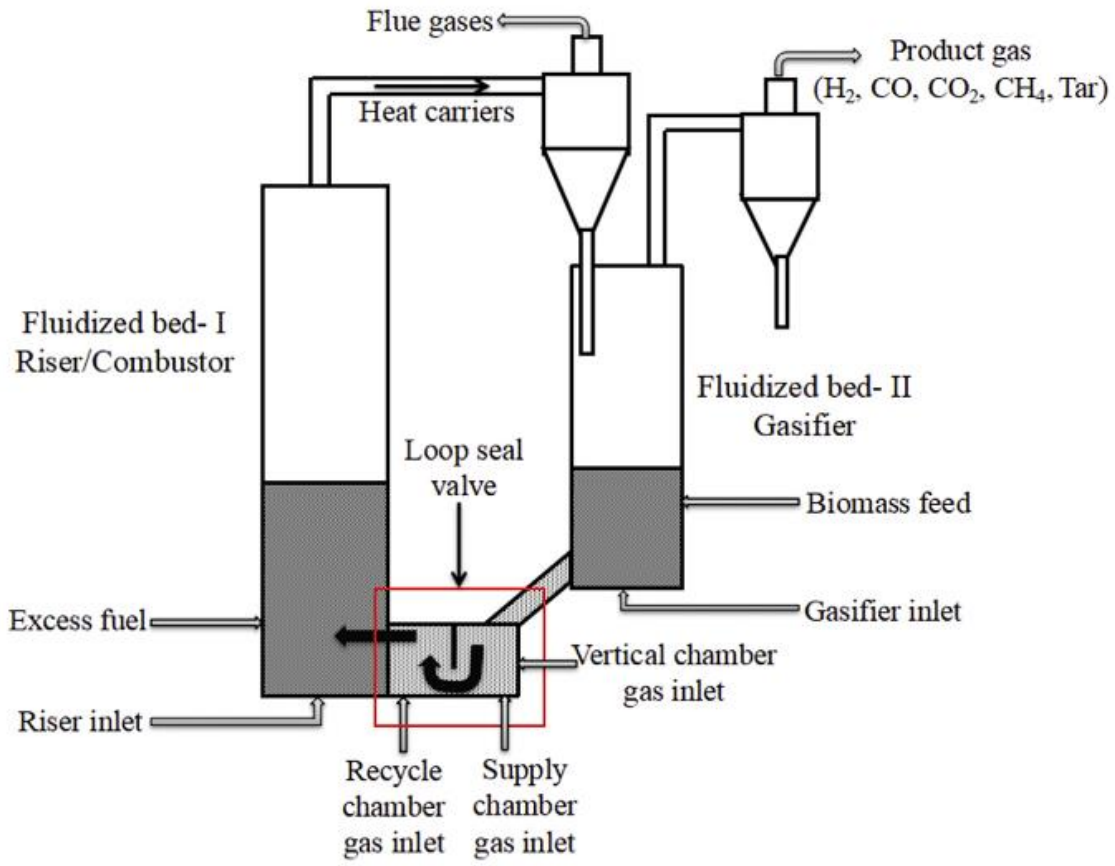

Figure 3.4: Schematic of the dual fluidised bed gasifier [205].

The DFB gasifier in this study is based on the Göteborg biomass gasification project (GoBiGas) plant in Sweden that produced bioSNG from woody biomass gasification [206]. The DFB gasifier is a gasifier where gasification occurs in one fluidised bed and the heat for gasification is generated in the other fluidised bed. In this gasifier, since air is introduced in a different zone, the syngas is practically nitrogen free. While thermodynamic modelling is suitable for first estimates and determining the limits of the system, it underestimates the hydrocarbons (C_1, C_2, tars) production and overestimates hydrogen production from gasification [179,185,207]. Kinetic modelling, which is more suitable for gasifier design, helps to reduce the inaccuracies but this is more complex and cannot be easily applied [190,196,197]. In this model, to reduce the inaccuracies from thermodynamic modelling, non-ideal corrections are applied to account for the formation of hydrocarbons especially methane and tar. This is based on similar equilibrium modelling techniques in [208–210]. An RStoic block is introduced in the model where the fractional carbon conversions of each reaction is set to match the experimental data in Alamia et al. [211] and simulate hydrocarbons formation to account for the non-equilibrium nature of gasification. This step is important in accounting for the formation of hydrocarbons especially methane and tar

[208–210] hence sensibly predicting the syngas composition. To reduce the number of sub processes and simplify the model, the following assumptions were made.

- Zero-dimensional reactor,
- Steady state process with no heat losses,
- N, Cl and S are converted to NH_3, HCl and H_2S respectively,
- Char contains only carbon and ash,
- Instantaneous devolatilization of biomass,
- Tar is $C_{10}H_8$ and other hydrocarbons formed are C_2H_2, C_2H_4, C_2H_6, C_6H_6 and C_7H_8.

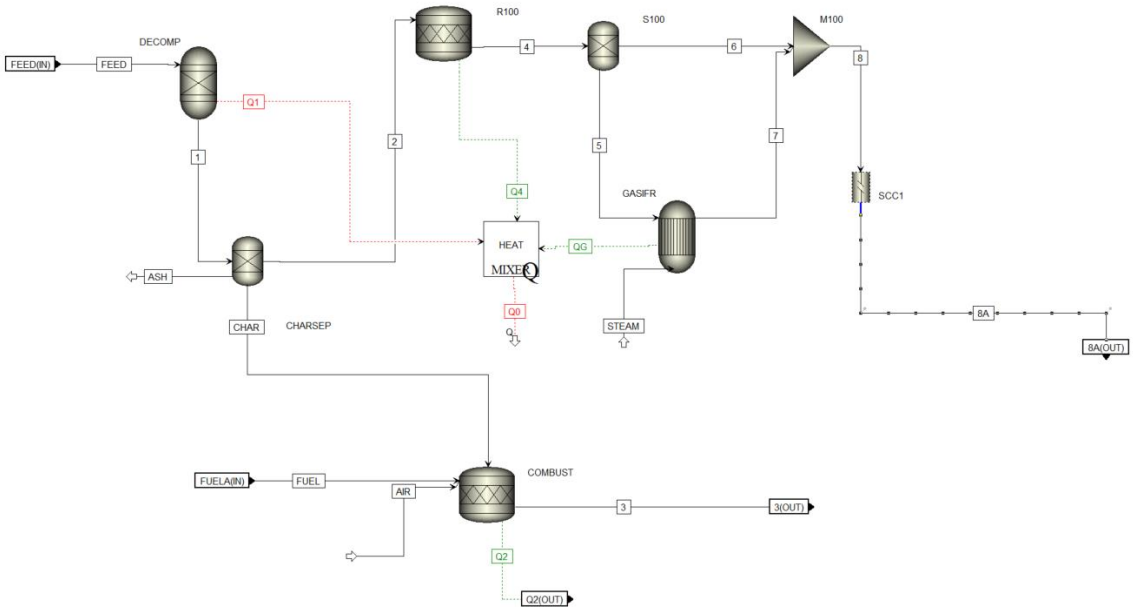

Figure 3.5: Aspen Plus flowsheet of the dual fluidised bed gasifier model.

The Aspen Plus model of the DFB gasifier is presented in Figure 3.5. In the DECOMP block (an RYield reactor), biomass is decomposed to its constituent elements based on the ultimate analysis of biomass. In the CHARSEP block, 15% of solid carbon is separated from the stream for combustion in the COMBUST block generate heat for the gasification reaction. In the actual gasifier, this heat is transported to the gasifier by some medium such as sand. Ash is also separated out in the CHARSEP block. The rest of the stream goes to R100, an RStoic reactor which accounts for the non-equilibrium nature of this type of gasification. In R100, a mix of tar and other hydrocarbons are formed. The hydrocarbons are separated from the stream before the GASFR block to prevent destruction in the subsequent reactor. The GASFR block is an RGibbs reactor with restricted equilibrium where steam as a gasifying agent is introduced and the gasification reactions are simulated. The stream from the GASFR

is mixed with hydrocarbons stream separated earlier on in the process for a final raw syngas stream. This gasifier model is validated against experimental data from Alamia et al. [211] and presented in Table 3.1.

Table 3.1: Model data validated against experimental data.

	Experimental	Model	% Difference
H_2 (vol% dry)	42.10	42.70	1.40
CO (vol% dry)	24.10	22.60	6.20
CO_2 (vol% dry)	23.50	20.20	14.00
CH_4 (vol% dry)	8.60	8.90	3.50
C_2H_2 (vol% dry)	0.13	0.13	0.00
C_2H_4 (vol% dry)	2.00	2.10	5.00
C_2H_6 (vol% dry)	1.90×10^{-1}	1.96×10^{-1}	3.20
C_3H_6 (vol% dry)	0.00	-	-
H_2O(vol%)	6.30	2.94	53.30
Tar (g/Nm^3)	7.00	6.88	1.70
BTX (g/Nm^3)	3.00	3.14	4.60

3.7.2 Entrained gasifier model

An Aspen plus flowsheet of the entrained gasifier model used in this study is depicted in Figure 3.6. The model was developed in Aspen Plus v10 and the Peng Robinson equation of state with Boston Mathias alpha function (PR-BM) was the thermodynamic package chosen to estimate phase equilibria and properties in gasification.

Table 3.2: Entrained gasifier model validation [212].

	Model	MIT model [212]	Experiment data [213]	% Difference
Ar (vol%)	0.007	0.008	-	-
CH_4 (vol%)	0	0.000	0.003	95.0
CO (vol%)	0.389	0.389	0.410	5.0
CO_2 (vol%)	0.105	0.105	0.102	3.0
COS (vol%)	0	0.000	-	-
H_2 (vol%)	0.295	0.294	0.298	1.0
H_2O (vol%)	0.186	0.186	0.171	9.0
H_2S (vol%)	0.007	0.007	0.011	36.0
N_2 (vol%)	0.009	0.009	0.008	12.5
NH_3 (vol%)	0	0.00	-	-
Temperature (°C)	1370	1370	-	-
Heat loss (%)	1	1	-	-
Equilibrium constant of WGS	0.426	0.426	0.427	0.23

The entrained gasifier model in this study is modelled according to the data in Field and Brasington [212] and Swanson et al. [155]. With the gasifier operating at 1300 °C, the gasifier is assumed to be operating at equilibrium [155,214] and is modelled as an RGibbs reactor using the equilibrium approach. However, a temperature approach of -10 °C (in quench mode) is applied to the water-gas shift reaction because there is a temperature difference between the equilibrium reaction temperature of the WGS reaction and the gasifier exit temperature [215]; also, the WGS equilibrium reaction temperature is dependent on the rate of cooling. The model had also been validated against experimental data [212] (see Table 3.2) making it suitable to be used in this study.

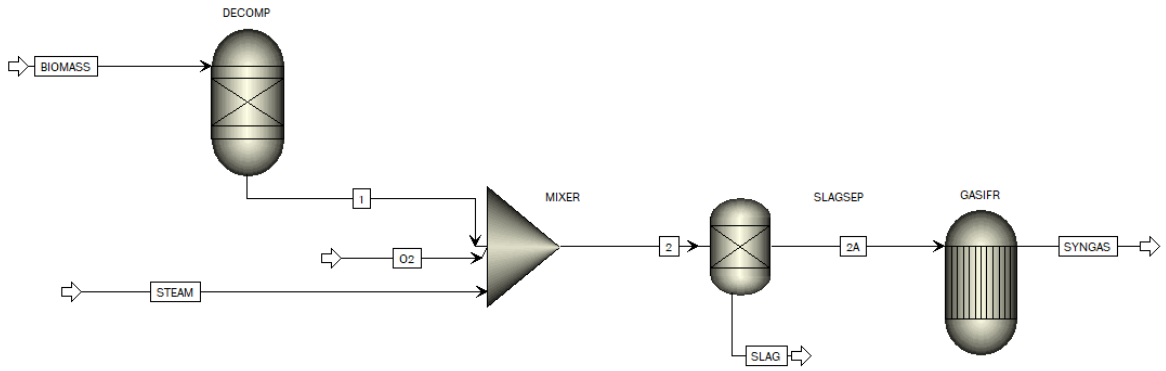

Figure 3.6: Aspen Plus flowsheet of the entrained gasifier model.

The DECOMP block is an RYield reactor where biomass is converted from a non-conventional component to conventional elements (C, H, O, N, S, Cl) based on the ultimate analysis of the biomass feed. Biomass is mixed with the gasifying agents – steam and oxygen – based on steam to oxygen ratio and oxygen to carbon ratio for the investigated case in a mixer and sent to a SEP block to remove the ash content. Finally, the elements are sent to an RGibbs block labelled GASIFR where the gasification reactions occur using the restricted equilibrium approach.

3.8 Assessment Approach

Following modelling and simulation of various production routes, some assessments are performed to interpret the data and present the information obtained. The methodology for the techno-economic assessments completed in this research is provided in this section. This methodology is based on guidelines available in literature to produce a harmonised way of presenting results.

3.8.1 Scope definition

Before proceeding with an assessment, the scope and the boundaries of project to be evaluated needs to be clearly defined [216,217]. This step involves determining the following:

- The feed, product, by-products and their units,
- Plant size and location,
- Plant lifetime,
- Plant year (to set the plant index and current cost values),
- Technology and operating conditions,
- Essential data, decisions and general assumptions,
- Utilities including cooling water, fired heat, steam, electricity, air and refrigerant,
- Fuel type and characteristics (wood, proximate and ultimate analysis),
- Storage,
- Waste management and
- Benchmark system, such as coal against biomass.

3.8.2 Performance indicators

The next step involves in the assessment involves defining the performance indicators. These indicators measure the technical and economic performance. From the literature, the key technical performance indicators include the energy efficiency, mass yield, carbon conversion and energy demand. The calculations for indicators are presented in Table 3.3.

Table 3.3: Calculation for key technical performance indicators.

Indicator	Calculation
Energy efficiency	$\eta = \frac{\text{Net energy output (MW)}}{\text{Net energy input (MW)}}$
Mass yield	$\eta_{mass} = \frac{\text{Product mass flow (kg/s)}}{\text{Feed mass flow (kg/s)}}$
Carbon conversion	$\eta_C = 1 - \frac{\text{Total rate of carbon in the outlet stream (mols/s)}}{\text{Total rate of carbon in the inlet stream(mol/s)}}$

As mentioned in sub-section 3.8.1, assumptions need to be listed in defining the scope. In the case of the economic assessment, these assumptions include the breakdown of financing, interest rates, plant construction duration and choice of constant or current currency value [216]. The economic performance indicators with some of the calculations presented in Table 3.4 include CAPEX, OPEX, levelised cost of energy, minimum selling price, cost of CO_2 avoided and cost of CO_2 captured.

Table 3.4: Calculation for key economic performance indicators.

Indicator	Calculation
Levelised cost of energy	$\text{LCOE (£/MWh)} = \frac{\text{Total levelised annual cost (£/yr)}}{\text{Total levelised energy output (MWh/yr)}}$
Cost of CO_2 avoided	$\text{Cost of } CO_2 \text{ avoided (£/t } CO_2) = \frac{(\text{LCOE})_{CCS} - (\text{LCOE})_{ref}}{(\text{t } CO_2/\text{MWh})_{ref} - (\text{t } CO_2/\text{MWh})_{CCS}}$
Cost of CO_2 captured	$\text{Cost of } CO_2 \text{ captured (£/t } CO_2) = \frac{(\text{LCOE})_{CC} - (\text{LCOE})_{ref}}{(\text{t } CO_2/\text{MWh})_{captured}}$

The CAPEX refers to the plant capital expenditure and this covers both direct and indirect costs including the purchase of major process equipment, installation, instrumentation and control, piping, buildings, yard improvements, engineering and supervision, land, construction expenses, contractor's fee, legal expenses, contingency and working capital [218,219]. The capital expenditure can be estimated via several ways including the cost curve method, economy of scale, step count method and reverse engineering methods discussed in Towler and Sinnott [220]. However, for this research, the cost curve method is employed to scale the plant cost by section from published data due to the simplicity and ease of use of the method. This method requires only the production rate and an exponent is applied depending on the mechanical intensity required by the plant [220]. The equation for this method is:

$$\text{Cost} = \text{Cost}_0 \times \left(\frac{\text{Scale}}{\text{Scale}_0}\right)^n \tag{3.4}$$

where 'Cost_0' and 'Scale_0' represent the cost and capacity of the base unit; 'Cost' and 'Scale' represent the estimated cost and actual size of the plant equipment; and 'n' is the scaling factor. To update the cost from previous years, the Chemical Engineering Plant Cost Index (CEPCI) is used updating the equation to:

$$\text{Cost} = \text{Cost}_0 \times \left(\frac{\text{Scale}}{\text{Scale}_0}\right)^n \times \left(\frac{\text{CEPCI}_{\text{current year}}}{\text{CEPCI}_0}\right) \tag{3.5}$$

Likewise, the purchase costs of major process equipment are estimated. These costs are commonly estimated using the factorial method with Lang factors due to the preliminary nature of this study as determined by the AACE International Cost Estimate Classes [221]. The equation for this method [222] is:

$$C_f = f_L \times C_e \tag{3.6}$$

where 'C_f' is the estimated fixed capital cost, 'f_L' is the Lang factor dependent on process type and 'C_e' is the total delivered cost of major process equipment.

The OPEX is the operating and maintenance costs associated with running a plant and this cost is made up of both fixed costs and variable costs. The fixed costs are independent of the plant operation and include labour costs, maintenance, rent, insurance and supervision. The variable costs are dependent and on the plant output and include the cost of raw materials, catalysts, utilities, effluent disposal and transport and storage [218].

Table 3.5: Parameters for estimating fixed operating and maintenance costs [222,223]**.**

Parameter	Value
Insurance, taxes & rent	2.5% fixed capital investment
Maintenance and repairs	2% fixed capital investment
Operating supplies	15% maintenance & repairs
Laboratory charges	10% operating labour
Overhead costs	50% operating labour
Royalties	1% fixed capital investment
Supervision	15% operating labour

The labour costs are estimated based on the number of shifts in a day and the number of personnel required per shift [222] and using information on the average salary available in open literature based on the plant location. The variable costs are estimated based on former expenditure in the literature and updated to account for inflation based on the plant year. The fixed costs are calculated as a percentage of the fixed capital investment. In this study, the values used are presented in Table 3.5.

The minimum energy selling price is the break-even selling price at which the future sales of energy produced and its by-products equal the present value of the total investment [224]. This price minimum selling price is determined by a discounted cash flow rate of return (DCFROR) analysis; it is calculated as the energy sale price when the net present value is 0. The net present value appraises the feasibility of a project. If the value is less than 0 (negative), the project will incur losses and if it is positive, the value of the initial capital is increased at the end of the project [225].

The DCFOR analysis calculates the present value of future earnings and is dependent on the assumed interest rate [222]. The underlining equations for this analysis are:

$$\sum_{n=1}^{n=t} \frac{CF_n}{(1+i)^n} = 0 \qquad (3.7)$$

$$CF_n = P(1 - r) + Dr \quad (3.8)$$

where 'CF_n' is the cash flow in year n; 't' is the project lifetime in years; 'P' is the gross profits in year n; 'r' is the tax rate; and 'D' is the depreciation.

To complete this DCFROR analysis, a flow sheet is modelled in MS Excel because of the functions (NPV, IF, solver, what if?) available in MS Excel which are required for the analysis, its ease of use and how it presents the information.

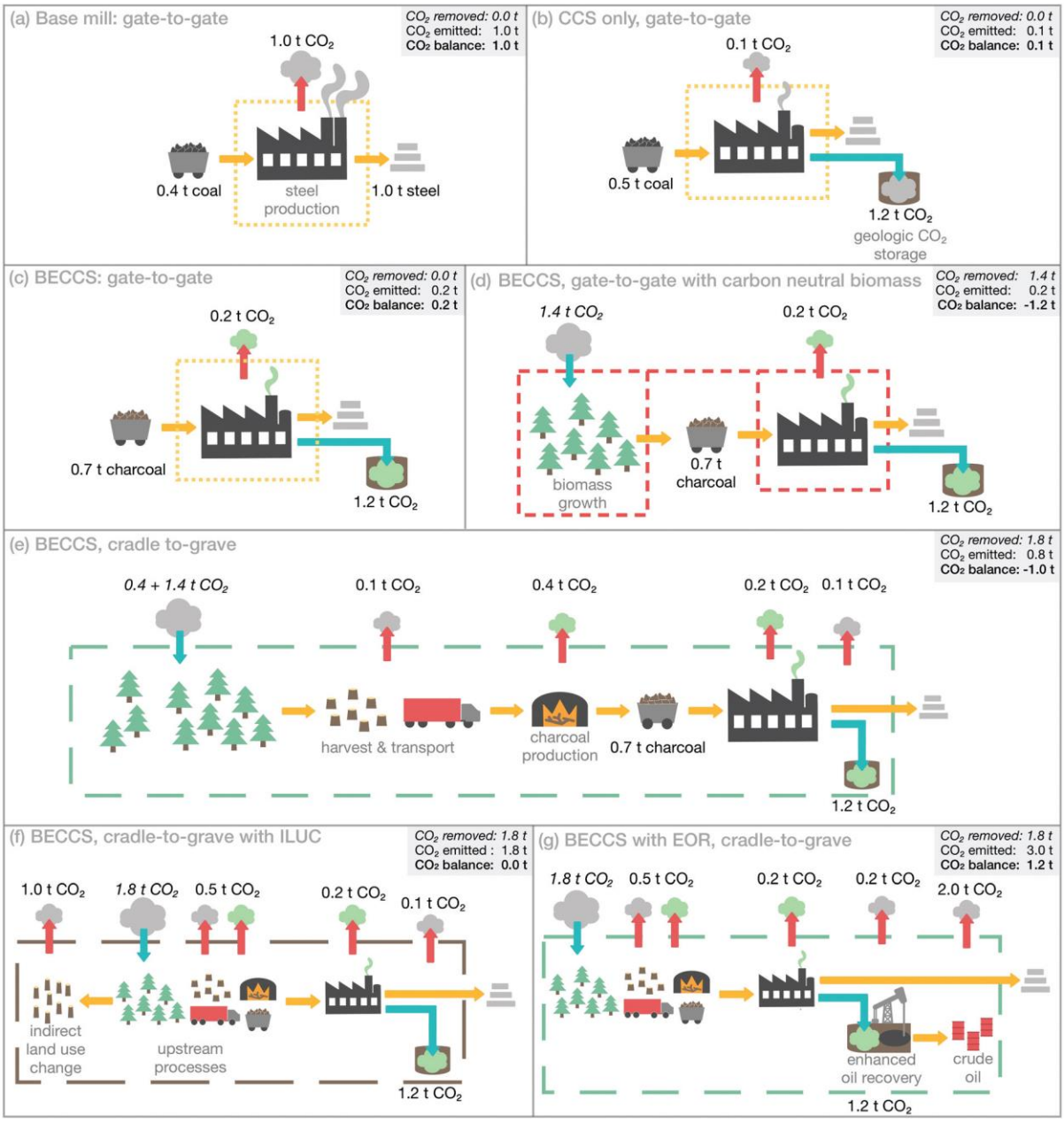

Figure 3.7: System boundary selection for estimating CO_2 emissions [226].

The environmental performance in this research is estimated using the United Kingdom Department of Business, Energy and Industrial Strategy (BEIS) greenhouse gas emission factors and a cradle-to-grave approach. The emission factor is the mass emission rate of greenhouse gases per unit energy produced. Tanzer and Ramirez [226] proposed information to be considered in accounting for negative emissions to prevent misinterpretation and miscounting and presented the different boundary systems used in NETs research.

Figure 3.7 [226] presents the different boundary systems commonly used in assessments. The cradle-to-grave approach considers emissions both upstream and downstream of the production plant including biomass harvesting and transporting as well as the product use. This approach is chosen for this study because it provides a more realistic representation of greenhouse gas emissions.

In the BEIS framework, emissions are characterised across three scopes - Scope 1, Scope 2 and Scope 3. Scope 1 accounts for direct emissions from a production process, such as is defined in a gate-to-gate system boundary. In biomass or biofuel combustion, this is the net emission from combustion. While biomass is considered CO_2 neutral and has a value of 0 for CO_2 emissions, other greenhouse gases such as N_2O and CH_4 have a value as these gases are utilised in biomass regeneration. Scope 2 accounts for indirect emissions from external energy (imported electricity and purchased heat) required to sustain the production process. Scope 3 accounts for indirect emissions from sources not owned or controlled by the plant, such as extraction, refining, transportation and distribution [227]. These are emissions from upstream processes as defined in the cradle part of a cradle-to-grave system boundary. These BEIS emission reporting factors are updated yearly to account for improvements in methodology and availability of new data [228].

3.9 Summary

The methodology presented in this chapter assists in understanding how the research study is carried out. It has provided the key steps to be followed to ensure that the research is completed properly and provides the information it intends to add to the literature. It has also presented the information needed to proceed with modelling and simulation in the next three chapters. The gasifier models which are key elements in both Chapters 4 and 5 have been validated and the assessment approach has been developed based on established methods in the literature.

The next chapter on BECCS in power generation is the first of the three assessments completed during this research.

4 BECCS in Power Generation for a Range of Biomass Feedstock

4.1 Introduction

As highlighted in sub-section 2.5.1, previous BECCS research in power generation has been focused on co-firing, biomass with a specific carbon capture technology and comparing biomass performance to coal performance with limited techno-economic assessments.

Biomass, a renewable energy source, exists worldwide and can even been likened to coal as explained in section 2.1. Different kinds of biomass feedstock are available around the world and to reduce feedstock importation, which directly drives up the price of the electricity production, it is important to find a suitable BECCS technology for the type of biomass available in each region. This is a step towards reducing costs and mitigating climate change.

The success of BECCS is dependent on the success of CCS. As CCS technology is currently being developed, there is no need to wait until its advancement before BECCS can be focused on; instead, it is important to develop both side by side so that the 2050 goal can be achieved. A lead-time of up to decades exists between research and implementation and now is the time to perform the research. Techno-economic assessments such as the present study can provide meaningful insights on the performance of BECCS projects and identify conditions for financial viability [229] [152].

This chapter contributes to BECCS research by filling the gap – lack of comparison of CO_2 abatement technology in BECCS – identified in Catalanotti et al. [141]. To the author's knowledge, there is no literature evaluating the performance of a range of biomass feedstocks in different CO_2 abatement technologies. The purpose of this study is to understand how different types of biomass will perform in different carbon capture technologies within the United Kingdom context. This involves investigating the performance of each feedstock in a BECCS scenario for power generation and the economic feasibility of deploying each option, then comparing with other scenarios to determine the best conditions for each type of biomass. The results of this study will provide a guide on suitable ways to couple each type of biomass with CCS technology when it moves to a commercial scale and highlight parameters that need to be controlled to sustain each configuration investigated.

4.2 Methodology

4.2.1 CO_2 abatement technologies

There exists an array of CO_2 abatement technologies. Dennis et al. [20] provides a comprehensive overview of the current ones while Lockwood [230] reviews the developing capture technologies. Currently, there are three main methods of CO_2 capture – pre-combustion capture, post-combustion capture and oxy-fuel capture and these are used for this study.

4.2.1.1 Post-Combustion Capture

Post-combustion capture, illustrated in Figure 4.1, involves the capture of CO_2 after combustion and it is the most common of all capture methods due to ease of retrofitting to already existing power plants. The widespread capture technique is by chemical absorption. Other capture techniques include adsorption, membrane separation and cryogenic separation. In absorption, a chemical solvent such as amine is used to absorb CO_2 from the flue gas; after the absorber, the CO_2-rich solvent is stripped by heating to release the CO_2 which is then compressed for transport and storage. The regenerated solvent is recycled to the absorber for further work. This method is the most established and is at the top when compared to other abatement technologies based on its technical readiness level (TRL)[139].

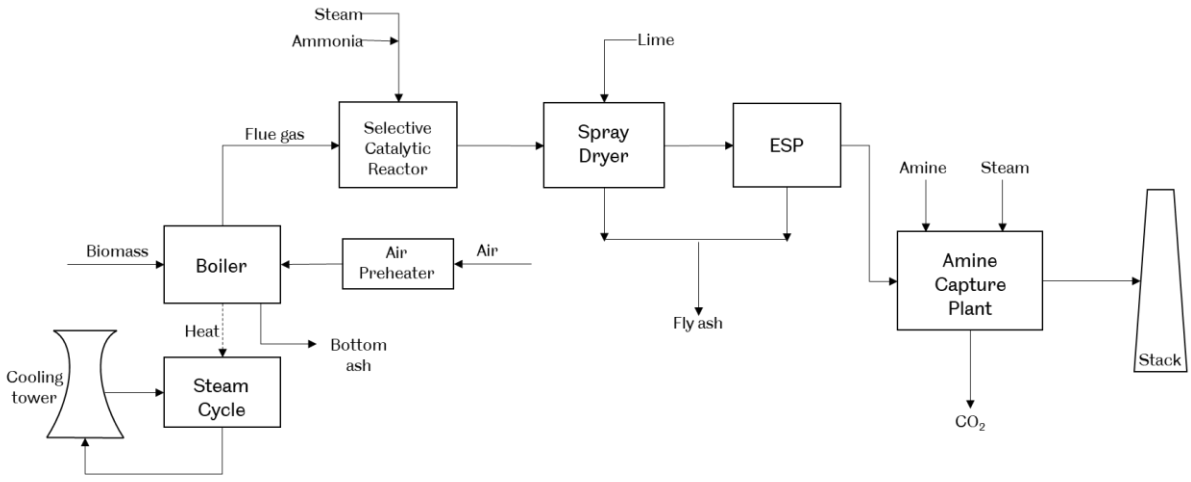

Figure 4.1: Schematic of the post-combustion capture plant used in this study.

There are currently several large-scale CCS facilities either in operation or under construction employing post-combustion capture and further pilot and demonstration-scale

facilities [231]. The largest in power generation is the 240 MW Petro Nova which captures 1.4 Mt of CO_2 per annum [231].

4.2.1.2 Oxy-fuel Combustion Capture

In oxy-fuel combustion, the fuel is burned in a nearly pure oxygen environment (~95%) rather than air resulting in flue gas concentrated with CO_2. Flue gas is recycled to the burner in order to keep and maintain flame temperature below the constraints [232] (combustion with oxygen results in higher flame temperature). As a result, the flue gas is predominantly CO_2 and H_2O for easy purification. To capture CO_2, the flue gas is cooled and dehydrated after removal of other impurities. While there are no commercial scale plants, there have been a few demonstration facilities such as the Vattenfall 30 MW facility [233] and the Callide Oxyfuel Project. A schematic of the oxy-fuel combustion plant in this study is depicted in Figure 4.2.

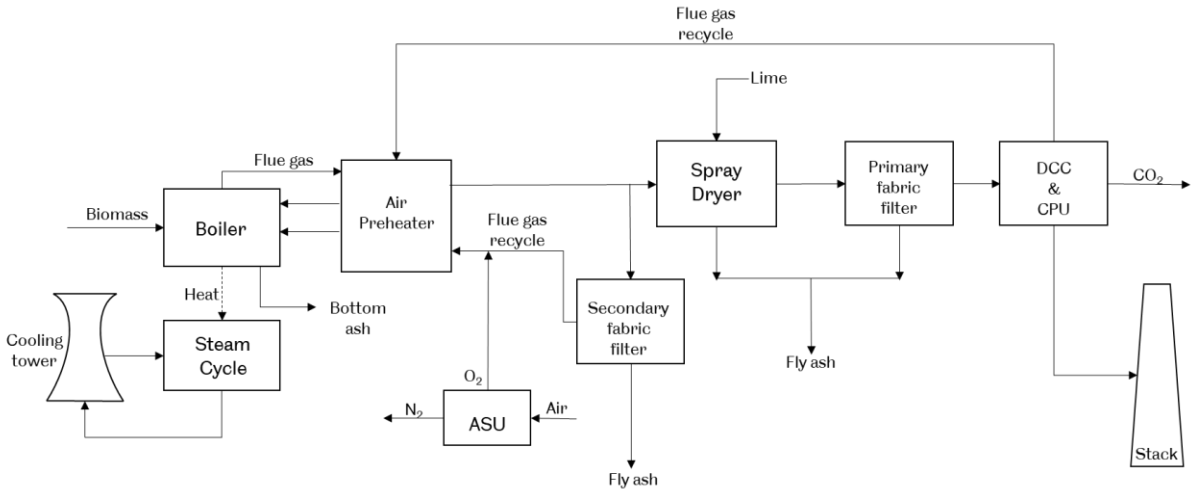

Figure 4.2: Schematic of the oxy-fuel combustion capture plant used in this study.

4.2.1.3 Pre-Combustion Capture

Pre-combustion capture involves CO_2 being captured before combustion. In this method, the fuel is combusted in limited oxidant to produce a synthetic fuel consisting mainly of H_2 and CO. In a shift reactor, most of the CO is converted to CO_2 and more hydrogen is produced when steam is added via the water-gas shift reaction:

$$H_2O + CO \leftrightarrow H_2 + CO_2 \quad (4.1)$$

CO_2 is commonly separated from hydrogen by scrubbing with a physical solvent such as Selexol. Hydrogen can now be used as a fuel in a combined cycle to generate electricity.

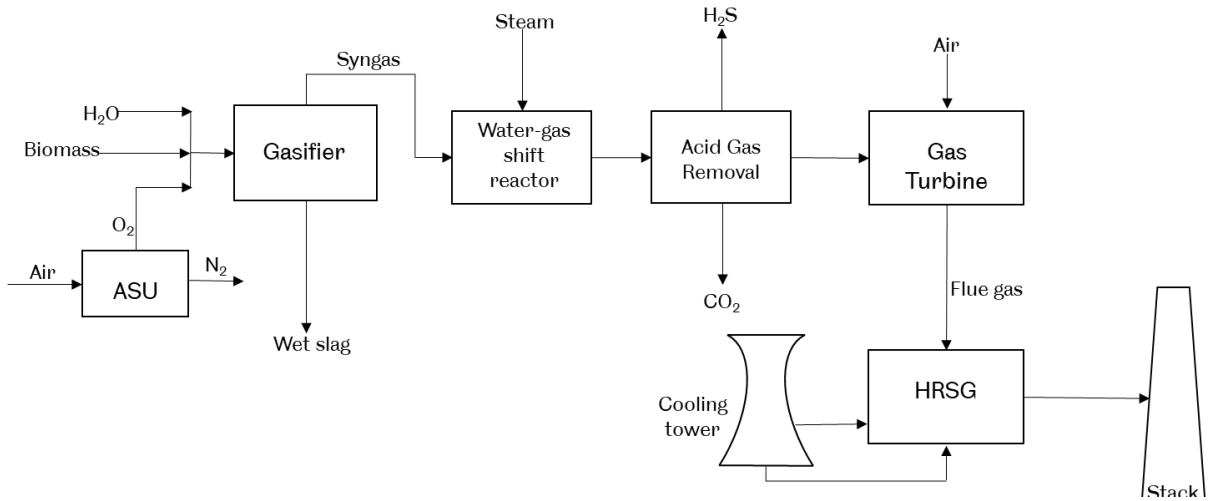

Figure 4.3: Schematic of the pre-combustion capture plant used in this study.

Figure 4.3 represents a schematic of the pre-combustion capture power plant used in this study.

4.2.2 Modelling approach

In this study, each case was modelled in the Integrated Environment Control Model (IECM) software. The IECM is a suitable software for this analysis but there are limitations to the model that should be accounted for. The software was designed for fossil fuels but there is the option to use a custom feed and one of the limitations is in the fuel handling. Biomass handling is more expensive than coal handling due to the moisture content and lower calorific value hence more storage, driers and grinders are required to increase the energy density of the feedstock. Also, the ash content from biomass is relatively more expensive to deal with in gas cleaning due to the presence of alkali and alkaline earth metals making it more fouling and corrosive [234]. While there is the option of a sub-critical, super critical and ultra-critical boiler, the only type of boiler available for the custom feed model is a conventional pulverised boiler. However, this is not suitable for all kinds of biomass and it may be suited for torrefied and ground wood pellets but not miscanthus and wheat straw. A subcritical circulating fluidised boiler is more suited to these type of biomass [235]. Again, boiler modifications are required to handle biomass such as the fuel feeding system, the burner and the ash handling but this is neglected in the IECM. Although coal (biomass in this study) and ash handling are covered in PCC and oxy-fuel, this is not an option in the IGCC

model. Likewise, for gasification, the only options available for gasifiers are the GE and Shell gasifiers which are both entrained flow gasifiers. Presently, there is no commercial entrained flow gasifier that can handle 100% biomass. Despite these limitations, the IECM remains highly suitable for providing estimates, preliminary modelling results and cost analysis which are the requirements for this study.

To handle the absence of driers, drying and pelletizing is included in the price of the biomass feedstocks. As biomass is a custom feed in the IECM, the IGCC module requires a syngas composition to be provided because it cannot calculate the syngas composition of arbitrary fuels. To do this, an entrained gasifier model was built in Aspen Plus v10 and this model calculated the syngas composition for each biomass. The model is explained in sub-section 3.7.2 and syngas compositions are available in Table A1 in Appendix A. Finally, as the model is not biomass focused, it does not account for negative emissions in a BECCS scenario hence, the cost avoidance it calculates does not include the effect of negative emissions. The cost avoidance in the BECCS scenario was calculated using the equation in Rubin [236]:

$$\text{Cost of } CO_2 \text{ avoided } (£/\text{tonne } CO_2) = \frac{(\text{LCOE})_{CCS} - (\text{LCOE})_{ref}}{(\text{tonne } CO_2/\text{MWh})_{ref} - (\text{tonne } CO_2/\text{MWh})_{CCS}} \quad (4.2)$$

where LCOE is the levelised cost of electricity and (tonne CO_2/MWh) is the CO_2 emission factor to the atmosphere.

4.2.3 Baselines and cases investigated

For each feedstock considered, two baselines are established to benchmark the feedstock performance. The first baseline is a conventional combustion plant without CCS referred to as the Ref plant and it serves as the baseline for the post-combustion and the oxy-fuel combustion capture cases. The second baseline is an integrated gasification combined cycle (IGCC) in power generation without CCS and this is referred to as the Ref-IGCC plant. This serves as the baseline for the pre-combustion capture case.

Three types of biomass were chosen based on their source. Wood is a forestry residue, miscanthus is an energy crop and wheat straw is an agricultural residue. Biogenic wastes were not considered in this study due to their unsuitability in combustion. Also, the moisture content of each biomass was fixed at 6.69%; this is the moisture value of white wood pellets as received [237].

Table 4.1: Proximate and ultimate analysis of biomass feedstocks [140,144,238,239].

Wt% (ar)	White wood pellet	Miscanthus	Wheat straw
Moisture	6.69	6.69	6.69
Volatile matter	78.10	76.61	72.13
Fixed carbon	14.51	15.30	15.21
Ash	0.70	1.40	5.97
C	48.44	45.16	44.04
H	6.34	5.88	5.41
N	0.15	0.28	0.65
S	0.02	0.09	0.16
Cl	0.01	0.12	0.17
O	37.69	40.38	36.91
HHV (MJ/kg)	19.41	18.27	17.82
Price (£/tonne)	189.90	118.90	132.20

There is no option of including a drier in the IECM, so it is assumed that the moisture biomass has been reduced to a certain level before combustion. Ideally, a certain level of moisture is permitted in the boiler but higher than this level and there would be negative effects on the boiler performance. To keep things uniform, the lowest moisture level was chosen as the baseline for other biomass; this happened to be that of white wood at 6.69%.

Table 4.2: Key operating parameters in the IECM [240,241].

Parameter	Ref	PCC	Oxy-fuel	Ref-IGCC	IGCC
Plant size (MW)	250	250	250	250	250
Capacity factor (%)	83	83	85	79	79
Plant life (yr)	25	25	25	15	15
Capture efficiency	0	87	92	0	88
CO_2 capture system	-	Amine	FG recycle + purification	-	Shift + Selexol
Boiler/Gasifier type	Supercritical	Supercritical	Supercritical	GE (Quench)	GE (Quench)
Boiler efficiency	86.7	86.7	91.0	-	-
Steam cycle heat rate (kJ/kWh)	9451	9451	7764	9496	9496
Excess air (%)	20	20	5	-	-
Steam mol input (H_2O/C)	-	-	-	0.7584	0.7584
Oxygen mol input (H_2O/O_2)	-	-	-	3	3

Also, the prices for the miscanthus and the wheat straw were retrieved by [144] and include the pre-processing to remove moisture and form pellets as well as transporting these pellets to the plant. It is assumed that miscanthus and wheat straw are sourced locally in the UK.

White wood is assumed to be imported from North America; the data and price of the feedstock is from the work by Al-Qayim et al. [140]. The composition for the wheat and the miscanthus was recovered from the ECN Phyllis database for biomass and waste [239] while the white wood from [237]. The properties of the biomass feedstocks are listed in Table 4.1 and this includes the price of the feedstocks.

In all cases, the plant size is fixed at 250 MW based on the gross electrical power output and located in the United Kingdom. The Ref plant includes a supercritical boiler and gas cleaning equipment. NOx removal with a 90% efficiency is by the in-furnace controls and a hot side selective catalytic reactor (this SCR is also present in post-combustion capture only). A cold side electrostatic precipitator (in oxy-fuel combustion, this is replaced by a fabric filter) handles particulate matter removal with a 98% efficiency and a lime spray dryer removes SO_2 with a 90% efficiency. The Ref-IGCC plant includes an air separation unit supplying 95% oxygen at 40 bar to the gasifier, a GE quench entrained flow gasifier operating at 1343°C and 42.4 bar and one gas turbine – GE 7FA – with an adiabatic efficiency of 84% is employed due to the size of the plant. Hydrogen sulphide (H_2S) is removed using Selexol and when CCS is added, it becomes a dual stage removal of acid gases.

Table 4.3: Economic assumptions in the IECM [242].

Parameter	Value
Discount rate	10%
Effective tax rate	20% (21% for IGCC)
Currency	Constant USD
Year	2017
Average exchange rate	£1 = $0.78

The key operating parameters are summarised in Table 4.2 and the economic assumptions in Table 4.3. The capacity factors, plant life and capture efficiency are based on average values from Finkenrath and the Department of Energy and Climate Change [240,241].

4.3 Results and Discussion

This section is divided into three parts. The technical analysis is covered in sub-section 4.3.1, the environmental analysis is covered in sub-section 4.3.2 and the economic analysis is covered by sub-sections 4.3.3 - 4.3.5 and 4.3.7. In sub-section 4.3.6, the results are bench-marked against the results of natural gas.

4.3.1 Effect of CCS on Net Plant Energy Efficiency

The net plant energy efficiency is the most common overall technical measure of a plant's performance. In this case, it is a measure of the ratio of the net electrical output to the energy input (calorific value of the biomass input).

Generally, the net plant efficiency generally decreases when a capture system is coupled to the plant due to the energy requirement of the additional equipment (energy penalty). This is true across all cases. White wood has the highest calorific value and miscanthus has a higher calorific value than wheat straw. The moisture and ash content are other factors that influence the plant efficiency; higher moisture and ash content result in reduced plant efficiency [243] but in this study, the moisture content is fixed and is thereby not a considered variable. From Figure 4.4, with the conventional reference plant and the post-combustion capture cases, the net plant energy efficiency decreases with decreasing calorific value of the biomass input.

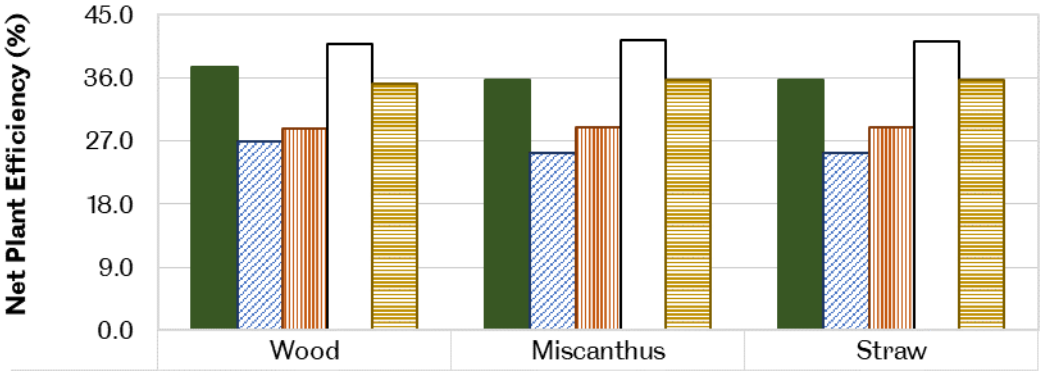

	Wood	Miscanthus	Straw
Ref	37.5	35.7	35.7
PCC	26.9	25.3	25.2
Oxy	28.7	28.9	28.9
Ref-IGCC	40.7	41.3	41.2
IGCC	35.2	35.7	35.6

Figure 4.4: The net plant efficiency a range of biomass feedstocks using different CO2 capture technologies.

This is not the case in oxy-fuel combustion capture. In this case, straw and miscanthus have a higher net plant efficiency than white wood. Looking at the different properties to determine the reason for this occurrence, the outstanding feature is the higher ash content of both miscanthus and straw compared to white wood. Based on this, the preliminary conclusion would be that oxy-fuel combustion capture may be a better fit for high ash biomass. Further information and data analysis would be needed to strongly prove or disprove this.

The IECM calculates the gross electrical power output of 250 MW after the air compressor use and turbine shaft losses in the IGCC module. In terms of fuel power input to the gasifier to meet this power output of 250 MW, white wood inputs 572.5 MW while miscanthus and wheat straw have similar power inputs at 565.8 MW and 566.1 MW, respectively.

In gasification, the higher hydrogen content of white wood results in a syngas of higher hydrogen content. As a result, a higher volume of air is required in combustion. The air compressor performs much work, which decreases the net electricity output, so the more air required for combustion and all other things being constant then the more the net electricity output decreases. Although the overall electricity generation of white wood is the highest with the highest fuel power input, a higher percentage goes towards the air compressor. The net efficiency is a ratio of the power output to the power input and the feedstocks considered all have similar power outputs calculated at approximately 201 MW and therefore a higher energy input will result in a lower net plant efficiency. This explains why the net plant efficiency of white wood, both in the reference case and in the capture case, is slightly less than that of miscanthus and wheat straw. Between wheat straw and miscanthus, a higher ash content in straw requires more energy usage in the gasifier which reduces the gasifier efficiency and overall plant efficiency.

For the three different technologies investigated, post-combustion capture has the largest decrease in net plant efficiency. The efficiency of a plant will always decrease when CCS is added due to the parasitic nature of capture plants. The capture plants require additional energy to operate and this reduces the energy output from the plant, energy that will have been sold as electricity. Post-combustion capture suffers the highest energy penalty due to the capture plant requirements, especially in the solvent regeneration which uses steam extracted from the steam cycle. Some suggestions to reduce the energy penalty include the change in solvent and effective heat integration [143]. The solvent selection in this study is MEA because this is what is currently used in commercial plants. Advanced solvents for chemical absorption have been developed [143] and these are capable of reducing the energy penalty.

When compared to physical absorption in IGCC, solvent regeneration is not as energy intensive and while the addition of the water-gas shift reactors (high temperature and low temperature) might raise costs and reduce energy output when CO is converted to CO_2 thus reducing the heating value of the resulting syngas, the thermal credit, which is the steam

available for power generation using steam turbines as a result of cooling between the two water-gas shift reactors, offsets this effect.

Overall, the results indicate that the IGCC is suitable for lower calorific value biomass and IGCC suffers the least energy penalty when CCS is retrofitted to a power plant; there is also an indication that oxy-fuel combustion capture might be a better-fit for high ash biomass; and the most common capture method – post-combustion – needs advanced solvents commercially to reduce its relatively high energy penalty.

4.3.2 Effect of CCS on the CO_2 emission factor

The CO_2 emission factor is an environmental measure of the effect of CCS. The emission factor is the mass emission rate of CO_2 to the atmosphere in tonne per MWh of electricity produced. Ideally, the goal is to reduce CO_2 emissions to the atmosphere whilst providing energy to achieve environmental sustainability.

Biomass is regarded as a CO_2 neutral fuel because the emissions from its combustion were initially fixed within the material and will be taken back up when it is regenerated. This explanation does not consider the emissions associated with the harvesting, transporting and refining of biomass for combustion but it is necessary to account for these emissions to determine the accuracy when reporting biomass as carbon neutral or carbon negative.

Table 4.4: Emission factors of the reference plant (this does not consider the type of plant).

Biomass	kg CO_2e/kWh
White wood pellets	0.0557
Miscanthus	0.0340
Straw	0.0332

The United Kingdom Department of Business, Energy and Industrial Strategy (BEIS) [244] outlines the emission factors for greenhouse gas reporting and how to use these factors. The BEIS framework categorises activities that release emissions into three classes known as scopes – Scope 1, Scope 2 and Scope 3. Scope 1 refers to direct emissions from fuel combustion; this is zero for CO_2 emissions in the case of biomass and biofuels due to its status as CO_2 neutral. However, N_2O and CH_4 released are not absorbed in biomass regeneration so Scope 1 covers these gases. A different class known as 'outside of scopes' is used to categorise the direct emissions of CO_2 from the combustion of biofuels. Scope 2 refers to the emissions associated with electricity and heat purchased for the plant, however, it is assumed that the plant is self-sustaining, so this is zero for the cases examined

in this work. Scope 3 refers to indirect emissions from sources not owned or controlled by the plant; this is the emissions as a result of harvesting, refining and transporting biomass. Scope 3 excludes electricity and heat purchased for the plant which is covered by Scope 2. The biomass carbon footprint for the reference plants obtained from the calculation of the emission factors in Table 4.4 includes Scope 1 and Scope 3 factors. More information about the calculation is given in Appendix A. Using this approach, Figure 4.5 represents the emission factors for all the cases investigated.

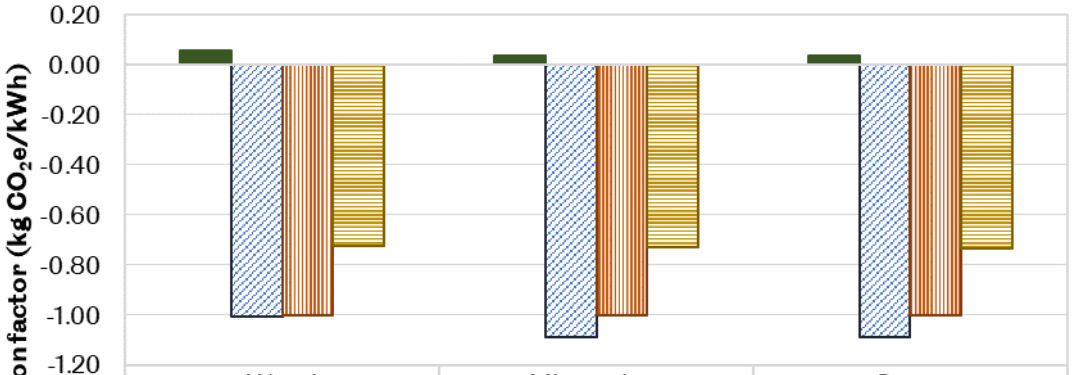

	Wood	Miscanthus	Straw
Ref	0.0557	0.0340	0.0332
PCC	-1.0071	-1.0877	-1.0913
Oxy	-1.0002	-1.0040	-1.0041
IGCC	-0.7272	-0.7321	-0.7336

Figure 4.5: Emission factor (kg CO_2e/kWh) of white wood, miscanthus and wheat straw in different CCS technologies.

For all feedstocks, the post-combustion capture has the most negative emission factors. This can be attributed to the high mass flowrate to the boiler required for a fixed gross power output and hence more CO_2 being produced and captured. Wheat straw has slightly more negative emissions than the other biomass feedstocks. From the analysis, this is mainly due to the lower indirect emissions during harvesting and transporting to the plant facility as indicated by the emission factors in Table 4.4. The most negative emission factor obtained in this study is with wheat straw in post-combustion capture and this is equivalent to a CO_2 mitigation potential of 1.52 Mt yearly.

Based on the emission factors of the reference plants alone, using white wood releases at least 60% more emissions per MWh of electricity produced than the emissions associated with miscanthus and wheat straw. Harvesting and processing wood into pellets is more energy intensive than processing miscanthus or straw. This goes further to reiterate the

point that it is important to make the right choices along the biomass production and supply chain to successfully enable negative emissions.

The emission factor calculated in the IECM is referred to as the outside of scope factors by the BEIS framework, i.e., the direct CO_2 emissions from burning biomass and the CO_2 emissions when discounting biomass neutrality. As explained in sub-section 4.2.2, the IECM was built for fossil fuels which are not carbon neutral. Figure 4.6 represents the outside of scope factors of using the various biomass feedstocks.

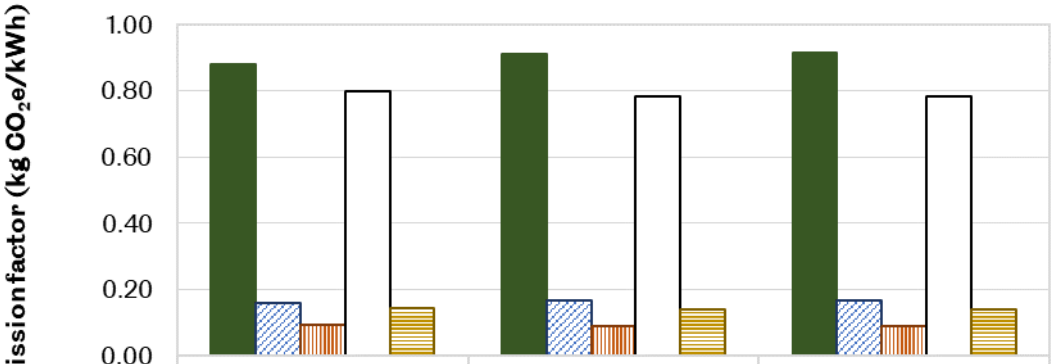

	Wood	Miscanthus	Straw
Ref	0.8782	0.9123	0.9139
PCC	0.1584	0.1676	0.1680
Oxy	0.0918	0.0903	0.0902
Ref-IGCC	0.8000	0.7834	0.7828
IGCC	0.1440	0.1395	0.1400

Figure 4.6: Emission factors discounting biomass carbon neutrality.

The direct emissions from biomass combustion need to be accounted for to show the short-term effect of BECCS on the environment. This is only short term because the emissions will be recycled over time to generate new biomass. This is true when using perennial grasses, such as miscanthus and wheat grass. Wood takes a relatively longer time to be generated but several magnitudes shorter when compared to fossil fuels.

Liu et al. [35] explain that the CO_2 emissions from combustion reduce with an increasing H:C ratio and increasing energy efficiency, i.e. CO_2 emissions are directly linked to the energy efficiency. Comparing Figure 4.4 and Figure 4.6, white wood is the most efficient in post-combustion capture and this corresponds to the least emission factor using this technology. This is the case for wheat straw in oxy-fuel combustion and miscanthus in pre-combustion capture. This impact should be considered when focusing on short to medium term effects of using BECCS.

4.3.3 Cost of CO_2 avoided and captured

The cost of CO_2 avoided is a common economic measure of CCS costs. It reflects the average cost of avoiding a unit of CO_2 emissions (e.g., tonne) to the atmosphere whilst providing a unit of useful product (e.g., MWh) from a reference plant. It is essentially the carbon tax that needs to be applied so that the LCOE of the plant with CCS equals that of the reference plant (without CCS) [236]. The cost of the CO_2 captured measures the cost of reducing CO_2 emissions to the atmosphere and reports the incremental cost of CO_2 capture from a particular facility. This measure excludes the cost of transportation and storage as it assesses the economic viability of capturing (producing) CO_2 relative to its market price as a commercial commodity (such as use in beverages and a precursor for chemicals) [216,236].

Table 4.5: Cost of CO_2 avoided and captured based on a reference plant of the given technology for a range of biomass feedstocks (a – discounting negative emissions, b – BECCS scenario).

	Wood			Miscanthus			Straw		
	PCC	**Oxy**	**IGCC**	**PCC**	**Oxy**	**IGCC**	**PCC**	**Oxy**	**IGCC**
Cost of CO_2 avoided[*a] (£/t)	98.3	122	66.5	87.4	97.5	60.5	93.6	99	62.7
Cost of CO_2 avoided[*b] (£/t)	60.8	87.5	50.2	51.8	73.2	44.7	55.5	74.8	46.2
Cost of CO_2 captured (£/t)	60.5	83.5	46.3	51.7	70.2	41.2	55.8	71.9	43.1

While the cost of CO_2 captured is straightforward, as obtained from IECM, the cost of CO_2 avoided is not. IECM does not include an option for biomass so it cannot account for the negative emissions associated with biomass and hence the cost of CO_2 avoided is based on the outside of scope emission factors. However, it is important to explore how negative emissions affect these costs, as this is within the scope of this work. Table 4.5 reports these costs and the avoidance cost is reported in two ways – discounting negative emissions and in a BECCS scenario (including negative emissions). Ideally, the CO_2 avoidance cost should be calculated based on various reference plants [216] but this cannot be reported in this work due to the limited information available on different biomass feedstocks in power generation.

Generally, the costs decrease with decreasing feedstock price and CAPEX. White wood pellets report the highest cost due to the high cost of electricity as a result of a high feedstock price while the costs of avoidance and capture is cheapest with miscanthus due to miscanthus having the lowest feedstock price. Accounting for negative emissions decreases the avoidance cost by up to £38/tCO_2. In summary, a minimum carbon tax of £45/tCO_2 and a

maximum price of £87/tCO_2 is needed to match the LCOE of the plants without CCS. These values fall within the projected carbon prices of \$50/tCO_2 to \$140/tCO_2 in Canada [245] and the DECC predicted central carbon values of £60/tCO_2 to £135/tCO_2 [246]; all between 2020 and 2040.

4.3.4 Effect of CCS on the Levelised Cost of Electricity

The Levelised Cost of Electricity (LCOE) is an economic parameter that allows the comparison of different power plants and technologies and it is defined as the unit cost of electricity generation over the lifetime of a plant. This value represents the minimum revenue that a power plant should generate to cover the costs of building and running the plant during its economic lifetime. Figure 4.7 presents the results of the LCOE for all the cases using 2017 constant GBP. The economic assumptions are listed in Table 4.3.

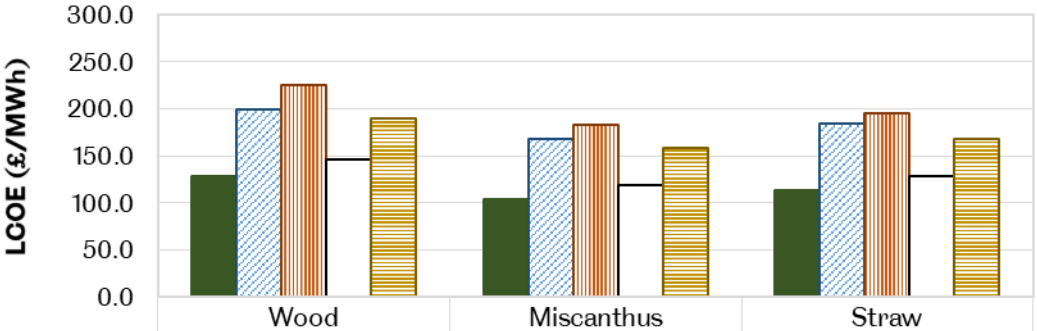

	Wood	Miscanthus	Straw
Ref	128.9	103.2	113.7
PCC	199.8	168.2	183.5
Oxy	224.4	183.2	195.5
Ref-IGCC	146.5	118.8	127.8
IGCC	190.2	157.7	168.1

Figure 4.7: Levelised cost of energy for a range of biomass feedstocks using different CO_2 capture technologies.

Without a capture plant attached to the power plant in all cases, the conventional power plant gives an LCOE that is £14/MWh to £18/MWh less than the IGCC power plant. However, when the capture plants are added, the LCOE of the all the IGCC cases are affected the least with increases between 30% and 33%, thus leading to them being the most economically favourable cases for the three biomass feedstocks in a retrofitting scenario.

(a)

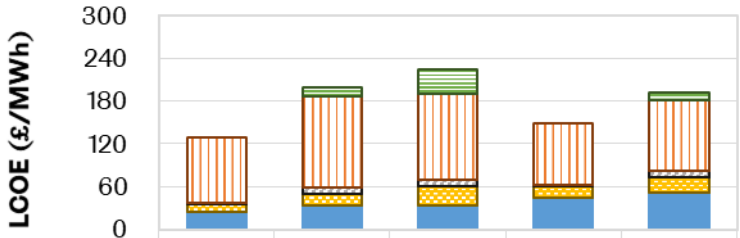

	Ref	WW-PCC	WW-Oxyfuel	Ref-IGCC	WW-IGCC
CCS	0.0	13.0	35.0	0.0	10.9
Fuel	92.4	128.5	120.6	86.1	99.6
VOM	0.8	8.5	8.4	1.3	9.1
FOM	10.6	16.8	27.7	16.1	21.6
Capital charges	25.1	32.6	32.6	44.9	51.3

(b)

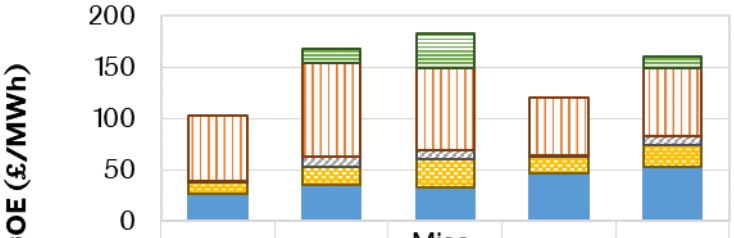

	Ref	Misc-PCC	Misc-Oxyfuel	Ref-IGCC	Misc-IGCC
CCS	0.0	13.8	34.6	0.0	10.8
Fuel	64.7	91.4	80.0	56.7	65.7
VOM	0.9	10.4	8.5	1.5	9.1
FOM	11.2	18.0	27.7	16.4	21.9
Capital charges	26.4	34.6	32.4	45.8	52.2

(c)

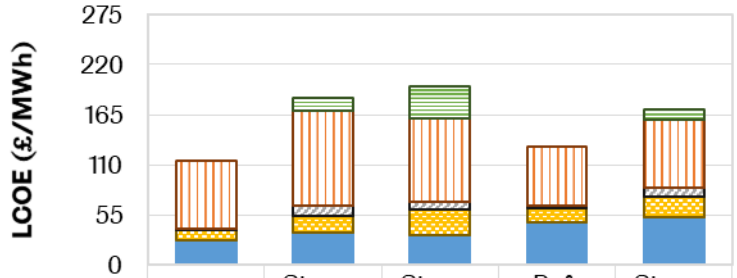

	Ref	Straw-PCC	Straw-Oxyfuel	Ref-IGCC	Straw-IGCC
CCS	0.0	13.8	34.5	0.0	10.8
Fuel	73.9	104.5	91.1	64.7	75.0
VOM	1.3	11.3	9.0	1.7	9.4
FOM	11.4	18.3	27.8	16.5	22.1
Capital charges	27.1	35.7	33.1	46.4	53.0

Figure 4.8: The LCOE breakdown of (a) white wood, (b) miscanthus and (c) wheat straw.

This minimal increase in LCOE for IGCC can be attributed to the more efficient capture process in IGCC [247]. The oxy-fuel combustion process has the highest LCOE with 16% to 19% of the LCOE associated with the capture plant. When compared to the effect of CCS on the LCOE in post-combustion and pre-combustion capture, CCS in the oxy-fuel is a significant contributor to the LCOE due to the addition of an air separation unit to produce oxygen, which is currently an expensive piece of technology. Figure 4.8 depicts the breakdown of the LCOE contributors. From this figure, the effect of adding CCS is clear, it drives the total costs of the plant up.

The addition of CCS drives up other costs, such as the feedstock expenditure, due to more biomass being needed to meet the gross electrical power output, more raw materials, such as reagents, are needed in the gas cleaning, labour costs and additional equipment.

With all the biomass feedstock, the fuel cost appears to be the most significant contributor to the LCOE. The next visible significant contributor to the LCOE is the CAPEX. Across the three biomass feedstocks, the contribution of CAPEX to the LCOE is higher in IGCC while the contribution of CCS is the least. This reinforces the point that it is cheapest to include carbon capture and storage to an already existing biomass gasification plant for power production.

The LCOE is dependent on several variable parameters including plant capacity factor, capital requirement, discount rate, fuel cost and variable operating and maintenance costs. These variables are fixed in this study, but these factors will be subject to market forces over the years and therefore it is crucial to understand how the variance of these factors will affect the plant output and income.

A sensitivity analysis on the LCOE is performed in the next sub-section and this reveals the key driving parameters on the LCOE.

4.3.5 LCOE sensitivity analysis

As mentioned in sub-section 4.3.4, the LCOE is dependent on several factors. As the LCOE represents the minimum selling price of electricity from a plant, it is important to understand how these variable parameters affect the LCOE. A sensitivity analysis was performed by varying these parameters and evaluating their individual effect on the LCOE based on a high-cost and low-cost scenario. The high and low-cost scenarios for the CAPEX and fuel cost used in this analysis are from the AACE classification [221]. As this study is to

assess the initial viability of the various feedstocks, it is classified as a Class 5 project. The estimates for the capacity factor, discount rate and operational lifetime are an average of the values commonly used in the literature for power plants. In the IGCC case, as the plant already operates at the low-cost estimate, only the high-cost scenario was evaluated.

Table 4.6: The high and low-cost estimates utilised in the LCOE sensitivity analysis.

Parameter	Low	High
CAPEX	-30%	+50%
Fuel cost (FC)	-50%	+50%
Capacity factor (CF)	50%	90%
Discount rate (DR)	8%	13%
Operational lifetime (OL) in years	15	30

From Figure 4.9, it is observed that the fuel price is the most crucial driver in the LCOE in the case of a high-cost fuel, such as white wood followed by the capacity cost and the CAPEX.

Going from post-combustion capture to oxy-fuel capture and then pre-combustion capture, the impact of the fuel cost on the LCOE decreases.

The least LCOE is achieved in all cases of post-combustion capture using a low-cost fuel while the highest LCOE is achieved with a capacity factor of 50% except in the case of white wood in post-combustion factor where the high-cost fuel results in the highest LCOE. This trend suggests that post-combustion capture results in the lowest LCOE for low-cost fuels but the volatile impact of a high-cost fuel on the LCOE along with the energy penalty associated with this abatement technology limits it.

The plant capacity factor is another crucial driver of the LCOE. The capacity factor represents the productivity of a plant and plays a major role in the LCOE price; increasing the capacity factor causes the LCOE to decrease.

A common reason why the plant capacity will drop is mainly due to equipment failure and operating maintenance, but this is a consideration in the planning stage. Increasing this factor above the current level will slightly decrease the LCOE but decreasing the capacity factor has a drastic impact on the LCOE. It significantly increases the LCOE, more than increasing the fuel cost will do. As the fuel cost decreases, the effect of the capacity factor becomes more visible, as seen with miscanthus which costs the least among the three feedstocks considered.

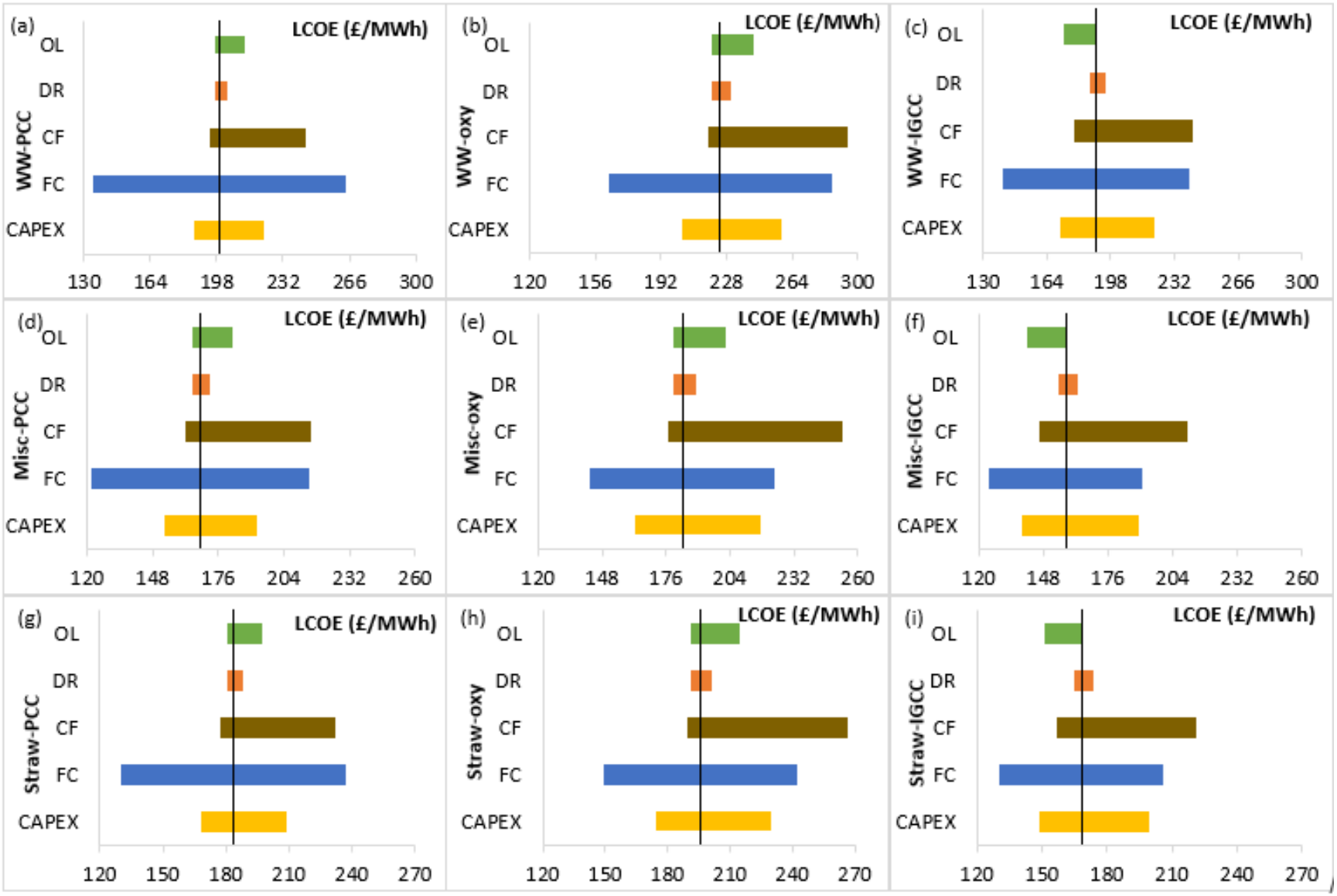

Figure 4.9: Result of the LCOE sensitivity analysis (a), (b), (c) white wood, (d), (e), (f) miscanthus, (g), (h), (i) wheat straw.

The final factor with a visible impact on the LCOE is the CAPEX; efforts to decrease the capital charges can cause a substantial decrease in the LCOE. Using biomass, feedstock availability is a factor that will affect the LCOE. A plant relying on agricultural residue, such as wheat straw, might not have this available all year round, thus resulting in a reduced plant capacity [248]. Also, the world is moving away from fossil fuels and towards renewable energy, hence the capacity factor of power plants is certain to reduce as more renewable energy sources (that have no fuel cost – e.g., solar) enter the market to diversify the energy mix.

While the discount rate and operational life are non-trivial, increasing the operational life of an IGCC plant will lead to a decrease in the LCOE. In all cases of white wood, the fuel cost is the clear barrier that needs to be overcome to reduce its LCOE especially with white wood. The feedstock price is a function of its source, availability, supply and demand.

Currently white wood is expensive while miscanthus is relatively cheaper. In the grand scheme of achieving a low-carbon economy, wood is a more effective CO_2 reduction option in construction, storing carbon while displacing the use of cement and steel [64].

While the CAPEX may be higher in one country or region, it could be lower in another country or region but ultimately it also drives the LCOE. Therefore, it is highly recommended to perform this study in different countries to see how each country favours the proposed BECCS technologies.

Ways to handle these variabilities and thus limit the impact on the LCOE, include investing in equipment such as thermal gasifiers that can handle a range of biomass feedstock and a circulating fluidised bed that can handle high moisture fuel, such as biogenic waste, to ensure a constant plant output [248–250]; increasing the plant scale (up to 500 MW_e) as plants benefit from economies of scale [251], however, an analysis to determine the optimum range of the plant size is required; and finally considering a combined heat and power plant to improve the overall efficiency and possibly generate additional revenue for the plant. Another advantage of using a circulating fluidised bed, apart from its fuel flexibility and ability to handle low grade fuels, is that pre-processing of the biomass feed is not required [250]; this can significantly reduce the cost of the feedstock which at present accounts for the pre-processing including moisture removal and pelletizing and transportation.

4.3.6 Benchmarking against natural gas

This sub-section details how the evaluated parameters compare to natural gas without and with CCS and the summary of the results is presented in Table 4.7. As expected, the plant efficiency of natural gas is higher in a range of 14% to 40% than the efficiencies of the biomass feedstocks due to the higher calorific value, no ash and minimal impurities in natural gas. The absence of ash and impurities in natural gas eliminates the need for a significant clean-up system which boosts the efficiency and reduces costs associated with running the plant. Comparing the LCOE, on the average that of white wood is 2.7 times natural gas without CCS and 2.9 times natural gas with CCS, that of miscanthus is 2.2 times natural gas without CCS and 2.4 times natural gas with CCS and the LCOE of straw is 2.3 times natural gas without CCS and 2.6 times natural gas with CCS.

Table 4.7: Summary of results using natural gas without and with CCS.

	Ref	PCC
Plant efficiency (%)	48.3	42.0
LCOE (£/MWh)	51.4	71.5
CO_2 emission factor (kg/kWh)	0.4057	0.0848
CO_2 avoided (£/tonne CO_2)	-	62.7
CO_2 captured (£/tonne CO_2)	-	42.7

Based on the technical and economic factors, natural gas outperforms biomass and this is due to the lower feedstock price of natural gas at £5.5/GJ [252], higher efficiency and its developed status from years of experience. Considering the emission factors, the natural gas reference plant has a lower emission factor than biomass (based on direct short to medium term emissions) but when coupled with CCS, biomass offers a better option due to negative emissions. Including the long-term effect of bioenergy, i.e., its ability to remove CO_2 relatively faster from the atmosphere, takes the option of natural gas out of negative emissions.

The effect of bioenergy without CCS in the short to medium term is more detrimental to the environment than natural gas without CCS; this should not be overlooked when planning bioenergy projects. Power generation technologies using fossil fuel enjoy years of experience resulting in relatively lower LCOE. If only the costs are considered, there would be no incentive to move towards bioenergy hence development opportunities and policy tools should be focused on to help decrease the costs associated with BECCS in power

generation. Decreased costs of BECCS and the effect on the environment will make BECCS competitive and possibly phase out the use of natural gas.

4.3.7 Effect of carbon pricing on LCOE

Carbon pricing is a major policy tool applied by governments to reduce carbon emissions and hence, protect the environment. The idea of carbon pricing serves to discourage emissions by increasing the cost of doing business. There are various forms of carbon pricing instruments but the most common ones are – carbon tax and emission trading scheme [253].

In the emissions trading scheme, a limit is set on the total amount of greenhouse gases emissions and with time, the limit is reduced. A major example where this system exists is in the EU. The EU ETS currently operates in 31 countries and has been in effect since 2005. In a carbon tax system, a direct price is applied to each unit of GHG emissions and there is no limit on the amount of emission reduction creating an incentive for lower emissions by adopting more efficient processes or low carbon fuels. British Columbia has used this system since 2008 and is currently at $\$40/tCO_2e$ in 2019 to increase by $5 every year until 2021 [254].

While carbon pricing has been adopted by some countries and is effective at reducing emissions, the rate at which the carbon pricing gap is decreasing is slow [255]. The carbon pricing gap summarises how countries use carbon pricing effectively and this gap has decreased by 3 percentage points between 2015 and 2016. To close the gap faster and for a cost-effective transition to low-carbon economies, carbon prices need to be increased quicker than the current rate.

However, while carbon pricing as a tool encourages switching to renewables such as biomass, fossil fuel technologies enjoy years of experience and optimisation resulting in cheaper cost of power production as opposed to relatively new renewable technologies which are expensive. The low carbon prices means that the emitters are not fully confronted with the cost of emissions to the society [255] and would rather pay the carbon price which is still cheaper than switching. To achieve low carbon economies, the carbon price needs to be high enough to force the rapid development of renewables such as BECCS.

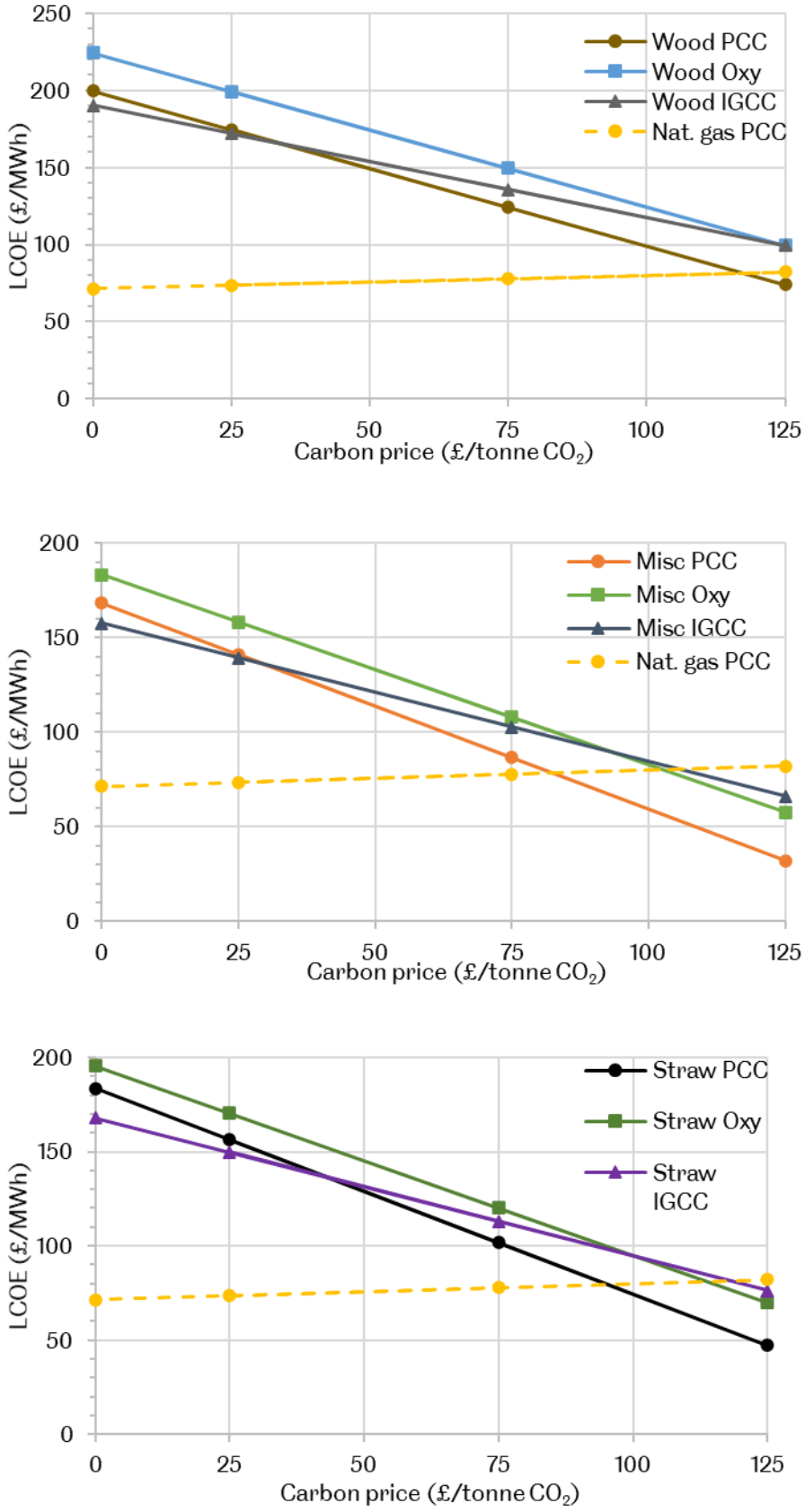

Figure 4.10: Sensitivity analysis of carbon price on LCOE using (a) wood, (b) miscanthus and (c) straw with respect to natural gas.

As mentioned earlier in sub-section 1.4.1, a major limitation to the commercial deployment of BECCS is the lack of economic policies especially in power generation. While different countries have renewable incentives to promote renewable energy investments [256], there are relatively none for CCS, likewise negative emission technologies.

The potential of carbon pricing in BECCS to quickly transition an economy is highlighted in Figure 4.10. Three carbon price cases - low case at £25/tCO_2, a medium case at £75/tCO_2 and a high case at £125/ tCO_2 – are applied to the range of BECCS technology investigated in this study. The BECCS cases are compared against natural gas with CCS scenario. In the BECCS cases, as a result of the negative emissions, revenue is generated for the plant eventually reducing the LCOE while in the natural gas with CCS case, the plant has to pay for its emissions, thus resulting in an increased LCOE.

At low and medium price carbon price scenarios, none of the biomass feedstocks can compete with natural gas, making BECCS an unattractive form of power generation. With an expected increase in carbon pricing, LCOEs as low as £32/MWh when using miscanthus can be achieved.

Table 4.8 shows the carbon prices at which the different biomass feedstocks break even with natural gas when coupled with CCS. Miscanthus in post combustion capture requires the least price to break even with natural gas at a carbon price of £83/tCO_2 implying that this is the minimum carbon price that can be applied to encourage competition with fossil fuels. While the LCOE of white wood decreases, even in the high case scenario, it is still not a favourable choice of feedstock owing to the high cost of obtaining it; a break-even carbon price of £141/tCO_2 in oxy-fuel capture and £146/tCO_2 in pre-combustion capture will be required. Overall, this table displays the potential of BECCS to rapidly decrease the carbon pricing gaps where negative emission credits (NECs) is established as a form of carbon pricing.

Table 4.8: Break-even carbon prices for a range of biomass feedstocks using different CO_2 capture technologies with respect to natural gas.

	PCC (£/tCO_2)	Oxy-fuel (£/tCO_2)	IGCC (£/tCO_2)
Wood	118.0	141.0	146.0
Miscanthus	82.5	103.0	106.0
Straw	95.2	114.0	118.0

Comparing the different CCS technologies, post-combustion capture shows the highest decrease at 81% in LCOE for the high case scenario when using miscanthus and this

compares to a 58% decrease using pre-combustion capture and 69% using oxy-fuel combustion capture. This high LCOE decrease observed with post-combustion capture can be directly related to the negative emission factor – which represents the amount of CO_2 removed from the atmosphere per unit of electricity produced so increasing the emission factor directly increases the amount of negative emission credits that can obtained. Although, post-combustion capture experiences the highest energy penalty with a decreased efficiency, in the grand scheme, the cheapest LCOE can be achieved here with sufficient carbon pricing. For natural gas with CCS, a maximum increase of 13% in the LCOE is observed; without CCS, the LCOE would be even larger and render power production from natural gas infeasible. This further demonstrates the power of carbon pricing in driving down the use of fossil fuels in power generation.

Applying carbon pricing to NETs such as BECCS in the form of NECs is a certain way to transition to a low-carbon economy. Cabral et al. [145] proposed a method of accelerating the decarbonisation of the power and industrial sectors by auctioning NECs generated from BECCS in a form of emissions trading scheme. The negative credits essentially generate revenue for BECCS plant without relying on government subsidies ultimately lowering the LCOE.

Eventually, it will be left for governments to decide the form in which carbon pricing can be applied to BECCS – in an emission trading scheme form, a carbon tax form or a mix of both forms? In whatever form it is implemented, it is evident that this instrument can adequately decarbonise an economy quickly.

4.4 Conclusion

As the world moves towards mitigating climate change by reducing CO_2 emissions in the atmosphere, negative emission technologies (NETs) such as BECCS need to be better understood and further developed. In this study, the performances of a range of biomass feedstock in power generation with different CCS technologies were compared using techno-economic models built in the IECM.

The results of this study indicate that the most suitable BECCS technology for each type of biomass is dependent on certain factors. In all cases, adding a capture plant decreases the plant efficiency by up to 29% with post-combustion capture experiencing the highest energy penalty and pre-combustion capture experiencing the least at 13.5%. In post-combustion

capture, a higher calorific value biomass such as white wood results in higher net plant efficiency while pre-combustion capture is more suited to a lower calorific value biomass, however a high ash content in the biomass will still reduce the efficiency in both cases. Across all CCS technologies considered, pre-combustion is the most efficient with the least power production cost.

In terms of the range of feedstock and environmental effect, preliminary analysis of the type of feedstock suggests that the energy usage in harvesting and processing of biomass will significantly affect the overall negative emissions. Also, in the short to medium term, the energy efficiency of the biomass feedstock directly impacts the emission factor. While BECCS is a long-term mitigation strategy, bioenergy without CCS is not suitable in power generation as evidenced by the emission factors when compared to natural gas; it is actually worse. With BECCS, a 250 MW power plant can remove between 1.0 Mt and 1.52 Mt of CO_2 per year from the atmosphere in the long-term.

In terms of the economics, adding CCS to a power plant increases the LCOE. In post-combustion capture this increased by 37%, 43% in the oxy-fuel capture and 24% in the pre-combustion capture. In order for the bio-CCS cases to match the LCOE without CCS, the cost of CO_2 avoidance should be £56/tCO_2 in post-combustion capture, £79/tCO_2 in oxy-fuel capture and £47/tCO_2 in pre-combustion. Furthermore, if carbon pricing as a climate change mitigation tool is employed, a carbon price between £83/tCO_2 and £146/tCO_2 based on the three feedstocks considered is required to create competition with natural gas, promote the commercial deployment of BECCS and phase out natural gas in power generation. The carbon price is a function of the emission factor therefore more negative emissions results in minimal carbon prices to achieve feasibility. Among the feedstocks, miscanthus had the lowest costs (LCOE and avoidance cost) while white wood had the highest costs, the costs showed a direct relationship to the feedstock price. A sensitivity analysis on the LCOE revealed that the capacity factor, fuel cost and CAPEX are key drivers in the plant revenue; the high cost of obtaining white wood and its carbon footprint overshadowed its benefits (i.e. energy efficiency) in power production indicating that if white wood is not sourced locally, then its usage should be avoided.

Finally, this study has highlighted how different biomass feedstocks will fare in different CO_2 abatement technology for power generation. The results can serve as a preliminary assessment guide when exploring BECCS projects in different regions to ensure a minimal to positive impact on the environment, maximum plant operational life, maximum product

output and a profitable venture. Ultimately, this study has contributed to the ongoing BECCS research. BECCS is dependent on CCS and this can inform the current CCS research. There are many challenges with BECCS, such as the relatively high cost when compared to fossil fuels, which enjoy the privilege of experience. With no incentives in place to move towards renewable energy sources, the climate will suffer.

5 BECCS in Fuel Generation for Three Biofuel Production Routes

5.1 Introduction

Previous and current BECCS research has focused on its role in power generation neglecting the possible benefits in fuel generation. Compared to BECCS in power generation, carbon capture is intrinsic in the fuel generation plant, thus creating an initial economic advantage. BECCS In fuel generation can assist the decarbonisation of the transport and heating sectors.

To this end, the chapter examines the technical, economic and environmental feasibility of three fuel production routes using a second-generation biomass, i.e., lignocellulosic woody biomass, as a potential BECCS technology. As many economies move towards decarbonisation, conventional fuels cannot be displaced due to their importance, instead they can be replaced by alternatives that can help meet the goal. Suitable alternatives involve conversion of biomass by various routes. Biomass is an important fuel in a low-carbon economy because of its composition and similar processes to fossil fuels that it can undergo. Also, it should be noted that in this work, since carbon capture is an integral part of each production process, carbon capture and storage (CCS) refers to the captured CO_2 compression, transportation and storage. The use of second-generation biomass in this study is rooted in the fact that the production of this class of biomass does not compete with food production and also that the technology for these routes are readily available but not developed to a commercial scale [257–259]. Previous studies [155,260–263] on the biofuels production from second-generation biofuels has solely focused on the need to increase biofuel production to displace fossil-fuels but the economic and environmental impact of employing CCS has not been fully considered.

This chapter focuses on the use of biomass in addition to CCS to produce biofuels while removing CO_2 from the atmosphere. In addition to the technical and economic feasibility of the routes examined, the environmental impact is determined in terms of the mitigation potential. The routes considered are the common Fischer-Tropsch synthesis (FTS) to produce hydrocarbons, methanation to produce bio-synthetic natural gas (bioSNG) and oxymethylene ethers synthesis to produce OMEx. All three production routes are thermochemical processes and selected based on a common gasification process.

The chapter updates the work in the literature and adds much more information on the economic and environmental impact of deploying BECCS in the investigated fuel production routes. The results of this study answer the following questions:

- Is biofuel generation suitable to create substantial negative emissions?
- What are the savings created when compared to conventional fuels?
- How relevant is BECCS in fuel generation to climate change mitigation?
- Are there opportunities present in current processes to maximise carbon removal?
- Are the biofuels produced competitive with conventional fossil fuels in transportation?
- What role will carbon pricing in fuel generation play in transiting to a low-carbon economy?

5.2 Process Simulation and Description

All the examined processes were modelled using the sequential-modular approach in the Aspen Plus V10 software. Aspen Plus is capable of simulating large complex processes even those involving solids and non-ideal components such as biomass. Thermodynamic models were used to solve the mass and energy balances in the system. Generally, the Peng Robinson equation of state with Boston Mathias alpha function (PR-BM) was chosen to estimate phase equilibria and properties and steam tables for the power generation section [264]. The enthalpy of formation, specific heat capacity and density of the non-conventional components (biomass and ash) were estimated using the HCOALGEN and DCOALGIT property methods [265]. In Aspen Plus, the gasification process can either be equilibrium modelled or kinetic modelled. The complexity of the involved reactions prevents the simulation of the gasification process as a single unit operation model in Aspen Plus, so the process is simulated using various reactor models. In this work, equilibrium modelling [184,185] is applied across all processes due to its suitability for providing good estimates as is the scope of this work and create a solid foundation for techno-economic assessments. The acid gas removal (AGR) section with MEA is not modelled in Aspen Plus but instead the mass and energy requirements are calculated using equations provided in the Gas Processors Suppliers Association (GPSA) Engineering Databook [266]. There is little information on OMEx modelling which is mostly based on kinetics so as to simplify the OMEx reactor, mass yield fractions are implemented based on the work of Schmitz et al. [134]. In the gasification section, two types of gasifiers are considered based on the final product. An

entrained flow gasifier (EFG) is used in FTS and OMEx synthesis while a dual fluidised bed (DFB) gasifier is used in methanation. This is because a DFB gasifier promotes the formation of methane thereby maximising the final output (bioSNG) while the entrained flow gasifier destroys hydrocarbons such as methane formed during the gasification process. The cryogenic air separation unit for the EFG is not modelled in this work. Instead it is represented by an MCOMPR block and the power requirements are calculated based on the report in [267] that a cryogenic air separation system consumes about 260 to 340 kWh of energy per ton (1,016 kg) of oxygen produced with 90% used by the main compressor depending on the plant capacity. Additional modelling information for this chapter is available in Appendix D.

5.2.1 Biomass preparation

Wood is used as the main feedstock in all production routes. The estimated amount of waste wood biomass used in the UK in 2019 was 3.98 million tonnes per year [268] and based on the figures in previous years, this figure is expected to increase year on year. In 2013, the overall potential availability of wood fibre in Britain was 15.6 million tonnes per year and this figure was expected to grow up to over 18 million tonnes per year by 2029 [269]. This highlights the potential for the use of wood as biomass.

In this study, it is assumed that the wood is received without any pre-processing. All drying and processing is performed on the plant and the feed rate of wood to the plant is 1200 tonnes per day (t/d) on a wet basis with 15% moisture for large-scale fuel production. The composition of the wood is detailed in Table 5.1.

Table 5.1: Proximate and ultimate analysis of woody biomass [237].

White wood pellet	Wt%
Moisture	15.00
Volatile matter	83.70
Fixed carbon	15.55
Ash	0.75
C	51.89
H	6.79
N	0.16
S	0.02
Cl	0.01
O	40.38
LHV (MJ/kg)	16.28
Price (£/tonne)	50.00

In the preparation section of the plant, wood is dried and milled to 1 mm for EFG and 6 mm for the DFB gasifier. For the entrained flow gasifier, a chopper is first employed to reduce the size of the wood to 12 mm and then a grinder is used to further reduce the size to 1 mm. The electrical requirement for the chopper is scaled from Swanson et al. [155] while the electrical requirement of the grinder is calculated using the regressions from Mani et al. [270].

The chopped wood is sent to the drier to reduce the moisture level to 10%. This is achieved by steam drying and the reaction is modelled in an RSTOIC reactor based on the equation:

$$\text{Wood (wet)} \rightarrow 0.0555\text{H}_2 \tag{5.1}$$

A calculator block using FORTRAN statements defined in Aspen Plus determines the amount of steam to the reactor and the extent of drying (the final moisture content is 10%).

5.2.2 Biomass gasification

The gasification process involves several steps which can be split into different zones in the gasifier. The steps include the drying stage where the moisture content of biomass is reduced and removed in the form of steam; the pyrolysis stage where the biomass feed is thermally decomposed in the absence of an oxidising agent releasing volatile matter, tar and char; and the oxidation stage where the volatile matter and some of the char undergo oxidation with limited oxygen present in the gasifying media supplied to the gasifier.

The gasifying media could be air, oxygen (O_2), steam (H_2O) or carbon dioxide (CO_2). However, the choice of gasifying agent affects the heating value of the product gas. Air is the poorest choice as it results in the lowest heating value range of 4 – 7 MJ/Nm^3 [62] because the high amount of nitrogen present in the product gas dilutes the quality of the product gas. Steam is a better gasifying agent which gives a product gas with a heating value in the range of 10 – 18 MJ/Nm^3; this higher heating value is because of the increased H/C ratio. Pure oxygen results in a product gas with a heating value in the range of 12 – 28 MJ/Nm^3 [62] however, caution needs to be exercised when using oxygen; Ghassemi and Shahsavan-Markadeh [271] observed that while increasing the O/C content would increase the cold gas efficiency and heating value of the product gas, there is a threshold beyond which the effect becomes negative.

Gasification occurs in different types of gasifiers – fixed or moving bed, fluidised and entrained flow bed. The choice of gasifier is dependent on the range of application and desired outcome. Fixed or moving bed gasifiers include the updraft gasifier, downdraft gasifier and crossdraft gasifier, which are suitable for applications in the range of 10 kW – 10 MW but it experiences problems such as tar production and entrainment and difficulty maintaining uniform temperature due to poor mixing. The fluidised bed gasifier includes the bubbling fluidised bed and circulating fluidised bed gasifiers which are capable of perfect mixing and maintaining a uniform temperature. Fluidised bed gasifiers operate at moderately high temperatures (1000°C) but experience char entrainment in the product gas; a cyclone is used to solve this problem. The entrained flow gasifier (EFG) is commonly used in large scale operations and basically acts like a plug flow reactor. Conditions in the gasifier are such that the residence time of biomass particles in the reactor is short, carbon conversion is up to 99.5% and the product gas contains very little or even no tar. These conditions include high temperatures of up to 1600°C and high pressure, up to 80 bar and finely reduced biomass below 75 µm [62].

The gasification module consists of a combination of unit operations. An RYIELD reactor present in both gasifiers decomposes the non-conventional biomass into conventional components based on the ultimate analysis. The entrained flow gasifier is modelled after the GE gasifier which is approximately at equilibrium using an RGIBBS reactor, which estimates the composition of the syngas product by minimising the Gibbs free energy. The option to restrict equilibrium by specifying the temperature of individual reactions is employed and applied to the water-gas shift reaction, see (Eqn. 5.4). The equations modelled in the gasifier are given as follows:

$$C + 2H_2 \rightarrow CH_4 \tag{5.2}$$

$$2C + 1.5O_2 \rightarrow CO + CO_2 \tag{5.3}$$

$$CO + H_2O \rightarrow CO_2 + H_2 \tag{5.4}$$

$$2CO + O_2 \rightarrow 2CO_2 \tag{5.5}$$

$$H_2 + S \rightarrow H_2S \tag{5.6}$$

$$0.5N_2 + 1.5H_2 \rightarrow NH_3 \tag{5.7}$$

$$CO + H_2S \rightarrow COS + H_2 \quad (5.8)$$

$$H_2 + Cl_2 \rightarrow 2HCl \quad (5.9)$$

Steam and oxygen are used as the gasifying agents. The oxygen to carbon mole ratio is set at 0.25 while the steam to carbon mole ratio is set at 0.75 based on the stoichiometric equation for syngas formation[272].

$$1.34C + 0.34O_2 + H_2O \rightarrow 0.34CO_2 + CO + H_2 \quad (5.10)$$

Oxygen at 95% purity from an air separation unit is fed in at 149 °C and 28 bar while steam generated on the plant is fed in at 120 °C and 28 bar. Before the dried biomass goes into the Gibbs reactor, it is pressurised in a lock hopper using CO_2, an inert gas, produced from the AGR section at 0.09 kg/kg dry biomass as reported by Higman and van der Burgt [76] for gasifiers at 25 bar. The EFG operates at 1300 °C and 28 bar.

Table 5.2: Syngas compositions from EFG and DFB gasifier (vol% dry basis).

	EF gasifier	DFB gasifier
H_2	47.50	45.40
CO	40.80	23.10
CO_2	8.34	16.50
N_2	3.35	0.09
H_2O (vol% wet)	21.5	4.37
CH_4	1.42×10^{-2}	8.24
NH_3	6.75×10^{-7}	2.85×10^{-8}
HCl	6.40×10^{-7}	5.14×10^{-7}
H_2S	3.54×10^{-7}	0.01
C_2H_2	-	0.12
C_2H_4	-	1.98
C_2H_6	-	0.18

The DFB gasifier is based on the Göteborg biomass gasification project (GoBiGas) plant in Sweden that produced bioSNG from woody biomass gasification [273]. In the DFB gasifier, gasification occurs in one fluidised bed and the heat for gasification is generated in the other fluidised bed. In this gasifier, since air is introduced in a different zone, the syngas is practically nitrogen free.

Steam is introduced to the gasifier for steam to biomass (dry ash free) mass ratio of 0.5. The DFB gasifier operates at 1.24 bar and 870 °C. The syngas compositions for both gasifiers are presented in Table 5.2.

5.2.3 Syngas cleaning and conditioning

Syngas leaving the gasifier contains impurities such as tar, particulate matter (PM) and poisonous gases including hydrogen sulphide (H_2S), sulphur dioxide (SO_2), hydrogen chloride (HCl) and ammonia (NH_3). These contaminants need to be removed before downstream applications to prevent hazards including plugging, deactivation of catalysts and corrosion which would consequently affect the process efficiency [274,275]. The gas cleaning method is based on the cleaning temperature – hot gas cleanup and cold gas cleanup.

In this study, the cold gas cleanup method is applied as it is the most common method across fuel production processes. For the EFG, the syngas is cooled by direct-contact water quench to 203 °C and then slag from melted ash is removed from the syngas using a separator. Wet scrubbing using water is applied in a flash unit to simulate removal of impurities such as NH_3, HCl and Cl_2. In FTS, the H_2/CO ratio is 1.17 which quite low. To adjust the ratio to the optimal value of 2.1 for FTS, a sour water-gas shift (SWGS) reactor is used. This reaction is modelled in an REQUIL reactor. For suitable WGS activity and to reduce the volume of the SWGS reactor, only a portion of the syngas undergoes the reaction. To achieve the optimal ratio, a design specification to set the temperature of the reactor and a calculator block to set the steam flow rate to the reactor at 3 times the flow rate of CO in syngas to the reactor are used. In OMEx synthesis, the H_2/CO ratio is adjusted to 3 for methanol synthesis in an SWGS reactor. This is achieved in an REQUIL reactor and a design specification where the flow rate of steam is varied.

The adjusted syngas is further cooled and water removed in three flash units before the acid gas removal (AGR) section. In the AGR section, CO_2 and H_2S are removed using 30 wt% MEA. This is not modelled in Aspen Plus but the reboiler duty, cooling duty and pump requirements are calculated based on the equations in the Engineering Date Book [266]. In OMEx synthesis, the amount of CO_2 removed is set by the stoichiometric ratio of $(H_2 - CO_2)/(CO+CO_2)$. This is set at 2.1 as the optimal value should be greater than 2 [110]. Also, this keeps the CO_2 composition in the syngas at ≤ 7% in order to improve the methanol productivity [276]. In FTS, CO_2 and H_2S removal are set at 96% and 99%, respectively.

In methanation, after the dual fluidised bed gasifier, tar is condensed from the raw syngas in a three-phase flash unit and recycled to the combustor to be burnt alongside char for heat generation.

Table 5.3: Acid Gas Removal (AGR) estimated parameters.

Acid Gas parameter	FT Synthesis	Methanation	OMEx synthesis
Circulation rate (m^3/h)	537.4	382.5	634.7
Absorber pressure (bar)	22.1	15.6	24.8
Stripper pressure (bar)	1.01	1.01	1.01
Reboiler duty (MW)	49.9	35.5	59.0
Condenser duty (MW)	20.8	14.8	24.6
Amine cooler duty (MW)	10.4	7.4	12.3

After this, the cyclic hydrocarbons - benzene and toluene - are removed from the syngas and also recycled to be burnt with tar and char. This occurs when the raw syngas is passed through an activated carbon bed modelled by a separator unit. Before removing the rest of the impurities, the syngas is compressed to the methanation pressure of 16 bar then cooled to 40 °C for acid gas removal using 30 wt% MEA. CO_2 and H_2S removal are set as the same in FTS. A guard bed located after the AGR section and before the water-gas shift (WGS) reactor absorbs impurities to prevent possible contamination of catalysts upstream. In the WGS reactor, a design specification to maintain a desired H_2/CO ratio of 3.5 in the clean syngas is used. This is due to the optimal value of the methane synthesis being greater than 3 as seen in the equation:

$$3H_2 + CO \rightarrow CH_4 + H_2O \tag{5.11}$$

5.2.4 Fuel synthesis

5.2.4.1 Fischer-Tropsch Synthesis

A block flow diagram of the FTS is seen in Figure 2.7. In the FTS, syngas is compressed to 25 bar and heated to 200 °C before passing through a zinc-oxide guard bed modelled using a separator unit to reduce H_2S to 200 ppb/50 ppb to avoid catalyst poisoning in the FTS reactor. Before the FTS reactor, a pressure swing absorber (PSA) isolates a stream of hydrogen from a fraction of the syngas for hydroprocessing of wax downstream of the FTS reactor. The FTS reactor operates at 25 bar and 200 °C using a cobalt-based catalyst [155] and is modelled as a RSTOIC reactor. The product distribution was estimated by the Anderson-Schluz-Flory (ASF) model (described in Song et al. [277]) with a chain growth factor of 0.9 and carbon monoxide per-pass conversion of 40% [155]. This was implemented using a calculator block with FORTRAN statements. The output of the FTS reactor consisted of unconverted syngas, light gases and hydrocarbons. The hydrocarbons produced were all alkanes from C_1 – C_{20} and C_{30}. Alkanes from C_5 to C_{10} were grouped as naphtha, C_{11} to C_{20}

were grouped as diesel and C_{20} to C_{30} was wax. The products were separated in a series of flash units and vacuum distillation (RADFRAC) columns. Wax was further cracked to naphtha and diesel using the hydrogen stream isolated earlier on in a RSTOIC reactor operating at 370 °C and 0 bar. A small portion of the unconverted syngas stream was sent to the power generation to prevent accumulation in the FTS reactor and generate power for the plant. The recycle ratio observed was 1.38; however, this is not an optimised recycle ratio as this is not included in the scope of this work.

5.2.4.2 Methanation

The methanation process is modelled after the GoBiGas setup [211]. In a premethanation reactor, hydrocarbons present in the syngas are cracked using steam while some of the CO and CO_2 present are converted to methane. The steam to hydrocarbon ratio is set at 0.5 [278]. Syngas goes into methanation at 16 bar and 300°C. Methanation takes place in a series of four reactors without recycle based on the Topsøe Recycle Energy-efficient Methanation Process (TREMP) using the MCR catalyst [121]. Coolers are situated between reactors due to the exothermic nature of the reaction and to maintain catalyst activity. The heat removed is recovered later in the process to generate steam for parts of the plant. Steam is added to the first reactor to prevent the formation of carbon on the catalyst. The methanation reactors are modelled as RGIBBS reactors with a pressure drop of 0.5 bar in each reactor. BioSNG is upgraded to recover unconverted H_2 and reduce CO_2 in the final product.

5.2.4.3 Oxymethylene ethers Synthesis

OMEx is synthesised via the methanol and formaldehyde route seen in Figure 2.8 so the first step in this process is the conversion of syngas to methanol. Methanol synthesis was modelled after the ICI Synetix Methanol process available from the Aspen Plus database. Syngas is compressed to 80 bar in two stages and then cooled to 230 °C before the reactor. In the ICI Synetix process, the methanol reactor is modelled as four RPLUG reactors in series with fresh syngas introduced between each reactor for cooling. In this work, the reactor is modelled as a single REQUIL reactor operating at 250 °C and 80 bar (see Appendix D). The reactions occurring in the reactor include the WGS reaction in equation (4) and the following:

$$3H_2 + CO_2 \rightarrow CH_3OH + H_2O \tag{5.12}$$

$$2H_2 + CO \rightarrow CH_3OH \quad (5.13)$$

Crude methanol is cooled to 38 °C and flashed where most of the methanol leaves in one stream. The other stream containing unconverted syngas and some methanol is compressed and recycled to the reactor. However, a fraction of this purged and sent to power generation to prevent build up. The methanol stream is sent to methanol recovery where a couple of flash units and distillation (RADFRAC) columns are used to separate methanol from CO_2 and H_2O. The CO_2 recovered in this part of the plant is sent to compression in the CCS plant while H_2O is sent to wastewater treatment.

In an RSTOIC reactor operating at 200 °C and 3 bar, methanol (MeOH) is converted to formaldehyde (FA) using air at a conversion rate of 87%. Based on the stoichiometric reaction and required conversion, the air flow to the reactor is determined by a calculator block. The product contains 37 wt% FA. In the OMEx reactor, H_2O, FA and MeOH go through a series of reactions forming hemiacetals and glycols, which in turn react with FA and MeOH to form OMEx. The reaction pathways are detailed in Schmitz [279]. In this work, this is modelled as an RYIELD reactor operating at 96 °C and 3.04 bar over Amberlyst-36 catalyst based on mass fractions calculated from the mass balance in the model by Ai [280]. Ai [280] modelled the OMEx synthesis and this consisted of a CSTR and distillation columns to separate the products and recycle $OME_{1\text{-}2,4\text{-}8,}$ FA and MeOH. The energy requirements in distillation of the products (modelled as separator units) were calculated from this work at 44.7 MJ/kg of OMEx produced for the heating duty and 47.1 MJ/kg for the cooling duty. The final OMEx product is a mix of OME_3 – OME_5.

5.2.5 Power and steam generation

Heat recovery from syngas cleaning is used to generate steam for different parts of the plan. In FTS, unconverted syngas is burnt in a combustor with 25% excess air to fully combust the purge gas. The flue gas generates electricity after passing through a gas turbine before heat recovery from the flue gas to generate steam for the drier, gasifier and SWGS reactor. Also, heat from the syngas cooling section is recovered to generate steam for the steam turbine. In methanation, a portion of the bioSNG produced (10% without CCS and 30% in the CCS case) is sent to a combined cycle where electricity is produced to meet the plant demand. Heat is recovered from the flue gas in a similar manner in order to generate steam for parts of the plant (gasification, WGS reactor, methanation) and the steam turbine. Other streams for

heat recovery include the flue gas from the dual gasifier and intermediate streams from the methanation reactors. In OMEx synthesis, methanol purge streams from the methanol synthesis are burnt and used to generate steam to drive the steam turbine.

5.2.6 CO_2 compression

For the cases with CCS, the CO_2 captured from the amine plant needs to be compressed and liquefied (supercritical fluid) before pipeline transportation and geological storage. This is achieved by multiple compressors with interstage cooling and then a pump and a final cooler. CO_2 is compressed up to 110 bar [281] and cooled to 35 °C. This final condition is based on the phase diagram of CO_2 [282]; at this pressure and temperature, CO_2 exists as a supercritical fluid and can be easily transported using pipelines to a final underground storage site. It is essential that impurity and water levels are kept below the recommended levels [282] to prevent corrosion of the transportation pipelines. To achieve this, CO_2 entering the CO_2 compression undergoes gas conditioning to minimise the concentration of impurities and water level.

5.3 Economic Assessment

An economic model was built to determine the feasibility of production of each product as well as monitor the effect of certain parameters on the price. Discounted cash flow rate of return (DCFROR) analysis, net present value (NPV) break-even analysis to estimate the minimum selling price (MSP) of the biofuels. The major economic assumptions are listed in Table 5.4.

Table 5.4: Process economic assumptions.

Parameter	Value
Location	United Kingdom
Currency	GBP
Base year	2018
Project lifetime (years)	20
Construction period (years)	2.5
Start-up time (years)	0.5
Capacity factor (%)	85
Tax rate (%)	30
Equity/Debt (%/%)	100/0
Discount rate (%)	10
Depreciation	Straight-line
Depreciation period (yr)	10
Salvage value (£)	0

5.3.1 Capital, operating and maintenance expenditures

The total capital investment (TCI) estimates are commonly based on the total purchased equipment costs (TPEC), installation factors and contingency. The methodology for TCI estimation is listed in Table 5.5.

Non-installed direct costs are broken down into 29% buildings, 12% yard improvements and 6% land while indirect costs are broken down into 32% engineering and supervision, 34% construction expenses and 23% contractor's fee and legal expenses [154,155].

In this work, the TCI for each plant was calculated using the factorial estimation method and the costs for the major components were taken from the open literature.

Table 5.5: Total Capital Investment (TCI) estimation methodology.

Parameter	Method
Total Purchased Equipment Cost (TPEC)	Aspen Process Economic Analyzer, open literature
Total Installed Cost (TIC)	TPEC Installation factor
Non-installed Direct Costs (NDC)	47% of TPEC
Indirect Costs (IC)	89% of TPEC
Contingency (CC)	20% of TPEC
Fixed Capital Investment (FCI)	TIC + CC + NDC + IC
Working Capital (WC)	15% of FCI
Total Capital Investment (TCI)	FCI + WC

Other unit operations that are not available in the open literature were estimated using the Aspen Process Economic Analyzer (APEA). However, due to the installation factors by APEA being generally low, an overall installation factor of 3.02 was used as suggested by Peters et al. [219] for solid-liquid plants. Equipment costs were calculated using Eqn. (5.14).

$$\text{Cost} = \text{Cost}_0 \times \left(\frac{\text{Scale}}{\text{Scale}_0}\right)^{\text{n}} \tag{5.14}$$

Where 'Cost_0' and 'Scale_0' represent the cost and capacity of the base unit; 'Cost' and 'Scale' represent the estimated cost and actual size of the plant equipment; and 'n' is the scaling factor. The base capacity and cost for units obtained from the open literature are listed in Table B1 in the Appendix B. After converting currencies using the average yearly exchange rate of the corresponding years, the costs were converted to GBP using the Chemical Engineering Plant Cost Index (CEPCI). The scaling factors were obtained from Tagomori et al., Thunman et al. and Sinnott and Towler [150,156,218].

The operating and maintenance (OPEX) costs (summarised in Table B2 and Table B3 in the Appendix B) covers every other cost for the day-to-day running of the plant. This includes labour costs, maintenance, insurance and purchase of raw materials. For this study, the fixed costs were estimated using guidance from Peters et al. and Sinnott and Towler [218,219]. The labour costs were estimated using data from Glassdoor and Payscale [283,284]. The number of employees and shifts were derived from Phillips et al. [285]. In FTS and methanation, there are 8 maintenance technicians and 20 shift operators while in OMEx synthesis, there is an extra section for methanol synthesis, increasing the number of maintenance technicians and shift operators to 12 and 30, respectively.

5.3.2 Levelised cost of fuel (LCOF)

The levelised cost of fuel represents the cost of producing a unit of fuel. This includes the amortized capital investment over the life of the plant and the yearly operating and maintenance costs. For each process, it is calculated as follows:

$$\text{LCOF } (£/\text{GJ}) = \frac{(\text{FCF} \times \text{TCI}) + \text{OPEX} - \text{Revenues from by-products}}{Q_{\text{fuel}} \times \text{CF} \times 8766} \tag{5.15}$$

$$\text{FCF} = \frac{i(1+i)^n}{(1+i)^n - 1} \tag{5.16}$$

Where 'FCF' is the fixed charge factor determined by the discount rate (i) and plant lifetime (n); 'TCI' is the total capital investment in GBP, 'OPEX' is the yearly operating costs including the cost of feedstock in £/yr; 'by-products' is the revenue generated from sale of by-products such as electricity in £/yr; 'Q_{fuel}' is the fuel energy output in GJ/hr; 'CF is the plant availability; and 8766 represents the total number of hours in a year.

5.3.3 Minimum selling price (MSP)

After determining the capital, operating and maintenance costs, the minimum fuel selling price is determined using a DCFROR analysis. The MSP is the calculated at the selling price of fuel when the NPV is equal to zero at the fixed discount rate over the plant lifetime. This is achieved using the NPV function and solver in Excel. The equation for the DCFROR is outlined as follows:

$$\sum_{n=1}^{n=20} \frac{CF_n}{(1+i)^n} = 0 \tag{5.17}$$

$$CF_n = P(1 - t) + Dt \quad (5.18)$$

where 'CF_n' is the cash flow in year n; 'P' is the gross profits in year n; 't' is the tax rate; and 'D' is the depreciation.

5.3.4 CO_2 avoidance cost

The CO_2 avoidance cost represents the minimum carbon tax to be paid when the CCS plant is compared to a similar plant without CCS. In comparison to a similar plant, the cost is calculated on the basis of transportation and storage costs as capture is included in all scenarios. The avoidance cost is calculated as follows:

$$CO_2 \text{avoided } (£/tCO_2) = \frac{LCOF_{CCS} - LCOF_{ref}}{(tCO_2/MWh)_{ref} - (tCO_2/MWh)_{CCS}} \quad (5.19)$$

where LCOF is the levelised cost of fuel and (tCO_2/MWh) is the emission factor to the atmosphere. In this chapter, the CO_2 avoidance cost is compared to two plants; the first plant is a conventional fossil-derived fuel production plant such as the production of natural gas or diesel and the second plant is a biorefinery where biomass is converted to a biofuel. On both plants, CO_2 is not transported and stored, rather it is released to the atmosphere.

5.3.5 Process performance indicators

The performance of each plant can be quantified by several indicators. These performance indicators determine how efficient a production process is. The performance of the gasifier is determined by the cold gas efficiency which is calculated as the energy content of the resulting syngas against the energy content of dry ash free biomass sent to the gasifier.

$$CGE\% = \frac{\dot{m}_{syngas} \times LHV_{syngas}}{\dot{m}_{biomass} \times LHV_{biomass}} \times 100 \quad (5.20)$$

where $\dot{m}$ is the mass flowrate in kg/s and LHV is the lower heating value in MJ/kg.

Another important technical parameter considered is the overall energy conversion efficiency and it represents the amount of biomass energy present in the fuel generated. This value also considers the electricity input and output on the plant.

$$\eta = \frac{Q_{fuel}+El_{out}}{Q_{biomass}+El_{in}+Q_{in}} \quad (5.21)$$

where Q is the energy content in MW and El_{in} is the net electricity imported, El_{out} is the net electricity exported from the plant both in MW and Q_{in} is purchased heat in MW.

5.4 Results and Discussion

This section covers the technical, environmental and economic results and interpretation of the three production routes. For each route, with and without CCS scenarios are investigated. Then the results are compared to the conventional fossil-derived fuel counterparts. In addition, financial analysis is presented for all cases and a sensitivity analysis has been carried out for the CCS cases.

5.4.1 Mass balance

The diagrams in Figure 5.1 show the mass balance on the plant. A carbon balance is available in Appendix B. In both FTS cases, 43.9% of carbon in the feedstock to plant is stored in the resulting FT-fuels. In the FTS+CCS case, 46.8% of carbon is captured and 9.3% is vented in the flue gas from the power generation while 0.1% is lost in wastewater; in the FTS case, 56.1% is vented to the atmosphere. In both bioSNG cases, 32.6% of carbon is stored in bioSNG; in the bioSNG+CCS case 32.5% is captured and 34.9% is vented in the flue gas from the power generation and gasification; without CCS, 67.4% is vented to the atmosphere. In both OMEx synthesis cases, 52.9% of carbon to process is stored in OMEx. In OMEx+CCS, 45.4% of carbon is captured and 1.7% is vented to the atmosphere from waste streams; without CCS, 47.1% of carbon is vented to the atmosphere. The system with the least CO_2 venting is in the OMEx production while the most venting occurs in bioSNG production due to the flue gas generated from the dual fluidised gasifier.

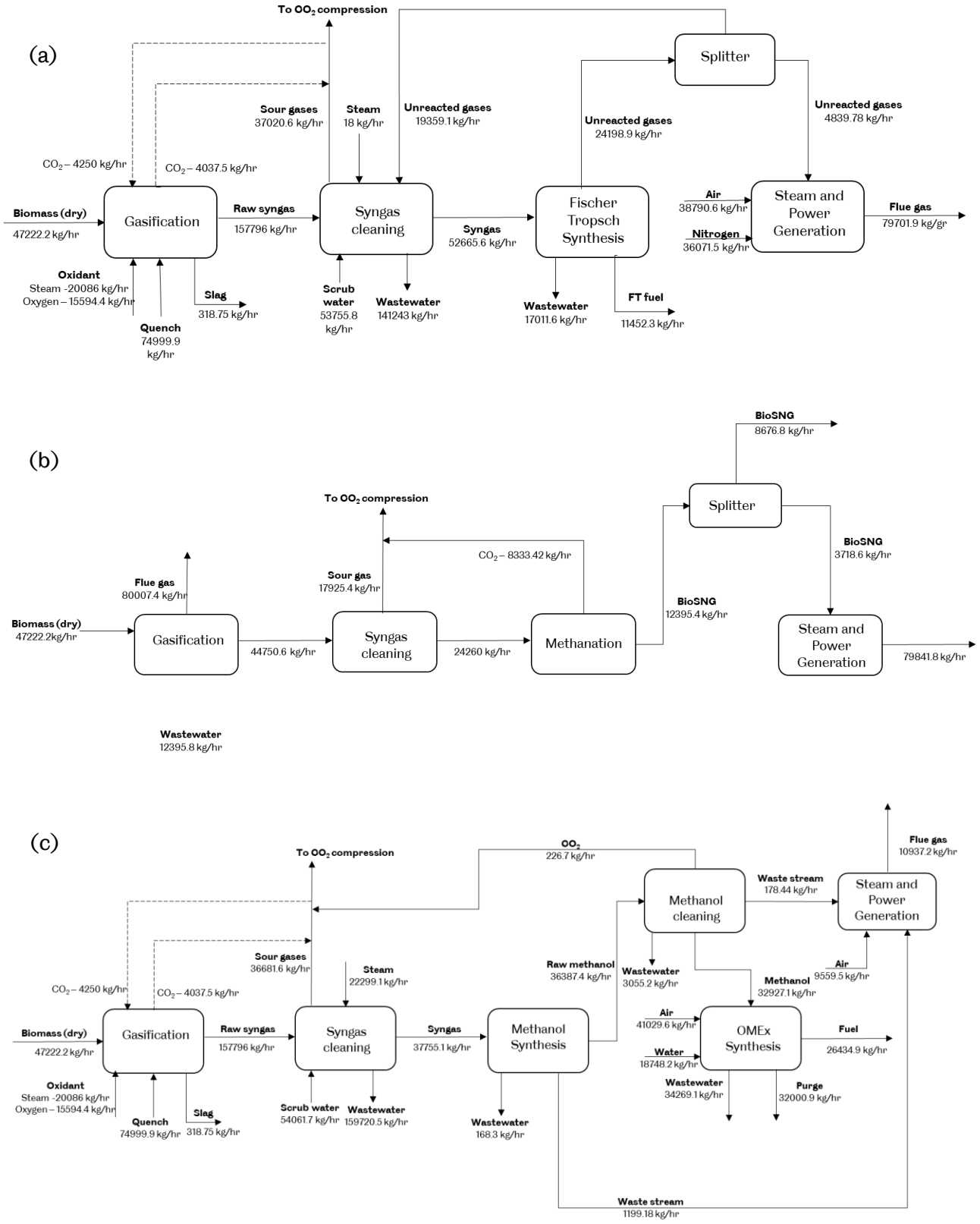

Figure 5.1: Mass balance investigated for the production routes (a) Fischer-Tropsch synthesis, (b) Methanation and (c) Oxymethylene ether synthesis.

5.4.2 Energy balance

Table 5.6: Power requirements and generation for three production routes without and with CCS.

Power (MW)	Fischer-Tropsch		Methanation		Oxymethylene ethers	
		CCS		CCS		CCS
USAGE						
Chopper	0.26	0.26	0.26	0.26	0.26	0.26
Grinder	1.36	1.36	0.32	0.32	1.36	1.36
Lock hopper system	0.10	0.10	-	-	0.10	0.10
AGR pumps	1.02	1.02	0.78	0.78	1.47	1.47
Syngas booster compressor	0.87	0.87	7.72	7.72	-	-
PSA compressor	0.08	0.08	-	-	-	-
Methanation compressor	-	-	0.18	0.18	-	-
BioSNG compressor	-	-	1.01	1.01	-	-
Naphtha pump	3.30E-04	3.30E-04	-	-	-	-
Diesel pump	7.10E-04	7.10E-04	-	-	-	-
MeOH synthesis compressors	-	-	-	-	4.86	4.86
MeOH cleaning pumps	-	-	-	-	2.20E-03	2.20E-03
OMEx pump	-	-	-	-	3.10E-03	3.10E-03
Air compressor (OMEx)	-	-	-	-	1.48	1.48
Hydroprocessing	0.21	0.21	-	-	-	-
Air compressor (GT)	2.82	2.82	7.88	7.88	-	-
Air Separation Unit	5.00	5.00	-	-	5.00	5.00
Oxygen compressor (ASU)	2.38	2.38	-	-	2.38	2.38
Water pumps (Steam generation)	0.05	0.05	0.02	0.02	0.31	0.31
CO_2 compression	0.00	5.00	0.00	3.60	0.00	4.68
Refrigeration	1.82	1.82	0.00	0.00	0.00	0.00
Total	16.20	21.20	18.20	21.80	17.70	22.40
GENERATION						
Gas Turbine	10.70	10.70	17.60	17.60	4.80	4.80
Steam Turbine	4.60	4.60	3.70	3.70	0.70	0.70
NET ELECTRICITY	-1.00	-6.00	3.18	-0.43	-12.30	-16.90
*negative net electricity signifies that electricity is imported						

In all production routes, the common sources of heating demand include the distillation columns, gasifier, dryers, intermediate heaters and power generation unit. The sources of cooling demand include distillation columns and intermediate coolers. Suitable heat integration was performed to recover useful heat from different streams and minimise heat

waste on the plant. This allowed manufacture of low pressure to high pressure steam where necessary for use in different locations in each plant. Where further heating was required, fired heat from natural gas was used. Further cooling was achieved with air, cooling water and refrigerants. Electricity was imported from the grid to meet power requirements in the case that a plant is not self-sustaining. Table 5.6 shows a breakdown of the power usage and generation for each production route.

5.4.3 Plant efficiency

The cold gas efficiency, given in Eqn. (5.20) is a technical parameter that represents the efficiency of the EFG and DFB gasifiers. A heat loss from the reactor is assumed as 1% of the biomass energy input. The efficiency of the EFG was calculated from Aspen at 87.2% and that of the DFB gasifier was calculated at 70.1%. The difference in these efficiencies lies in the operation of the gasifiers. In the DFG gasifier, further efficiency is lost due to char and tar formation when compared to the EFG which operates near equilibrium and destroys tar and char formed during the gasification process. The summary of the results from the process simulation are presented in Table 5.7.

Table 5.7: Summary of the process simulation results.

	FTS	FTS +CCS	BioSNG	BioSNG +CCS	OMEx	OMEx +CCS
Product yield (%)	22.9	22.9	19.8	19.8	52.9	52.9
Energy produced (MW)	111.1	111.1	131.8	131.8	140.4	140.4
Energy conversion (%)	44.9	44.0	59.7	58.2	48.5	47.7
Net heat input (MW)	20.5	20.5	0.0	0.0	51.3	51.3
Electricity produced (MW)	15.1	15.1	21.3	21.3	5.5	5.5
Electricity demand (MW)	16.2	21.2	18.2	21.8	17.7	22.4
Net electricity (MW)	-1.0	-6.0	3.18	-0.4	-12.3	-16.9

For all the biofuels considered, without CCS, the bioSNG route has the highest energy efficiency at 59.7% while the FT-fuel route has the lowest at 44.9%. With the CCS route, it is the same with bioSNG at 58.2% and the FT-fuel route at 44%. Across all three cases, the addition of CCS results in no more than a 1.5-percentage point drop.

In terms of mass yield, the OMEx route has the highest product yield at 53%. which is almost three times the yield of bioSNG even with additional synthesis steps, such as methanol synthesis and formaldehyde synthesis. Due to the recycling in OMEx synthesis to optimise the process, the OMEx yield from methanol increases from 38% reported in Zhang et al. [286], to 83%, as proposed by Ai et al. [280]. This 83% mass yield corresponds to a methanol conversion of 99.9%. Also, the syngas conversion to methanol process is 95%. In FTS, the single pass conversion is 40%; by recycling unconverted syngas, this goes up to 73%.

Energy efficiency loss in routes using the EFG (FTS and OMEx synthesis) is due to the cooling method of the raw syngas. Quench cooling is used and, in this way, sensible heat that would otherwise be recovered for heat integration is lost. Cool gas cleanup is used with the EFG and this induces energy penalties on the plant but switching to hot gas cleanup can reduce waste streams and costs while the overall plant efficiency is improved when compared to cold gas cleanup. To improve the efficiency, radiant cooling is more suitable, but the capital costs will increase. For the bioSNG route, the product yield decreases due to a portion being sent off to generate power for the plant demand; this in turn reduces the energy conversion efficiency.

The FT-fuel yield of 22.9% is comparable to values reported in the literature; Tagomori et al. [150] reports a yield of up to 15% for FT-liquids from forestry residue while Dimitriou et al. [154] reports a yield of 20.4% using an entrained flow gasifier and woody biomass to produce FT-fuel. The initial yield of bioSNG at 25% is consistent with the value of bioSNG yield of 24% obtained using a gasifier operating at 1 bar as reported by Vitasari et al. [287]. For the OMEx yield, there is not much data available in the literature to compare the yield. Based on the experiment and modelling by Zhang et al. [286], the OMEx yield is 20% but the product contains mainly OME_1 and there is no recycling of the products to increase conversion. However, the methanol yield from biomass is compared. The stoichiometric ratio of $(H_2 - CO_2)/(CO+CO_2)$ in the syngas is set at 2.1 in this work as advised by E4Tech [110] and this gives methanol yield of 67%. In the models on OMEx production by Zhang et al. and Oyedun et al. [135,286], this ratio is set between 0.29 and 0.55 resulting in methanol yields between 29% and 52%. Also, in Phillips et al. [276], a stoichiometric ratio of 1 results in a methanol yield of 49%.

5.4.4 Capital, operating and maintenance expenditures

The total capital investment breakdown for all cases is presented in Figure 5.2. The capital cost is in the range of £146 - £ 296 million. The only contribution costs of CCS to the capital cost is associated with CO_2 compression as a capture unit is present in both cases. Likewise, the contribution costs of CCS to the operating and maintaining expenditure is associated with transport and storage. The highest capital cost is encountered in OMEx production. In this process, the major contribution to the capital cost is the fuel synthesis which is 41% of the entire cost. This fuel synthesis includes OMEx production from methanol and trioxane. In essence, this includes 4 synthesis units – formaldehyde, trioxane, methylal and OMEx syntheses.

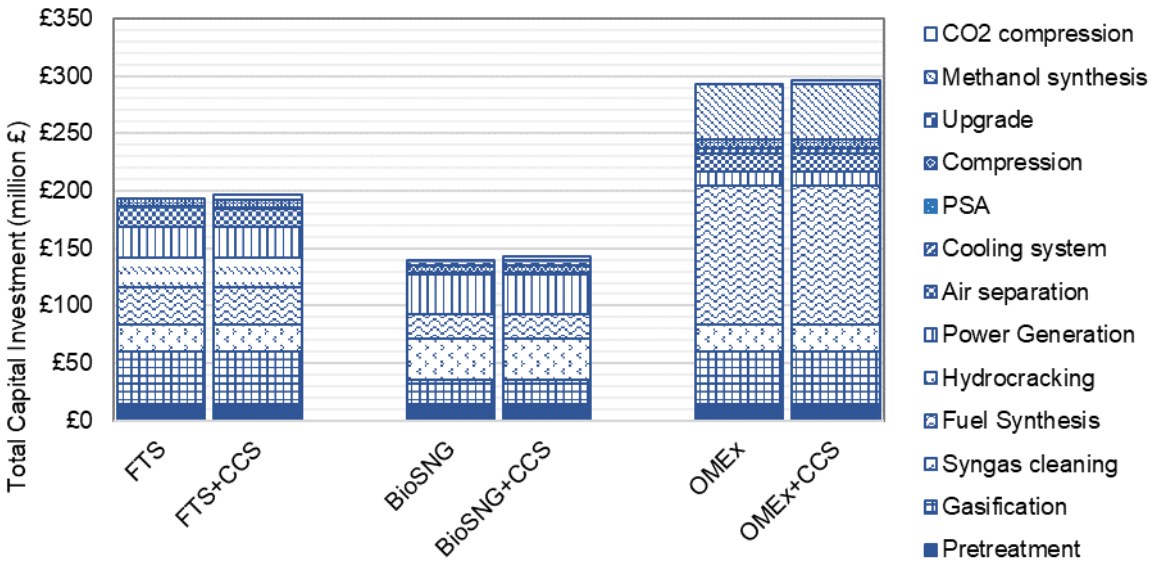

Figure 5.2: Total Capital Investment breakdown of three production routes without and with CCS.

For the FTS, gasification is the most significant contributor to the capital cost accounting for 24% of the total investment. In bioSNG production, syngas cleaning and the power generation section are the biggest contributors to the capital cost, each accounting for 25% of the overall cost. In bioSNG without CCS, excess electricity from burning a fraction of the product to meet plant demand is sold to generate revenue. In OMEx production, the fuel synthesis section accounts for 41% of the overall cost as a result of the additional synthesis steps required in the production process.

The cost of the entrained gasification units used in FTS and OMEx synthesis is noticeably higher than the cost of the dual fluidised gasifier used in methanation. The operating conditions of the gasifiers influence the gasification unit cost. The EFG operates at a significantly higher pressure of 28 bar than the DFB gasifier operating at atmospheric pressure. Also, the EFG operates at 1300 °C while the DFB operates at 870 °C. These are the conditions considered when designing the pressure vessel for the gasifier as these factors determine the thickness of the vessel and amount of materials required to build the gasifiers.

In all cases, the cost of additional CO_2 compression is between 1% and 2% of the total investment, thus indicating that the additional investment for CCS is minimal.

The annual operating cost and maintenance costs are presented in Figure 5.3. The feedstock cost is the same across all processes as the feed input is fixed at 1020 dt/d. In terms of the fixed cost which includes labour, insurance and rent; the methanation process has the lowest annual cost while OMEx has the highest cost.

This is the same trend as the total capital investment as the fixed costs are a fraction of the fixed capital investment. The feedstock cost is the major contributor to the operating costs in all cases except OMEx production where the variable cost dominates. The addition of transport & storage minimally affects the overall OPEX contributing to between 5.3% and 7.3% of this cost. While the variable cost is constant in FTS and methanation with the addition of CCS, the variable cost in OMEx production increases due to an increase in electricity demand in the OMEx plant which is not self-sufficient. The OMEx production clearly is the most expensive to run. This is due to several reasons such as the daily cost of electricity; the use of fired heat compared to the other plants to vaporise water for steam generation; and also, daily wastewater treatment and cooling water for heat exchange on the plant is significantly higher than the other plants due to more synthesis units required.

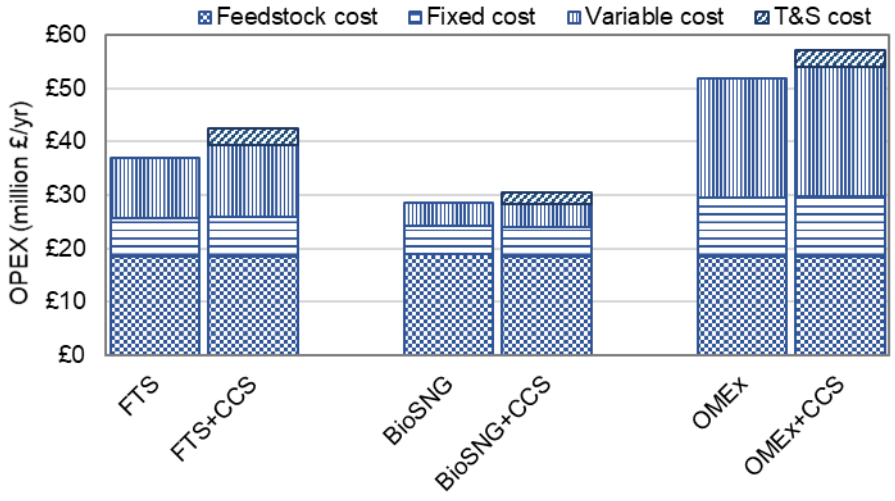

Figure 5.3: Operating and maintenance expenditure of three production routes without and with CCS.

5.4.5 Levelised cost of fuel (LCOF)

The levelised cost of fuel production is presented in Figure 5.4. It represents the costs – capital, operating and maintenance – required to produce one unit (GJ) of fuel based on the lower heating value. The cost of production of these biofuels is in the range £12/GJ - £23/GJ without CCS and £13/GJ - £24/GJ with CCS.

For all routes, the increase in the production costs is as a result of adding transport and storage; this includes the cost of additional compressors to prepare CO_2 for transportation, pipeline costs and storage costs. In FT-fuel and bioSNG, a value of 10% is observed and 7% in OMEx production mainly due to the decrease in electricity export revenue and an increased operating expenditure. Overall, bio-SNG production still has the least production cost with and without CCS while OMEx has the highest production cost. The production cost is a function of the capital cost, fixed charge factor, by-products and fuel output as presented in Eqn. (5.15).

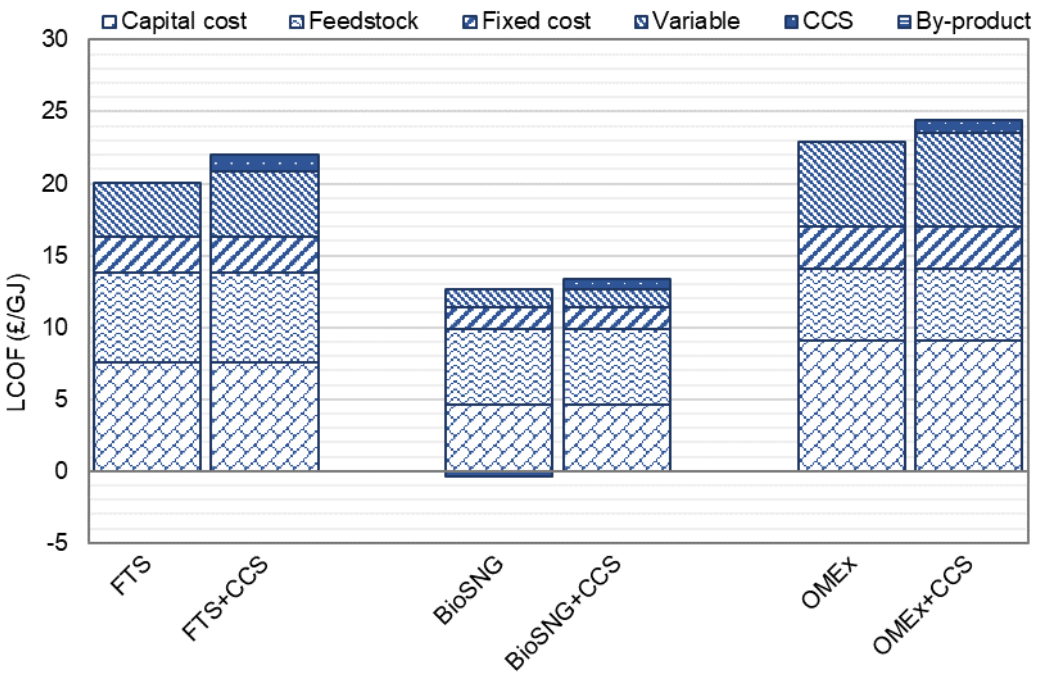

Figure 5.4: Levelised cost of fuel production for three production routes without and with CCS.

Based on the trend of the total capital investment, it would be expected that the highest production cost would be for OMEx while the least would be for bioSNG and this is what is observed. The LCOF is dependent on the capital investment, operating expenditure and energy output. The production cost of FT-fuel and methane from biomass falls within the range 18.3 – 35.3 £/GJ and 15.3 – 27.5 £/GJ (1 £/GJ = 3.6 £/MWh) respectively as reported by Brown et al. [288]. The values calculated in our work are comparable to this range for FT-fuels and bioSNG. Comparing the OMEx production cost, Oyedun et al. [135] report a value of £1.24/L (from $1.67/L using exchange rate values for 2016) when processing 500 t/d of woody biomass day. While Schmitz et al. [134] report a value £0.41/L (from $614.8/t assuming OMEx density of 1097 kg/m^3 and exchange range values for 2014) when producing OMEx at 1 Mio. t/yr. For this work, the values are 0.47 – 0.50 £/L when processing 1200 t/d for an output of 0.2 Mio. t/yr.

5.4.6 Greenhouse gas (GHG) emissions

Greenhouse gas (GHG) emissions are a source of environmental concern when establishing a production plant. In this sub-section, the GHG emissions for each production route are characterised by emission factors. The emission factor estimates how much greenhouse gases in CO_2 equivalent is released per unit of energy output; this also measures the potential for negative emissions. This emission factor includes the biomass harvesting and processing emissions, natural gas for fired heat on the plant, electricity imported to the plant and CH_4

and N_2O emissions in the resulting biofuels. It basically covers the lifetime emissions of biomass use but excludes emissions from transportation and distribution of the biofuels.

The emission factors used in this study are GHG conversion factors based on the outline from the UK Department of Business, Energy and Industrial Strategy (BEIS) [289]. The BEIS framework categorises the emissions based on activities into three scopes – Scope 1, Scope 2 and Scope 3. In this chapter, Scope 1 covers direct emissions from the plant itself such as fuel combustion which is zero for CO_2 emissions in the case of biomass and biofuels due to its status as CO_2 neutral. However, N_2O and CH_4 released are not absorbed in biomass regeneration so Scope 1 covers these gases. Scope 2 covers indirect emissions from the plant such as imported electricity and heat purchased to cover internal needs. Scope 3 covers indirect emissions from sources not owned or controlled by the plant such as the emissions due to harvesting, refining and transporting biomass. The values used in this study are presented in Table 5.8.

Table 5.8: Emission factors used in greenhouse gas reporting in this study [289].

Fuel	Scope 1 (kg CO_2e/kWh)	Scope 2 (kg CO_2e/kWh)	Scope 3 (kg CO_2e/kWh)	Overall emission factor (kg CO_2e/kWh)
Wood pellets	0.01563	--	0.03744	0.05307
Natural gas	0.20428	--	0.02657	0.23085
Electricity	--	0.25560	--	0.25560

The values for the three routes investigated with and without CCS are presented in Figure 5.5. Without CCS, all the production routes are net positive for GHG emissions. With CCS, there is a significant decrease of over 250% in the emission factors. While adding CCS is minimal to production costs (economics) – as seen in previous sub-section – the effect on the environment is significant in terms of huge emission savings.

Adding CCS to FT-fuel production results in negative emissions equivalent to a GHG mitigation potential of 519,000 tCO_2 per year; for bioSNG production, there exists a mitigation potential equivalent to 301,000 tCO_2 per year; and for the OMEx route, there is a mitigation potential equal to 303,000 tCO_2 per year. The OMEx route without CCS has the highest emission potential at 201,000 tCO_2/yr and this is mainly due to the indirect emissions from the purchased electricity. The OMEx route purchases the most electricity from the grid. This also limits the emission saving potential with CCS applied. The bioSNG route has the least emission savings potential with CCS. This is mainly due to the amount of captured and

stored carbon; looking at the carbon balance in Figure 5.1, the most amount of carbon is vented within this process due to the required gasification technology and power generation.

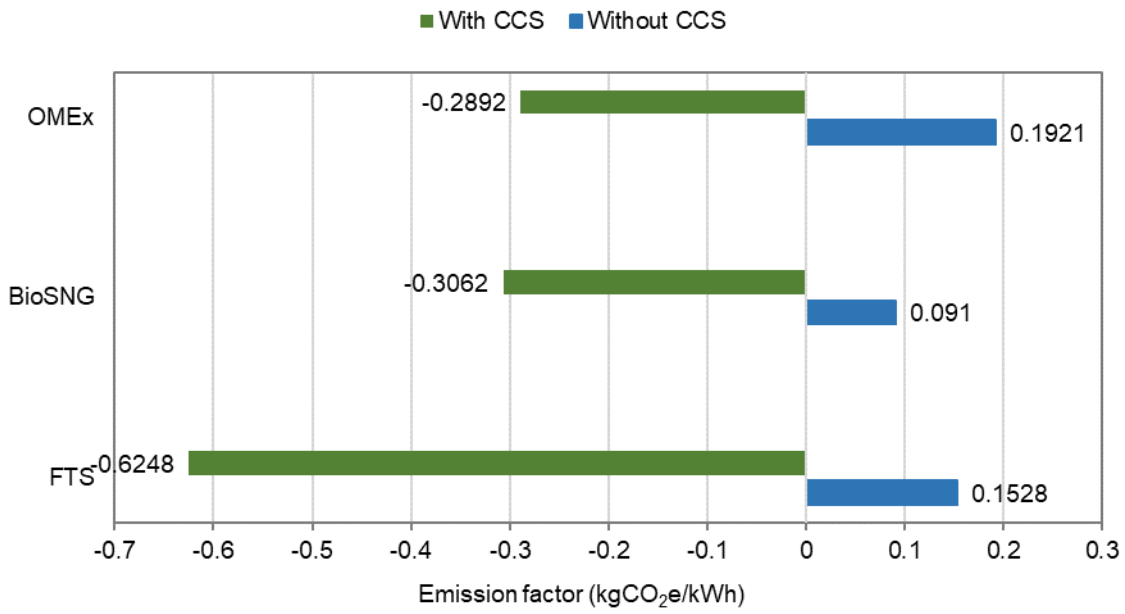

Figure 5.5: Emission of production routes without and with CCS.

While the OMEx route imports much electricity which contributes to emissions, a higher energy output and CO_2 capture helps in reducing the emission factor. The emission factor is also a function of energy output, so to decrease emissions and improve environmental performance, improving the plant efficiency, which results in a higher output is one way. Other ways include decreasing the amount of CO_2 vented to the atmosphere (especially with the bioSNG route) and limiting electricity imports from the grid by coupling to renewable energy power generation.

5.4.7 CO_2 avoidance cost

The CO_2 avoidance cost (in the CCS cases) Plant A refers to a conventional fossil fuel plant (natural gas for bioSNG and diesel for FT-fuel and OMEx) while Plant B refers to the biomass-based plant without CCS. These values represent the minimal carbon tax to be paid on CO_2 emissions. With the conventional plant, the values are much higher due to the lower cost of fuel production using fossil fuels. A maximum avoidance cost of £119/tonne CO_2 is reported in this study and it is comparable to the 2011 values reported for the UK. Charles et al. [290] reported an abatement cost of biofuels of £115/tonne CO_2 for bioethanol and £154/tonne CO_2 for used cooking oil diesel.

Table 5.9: CO_2 avoidance cost in £/tonne CO_2 with reference to a conventional plant and a bio-refinery.

	Plant A	Plant B
FTS	75.0	21.7
BioSNG	91.0	22.4
OMEx	119.0	25.7

Fuel switching to biomass resources results in a reduced avoidance cost as seen in the case of Plant B. Across the three routes, production of OMEx generally has the highest cost due to its relatively low emission factor as more emissions to the atmosphere needs to be paid for. In the bioSNG route, although a higher percentage of carbon is vented in the process, minimal electricity is purchased and there is no heat or steam purchase to indirectly increasing the CO_2 emissions from the process. The FT-fuel route has the lowest avoidance cost even with electricity and heat imports; however, the amount of emissions from these imports are offset by a higher amount of CO_2 capture in the process. Note that electricity and heat imports are less than half of what is required in the OMEx route. This is because the avoidance cost is a function of the emission factor and the more negative emissions achieved by a plant, the lower is the cost. Alternatively, increasing the price of conventional fossil-derived fuels will lower the avoidance cost. Finally, including BECCS in carbon trading systems will further result in reduced avoidance costs.

5.4.8 Comparison with fossil-derived fuels – diesel and natural gas

In this sub-section, the minimum selling price (MSP) of each biofuel is compared to the market price of conventional fossil fuels. While OMEx is a diesel additive, its production route will also be compared to diesel production cost. Using a DCFROR and NPV break-even analysis, the MSP was determined for all routes and presented in Table 5.10.

Table 5.10: Minimum biofuel selling price of three production routes without and with CCS.

	Without CCS (£/GJ)	With CCS (£/GJ)
FTS	22.5	23.4
BioSNG	14.3	14.5
OMEx	25.8	26.5

The average 2018 UK wholesale price of natural gas was £5.5/GJ [291] while that of diesel excluding UK fuel duty was £13.23/GJ [252] (for a diesel energy density of 32 MJ/l). The MSP for bioSNG with and without CCS is at least 2.5 times the cost of producing natural gas while the MSP of FT-fuels and OMEx is up to two times the price of conventional diesel price. This

means that the three routes investigated cannot compete with natural gas and diesel without process improvements to decrease costs and incentives such as policy schemes.

To encourage the production of these biofuels to compete with and phase out the dependence on fossil-derived fuels, policy instruments such as subsidies and carbon taxes are required. The next sub-section covers the existing policy schemes within the UK that support the production of biofuels and suggest a possible scheme to assist with decarbonisation.

5.4.9 Financial tools analysis

The UK government introduced the Renewable Transport Fuel Obligation (RTFO) in 2008 with the aim of reducing GHG emissions from fuel used for transport purposes. It lays out an obligation for fuel suppliers to meet a target of renewable fuel in each obligation period. Renewable Transport Fuel Certificates (RTFCs) are issued for each litre or kg of biofuel produced. For certain biofuel sources such as waste, double RTFCs are issued. As such, these RTFCs can be traded and the price is dependent on demand and supply. In the past, the trade prices have varied between £0.09 and £0.20 per certificate [292,293]. For this analysis, an RTFC price of £0.145/RTFC will be used. Based on the RTFO guidelines, for each litre of biofuel produced, 1 RTFC has been issued.

The Renewable Heat Incentive (RHI) established in 2009, provides financial support for renewable heat technologies. A tariff is paid to the renewable heat generator for each unit of energy generated. Currently, for biomethane produced and injected to the grid, the current tariff is an average of £22.16/MWh [294]; this is the value assumed for the plant's lifetime. BioSNG is also eligible for RTFCs at 1.9 RTFCs for each kilogram of biomethane, using feedstocks that are wastes or residues or dedicated energy crops doubles the RTFCs to 3.8 RTFCs/kg. In this case, biomass feedstock is assumed to be woody biomass and thus qualifies for the 1.9 RTFCs/kg and with preliminary calculations, the RHI provides more savings. The RHI is applied to bioSNG while the RTFO is applied to FT-fuels and OMEx.

Figure 5.6 depicts the effect of the RTFCs and the RHI on biofuel production. While the application of the RTFCs is beneficial to the production routes without and with CCS, it is still not enough to comfortably compete with the conventional diesel, only FTS without CCS is close enough.

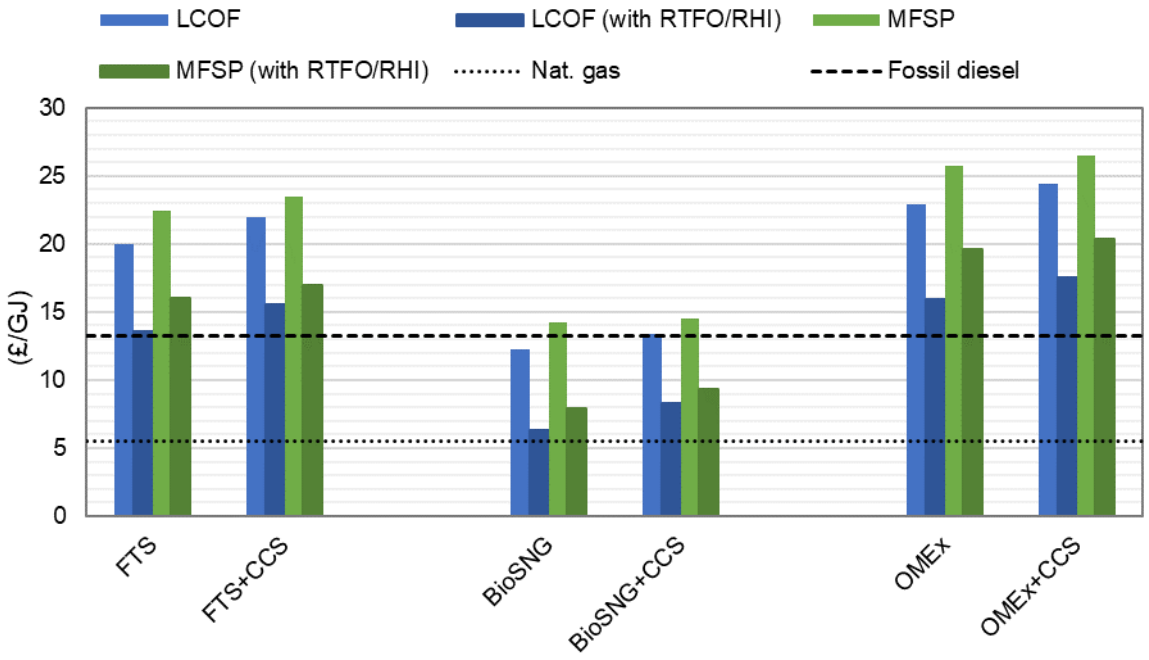

Figure 5.6: Effect of RTFO and RHI on the production cost and minimum fuel selling price of three production routes without and with CCS.

The MSP sees up to a 28% decrease for FT-fuels and up to a 24% decrease for OMEx. While the implementation of the RHI to bioSNG production decreases the minimum selling price by 44% without CCS and 36% with CCS, it is still not profitable and competitive with natural gas production. Further decreasing the MSP of all production routes will require switching to waste as feedstock so that the bioSNG process can qualify for 3.8 RTFCs/kg under the RTFO and the FT-fuels and OMEx can qualify for 2 RTFCs/l; also, this switch could result in a decrease in the feedstock price but at the same time the technical feasibility of waste to fuels is more challenging and less mature compared to virgin wood.

Carbon price is an effective tool in reducing GHG emissions when applied effectively. In the current EU emissions trading scheme applied by the UK, there is no credit for negative emissions. Applying a sufficient carbon price to close the carbon pricing gap will assist renewable technologies to fairly compete with fossil-fuel technologies and eventually decrease the dependence on fossil fuels by lowering the levelised cost of fuel of biofuels whilst increasing that of fossil-based fuels. Introducing a carbon price for negative emissions could boost the feasibility of producing biofuels because while revenue will be generated through this means, the price of fossil-derived fuels will increase as a result of paying the environmental price for positive emissions.

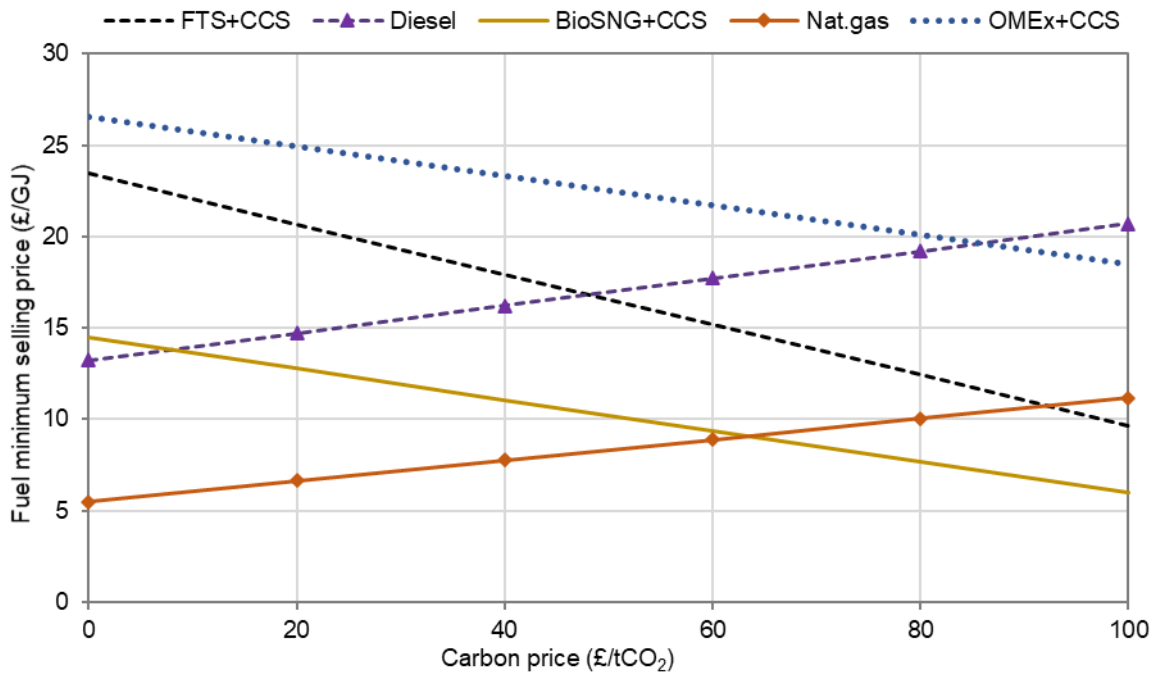

Figure 5.7: Effect of negative emission credit on minimum selling price of biofuels and fossil-derived fuels.

Figure 5.7 illustrates the dependency of the minimum selling price for the CCS cases on the carbon price (RTFO and RHI payments are not included). In this study, a break-even carbon price of £48/tCO_2 is required for FT-fuels to compete with fossil-derived diesel and a price of £86/tCO_2 is required for OMEx to compete. Higher carbon prices will discourage the production of diesel and favour the production of FT-fuels with CCS and OMEx with CCS as well as drive the development and deployment of this technology. With bioSNG, even with the increase in natural gas prices where a carbon price is introduced, a carbon price up to £63/tCO_2 is required to break even. The major barrier to the deployment of the bioSNG route is the very low price of natural gas. These break-even carbon prices are dependent on the emission factor of the production route. To further decrease the minimum carbon price required, the routes, especially the OMEx route will need to generate more negative emissions; doubling the emission factor halves the break-even carbon price.

Natural gas production currently enjoys a lot of benefits as it produces 50% less CO_2 emissions than coal [295] and is currently being used as a transition fuel. However, now is the time to prepare and cut the costs associated with bioSNG production to boost its feasibility as economies move towards decarbonisation.

5.4.10 Sensitivity analysis

The production cost of biofuel is dependent on different parameters. In this sub-section, a sensitivity analysis is performed to pinpoint the parameters that have a significant effect on the production cost. This analysis highlights the parameters to be focused on in making each route feasible and competitive. Generally, the parameters (CAPEX, plant life, biomass cost) are changed by ±30% of the base case scenario with the exceptions of the fuel output at ±10%, the interest rate at ±20%, the operating hours where the capacity factor is between 70% and 90% as not to the exceed the maximum hours in a year and CCS costs. Also, this analysis is only carried out for the CCS cases as the focus is on BECCS technologies and it is only the CCS cases that provide negative emissions. The results of the analysis are displayed in Figure 5.7.

The bars in the Figure 5.8 represent the sensitivity of each parameter to the production cost. Longer bars depict higher sensitivity while shorter bars depict lower sensitivity. From this, the most significant factor that will affect the production cost is the operating hours. The plant operating hours in a year is dependent on the capacity factor. Increasing the capacity factor to 90% while other factors are kept constant, decreases the production cost by 6% while decreasing the capacity factor to 70% results in a 21% increase in the production cost. Apart from maintenance, the capacity factor is affected by the feedstock availability. Where there is a shortage of supply, the capacity factor is reduced, thus resulting in decreased output. It is important that the supply of the biomass is sustainable and secure for each production route; this should also be applied for the biomass price to avoid fluctuations in price (at 30% uncertainty of feedstock price, fluctuations in production cost are -6% to +10%). Alternatively, considering a mix of biomass sources could be beneficial.

The next factors that significantly affect the production cost are the capital investment and the fuel output. Fluctuations of -15% to +15% in production cost are seen for an uncertainty of 30% in the capital investment while fluctuations of -9% to +11% are seen for an uncertainty of 10% in the fuel output. The possible decrease in production cost highlights the importance of improving the plant efficiency to increase the fuel output. As the data for the capital investment is acquired from factorial estimation and open literature, it is difficult to accurately predict the capital expenditure.

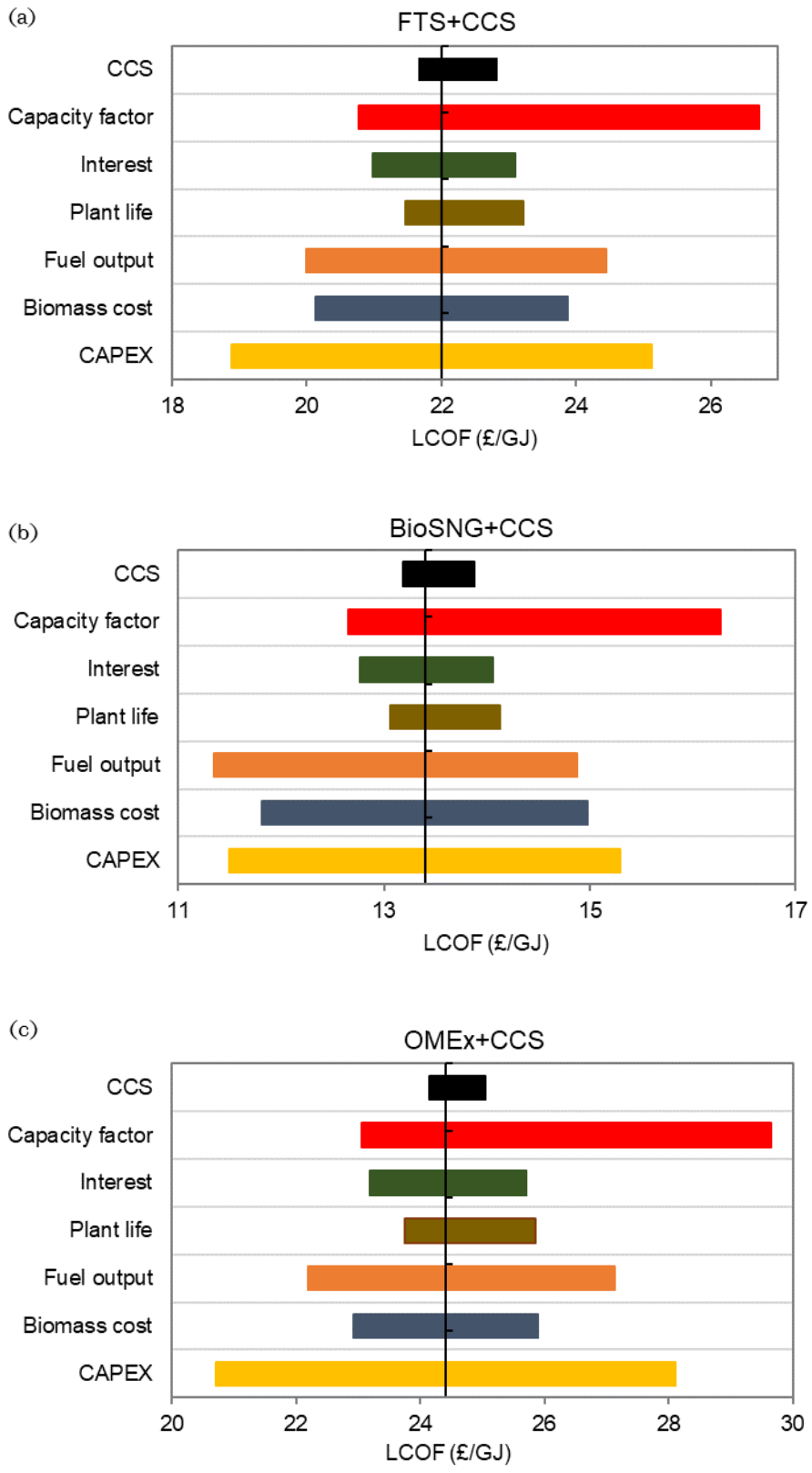

Figure 5.8: Sensitivity analysis on the production cost for three production routes with CCS (a) Fischer-Tropsch synthesis, (b) Methanation and (c) Oxymethylene ether synthesis.

Also, the capital investment is subject to location; importation of equipment attracts import duties and could result in increased CAPEX while producing within the country will not have such duties. Accurate data will be available where there are existing commercial plants. Until then, the initial estimates provided in this chapter are suitable for preliminary feasibility studies. Other parameters – CO_2 transport & storage costs and plant life – have minimal effect on the production cost.

5.5 Conclusion

BECCS is an integral concept to stabilizing and eventually reducing CO_2 levels in the atmosphere. Fuel generation already has an advantage due to the intrinsic capture unit and pure stream of CO_2 available providing an opportunity for easy CCS retrofitting. This work investigated the technical, economic and environmental performance of three biofuel production routes that have the potential to be BECCS technologies. The fuel synthesis routes – Fischer-Tropsch synthesis, methanation and oxymethylene ethers synthesis – were modelled using Aspen Plus. A sensitivity analysis was performed to highlight the parameters for process improvements.

The energy conversion was in the range of 44.9% - 59.7% without CCS and 44.0% - 58.2% with CCS. BioSNG production had the highest efficiency due to high CO conversion to CH_4 as well as optimised heat integration with no external heat input. FT synthesis had the least efficiency due to the overall CO conversion pass of 72.7%. In all three cases, the energy conversion decreases by less than 1.5 percentage points when CCS is added to the plant due to intrinsic nature of CO_2 capture in biofuel generation.

Regarding the effect on the environment, adding CCS results in substantial negative emissions for the three routes considered. 301,000 – 519,000 tCO_2 can be removed from the atmosphere per year using the investigated routes. The OMEx route has the least emission factor at -0.2892 $kgCO_2$/kWh due to purchased heat, steam and electricity to meet the plant demand. The bioSNG route has a lower emission factor than the FT-fuel route due to the amount of CO_2 that is vented to the atmosphere during the process especially in the gasification section that uses dual fluidised bed gasifier to maximise the product yield. However, more negative emissions can be achieved by capturing CO_2 in the flue gas and limiting electricity imports which increase indirect emissions, thus maximising carbon removal.

The production costs are in the range of £12/GJ - £23/GJ without CCS and £13/GJ - £24/GJ with CCS. BioSNG is relatively the cheapest fuel to produce while FT-fuel is relatively the most expensive to produce as a result of high capital investment and low product yield. The addition of CCS does not have a drastic effect on the production costs while providing huge environmental benefits. However, in comparison to fossil-derived fuels on the market, the biofuel counterparts cannot feasibly compete without financial incentives due to minimum selling prices of the biofuels being at least two times more than fossil-derived fuels. With the application of the current RTFO and the RHI prices, competition is still not feasible with the current feedstock – woody biomass. Applying carbon pricing as an economic tool, a price in the range £48/tCO_2 – £86/tCO_2 is required to break-even with the current market price of the fossil-derive fuels. These figures are a function of the emission factor hence more negative emission credits need to be generated by the plants to achieve a lower carbon price. Combining the current financial incentives (RTFO and RHI) with carbon pricing could result in a much lower breakeven price. The sensitivity analysis highlights the capacity factor as the critical process parameter affecting the production cost. Other important parameters include the fuel output, the capital expenditure and feedstock costs.

Overall, the three routes with CCS are promising BECCS technologies but cannot currently compete with fossil-fuels without carbon pricing. Process improvements to boost the product yield and capture more CO_2 are required. Also, more aggressive policies and incentives focused on decarbonisation are needed to drive development and deployment and eventually favour competition to phase out fossil-derived fuels.

6 Potential for CO_2 Utilisation in Three Electrofuel Production Routes

6.1 Introduction

This chapter focuses on the potential of carbon dioxide utilisation in meeting the 2050 targets set by the Paris Agreement in 2015. Carbon dioxide is a valuable feedstock across several industries such as the petrochemical industry, welding, food and soft and it can be used either directly in cultivating microalgae [296] and enhanced oil recovery or by converting to chemicals including urea and polymers. CO_2 serves as a material for chemical energy storage mainly by converting it to a synthetic fuel or intermediate [297]. Converting CO_2 to synthetic fuel as a chemical energy form of electricity storage involves the use of electricity sources that are independent of energy demand such as nuclear energy. Electricity for this process could be from excess electricity from intermittent renewable energy plants or dedicated renewable energy plants. Where the electricity is not from a dedicated source, the energy demand independency results in excess electricity due to certain constraints and the excess electrical energy can be converted to chemical energy, typically via electrolysis [298]. Also, due to the intermittent nature of electricity from renewable energy, such as wind and solar, storing the excess energy in synthetic fuels can help to balance this out.

When fuels are produced via electrolysis, the resulting fuel is termed an electrofuel. By converting CO_2 derived from another process to electrofuels (a useful resource), a CO_2 circular economy can be formed [97] which promotes efficient use of materials and further reduce greenhouse gas emissions [299]. The main components of electrofuels are hydrogen (H_2) and CO_2 mixed in different ratios depending on the product. High purity oxygen is a by-product which can be sold to generate more revenue.

This chapter explores the future potential of three electrofuels from carbon dioxide (CO_2) and hydrogen via water electrolysis. The study examines the current technical, economic and environmental feasibilities and compares it to the biofuel route via gasification from Chapter 5. While there is a focus is on the use of biofuels to replace existing fossil fuels (especially in the transport sector), electrofuels could potentially augment the supply of biofuels by utilising the excess CO_2 from biofuel production and assist in decarbonising the transport sector [161]. Also, there is the issue of the sustainability of biomass resources which limits the

supply of biofuels and thereby it is essential to maximise the fuel yield from its production process by increasing the carbon conversion in the form of CO_2 utilisation [300]. A number of electrofuels exist, including dimethyl ether (DME), liquefied natural gas, methane, fuel oil, diesel, methanol, biodiesel and oxy methylene ethers (OMEx). For this chapter, the production of the following electrofuels – diesel and gasoline from Fischer-Tropsch Synthesis, OMEx and methane – are focused on. The three production routes chosen are based on the previous chapter on biofuel production and their potential as energy carriers in the transport sector. This chapter considers the electrolysis route to determine its potential in a circular economy and how it compares to the gasification (thermochemical) route.

Water electrolysis to produce hydrogen is not a new technology and the most common electrolysers are alkaline, proton exchange and solid oxide. The most mature electrolyser [301] is the alkaline water electrolyser which is used in this study due to its maturity level and lower cost when compared to the other types of electrolyser. In accessing the technical maturity of the production route using the technical readiness level (TRL) adopted from the European Commission classification [302], the FT synthesis route is 6 [303]. Although, FT synthesis is a mature technology with a TRL of 9 due to the availability on a commercial scale and the property data available in the literature, this is only for non-renewable feedstocks. Consequently, in the context of renewable CO_2 utilisation requiring technologies such as the reverse water-gas shift reaction which has a lower maturity [304], this value decreases to 6. The TRL of methanation via CO_2 utilisation is 9 [304] due to the commercial availability; since 2013, Audi e-gas, synthetic methane via CO_2 hydrogenation and electrolysis, has been in production [305,306]. The TRL of OMEx stands at 4 as there is a proof of concept and laboratory validation but it lacks process data or publicly available detailed properties [307].

This chapter updates and improves the information on electrofuel production in the literature. Also, this study aims to provide more information on the Power-to-OMEx route. It goes further and highlights the environmental impact of each process regarding achieving a CO_2 circular economy and assesses the potential of CO_2 utilisation in mitigating climate change.

6.2 Scope of Evaluation

The evaluation in this paper focuses on the production of electrofuels from CO_2 and renewable electricity. The system consists of an electrolyser, hydrogen storage, fuel synthesis infrastructure and utilities. Where excess power is available and supply exceeds

demand, the hydrogen storage facility buffers this to allow continuous operation of the plant. In this system, renewable energy comes from offshore wind production.

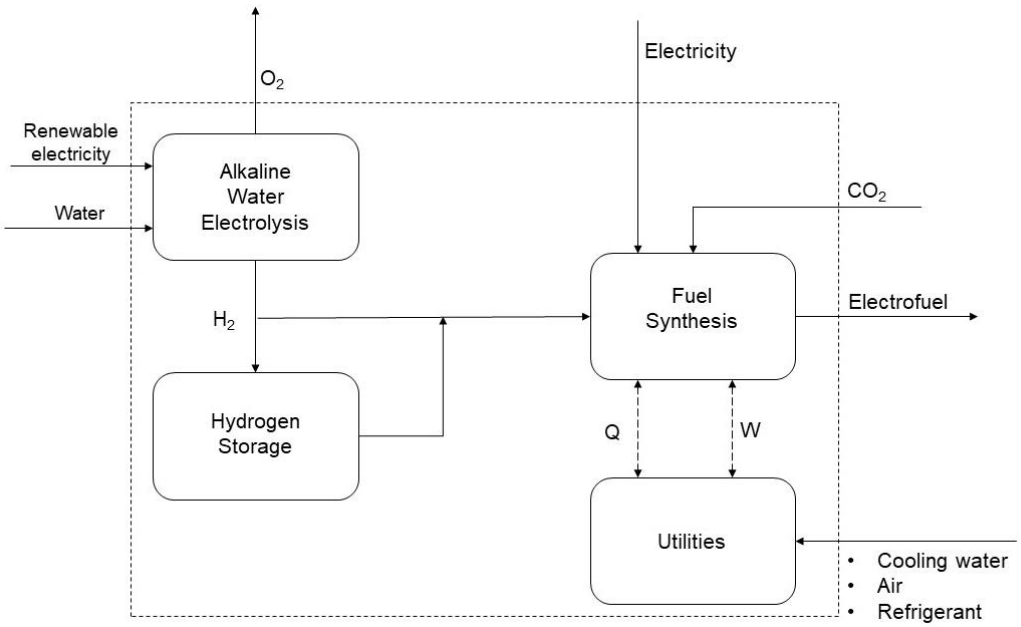

Figure 6.1: Boundary system for the evaluation for electrofuel production.

The scope of this evaluation is presented in Figure 6.1. The system inputs are deionised water, captured CO_2 and renewable electricity. H_2 is an intermediate feed and CO_2 is purchased at the market price; however, the CO_2 source varies from either a bioenergy power generation plant or a biofuel production (the criterion is that it comes from bioenergy generation for the context of BECCUS). Additional feed, such as nitrogen (N_2) and electrolyte make-up solution are also purchased at their market prices. In fuel synthesis, the FT synthesis route includes gas conditioning, FT synthesis, fuel separation; methanation includes synthesis in three reactors in series and a fuel upgrade; and OMEx synthesis includes methanol synthesis, methanol dehydration, formaldehyde synthesis, trioxane synthesis, methylal synthesis and OMEx synthesis [134]. The utilities section includes waste heat recovery and power generation units.

6.3 Process Modelling

A simple model is built for each electrofuel process in the Aspen Plus environment using the sequential-modular approach. The mass and energy balances are solved using the Peng-Robinson equation of state with the Boston Mathias alpha function (PR-BM) thermodynamic model. Also, a steam table model is used where power generation via steam turbines is

required. The modelling of the units in each production route is explained in this section and detailed modelling in Aspen is available in Appendix D.

6.3.1 Electrolyser unit

The model of the electrolyser unit is the same for the three process routes. Hydrogen production via alkaline water electrolysis (AWE) was modelled using a combination of units. In AWE, water is dissociated into hydrogen and oxygen. This system includes two electrodes immersed in a concentrated alkaline aqueous solution (potassium hydroxide) and a porous material between the electrodes permits the transportation of hydroxyl (OH^-) ions but limits the movement of oxygen and hydrogen [308]. When sufficient current is applied to the system, water oxidation in Eqn. (6.1) occurs at the anode and water reduction in Eqn. (6.2) occurs at the cathode simultaneously.

$$4OH^- \rightarrow O_2 + 2H_2O + 4e^- \quad (6.1)$$

$$4H_2O + 4e^- \rightarrow 2H_2 + 4OH^- \quad (6.2)$$

Using values available in literature including estimates for the near future of alkaline electrolysers, the electrical requirement for this process is calculated based on a 71% electricity-to-hydrogen efficiency (LHV basis) [309]. An additional 10% of this electrical requirement is assumed for the rest of the equipment in the hydrogen production process [310] with a 95% AC/DC conversion efficiency. The stack lifetime is 95,000 h [311] and the electrolyte solution is topped up at 1mg/Nm^3H_2 to make up for losses through the product gases [308]. The technical parameters of the electrolyser modelled in this study are presented in Table 6.1.

Table 6.1: Technical parameters of the alkaline electrolyser.

Parameter	Value
Stack efficiency (%)	71
Temperature (°C)	80
Pressure (bar)	20
Stack lifetime (h)	95,000
System lifetime (yr)	28
Water consumption ($m^3\ kg^{-1}H_2$)	0.01
Electrolyte	Potassium hydroxide (KOH)
Electrolyte concentration (wt%)	30
Electrolyte makeup (mg Nm^{-3} H_2)	1

An RSTOIC reactor operating at 80 °C and 20 bar [301] is used to model this process. A SEP block after the reactor is used to represent the diaphragm which allows the OH^- ions move to the anode for the anodic reaction. It also represents the collection of oxygen and hydrogen at the anode and cathode, respectively. Oxygen collected from the process is dehydrated and liquefied for commercial purposes while hydrogen is cooled to 25 °C and dehydrated via pressure swing adsorption (modelled as a flash unit maintained at 20 bar) to a 99.9% purity before being sent to storage to be used as required downstream. The stack electricity consumption for this electrolyser is 46.9 kWh_{el} kg^{-1} H_2 and the overall system electricity consumption is 51.59 kWh_{el} kg^{-1} H_2.

6.3.2 Fischer-Tropsch synthesis unit

A general overview of the Fischer-Tropsch process including a flow diagram is presented in sub-section 2.4.3. Also, detailed modelling of the process is available in Appendix D. In this chapter, a mix of H_2 and CO_2 with a ratio of 2.1:1 is compressed to 300 °C and 22.5 bar [155] and fed to the e-FTS process. In this process, a reverse water-gas shift (RWGS) reactor is required to produce carbon monoxide (CO) and adjust the H_2/CO ratio to 2.1. This step is modelled in an REQUIL reactor operating at 879°C and a pressure drop of 0.5 bar to promote CO formation via the reverse water-gas shift reaction as given in Eqn. (6.3):

$$CO_2 + H_2 \leftrightarrow CO + H_2O \tag{6.3}$$

Syngas after this reactor is cooled down and passed through a series of flash units to condense the water out of the mixture before passing through an acid gas removal unit to remove excess CO_2. A pressure swing absorber (PSA) before the main reactor isolates a portion of the H_2 in syngas for wax hydroprocessing downstream. An RSTOIC reactor is used to model the FT synthesis reaction (see Eqn. (6.4)) which is a polymerisation of CO and H_2 to hydrocarbons over a cobalt-based catalyst.

$$nCO + 2nH_2 \rightarrow (-CH_2-)_n + nH_2O \tag{6.4}$$

The product distribution (hydrocarbons composed of alkanes from C_1 – C_{20} and C_{30}) was estimated by the Anderson-Schluz-Flory (ASF) model (described in Song et al. [277]) with a chain growth factor of 0.9 and carbon monoxide per-pass conversion of 40% [155]. The products of the reaction are purified and separated in a series of flash units, absorbers and

distillation columns. Unconverted syngas is recycled and split between the FT synthesis reactor and the power generation unit.

6.3.3 Methanation unit

H_2 and CO_2 are compressed to 20 bar and 250 °C to favour the thermodynamics and kinetics of the reaction before being fed to the methanation unit with a stoichiometric ratio of 4:1 based on Eqn. (6.5):

$$4H_2 + CO_2 \rightarrow CH_4 + 2H_2O \tag{6.5}$$

The reaction takes place in a series of three reactors without a recycle stream. Between each reactor, the intermediate stream is cooled via heat recovery in an Organic Rankine Cycle (ORC) then water is condensed out in a flash unit. Before entering the next reactor, the stream is heated back to 250 °C in a heat exchanger by the outgoing stream of the reactor. Steam is introduced to the reactors to prevent carbon formation; the amount of steam is set by a design specification. The methanation reactors are modelled as RGIBBS reactors with a pressure drop of 0.5 bar in each reactor and the methane is upgraded to meet requirements for grid injection. This involves removal of water vapour and CO_2 such that the concentration in the methane is below the required levels and then it is compressed to 70 bar.

6.3.4 Oxymethylene ethers synthesis unit

OMEx is synthesised via the intermediate route as described in Schmitz et al. [134]. This is via the methanol and formaldehyde route in the block flow diagram in Figure 2.8 and intermediate reactions explained in sub-section 2.4.5. This involves the synthesis of formaldehyde from methanol, trioxane from aqueous formaldehyde, methylal from aqueous formaldehyde and methanol and finally OMEx from trioxane and methylal. This process is a 5-unit synthesis process. However, in this study, trioxane, methylal and OMEx synthesis are lumped into one process. A stream of H_2 and CO_2 compressed to 80 bar and 230 °C and it is fed to methanol synthesis with a stoichiometric ratio of 3:1 according to Eqn. (6.6).

$$3H_2 + CO_2 \rightarrow CH_3OH + H_2O \tag{6.6}$$

$$CH_3OH + 0.5O_2 \rightarrow CH_2O + H_2O \tag{6.7}$$

This is modelled in a single REQUIL reactor operating at 250 °C with no pressure drop. Methanol from the reactor is cooled and the unconverted H_2 and CO_2 is separated in a flash unit. This is recycled to the reactor. The methanol stream goes to the methanol recovery stage where distillation (RADFRAC) columns remove water and CO_2 from the methanol stream. Methanol is converted to formaldehyde using air via Eqn. (6.7) in an RSTOIC reactor operating at 200 °C and 3 bar. The product containing 37 wt% formaldehyde goes into an RYIELD reactor operating at 96 °C and 3.04 bar over an Amberlyst-36 catalyst representing the lumped trioxane, methylal and OMEx synthesis units. The OMEx product distribution is determined by the mass yield based on the model by Ai [312].

6.3.5 Utilities

Unreacted syngas from the FT synthesis is sent to the power generation section and it is combusted with 3% excess oxygen from the electrolyser. The flue gas is expanded in a gas turbine to generate electricity and heat is recovered from the exhaust stream and converted to work in a steam cycle. The flue gas leaves the combined cycle at 371 °C and a portion is recycled to the combustion chamber in order to control the temperature of the exhaust stream and protect the gas turbine blades. In the steam cycle, electricity is generated by the expansion of steam in the turbines. The intermediate stream is heated with the flue gas to boost heat recovery. A total of 16.7 MW is recovered from this combined cycle.

In methanation, heat is recovered from the stream between reactors. After the outgoing stream from the reactor has heated up the incoming stream in a heat exchanger, it goes into the ORC where pentane is the working fluid before exiting the ORC at 135 °C. Pentane is selected as the working fluid due to the relatively low temperature and limited heat transfer available. A total of 4 MW is recovered via the ORC.

In the OMEx synthesis, a purge stream from methanol synthesis and dehydration goes to the power generation section, similar to the FT synthesis case, thus generating a total of 4.1 MW.

6.4 Economic Modelling

An economic model is built based on the simulation performed to investigate the cost breakdown and examine the influence of different parameters such as the capital expenditure (CAPEX) and the operating and maintenance cost (OPEX) on the electrofuel price. The minimum fuel selling price for each electrofuel was estimated using a discounted

cash flow rate of return (DCFROR) analysis and net present value (NPV) break-even analysis. The economic parameters for the model are presented in Table 6.2.

Table 6.2: Process economic assumptions.

Parameter	Value
Location	United Kingdom
Currency	GBP
Base year	2019
Project lifetime (years)	25
Construction period (years)	2.5
Start-up time (years)	0.5
Capacity factor (%)	90
Tax rate (%)	19
Equity/Debt (%/%)	100/0
Discount rate (%)	8
Depreciation	Straight-line
Depreciation period (yr)	10
Salvage value (£)	0

The CAPEX for each production route is estimated using the factorial estimation method and purchased equipment costs (PEC), installation factors and the contingency available in the open literature. The method is outlined in Table 6.3.

The equipment costs were estimated according to Eqn. (6.8) with scaling factors accounting for the economies of scale and the Chemical Engineering Plant Cost Index (CEPCI) updating the prices from previous years.

$$\text{Cost} = \text{Cost}_0 \times \left(\frac{\text{Scale}}{\text{Scale}_0}\right)^{\text{n}} \times \left(\frac{\text{CEPCI}_{2019}}{\text{CEPCI}_0}\right) \tag{6.8}$$

Where $'\text{Cost}_0'$, $'\text{Scale}_0'$ and $'\text{CEPCI}_0'$ represent the cost, capacity of the base unit and CEPCI of the base unit year, respectively; 'Cost', 'Scale' and $'\text{CEPCI}_{2019}'$ represent the estimated cost, actual size of the plant equipment and the CEPCI of the study year; and 'n' is the scaling factor. The values for the base unit capacity, costs and scaling factor can be found in Table B1

in Appendix B the size of the hydrogen storage was roughly estimated based on the work of König et al. [158].

Table 6.3: Estimation methodology for CAPEX.

Parameter	Method
Total Purchased Equipment Cost (TPEC)	Aspen Process Economic Analyzer, open literature
Total Installed Cost (TIC)	**TPEC Installation factor**
Buildings	0.29 x TPEC
Yard Improvements	0.12 x TPEC
Land	0.06 x TPEC
Non-installed Direct Costs (NDC)	**47% of TPEC**
Engineering and Supervision	0.32 x TPEC
Construction Expenses	0.34 x TPEC
Contractor's Fee and Legal Expenses	0.23 x TPEC
Indirect Costs (IC)	**89% of TPEC**
Contingency (CC)	20% of TPEC
Fixed Capital Investment (FCI)	**TIC + CC + NDC + IC**
Working Capital (WC)	15% of FCI
Total Capital Investment (TCI)	**FCI + WC**

The operating and maintenance expenditure (OPEX) includes the costs for maintenance, insurance, labour and raw materials. The prices for the raw materials, catalysts and utilities presented in Table B3 in Appendix B are based on the former expenditure and this is updated to account for inflation. The fixed costs – maintenance, depreciation, local taxes, insurance and rent – were estimated with guidance from Sinnott and Towler [218]. The labour costs were estimated using data from Glassdoor and Payscale [283,284].

The levelised cost of fuel is the cost of producing a unit of fuel and it is dependent on the annualised capital cost (ACC), OPEX and revenue from the by-products. The net production cost is calculated via Eqns. (6.9) and (6.10) where 'i' is the discount rate and 'n' is the plant lifetime in years.

$$\mathrm{ACC} = \mathrm{TCI} \times \frac{\mathrm{i}(1+\mathrm{i})^{\mathrm{n}}}{(1+\mathrm{i})^{\mathrm{n}}-1} \tag{6.9}$$

$$\text{LCOF} = \frac{\text{ACC + OPEX} - \text{Revenues from by-products}}{\text{Fuel production rate}} \quad (6.10)$$

After the CAPEX and OPEX are determined, the cash flow for each year is determined and the minimum fuel selling price (MFSP) is determined via a DCFROR analysis. The MFSP is calculated as the fuel selling price when the NPV = 0 in Excel. The equation for the DCFROR is outlined below in Eqns. (6.11) and (6.12) where 'CF_n' is the cash flow in year n; 'P' is the gross profits in year n; 't' is the tax rate; and 'D' is the depreciation:

$$\sum_{n=1}^{n=25} \frac{CF_n}{(1+i)^n} = 0 \quad (6.11)$$

$$CF_n = P(1-t) + Dt \quad (6.12)$$

6.5 Results

6.5.1 Process performance indicators

The mass and energy balances for the modelled processes were completed and the performance indicators are summarised in this sub-section. Each process performance was based on the chemical, energy and carbon conversion efficiencies and the definitions are presented in Table 6.4. The chemical conversion efficiency represents amount of energy in the feed (H_2) that is stored in the resulting fuel and accounts for the losses in the fuel synthesis conversion process. The overall energy efficiency is also the Power-to-X efficiency in this case as it is based on the net amount of electricity supplied to each plant. This includes electricity for electrolysis and other plant utilities. A breakdown of the overall electricity requirement for each plant is presented in Table C1 in the Appendix C.

Table 6.4: Process performances parameters.

Parameter	Formula
Chemical conversion efficiency	$\eta_{CCE} = \frac{\dot{m}_{efuel} \times LHV_{efuel}}{\dot{m}_{H_2} \times LHV_{H_2}}$
Power-to-X efficiency	$\eta = \frac{\dot{m}_{efuel} \times LHV_{efuel}}{\text{Net electricity input} + \text{heat input}}$
Carbon conversion efficiency	$\eta_{CC} = \frac{\dot{n}_{C,efuel}}{\dot{n}_{C,feed}}$
*$\dot{m}$ is the mass flowrate in kg/h, LHV is the calorific value in MJ/kg and $\dot{n}$ is the number of moles.	

The electrolyser accounts for over 95% of the electricity requirement on each plant. While some electricity is generated in each process from waste heat recovery, the amount is not substantial enough to offset the consumption. FT synthesis has the lowest chemical conversion and energy efficiency at 55.9% and 35.1% respectively due to an overall CO conversion at 72.7%. In e-SNG and e-OMEx synthesis, the conversion across the synthesis reactor is 98% and 99% respectively. The fuel synthesis section of the FT synthesis model is based on the work of Swanson et al. [155] and while the recycle ratio of the unreacted syngas from the reactor is increased to 1.38, a small portion of the recycle stream is sent to power generation. In the power generation section, the unreacted syngas to electricity has a 53% efficiency, thus indicating how much energy is lost from this process. With a low per-pass CO conversion of 40%, recycling unreacted syngas improves the energy conversion; however, the recycle ratio in this work has not been optimised as it is beyond the scope of this study. König et al. [158] reports a power-to-liquid efficiency for FT-fuel production at 44.6% due to recycling most of the unreacted syngas.

Table 6.5: Summary of the key process performance indicators.

	e-FTS	e-SNG	e-OMEx
Energy output (MW)	114.9	165.0	148.0
Mass yield (%)	23.5	30.8	51.3
Carbon conversion (%)	83.1	99.9	94.4
Carbon vented (%)	16.9	0.1	5.6
Chemical conversion (%)	55.9	82.9	67.6
Power-to-X (%)	35.1	49	38.5
Net power required (MW)	327	337	366

The e-SNG and e-OMEx routes achieve a Power-to-X efficiency of 49% and 38.5% respectively, which is comparable to the results published in the literature for electrofuels production. In these two cases, conversion in fuel synthesis is over 90% which boosts the plant efficiency.

The mass balance reveals how carbon is transformed in the system. In both e-SNG and e-OMEx, most of the carbon is stored in the fuel while in e-FTS, a significant amount is vented in power generation. Also, because of the water-gas shift reaction required to produce CO for the downstream reaction, there is an initial excess of CO_2 to the system. A large amount of CO_2 is required to drive the RWGS reaction but the excess needs to be removed after to

meet the stoichiometric ratio for the FT synthesis reaction; this amount is recycled to the CO_2 inlet stream. One suggestion to avoid this system is to switch to co-electrolysis of CO_2 and H_2O; this eliminates the need of a RWGS reactor and carbon capture unit. However, co-electrolysis takes place in a solid oxide electrolyser which is still in the demonstration [301] stage and more expensive than the alkaline electrolyser.

6.5.2 Economic analysis

The total capital expenditures for the three electrofuel production routes are presented in Figure 6.2. The CAPEX is £383 million for e-FTS, £269 million for e-SNG and £483 million for e-OMEx. These costs are generally higher than that of the biofuel counterparts whose CAPEX falls into the range of £143 - £ 292 million even with a decrease in the number of unit operations. Also, the electrolyser unit is the major contributor to this price, accounting for 75% of the CAPEX in e-FTS, 91% in e-SNG and 55% in e-OMEx. The e-OMEx route has another significant contributor which is the fuel synthesis route at 38% of the CAPEX. This is due to the 5 synthesis units being involved in the production process.

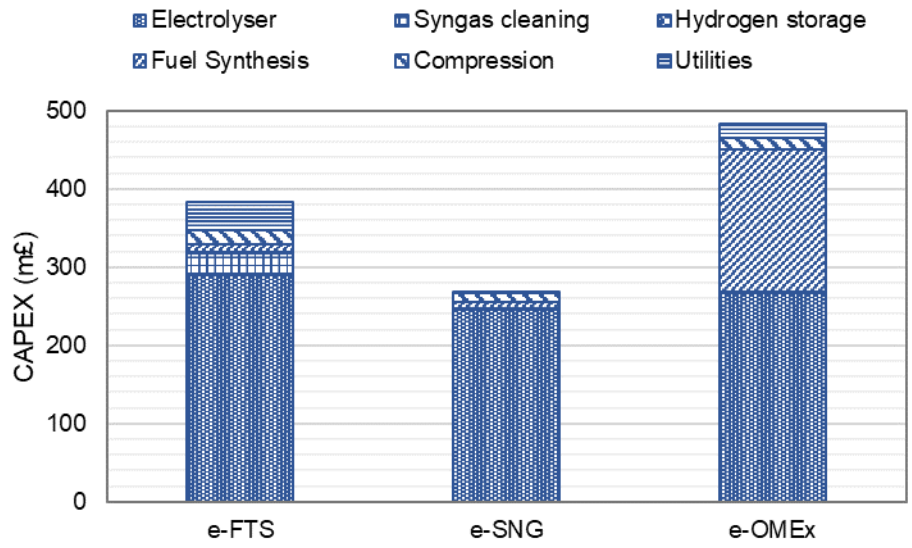

Figure 6.2: CAPEX breakdown of the three electrofuel production routes.

The OPEX breakdown for the three routes is presented in Figure 6.3 while the breakdown of the LCOF is presented in Figure 6.4. Electricity is separated from the variable costs as it accounts for over 89% of the OPEX and LCOF as seen in both figures. The electricity used for each plant comes from offshore wind energy and is priced at £106/MWh [240] based on central generating costs in 2020. This figure is estimated to go as low as £85/MWh by 2030. However, this is still too high based on the electricity demand. Switching to a large-scale

solar PV as the electricity source will give an electricity price as low as £52/MWh while a nuclear plant will give a price as low as £69/MWh by 2030.

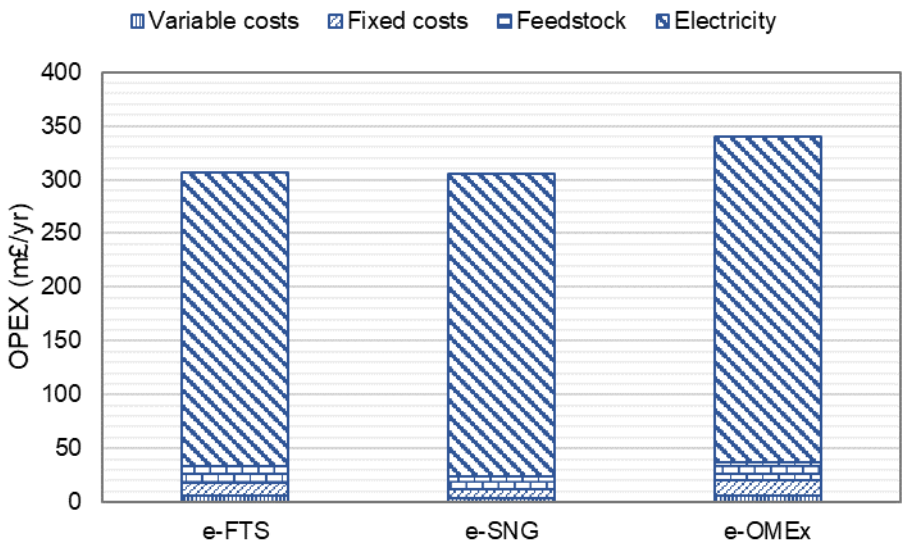

Figure 6.3: OPEX breakdown of the three electrofuel production routes.

The electricity price is a critical factor affecting the price of the electrofuels and this is in agreement with studies on electrofuels [161,163,313]. A sensitivity analysis is conducted in order to identify other parameters influencing the plant economics.

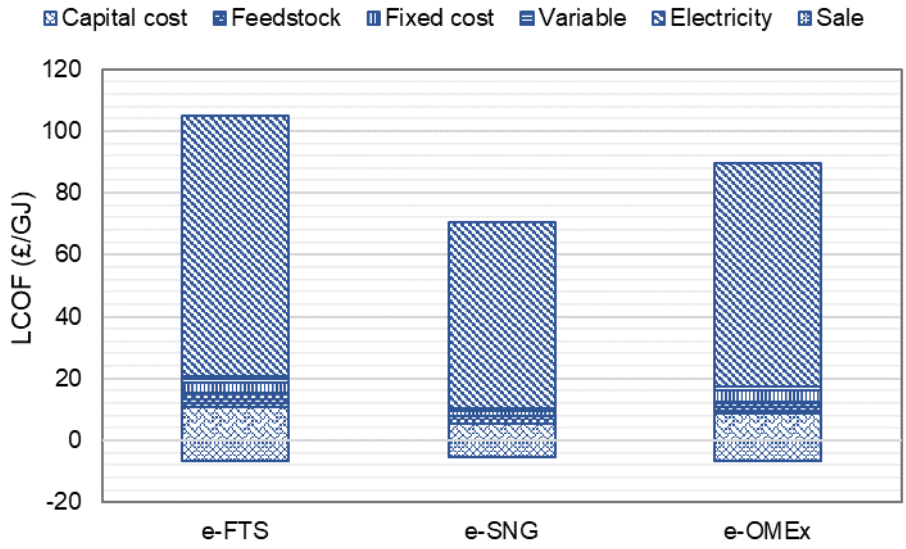

Figure 6.4: Levelised cost of fuel production for the three production routes.

The LCOF for the e-FTS route is £3.46/kg (£352/MWh) and this is comparable to the value of $6.83/kg (£4.48/kg accounting for inflation) reported in König et al. [158] and falls on the higher end of the 2015 reference scenario range reported in Brynolf et al. [161]. The LCOF of

e-SNG production at £3.25/kg (£234/MWh) also falls within the same range. With e-OMEx, this study reports an LCOF value £82.80/GJ (£299/MWh) which is close to the value presented in Zimmerman et al. [307] at $89/GJ (£261/MWh) for the production of OMEx via PEM electrolysis; however, it should be noted that assumed electricity price which is the major contributor to the LCOF is different to the price in this study due to the electricity source assumed.

Table 6.6: Comparison of the minimum fuel selling price with conventional fossil fuels.

	Electrofuel (£/GJ)	Biofuel (£/GJ)	Fossil fuel (£/GJ)
FTS	96.90	28.90	13.23
SNG	59.90	19.10	5.50
OMEx	64.10	26.30	13.23

The minimum fuel selling price from the economic model is reported in Table 6.6 alongside the minimum biofuel selling prices and the market price of conventional fuels. These values are 3.0 times, on the average, the values reported to produce the corresponding biofuels and 7.7 times that of the corresponding fossil fuels, thus revealing the current unfeasibility of setting up such plants without reasonable incentives and policies. However, electrofuels are the fuels of the future and there is the opportunity to reduce the production costs over the coming years. Currently, there are no incentives or policies to boost or support electrofuel production, hence commercially producing electrofuel could remain unfeasible. However, with the accelerated deployment of CCUS technologies and successful policy in creating a viable market [93], there is potential for the high cost of electrofuel production to substantially reduce.

6.5.3 Sensitivity analysis

A sensitivity analysis is executed to highlight the influence of certain parameters on the fuel production cost underlining the process factors for optimisation. The parameters are varied based on a high-cost and low-cost scenario. For the CAPEX (excluding the electrolyser), the low and high-cost scenarios use the AACE classification range [314] for a Class 5 project. The electrolyser low value is based on a 2030 estimate of 367 €/kW in Bertuccioli et al. [311] and the high value is a 2030 estimate of 1300 €/kW in Schmidt et al. [301]. The electricity range is based on the BEIS [240] estimated renewable energy values up to 2030.

Table 6.7: Parameters for the sensitivity analysis.

	Low	Nominal	High
CAPEX (£)	-30%	-	+50%
Electrolyser (€/kW)	367	1100	1300
Cost of electricity (£/MWh)	45	106	119
Price of oxygen (£/t)	49	70	91
Cost of CO_2 (£/t)	30	42	84
Interest rate (%)	6	8	10

The oxygen price is changed by ±30% of the base scenario while the high-cost CO_2 price is the maximum cost of CO_2 captured from a biomass power plant in Emenike et al. [148]. Table 6.7 summarises the low-values and high-values of the parameters investigated in the sensitivity analysis and the results are presented in Figure 6.5.

The bars in Figure 6.5 represent the sensitivity of a parameter's effect on the plant economics and the longer the bar, the higher the sensitivity is. As seen in Figure 6.5, as expected, the price of electricity is the most critical parameter which can reduce the LCOF by 51% at £45/MWh if the plant is powered by a large-scale onshore wind farm and the LCOF can increase by 11% when the electricity price increases to £119/MWh. If excess power to run the electrolyser is supplied free of charge, the LCOF can drop by over 88% of the base price. The investigated range of the electrolyser price causes the LCOF to vary between -5% and +2%. Electrolyser prices are expected to drop with increased spending in research and development. In addition, the electrolyser efficiency determines the amount of electricity required and the size of the electrolyser, an improvement in this efficiency could potentially lower the LCOF [158].

The CO_2 purchase price and oxygen sale price have a medium effect on the LCOF. In general, varying the CO_2 purchase price causes the LCOF to fluctuate between –1% and +4% while varying the oxygen sale price causes the price to fluctuate by ±2%. Other parameters, such as the CAPEX of the rest of the plant and the interest rate, have very little to no effect on the production cost.

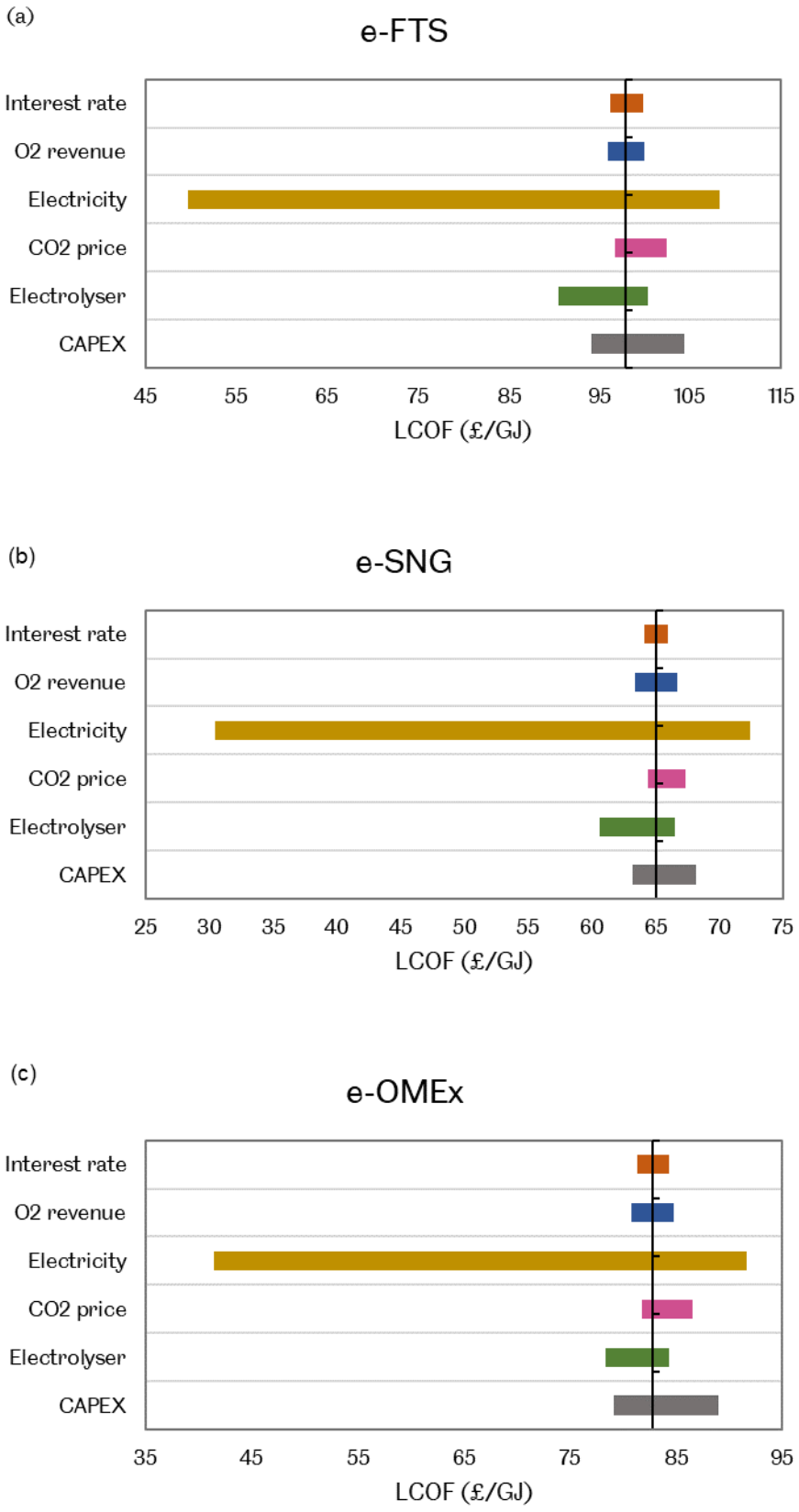

Figure 6.5: Sensitivity of economic parameters on the LCOF of three electrofuel production routes.

6.5.4 Environmental impact

The environmental impact of setting up each of the electrofuel production plants is considered in this sub-section using a CO_2 emission factor. The emission factor is the mass emission rate of greenhouse gases to the atmosphere per unit of fuel output. The emission factor considers the greenhouse gas emissions over the lifetime of the plant, such as during harvesting and processing, electricity import and purchased heat but this excludes emissions from transportation and the distribution of fuel.

Table 6.8: Emission factors used in this study [228,315–317].

Fuel	Emission factor (kg CO_2e /kWh)
Biomass (wood pellets)	0.05289
Natural gas	0.23023
Wind electricity	0.01200
Solar-PV electricity	0.04800

The United Kingdom Department of Business, Energy and Industrial Strategy (BEIS) [228] outlines the emission factors for greenhouse gas reporting and this is currently updated yearly. The BEIS framework categorises these emissions based on activities in three scopes – Scope 1, Scope 2 and Scope 3. In this study, Scope 1 covers direct emissions from the plant itself, such as use of process equipment and greenhouse gases from combustion within the plant. When using biomass and biofuels, this value is 0 for CO_2 emissions but not for N_2O and CH_4 which are not absorbed in the biomass regeneration. Scope 2 covers indirect emissions from the plant, such as imported electricity and heat purchased for the plant. Scope 3 refers to indirect emissions from sources not owned or controlled by the plant, such as the emissions due to harvesting, refining and transporting biomass; this is referred to as background emissions in this study. However, the BEIS framework does not cover the emission factors for other renewable energy, such as solar, wind and geothermal energy, so these factors are sourced from open literature. The values of the emission factors used in this study are presented in Table 6.8.

With CO_2 utilisation, calculating the emission factor of the subsequent production plant is difficult without considering the CO_2 source. In addition, in order to account for the CO_2 source, the final emissions when the electrofuel is combusted as well as the co-products need to be accounted for to give a true representation of the greenhouse gas emissions. There are three classifications of the CO_2 source [318]:

a. Non-biogenic point-sources: This covers CO_2 captured from industries using fossil fuel, such as coal fired power plants, natural gas combined cycle plant and cement production.
b. Biogenic point-sources: This covers CO_2 captured from biorefineries and biomass power plants.
c. Air capture: This covers CO_2 directly removed from the atmosphere via direct air capture.

In this sub-section, the boundary system for the analysis considering each CO_2 source is shown in Figure 6.6. Additional information on the assessment is available in Appendix C. The emission factor is calculated based on three CO_2 sources:

1. CO_2 captured via post combustion capture from a natural gas combined cycle power plant. The CO_2 capture efficiency is assumed to be 87% [241].
2. CO_2 captured via post combustion capture from a biomass-based power plant. The capture efficiency is assumed to be 87% [241].
3. CO_2 captured via direct air capture (DAC). The system is assumed to powered by a solar-PV system and operating at an 84% CO_2 capture efficiency [319,320].

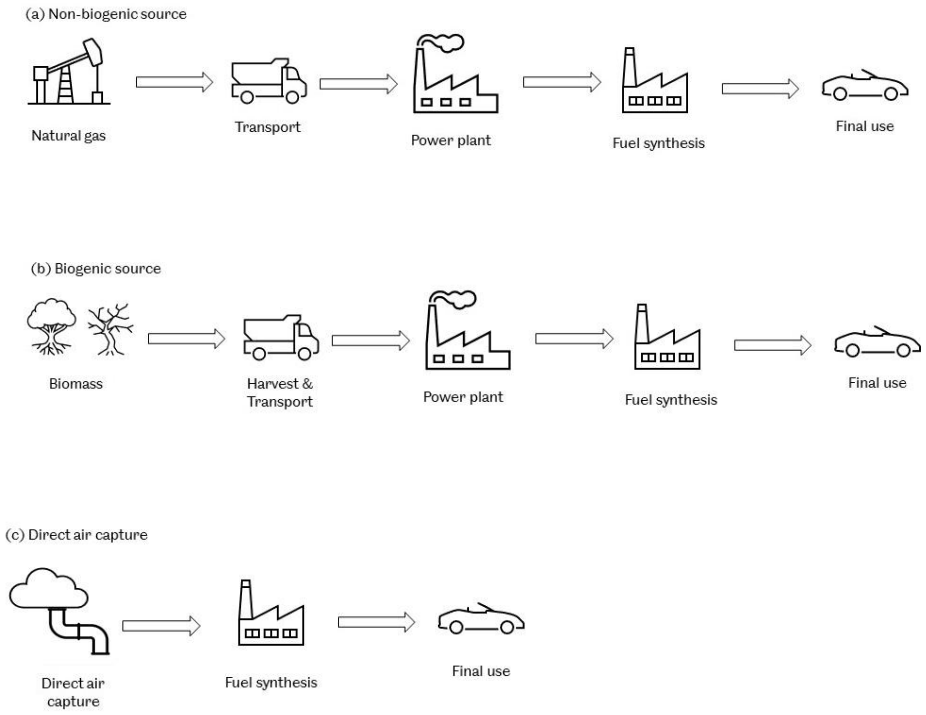

Figure 6.6: Boundary system for environmental assessment.

Figure 6.7 presents the emission factors for all the cases and the net emission factor is positive for all sources. This indicates that CO_2 utilisation does not achieve negative emissions in the fuel production routes. Using a non-biogenic CO_2 source has the highest emission factor and potentially releasing 370,000 – 530,000 tCO_2/yr with no reasonable carbon intake. With a biogenic CO_2 source, this range is lower at 76,000 – 99,000 tCO_2/yr while using CO_2 from air capture has the lowest range at 38,000 – 43,000 tCO_2/yr. When using CO_2 from direct air capture and biogenic sources, there are opportunities to reduce the emission factors, especially in the fuel synthesis process. A significant portion of CO_2 is vented to the atmosphere from the flue gas in power generation which could be further captured using membranes; also, the CO_2 capture efficiency could be improved to avoid losses; and combining CO_2 utilisation with storage as in CCUS could result in carbon neutrality or negative emissions. When comparing the biogenic sourced CO_2 route for electrofuel production to the biofuel production route via gasification, the biofuel route performs better environmentally as it achieves negative emissions and can remove up to 519,000 tCO_2/yr from the atmosphere.

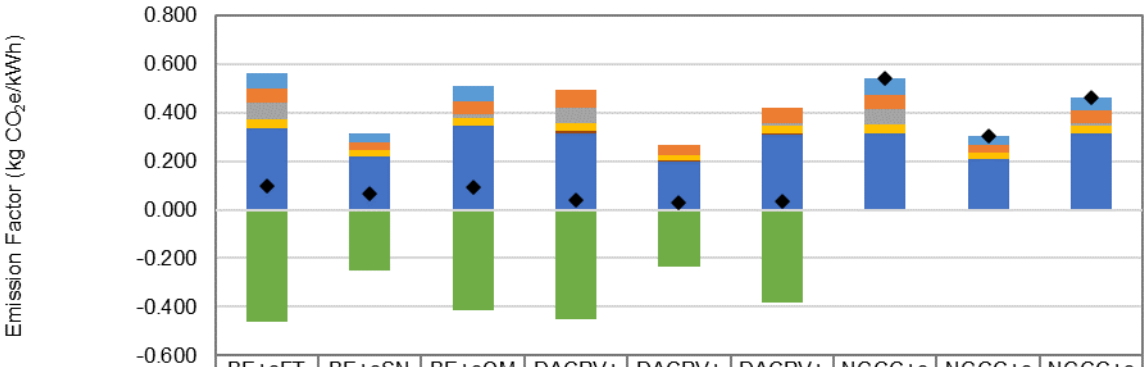

	BE+eFTS	BE+eSNG	BE+eOMEx	DACPV+eFTS	DACPV+eSNG	DACPV+eOMEx	NGCC+eFTS	NGCC+eSNG	NGCC+eOME
Background	0.063	0.038	0.062	0.000	0.000	0.000	0.072	0.035	0.055
CO2 capture loss	0.060	0.032	0.054	0.072	0.038	0.061	0.057	0.031	0.049
CO2 from process	0.068	0.000	0.014	0.064	0.000	0.012	0.064	0.000	0.012
CO2 intake	-0.463	-0.251	-0.415	-0.452	-0.235	-0.384	0.000	0.000	0.000
Wind electricity	0.036	0.027	0.033	0.034	0.026	0.030	0.034	0.026	0.030
PV Electricity	0.000	0.000	0.000	0.007	0.003	0.006	0.000	0.000	0.000
Fuel combustion	0.335	0.219	0.347	0.316	0.197	0.310	0.315	0.210	0.316
Total	0.099	0.065	0.095	0.042	0.029	0.035	0.542	0.303	0.463

Figure 6.7: Greenhouse gas emission factors breakdown of three electrofuel production routes with different CO_2 sources.

However, while direct air capture appears to be the most promising environmentally, it is an expensive technology with costs as high as \$300/tCO_2 [321]. Also, it is a technology set up to sequester carbon or produce carbon-neutral fuels; therefore, when it is applied to CO_2

utilisation, it is essential that meets this purpose. This result stresses the importance of evaluating the environmental impact of CO_2 utilisation and optimising the process to ensure that overall, CO_2 is removed from the atmosphere.

6.6 Conclusion

CO_2 utilisation is an integral part of transitioning to a net zero carbon economy [93]. Using CO_2 and renewable energy power, this work explores the technical, economic and environmental performance of producing electrofuels in comparison to their biofuel counterparts. The electrofuels production routes were modelled in Aspen Plus and the electrofuels considered were FT-fuels via the Fischer-Tropsch synthesis, SNG via methanation and OMEx via oxymethylene ether synthesis.

With CO_2 utilisation, the Power-to-X efficiency was 35.1% with e-FTS, 49% with e-SNG production and 38.5% with e-OMEx. The FT synthesis production route had the least efficiency due to an overall CO conversion in FT synthesis reactor of 72.7% which is relatively lower than the CO_2 conversion across the synthesis reactors in the other two processes. Also, in the mass balance, over 15% of carbon in the system is lost to the environment. In the other two production routes, higher conversion rates are achieved. In all routes, the electricity demand for the electrolyser accounts for over 90% of the power requirement.

From the economic model, the levelised cost of the investigated electrofuels are £352/MWh, £234/MWh and £299/MWh for FT-fuel, SNG and OMEx, respectively. The cost of electricity dominates the LCOF and OPEX and is responsible for the high cost. The minimum electrofuel selling price when compared to the corresponding biofuel price is 3.0 times higher and 7.7 times higher in comparison to fossil-derived fuels, thus rendering production unfeasible without process optimisation, significant financial incentives and policies. A sensitivity analysis highlights the electricity price as the most critical factor which could reduce the LCOF by 51% if the price of electricity dropped to £45/MWh and could reduce by 88% if excess renewable electricity is supplied free of charge. The other significant factors are the price of the electrolyser and the CO_2 purchase price.

An assessment of the emission factors over the plant lifetime to determine the environmental impact showed that electrofuel production results in net positive greenhouse gas emissions irrespective of the CO_2 source. Considering the use of CO_2 from a non-biogenic source, a biogenic source and direct air capture, the emissions potential

nonetheless is positive, but decreases significantly by over 80%. However, with direct air capture as the best choice in terms of emissions, it is an expensive technology and defeats its purpose to generate carbon-neutral fuels if improvements in the production routes are not made. Therefore, CO_2 capture losses during each process need to be minimised to improve the chances of achieving carbon-neutrality with CO_2 utilisation or combined with CO_2 storage for more environmental benefits.

Finally, while biofuels perform better than electrofuels, both could potentially contribute to a sustainable energy future. However, the existing electrofuels technology will not achieve this without improvements. Electrofuels are fuels for the future, hence it is imperative that the production process is optimised to achieve the purpose for which the fuels have been designed for while also achieving cost-effectiveness.

7 Conclusions and Recommendations

In the quest for reducing greenhouse gas emissions and mitigating climate change, alongside common CO_2 emission reduction strategies, negative emission technologies (NETs) have been identified as technologies to remove CO_2 from the atmosphere. This research focused on one of the NETs - bioenergy with carbon capture and storage (BECCS) as a climate change mitigation tool and its application in the energy generation sector. This research also considered carbon capture and utilisation as an emission reduction tool. The aim of this research was to contribute much more detailed information to the limited literature on BECCS in order to substantially improve the understanding and aid further development of this technology. This research thoroughly evaluated the technical, economic and environmental performance of the different energy production routes with and without CCS.

The literature review of the subject highlighted the demand for more detailed research into BECCS to discover the application potential of this NET. This research was divided into three parts and completed using process models and simulations, economic models and data from the open literature. Mass and energy balances, economic assessments, environmental assessments and sensitivity studies were applied to obtain detailed information. The main process modelling tools used were the IECM and Aspen Plus.

This next two sections summarise the results of this research and present recommendations for future research.

7.1 Conclusions

The first part on BECCS in power generation assessed the performances of a range of biomass feedstock (white wood pellets, miscanthus and wheat straw) with different CCS technologies - post combustion capture using amines, oxy-fuel combustion and pre-combustion capture using Selexol. The results of this project showed that:

- The most suitable BECCS technology for each type of biomass is dependent on a combination of factors including the biomass calorific value, moisture content and ash content.
- The addition of a capture plant to power generation decreases the plant efficiency by up to 29% with post-combustion experiencing the highest energy penalty.

- In comparison to other capture systems, pre-combustion capture experienced the least drop in energy efficiency with a decrease of 13.5%.
- Based on the calorific value of the biomass, post-combustion capture results in higher net plant efficiencies with higher calorific value biomass, such as white wood pellets while pre-combustion capture is more suited to lower calorific value biomass.
- A high content of ash in biomass reduces the efficiency in all cases.
- Pre-combustion capture is the most efficient capture system with the least power production cost.
- Upstream production of biomass such as the harvesting and processing significantly affects the overall negative emissions.
- In the short to medium term, bioenergy without CCS is not suitable with power generation when compared to natural gas based on the emission factors.
- Bioenergy with CCS can remove 1.0 - 1.52 $MtCO_2e\ yr^{-1}$ from the atmosphere in the long-term with a 250 MW power plant.
- Adding CCS to a power plant increases the LCOE by 37%, 43% and 24% in post-combustion, pre-combustion and oxy-fuel combustion capture, respectively.
- The LCOE of biomass combustion with CCS is in the range of £158 - £224 per MWh.
- The cost of CO_2 avoidance is £56/tCO_2 in post-combustion capture, £79/tCO_2 in oxy-fuel capture and £47/tCO_2 in pre-combustion capture.
- A carbon price in the range of £83/tCO_2 and £146/tCO_2 based on the three feedstocks considered, is required to create competition with natural gas if carbon pricing as climate change mitigation tool is employed.
- From the sensitivity analysis, the key drivers of the LCOE were the biomass cost, capacity factor and the CAPEX.

This first part provided information on the performance of different types of biomass in different CO_2 abatement technologies that was not previously available in BECCS literature and constituted a first attempt to fill the knowledge gap.

The second part assessed the performance of BECCS in fuel generation via gasification. The scope of this project focused on three biofuel production routes - FT-fuels (diesel and gasoline) via Fischer-Tropsch synthesis, bioSNG via methanation and OMEx via oxymethylene ether synthesis. These fuels were chosen based on their roles as alternative transport fuels. The results of this project showed that:

- The energy efficiency of the three production routes is in the range of 44.9% - 59.7% without CCS and 44.0% - 58.2% with CCS.
- In terms of technical performance, BioSNG synthesis is the most promising route of the three investigated with the highest energy efficiency as a result of high CO conversion to CH_4 as well as optimised heat integration with no external heat input.
- FT synthesis has the least energy efficiency due to the overall CO conversion pass of 72.7%.
- In all three cases, the energy conversion decreases by less than 1.5 percentage points when CCS is added to the plant due to intrinsic nature of CO_2 capture in biofuel generation.
- The addition of CCS results in negative emissions in the range of 301,000 – 519,000 $tCO_2e\ yr^{-1}$.
- The OMEx route has the least emission factor at -0.2892 $kgCO_2/kWh$ due to purchased heat, steam and electricity to meet the plant demand. The bioSNG route has a lower emission factor than the FT-fuel route due to the amount of CO_2 that is vented to the atmosphere in the gasification section. The dual fluidised bed gasifier is used in the gasification section in bioSNG production to maximise the product yield resulting in flue gas that is vented to the atmosphere. To generate more negative emissions, CO_2 can be captured from the flue gas using membranes and electricity imports be limited.
- The biofuel production costs production costs are in the range of £12/GJ - £23/GJ without CCS and £13/GJ - £24/GJ with CCS with bioSNG being the cheapest to produce and OMEx being the most expensive to produce due to the high capital investment and operating expenditure when compared to the other biofuel production routes.
- While the addition of CCS increases the LCOE, the maximum increase is by 10% in bioSNG production.
- Without financial incentives, the minimum selling price of the biofuels is at least two times more than that of the market price of fossil-derived fuels making competition unfeasible. Applying current financial incentives such as the RTFO and RHI reduces the gap but is still not enough to drive competition.
- Using a carbon pricing as an economic tool, competition with fossil-derived fuels can be possible with a carbon price in the range of £48/tCO_2 – £86/tCO_2. This range can be further reduced if the production routes generate more negative emissions.

- The capacity factor is the most crucial process parameter affecting the LCOE; other parameters are the fuel output, CAPEX and feedstock costs.

This second part of the research was a first attempt to comprehensively evaluate the techno-economic and environmental performance of applying BECCS in fuel generation.

The last part of this project assessed the production of electrofuels with CO_2 utilisation. The fuel production routes were the same routes from the previous part and the thermochemical conversion step was replaced with an electrochemical conversion step. This part assessed the potential of electrofuels in mitigating climate change using captured CO_2 and hydrogen from water electrolysis. The results of this project showed that:

- The Power-to-X efficiency is 35.1% with e-FTS, 49% with e-SNG production and 38.5% with e-OMEx. Similar to the thermochemical conversion route, FT synthesis has the lowest conversion efficiency.
- The capital investment required is at least 65% more than that required for the biofuel production routes mainly because of the electrolyser cost.
- In all production routes, the electrolyser power requirement accounts for over 89% of the overall plant power demand.
- The electrofuel production costs are £352/MWh, £234/MWh and £299/MWh for FT-fuels, SNG and OMEx, respectively with SNG being the cheapest to produce.
- The cost of electricity is the major contributor to the levelised cost of fuel and it dominates the OPEX. It is responsible for the high production costs.
- The minimum selling price is on the average 3.0 times that of the biofuel counterpart and 7.7 times the current market price of the fossil-derived fuels counterpart.
- There are no current financial policies to support the production of electrofuels in the UK.
- From the sensitivity analysis, the price of electricity is the most critical factor affecting the production cost of electrofuels. If the price of electricity decreased to £45/MWh, the LCOF could reduce by 51% and if excess electricity were supplied to the production plant free of charge, the LCOF could reduce by 88%. Other factors affecting the production cost include the electrolyser price and the cost of CO_2.
- Considering the CO_2 source to determine the environmental impact, three CO_2 sources were investigated - CO_2 captured from a natural gas combined cycle (non-biogenic source), CO_2 captured from a biomass power plant (biogenic source) and CO_2 captured directly from the air. All sources result in positive emissions but going

from a non-biogenic source to either a biogenic source or direct air capture decreases the emissions by at least 80%.

- To achieve carbon-neutral electrofuels, CO_2 capture losses from a biogenic source and direct air capture need to be minimised or combined with other CO_2 storage options such as geological storage.

This last part of the research provided more detailed information on electrofuel production to the available literature by including the environmental impact associated with the production route while assessing the potential of carbon dioxide utilisation as an emission reduction tool.

Overall, in this thesis, it has been shown biomass power generation and biofuel generation with CCS can achieve significant negative emissions, thus cementing the role they could play in decarbonising an economy and mitigating climate change while CO_2 utilisation to produce electrofuels shows a potential to reduce greenhouse gas emissions. However, the production costs are expensive and cannot compete with conventional fossil fuels and eventually phase out fossil fuels without aggressive policies. Effectively applying carbon pricing under schemes such as the emissions trading scheme and generating negative emissions credit appears to be a convenient tool to drive the application of BECCS and make large scale deployment feasible. Other ways to lower production costs are with process improvements and optimisation which would boost the product yield; environmentally, process improvements will increase the amount of CO_2 that could be removed from the atmosphere.

This research has provided much important information to the BECCS literature and CO_2 utilisation as regards the energy generation sector. This information that has been provided in this thesis can be used, with great advantage, for a preliminary assessment in exploring and prioritising BECCS projects; also, it has provided valuable information to inform current CCS research as BECCS is dependent on it.

7.2 Recommendations for Future Work

Based on the research completed in this thesis then it is recommended that the following investigations should be performed:

- The application of other negative emission technologies across sectors emitting CO_2 be comparatively assessed to guide the choice of NETs in a particular route sector.

- Biogenic waste such as municipal solid waste (MSW) should be considered in power generation with different types of CO_2 abatement technology and compared with other classes of biomass to obtain more information about the performance of the different classes of biomass combustion with CCS.
- In fuel generation, the scope of fuels investigated should be expanded to include more than the three fuels considered in this study.
- Due to time constraints, maximising the output from each energy generation route was not considered. Future work should include this as well as consider new technologies and materials that increase the production performance, then assessing the performance accordingly.
- In terms of financial tools, more incentives should be developed and applied to the assessments to provide more ideas for policymakers.
- In this research, the geography was limited to the UK. Applying this study to other countries would provide more information of BECCS application in energy generation on a global scale as this will consider the differences across countries.
- CO_2 utilisation should be coupled with CO_2 storage and the ratio optimised to achieve maximum negative emissions with CCUS.
- An uncertainty analysis study should be included in addition to the sensitivity analysis to account for the variability of the process model inputs and simplifications.

References

[1] IEA, Key World Energy Statistics 2020, Paris, 2020.

[2] IEA, World Energy Outlook 2016, (2016). https://www.iea.org/reports/world-energy-outlook-2016 (accessed January 26, 2021).

[3] EIA, EIA projects nearly 50% increase in world energy usage by 2050, led by growth in Asia , U.S. Energy Inf. Adm. (2019). https://www.eia.gov/todayinenergy/detail.php?id=41433 (accessed February 22, 2021).

[4] B. Gates, How energy makes life possible , Gates Notes. (2017). https://www.gatesnotes.com/Books/Energy-and-Civilization (accessed January 26, 2021).

[5] A. Jensen, Energy Resources in the Industrial Revolution, Sciencing.Com. (2017). https://sciencing.com/energy-resources-industrial-revolution-7639537.html (accessed January 26, 2021).

[6] IEA, Global Energy Review 2019, Paris, 2020. www.iea.org/t&c/ (accessed February 22, 2021).

[7] Union of Concerned Scientists USA, Why Does CO2 get more attention than other gases?, Union Concerned Sci. Inc. (2017). https://www.ucsusa.org/resources/why-does-co2-get-more-attention-other-gases#.W2LCvy3My3U (accessed January 26, 2021).

[8] Department of Energy & Climate Change, Local Authority Carbon Dioxide Emissions Emstimates 2014, London, 2016. https://www.gov.uk/government/collections/uk (accessed January 26, 2021).

[9] H. Ritchie, Sector by sector: where do global greenhouse gas emissions come from?, Our World Data. (2020). https://ourworldindata.org/ghg-emissions-by-sector (accessed February 22, 2021).

[10] IEA, Data & Statistics , (n.d.). https://www.iea.org/data-and-statistics?country=WORLD&fuel=CO2 emissions&indicator=CO2BySector (accessed January 26, 2021).

[11] UNFCCC, KYOTO PROTOCOL TO THE UNITED NATIONS FRAMEWORK CONVENTION ON CLIMATE CHANGE UNITED NATIONS, Kyoto, 1998.

[12] M. Jakob, M. Haller, R. Marschinski, Will history repeat itself? Economic convergence and convergence in energy use patterns, Energy Econ. 34 (2012) 95–104. https://doi.org/10.1016/j.eneco.2011.07.008.

[13] M. Jakob, J.C. Steckel, How climate change mitigation could harm development in poor countries, Wiley Interdiscip. Rev. Clim. Chang. 5 (2014) 161–168. https://doi.org/10.1002/wcc.260.

[14] E.& I.S. Department for Business, UK ENERGY IN BRIEF 2017, London, 2017. www.nationalarchives.gov.uk/doc/open-government- (accessed January 26, 2021).

[15] S. Evans, Analysis: UK's CO2 emissions have fallen 29% over the past decade, Carbon Br. (2020). https://www.carbonbrief.org/analysis-uks-co2-emissions-have-fallen-29-per-cent-over-the-past-decade (accessed February 22, 2021).

[16] Z. Hausfather, Analysis: Why the UK's CO2 emissions have fallen 38% since 1990, Carbon Br. (2019). https://www.carbonbrief.org/analysis-why-the-uks-co2-emissions-have-fallen-38-since-1990 (accessed February 22, 2021).

[17] A. Ajanovic, R. Haas, Economic challenges for the future relevance of biofuels in transport in EU countries, Energy. 35 (2010) 3340–3348. https://doi.org/10.1016/j.energy.2010.04.020.

[18] IPCC, CARBON DIOXIDE CAPTURE AND STORAGE, Cambridge University Press, Cambridge, 2005.

[19] T.F. Wall, Combustion processes for carbon capture, Proc. Combust. Inst. 31 I (2007) 31–47. https://doi.org/10.1016/j.proci.2006.08.123.

[20] D.Y.C. Leung, G. Caramanna, M.M. Maroto-Valer, An overview of current status of carbon dioxide capture and storage technologies, Renew. Sustain. Energy Rev. (2014). https://doi.org/10.1016/j.rser.2014.07.093.

[21] Zero CO2, What is CCS?, Zerom Emiss. Resour. Organ. (2017). http://www.zeroco2.no/introduction/what-is-ccs (accessed February 23, 2021).

[22] B.J.P. Buhre, L.K. Elliott, C.D. Sheng, R.P. Gupta, T.F. Wall, Oxy-fuel combustion technology for coal-fired power generation, Prog. Energy Combust. Sci. 31 (2005) 283–307. https://doi.org/10.1016/j.pecs.2005.07.001.

[23] N. Kampman, A. Busch, P. Bertier, J. Snippe, S. Hangx, V. Pipich, Z. Di, G. Rother, J.F. Harrington, J.P. Evans, A. Maskell, H.J. Chapman, M.J. Bickle, Observational evidence confirms modelling of the long-term integrity of CO2-reservoir caprocks, Nat. Commun. 2016 71. 7 (2016) 1–10. https://doi.org/10.1038/ncomms12268.

[24] EIA, Renewable energy explained , U.S. Energy Inf. Adm. (2020). https://www.eia.gov/energyexplained/renewable-sources/ (accessed February 24, 2021).

[25] N. Edomah, Economics of Energy Supply, in: Ref. Modul. Earth Syst. Environ. Sci., Elsevier, 2018. https://doi.org/10.1016/b978-0-12-409548-9.11713-0.

[26] EIA, Biomass explained, U.S. Energy Inf. Adm. (2020). https://www.eia.gov/energyexplained/biomass/ (accessed February 24, 2021).

[27] EIA, Wind explained, U.S. Energy Inf. Adm. (2020). https://www.eia.gov/energyexplained/wind/ (accessed February 24, 2021).

[28] EIA, Hydropower explained, U.S. Energy Inf. Adm. (2020). https://www.eia.gov/energyexplained/hydropower/ (accessed February 24, 2021).

[29] OpenLearn, An introduction to sustainable energy, (2018).

[30] Ocean Energy Council, Tidal Energy , Ocean Energy Counc. Inc. (2008). https://web.archive.org/web/20080513175027/http://www.oceanenergycouncil.com/index.php/Tidal-Energy/Tidal-Energy.html (accessed February 24, 2021).

[31] EASAC, Negative Emission Technologies: What Role in Meeting Paris Agreement Targets?, 2018.

[32] Climate ADAPT, Afforestation and reforestation as adaptation opportunity — Climate-ADAPT, Clim. Adapt. (2020). https://climate-adapt.eea.europa.eu/metadata/adaptation-options/afforestation-and-reforestation-as-adaptation-opportunity (accessed March 8, 2021).

[33] R. Cho, Can Soil Help Combat Climate Change?, Columbia Univ. (2018). https://blogs.ei.columbia.edu/2018/02/21/can-soil-help-combat-climate-change/ (accessed March 8, 2021).

[34] C. Chow, Enhanced Weathering for Carbon Capture |, Earth.Org. (2020). https://earth.org/enhanced-weathering-for-carbon-capture/ (accessed March 8, 2021).

[35] S. Fuss, W.F. Lamb, M.W. Callaghan, J. Hilaire, F. Creutzig, T. Amann, T. Beringer, W. De Oliveira Garcia, J. Hartmann, T. Khanna, G. Luderer, G.F. Nemet, J. Rogelj, P. Smith, J.V. Vicente, J. Wilcox, M. Del Mar Zamora Dominguez, J.C. Minx, Negative emissions - Part 2: Costs, potentials and side effects, Environ. Res. Lett. 13 (2018) 063002. https://doi.org/10.1088/1748-9326/aabf9f.

[36] IEAGHG, POTENTIAL FOR BIOMASS AND CARBON DIOXIDE CAPTURE AND STORAGE, 2011. www.ieaghg.org (accessed February 25, 2021).

[37] D. O'driscoll, Carbon Abatement Potential of Reforestation, 2018.

[38] J. Busch, J. Engelmann, S.C. Cook-Patton, B.W. Griscom, T. Kroeger, H. Possingham, P. Shyamsundar, Potential for low-cost carbon dioxide removal through tropical reforestation, Nat. Clim. Chang. 9 (2019) 463–466. https://doi.org/10.1038/s41558-019-0485-x.

[39] IPCC, Climate Change 2014: Synthesis Report. Contribution of Working Groups I, II and III to the Fifth Assessment Report of the Intergovernmental Panel on Climate Change, in: Core Writing Team, R.K. Pachauri, L. Meyer (Eds.), IPCC, Geneva, Switzerland, 2014: pp. 0–151. http://www.ipcc.ch. (accessed January 29, 2021).

[40] LSE, Climate Change Laws of the World, Grantham Res. Inst. Clim. Chang. Environ. (2021). https://climate-laws.org/ (accessed February 24, 2021).

[41] European Commission, Outcome of the October 2014 European Council, Brussels, 2014.

[42] European Commission, COMMUNICATION FROM THE COMMISSION TO THE EUROPEAN PARLIAMENT AND THE COUNCIL European Energy Security Strategy, Brussels, 2014. https://eur-lex.europa.eu/legal-

content/EN/TXT/PDF/?uri=CELEX:52014DC0330&from=EN (accessed February 24, 2021).

[43] S. Evans, The EU energy security strategy in 5 graphs, Carbon Br. (2014). https://www.carbonbrief.org/the-eu-energy-security-strategy-in-5-graphs (accessed February 24, 2021).

[44] European Commission, An EU Strategy to harness the potential of offshore renewable energy for a climate neutral future, Brussels, 2020. https://ec.europa.eu/environment/nature/natura2000/management/pdf/guidance_on_energy_transmission_infrastr (accessed February 24, 2021).

[45] CCC, The Sixth Carbon Budget: The UK's path to Net Zero, London, 2020. https://www.theccc.org.uk/publication/sixth-carbon-budget/.

[46] UK Parliament, Climate Change Act 2008, c.27, London, 2008. https://www.legislation.gov.uk/ukpga/2008/27/contents (accessed February 24, 2021).

[47] Department of Energy & Climate Change, Final Statement for the First Carbon Budget Period, London, 2014. www.nationalarchives.gov.uk/doc/open-government-licence/version/2/ (accessed February 24, 2021).

[48] Department for Business Energy & Industrial Strategy, FINAL STATEMENT FOR THE SECOND CARBON BUDGET, London, 2019. www.gov.uk/government/publications (accessed February 24, 2021).

[49] S. Evans, J. Gabbatiss, CCC: UK risks 'egg on face' unless it accelerates climate plans, Carbon Br. (2020). https://www.carbonbrief.org/ccc-uk-risks-egg-on-face-unless-it-accelerates-climate-plans (accessed February 24, 2021).

[50] UK Parliament, The CRC Energy Efficiency Scheme Order 2013, No.1119, 2013. https://www.legislation.gov.uk/uksi/2013/1119/contents/made (accessed February 25, 2021).

[51] UK Parliament, The Renewables Obligation Order 2006, No. 1004, 2006. https://www.legislation.gov.uk/uksi/2006/1004/made (accessed February 25, 2021).

[52] Ofgem, RO closure, (n.d.). https://www.ofgem.gov.uk/environmental-programmes/ro/about-ro/ro-closure (accessed February 25, 2021).

[53] UK Parliament, Energy Act 2013, c.32, 2013. https://www.legislation.gov.uk/ukpga/2013/32/contents (accessed February 25, 2021).

[54] Department of Energy & Climate Change, Electricity Market Reform: Policy Overview, London, 2012.

[55] UK Parliament, The Renewable Transport Fuel Obligations Order 2007, No. 3072, 2007. https://www.legislation.gov.uk/uksi/2007/3072/contents/made (accessed February 25, 2021).

[56] M.A. Quader, S. Ahmed, Bioenergy with carbon capture and storage (BECCS): Future prospects of carbon-negative technologies, in: Clean Energy Sustain. Dev. Comp. Contrasts New Approaches, Elsevier Inc., 2017: pp. 91–140. https://doi.org/10.1016/B978-0-12-805423-9.00004-1.

[57] C. Streck, Climate Focus Client Brief on the Paris Agreement III, Amsterdam, 2015. https://www.climatefocus.com/sites/default/files/20151228 COP 21 briefing FIN.pdf (accessed January 26, 2021).

[58] H.J. Buck, Challenges and Opportunities of Bioenergy With Carbon Capture and Storage (BECCS) for Communities, Curr. Sustain. Energy Reports. 6 (2019) 124–130. https://doi.org/10.1007/s40518-019-00139-y.

[59] S. Alberici, P. Noothout, G.U. Rehman Mir, M. Stork, F. Wiersma, ASSESSING THE POTENTIAL OF CO 2 UTILISATION IN THE UK Final Report, London, 2017.

[60] S. Heidenreich, P.U. Foscolo, New concepts in biomass gasification, Prog. Energy Combust. Sci. 46 (2015) 72–95. https://doi.org/10.1016/j.pecs.2014.06.002.

[61] Department of Energy, Hydrogen Production: Biomass Gasification, Off. Energy Effic. Renew. Energy. (2018). https://www.energy.gov/eere/fuelcells/hydrogen-production-biomass-gasification (accessed January 26, 2021).

[62] P. Basu, Biomass Gasification, Pyrolysis and Torrefaction: Practical Design and Theory, 2013. https://doi.org/10.1016/C2011-0-07564-6.

[63] ReEnergy Holdings LLC, What is Biomass?, (n.d.). https://www.reenergyholdings.com/renewable-energy/what-is-biomass/ (accessed January 26, 2021).

[64] B. Freeman, S.J. Harry, E. Kmietowicz, Biomass in a low - carbon economy, (2018).

[65] J. Lalak, D. Martyniak, A. Kasprzycka, G. Żurek, W. Moroń, M. Chmielewska, D. Wiącek, J. Tys, Comparison of selected parameters of biomass and coal, Int. Agrophysics. 30 (2016) 475–482. https://doi.org/10.1515/intag-2016-0021.

[66] M.J. Prins, K.J. Ptasinski, F.J.J.G. Janssen, From coal to biomass gasification: Comparison of thermodynamic efficiency, Energy. 32 (2007) 1248–1259. https://doi.org/10.1016/j.energy.2006.07.017.

[67] IEA Greenhouse Gas R&D Programme (IEA GHG), Biomass CCS Study, (2009) 358.

[68] IEA, Key World Energy Statistics 2019, Paris, 2019.

[69] WBA, GLOBAL BIOENERGY STATISTICS 2019 , Stockholm, 2019.

[70] BioFuel Information, History of Biofuels , Biofuel.Org.Uk. (2010). http://biofuel.org.uk/history-of-biofuels.html (accessed February 8, 2021).

[71] A.P. de Souza, A. Grandis, D.C.C. Leite, M.S. Buckeridge, Sugarcane as a Bioenergy Source: History, Performance, and Perspectives for Second-Generation Bioethanol, Bioenergy Res. 7 (2014) 24–35. https://doi.org/10.1007/s12155-013-9366-8.

[72] K. Addison, Ethanol fuel: Journey to Forever, Journey to Forever. (n.d.). http://journeytoforever.org/ethanol.html#ethintro (accessed February 8, 2021).

[73] K.L. Chin, P.S. Hng, A Real Story of Bioethanol from Biomass: Malaysia Perspective, in: Biomass Now - Sustain. Growth Use, InTech, 2013. https://doi.org/10.5772/51198.

[74] A. Campbell, N. Doswald, The impacts of biofuel production on biodiversity: A review of the current literature, Algae. (2009). https://doi.org/10.1111/j.1601-0825.2006.01350.x.

[75] J.C. Solarte-Toro, Y. Chacón-Pérez, C.A. Cardona-Alzate, Evaluation of biogas and syngas as energy vectors for heat and power generation using lignocellulosic biomass as raw material, Electron. J. Biotechnol. 33 (2018) 52–62.

https://doi.org/10.1016/J.EJBT.2018.03.005.

[76] C. Higman, M. van der Burgt, Gasification, 2003. https://doi.org/10.1016/B978-0-7506-7707-3.X5000-1.

[77] T. Damartzis, A. Zabaniotou, Thermochemical conversion of biomass to second generation biofuels through integrated process design-A review, Renew. Sustain. Energy Rev. 15 (2011) 366–378. https://doi.org/10.1016/j.rser.2010.08.003.

[78] G. Zanchi, N. Pena, N. Bird, Is woody bioenergy carbon neutral ? A comparative assessment of emissions from consumption of woody bioenergy and fossil fuel, GCB-Bioenergy. 4 (2012) 761–772. https://doi.org/10.1111/j.1757-1707.2011.01149.x.

[79] B.E. Law, E. Schulze, C. Ko, Large-scale bioenergy from additional harvest of forest biomass is neither sustainable nor greenhouse gas neutral, (2012) 611–616. https://doi.org/10.1111/j.1757-1707.2012.01169.x.

[80] Y. Wu, F. Zhao, S. Liu, L. Wang, L. Qiu, G. Alexandrov, Bioenergy production and environmental impacts, Geosci. Lett. (2018). https://doi.org/10.1186/s40562-018-0114-y.

[81] M. Fajardy, S. Chiquier, N. Mac Dowell, Investigating the BECCS resource nexus: Delivering sustainable negative emissions, Energy Environ. Sci. 11 (2018) 3408–3430. https://doi.org/10.1039/c8ee01676c.

[82] A. Yasar, S. Nazir, A.B. Tabinda, M. Nazar, R. Rasheed, M. Afzaal, Socio-economic , health and agriculture bene fi ts of rural household biogas plants in energy scarce developing countries : A case study from Pakistan, Renew. Energy. 108 (2017) 19–25. https://doi.org/10.1016/j.renene.2017.02.044.

[83] O. Lehtonen, L. Okkonen, Socio-economic impacts of a local bioenergy-based development strategy e The case of Pielinen Karelia , Finland, Renew. Energy. 85 (2016) 610–619. https://doi.org/10.1016/j.renene.2015.07.006.

[84] M.L.J. Brinkman, P. Marcelo, S. Heijnen, B. Wicke, J.J.M. Guilhoto, A. Walter, A.P.C. Faaij, F. Van Der Hilst, Interregional assessment of socio-economic e ff ects of sugarcane ethanol production in Brazil, Renew. Sustain. Energy Rev. 88 (2018) 347–362. https://doi.org/10.1016/j.rser.2018.02.014.

[85] B. Bohra, N. Sharma, S. Saxena, V. Sabhlok, Socio-economic impact of Biofuel Agroforestry Systems on Smallholder and Large-holder Farmers in Karnataka , India, Agrofor. Syst. 92 (2018) 759–774. https://doi.org/10.1007/s10457-016-0046-5.

[86] L. Okkonen, O. Lehtonen, Local , regional and national level of the socioeconomic impacts of a bio-oil production system – A case in Lieksa , Finland, Renew. Sustain. Energy Rev. 71 (2017) 103–111. https://doi.org/10.1016/j.rser.2017.01.003.

[87] J. Domac, K. Richards, S. Risovic, Socio-economic drivers in implementing bioenergy projects, 28 (2005) 97–106. https://doi.org/10.1016/j.biombioe.2004.08.002.

[88] E. Impacts, O.F. Bioenergy, Iv. s -, (n.d.) 57–64.

[89] Global CCS Institute, Understanding CCS , Glob. CCS Inst. (n.d.). https://www.globalccsinstitute.com/about/what-is-ccs/ (accessed January 29, 2021).

[90] L. Temple-Smith, G. Turan, Carbon capture and storage pipeline grows by 10 large-scale facilities globally, Glob. CCS Inst. (2020). https://www.globalccsinstitute.com/news-media/press-room/media-releases/carbon-capture-and-storage-pipeline-grows-by-10-large-scale-facilities-globally/ (accessed January 29, 2021).

[91] C. Consoli, 2019 Perspective - Bioenergy and Carbon Capture and Storage, 2019. https://www.globalccsinstitute.com/wp-content/uploads/2019/03/BECCS-Perspective_FINAL_18-March.pdf (accessed January 29, 2021).

[92] IEA, Transforming Industry through CCUS , (2019). https://www.iea.org/reports/transforming-industry-through-ccus (accessed January 26, 2021).

[93] IEA, CCUS in Clean Energy Transitions, Paris, 2020. www.iea.org/t&c/ (accessed January 4, 2021).

[94] Grand View Research, Carbon Dioxide Market Size | Industry Report, 2020-2027, Gd. View Res. (2020). https://www.grandviewresearch.com/industry-analysis/carbon-dioxide-market (accessed February 1, 2021).

[95] IEA, Putting CO2 to Use, Paris, 2019. https://www.iea.org/reports/putting-co2-to-use

(accessed January 29, 2021).

[96] I. Dimitriou, P. García-Gutiérrez, R.H. Elder, R.M. Cuéllar-Franca, A. Azapagic, R.W.K. Allen, Carbon dioxide utilisation for production of transport fuels: Process and economic analysis, Energy Environ. Sci. 8 (2015) 1775–1789. https://doi.org/10.1039/c4ee04117h.

[97] E.I. Koytsoumpa, C. Bergins, E. Kakaras, The CO2 economy: Review of CO2 capture and reuse technologies, J. Supercrit. Fluids. 132 (2018) 3–16. https://doi.org/10.1016/j.supflu.2017.07.029.

[98] B. Hu, C. Guild, S.L. Suib, Thermal, electrochemical, and photochemical conversion of CO2 to fuels and value-added products, J. CO2 Util. 1 (2013) 18–27. https://doi.org/10.1016/j.jcou.2013.03.004.

[99] Alternative Fuels Data Center, Hydrogen Production and Distribution, U.S. Dep. Energy. (n.d.). https://afdc.energy.gov/fuels/hydrogen_production.html (accessed February 1, 2021).

[100] S. Deutz, D. Bongartz, B. Heuser, A. Kätelhön, L. Schulze Langenhorst, A. Omari, M. Walters, J. Klankermayer, W. Leitner, A. Mitsos, S. Pischinger, A. Bardow, Cleaner production of cleaner fuels: Wind-to-wheel-environmental assessment of CO2-based oxymethylene ether as a drop-in fuel, Energy Environ. Sci. 11 (2018) 331–343. https://doi.org/10.1039/c7ee01657c.

[101] M. Puig-Arnavat, J.C. Bruno, A. Coronas, Review and analysis of biomass gasification models, Renew. Sustain. Energy Rev. 14 (2010) 2841–2851. https://doi.org/10.1016/j.rser.2010.07.030.

[102] G.C. Vaughan, Equilibrium Modeling of Coal and Biomass Gasification, Auburn University, 2015.

[103] C.Z. Li, Importance of volatile-char interactions during the pyrolysis and gasification of low-rank fuels - A review, Fuel. 112 (2013) 609–623. https://doi.org/10.1016/j.fuel.2013.01.031.

[104] NETL, Gasification Introduction , Natl. Energy Technol. Lab. (2017). https://www.netl.doe.gov/research/Coal/energy-

systems/gasification/gasifipedia/intro-to-gasification (accessed January 26, 2021).

[105] H. Jameel, D.R. Keshwani, Thermochemical Conversion of Biomass to Power and Fuels, in: J.J. Cheng (Ed.), Cheng, J.J., 2nd ed., CRC Press, Boca Raton, 2017: pp. 375–421. https://doi.org/10.1201/9781315152868-10.

[106] P. Basu, Biomass Gasification, Pyrolysis and Torrefaction: Practical Design and Theory, 2nd ed., Elsevier Inc., Oxford, 2013. https://doi.org/10.1016/C2011-0-07564-6.

[107] FAO, Wood gas as engine fuel, Rome, 1986.

[108] A. de Klerk, Fischer-Tropsch Process, in: Kirk-Othmer Encycl. Chem. Technol., John Wiley & Sons, Inc., Hoboken, NJ, USA, 2013: pp. 1–20. https://doi.org/10.1002/0471238961.fiscdekl.a01.

[109] H. Schulz, Short history and present trends of Fischer-Tropsch synthesis, Appl. Catal. A Gen. 186 (1999) 3–12. https://doi.org/10.1016/S0926-860X(99)00160-X.

[110] E4Tech, Review of Technologies for Gasification of Biomass and Wastes Final report, NNFCC Bioeconomy Consult. (2009) 1–130. http://www.e4tech.com/wp-content/uploads/2016/01/gasification2009.pdf%0Ahttp://www.nnfcc.co.uk/tools/review-of-technologies-for-gasification-of-biomass-and-wastes-nnfcc-09-008.

[111] G. Jacobs, B.H. Davis, Chapter 5 Conversion of Biomass to Liquid Fuels and Chemicals via the Fischer–Tropsch Synthesis Route, in: M. Crocker (Ed.), Thermochem. Convers. Biomass to Liq. Fuels Chem., The Royal Society of Chemistry, 2010: pp. 95–124. https://doi.org/10.1039/9781849732260-00095.

[112] P.L. Spath, D.C. Dayton, Preliminary Screening – Technical and Economic Assessment of Synthesis Gas to Fuels and Chemicals with Emphasis on the Potential for Biomass-Derived Syngas, 2003. http://www.osti.gov/bridge (accessed February 2, 2021).

[113] NETL, Fischer-Tropsch Synthesis , U.S. Dep. Energy. (n.d.). https://www.netl.doe.gov/research/coal/energy-systems/gasification/gasifipedia/ftsynthesis (accessed February 2, 2021).

[114] H. Mahmoudi, M. Mahmoudi, O. Doustdar, H. Jahangiri, A. Tsolakis, S. Gu, M. LechWyszynski, A review of Fischer Tropsch synthesis process, mechanism, surface

chemistry and catalyst formulation, Biofuels Eng. 2 (2018) 11–31. https://doi.org/10.1515/bfuel-2017-0002.

[115] 10.2. Fischer-Tropsch Synthesis | netl.doe.gov, (n.d.). https://www.netl.doe.gov/research/coal/energy-systems/gasification/gasifipedia/ftsynthesis (accessed June 29, 2020).

[116] S.S. Ail, S. Dasappa, Biomass to liquid transportation fuel via Fischer Tropsch synthesis - Technology review and current scenario, Renew. Sustain. Energy Rev. 58 (2016) 267–286. https://doi.org/10.1016/j.rser.2015.12.143.

[117] G.A. Mills, F.W. Steffgen, Catalytic methanation, Catal. Rev. 8 (1974) 159–210. https://doi.org/10.1080/01614947408071860.

[118] S. Rönsch, J. Schneider, S. Matthischke, M. Schlüter, M. Götz, J. Lefebvre, P. Prabhakaran, S. Bajohr, Review on methanation - From fundamentals to current projects, Fuel. 166 (2016) 276–296. https://doi.org/10.1016/j.fuel.2015.10.111.

[119] NETL, Technology for SNG Production, U.S. Dep. Energy. (n.d.). https://www.netl.doe.gov/research/coal/energy-systems/gasification/gasifipedia/coal-to-sng (accessed February 2, 2021).

[120] C. Wix, I. Dybkjaer, H. Topsøe, L. Denmark, N.R. Udengaard, Coal-To-SNG: The Methanation Process, n.d.

[121] Halder Topsøe, From solid fuels to substitute natural gas (SNG) using TREMP, Tech. Report, Halder Topsøe. (2009) 8. http://scholar.google.com/scholar?hl=en&btnG=Search&q=intitle:From+solid+fuels+to+substitute+natural+gas+(SNG)+using+TREMP?#4.

[122] Approval granted for £150m renewable gas plant in Cheshire - Energy Live News, (n.d.).

[123] BI Staff, Göteborg Energi winds down GoBIGas 1 project in advance, Bioenergy Int. (2018). https://bioenergyinternational.com/research-development/goteborg-energi-winds-gobigas-1-project-advance.

[124] Germany launches new study of oxymethylene ethers for optimizing clean diesel

combustion - Green Car, (n.d.).

[125] D.S. Moulton, D.W. Nageli, Diesel fuel having improved qualities and method of forming, 5746785, 1998.

[126] C.J. Baranowski, A.M. Bahmanpour, O. Kröcher, Catalytic synthesis of polyoxymethylene dimethyl ethers (OME): A review, Appl. Catal. B Environ. 217 (2017) 407–420. https://doi.org/10.1016/j.apcatb.2017.06.007.

[127] Z. Ma, Z. Huang, C. Li, X. Wang, H. Miao, Combustion and emission characteristics of a diesel engine fuelled with diesel-propane blends, Fuel. 87 (2008) 1711–1717. https://doi.org/10.1016/j.fuel.2007.09.011.

[128] H. Liu, Z. Wang, J. Wang, X. He, Y. Zheng, Q. Tang, J. Wang, Performance, combustion and emission characteristics of a diesel engine fueled with polyoxymethylene dimethyl ethers (PODE3-4)/ diesel blends, Energy. 88 (2015) 793–800. https://doi.org/10.1016/j.energy.2015.05.088.

[129] B. Lumpp, D. Rothe, C. Pastötter, R. Lämmermann, E. Jacob, OXYMETHYLENE ETHERS AS DIESEL FUEL ADDITIVES OF THE FUTURE, MTZ Worldw. 72 (2011) 34–38. https://doi.org/10.1365/s38313-011-0027-z.

[130] A. Feiling, M. Münz, C. Beidl, Potenzial des synthetischen Kraftstoffs OME1b für den rußfreien Dieselmotor, ATZextra. 21 (2016) 16–21. https://doi.org/10.1007/s35778-015-0109-7.

[131] H. Liu, Z. Wang, J. Zhang, J. Wang, S. Shuai, Study on combustion and emission characteristics of Polyoxymethylene Dimethyl Ethers/diesel blends in light-duty and heavy-duty diesel engines, Appl. Energy. 185 (2017) 1393–1402. https://doi.org/10.1016/j.apenergy.2015.10.183.

[132] J. Burger, E. Ströfer, H. Hasse, Production process for diesel fuel components poly(oxymethylene) dimethyl ethers from methane-based products by hierarchical optimization with varying model depth, Chem. Eng. Res. Des. 91 (2013) 2648–2662. https://doi.org/10.1016/j.cherd.2013.05.023.

[133] M. Härtl, K. Gaukel, D. Pélerin, G. Wachtmeister, Oxymethylene Ether as Potentially CO2-neutral Fuel for Clean Diesel Engines Part 1: Engine Testing, MTZ Worldw. 78

(2017) 52–59. https://doi.org/10.1007/s38313-016-0163-6.

[134] N. Schmitz, J. Burger, E. Ströfer, H. Hasse, From methanol to the oxygenated diesel fuel poly(oxymethylene) dimethyl ether: An assessment of the production costs, Fuel. 185 (2016) 67–72. https://doi.org/10.1016/j.fuel.2016.07.085.

[135] A.O. Oyedun, A. Kumar, The development of the production cost of oxymethylene ethers as diesel additives from biomass, (2018). https://doi.org/10.1002/bbb.1887.

[136] D. Bongartz, J. Burre, A. Mitsos, Production of Oxymethylene Dimethyl Ethers from Hydrogen and Carbon Dioxide - Part I: Modeling and Analysis for OME1, Ind. Eng. Chem. Res. 58 (2019) 4881–4889. https://doi.org/10.1021/acs.iecr.8b05576.

[137] S. Chattopadhyay, S. Ghosh, Techno-economic assessment of a biomass-based combined power and cooling plant for rural application, Clean Technol. Environ. Policy. 22 (2020) 907–922. https://doi.org/10.1007/s10098-020-01832-z.

[138] S. Restrepo-Valencia, A. Walter, Techno-economic assessment of bio-energy with carbon capture and storage systems in a typical sugarcane mill in Brazil, Energies. 12 (2019). https://doi.org/10.3390/en12061129.

[139] A. Bhave, R.H.S. Taylor, P. Fennell, W.R. Livingston, N. Shah, N. Mac Dowell, J. Dennis, M. Kraft, M. Pourkashanian, M. Insa, J. Jones, N. Burdett, A. Bauen, C. Beal, A. Smallbone, J. Akroyd, Screening and techno-economic assessment of biomass-based power generation with CCS technologies to meet 2050 CO2 targets, Appl. Energy. 190 (2017) 481–489. https://doi.org/10.1016/j.apenergy.2016.12.120.

[140] K. Al-Qayim, W. Nimmo, M. Pourkashanian, Comparative techno-economic assessment of biomass and coal with CCS technologies in a pulverized combustion power plant in the United Kingdom, Int. J. Greenh. Gas Control. (2015). https://doi.org/10.1016/j.ijggc.2015.10.013.

[141] E. Catalanotti, K.J. Hughes, R.T.J. Porter, J. Price, M. Pourkashanian, Evaluation of performance and cost of combustion-based power plants with CO2 capture in the United Kingdom, Environ. Prog. Sustain. Energy. (2014). https://doi.org/10.1002/ep.11894.

[142] J.C. Meerman, M. Knoope, A. Ramírez, W.C. Turkenburg, A.P.C. Faaij, The techno-

economic potential of integrated gasification co-generation facilities with CCS Going from coal to biomass, Energy Procedia. 37 (2013) 6053–6061. https://doi.org/10.1016/j.egypro.2013.06.534.

[143] M. Bui, M. Fajardy, N. Mac Dowell, Bio-energy with carbon capture and storage (BECCS): Opportunities for performance improvement, Fuel. 213 (2018) 164–175. https://doi.org/10.1016/j.fuel.2017.10.100.

[144] D. Zhang, M. Bui, M. Fajardy, P. Patrizio, F. Kraxner, N. Mac Dowell, Unlocking the potential of BECCS with indigenous sources of biomass at a national scale, Sustain. Energy Fuels. 4 (2019) 226–253. https://doi.org/10.1039/c9se00609e.

[145] R.P. Cabral, M. Bui, N. Mac, International Journal of Greenhouse Gas Control A synergistic approach for the simultaneous decarbonisation of power and industry via bioenergy with carbon capture and storage (BECCS), Int. J. Greenh. Gas Control. 87 (2019) 221–237. https://doi.org/10.1016/j.ijggc.2019.05.020.

[146] C. Cumicheo, N. Mac Dowell, N. Shah, Natural gas and BECCS: A comparative analysis of alternative configurations for negative emissions power generation, Int. J. Greenh. Gas Control. 90 (2019) 102798. https://doi.org/10.1016/j.ijggc.2019.102798.

[147] R.P. Cabral, M. Bui, N. Mac Dowell, A synergistic approach for the simultaneous decarbonisation of power and industry via bioenergy with carbon capture and storage (BECCS), Int. J. Greenh. Gas Control. 87 (2019) 221–237. https://doi.org/10.1016/j.ijggc.2019.05.020.

[148] O. Emenike, S. Michailos, K.N. Finney, K.J. Hughes, D. Ingham, M. Pourkashanian, Initial techno-economic screening of BECCS technologies in power generation for a range of biomass feedstock, Sustain. Energy Technol. Assessments. 40 (2020) 100743. https://doi.org/10.1016/j.seta.2020.100743.

[149] M. Fajardy, N. Mac Dowell, The energy return on investment of BECCS: Is BECCS a threat to energy security?, Energy Environ. Sci. 11 (2018) 1581–1594. https://doi.org/10.1039/c7ee03610h.

[150] I.S. Tagomori, P.R.R. Rochedo, A. Szklo, Techno-economic and georeferenced analysis of forestry residues-based Fischer-Tropsch diesel with carbon capture in Brazil, Biomass and Bioenergy. 123 (2019) 134–148.

https://doi.org/10.1016/j.biombioe.2019.02.018.

[151] G. Song, J. Xiao, Y. Yu, L. Shen, A techno-economic assessment of SNG production from agriculture residuals in China, Energy Sources, Part B Econ. Plan. Policy. 11 (2016) 465–471. https://doi.org/10.1080/15567249.2012.654595.

[152] S. Michailos, O. Emenike, D. Ingham, K.J. Hughes, M. Pourkashanian, Methane production via syngas fermentation within the bio-CCS concept: A techno-economic assessment, Biochem. Eng. J. 150 (2019) 107290. https://doi.org/https://doi.org/10.1016/j.bej.2019.107290.

[153] G. de. Álamo, J. Sandquist, B.J. Vreugdenhill, G.A. Almansa, M. Carbo, Implementation of bio-CCS in biofuels production - IEA Bionergy Task 33 special report, 2018.

[154] I. Dimitriou, H. Goldingay, A. V. Bridgwater, Techno-economic and uncertainty analysis of Biomass to Liquid (BTL) systems for transport fuel production, Renew. Sustain. Energy Rev. 88 (2018) 160–175. https://doi.org/10.1016/j.rser.2018.02.023.

[155] R.M. Swanson, A. Platon, J.A. Satrio, R.C. Brown, Techno-economic analysis of biomass-to-liquids production based on gasification, Fuel. 89 (2010) S11–S19. https://doi.org/10.1016/j.fuel.2010.07.027.

[156] H. Thunman, C. Gustavsson, A. Larsson, I. Gunnarsson, F. Tengberg, Economic assessment of advanced biofuel production via gasification using real cost data from GoBiGas, a first-of-its-kind industrial installation, Submitt. Energy Sci. Eng. (2018) 105–118. https://doi.org/10.1002/ese3.271.

[157] M.C. Carbo, R. Smit, B. Van Der Drift, D. Jansen, Bio energy with CCS (BECCS): Large potential for BioSNG at low CO 2 avoidance cost, Energy Procedia. 4 (2011) 2950–2954. https://doi.org/10.1016/j.egypro.2011.02.203.

[158] D.H. König, M. Freiberg, R.U. Dietrich, A. Wörner, Techno-economic study of the storage of fluctuating renewable energy in liquid hydrocarbons, Fuel. (2015). https://doi.org/10.1016/j.fuel.2015.06.085.

[159] M.A. Adnan, M.G. Kibria, Comparative techno-economic and life-cycle assessment of power-to-methanol synthesis pathways, Appl. Energy. (2020). https://doi.org/10.1016/j.apenergy.2020.115614.

[160] J. Gorre, F. Ortloff, C. van Leeuwen, Production costs for synthetic methane in 2030 and 2050 of an optimized Power-to-Gas plant with intermediate hydrogen storage, Appl. Energy. (2019). https://doi.org/10.1016/j.apenergy.2019.113594.

[161] S. Brynolf, M. Taljegard, M. Grahn, J. Hansson, Electrofuels for the transport sector: A review of production costs, Renew. Sustain. Energy Rev. 81 (2018) 1887–1905. https://doi.org/10.1016/j.rser.2017.05.288.

[162] V. Dieterich, A. Buttler, A. Hanel, H. Spliethoff, S. Fendt, Power-to-liquid via synthesis of methanol, DME or Fischer–Tropsch-fuels: a review , Energy Environ. Sci. 13 (2020) 3207–3252. https://doi.org/10.1039/d0ee01187h.

[163] S. Michailos, S. McCord, V. Sick, G. Stokes, P. Styring, Dimethyl ether synthesis via captured CO2 hydrogenation within the power to liquids concept: A techno-economic assessment, Energy Convers. Manag. 184 (2019) 262–276. https://doi.org/10.1016/j.enconman.2019.01.046.

[164] A. Sternberg, A. Bardow, Power-to-What?-Environmental assessment of energy storage systems, Energy Environ. Sci. 8 (2015) 389–400. https://doi.org/10.1039/c4ee03051f.

[165] C. Van Der Giesen, R. Kleijn, G.J. Kramer, Energy and climate impacts of producing synthetic hydrocarbon fuels from CO2, Environ. Sci. Technol. 48 (2014) 7111–7121. https://doi.org/10.1021/es500191g.

[166] S.R. Upreti, Process Modeling and Simulation for Chemical Engineers, 2017. https://doi.org/10.1002/9781118914670.

[167] S. Hall, Rules of thumb for chemical engineers, 2017. https://doi.org/10.1016/c2016-0-00182-1.

[168] D.C.Y. Foo, R. Elyas, Introduction to Process Simulation, in: Chem. Eng. Process Simul., 2017. https://doi.org/10.1016/B978-0-12-803782-9.00001-7.

[169] Process Systems Enterprise, The gPROMS platform, (n.d.). https://www.psenterprise.com/products/gproms/platform (accessed February 16, 2021).

[170] CMU EPP, Integrated Environmental Control Model (IECM), (2012).

[171] Carneige Mellon, Integrated Environmental Control Model, (n.d.). https://www.cmu.edu/epp/iecm/ (accessed February 16, 2021).

[172] K.J. Borgert, E.S. Rubin, Oxy-combustion Carbon Capture for Pulverized Coal in the Integrated Environmental Control Model, Energy Procedia. 114 (2017) 522–529. https://doi.org/10.1016/j.egypro.2017.03.1194.

[173] A.B. Rao, P.C. Phadke, CO2 Capture and Storage in Coal Gasification Projects, IOP Conf. Ser. Earth Environ. Sci. 76 (2017). https://doi.org/10.1088/1755-1315/76/1/012011.

[174] H. Gerbelová, C. Ioakimidis, P. Ferrão, A techno-economical study of the CO2 capture in the energy sector in Portugal, Energy Procedia. 4 (2011) 1965–1972. https://doi.org/10.1016/j.egypro.2011.02.077.

[175] A.B. Rao, E.S. Rubin, A technical, economic, and environmental assessment of amine-based CO2 capture technology for power plant greenhouse gas control, Environ. Sci. Technol. 36 (2002) 4467–4475. https://doi.org/10.1021/es0158861.

[176] CMU EPP, Integrated Environmental Control Model - Documentation, (n.d.). https://www.cmu.edu/epp/iecm/iecm_doc.html.

[177] I.. {Aspen Technology, Aspen Plus ® User Guide, Aspen Technol. Inc. (2000) 936.

[178] NIST/SEMATECH, Process Modeling, E-Handb. Stat. Model. (2013). https://www.itl.nist.gov/div898/handbook/pmd/section1/pmd13.htm (accessed January 26, 2021).

[179] L.P.R. Pala, Q. Wang, G. Kolb, V. Hessel, Steam gasification of biomass with subsequent syngas adjustment using shift reaction for syngas production: An Aspen Plus model, Renew. Energy. 101 (2017) 484–492. https://doi.org/10.1016/j.renene.2016.08.069.

[180] P. Kaushal, R. Tyagi, Advanced simulation of biomass gasification in a fluidized bed reactor using ASPEN PLUS, Renew. Energy. 101 (2017) 629–636. https://doi.org/10.1016/j.renene.2016.09.011.

[181] W. Doherty, A. Reynolds, D. Kennedy, Simulation of a Circulating Fluidised Bed Biomass Gasifier using ASPEN Plus : a Performance Analysis, Dublin Inst. Technol. (2008) 1241–

1248.

[182] C.A. Callaghan, Kinetics and Catalysis of the Water-Gas-Shift Reaction : A Microkinetic and Graph Theoretic Approach, (2006).

[183] S. Jarungthammachote, A. Dutta, Thermodynamic equilibrium model and second law analysis of a downdraft waste gasifier, Energy. 32 (2007) 1660–1669. https://doi.org/10.1016/j.energy.2007.01.010.

[184] X.T. Li, J.R. Grace, C.J. Lim, A.P. Watkinson, H.P. Chen, J.R. Kim, Biomass gasification in a circulating fluidized bed, Biomass and Bioenergy. (2004). https://doi.org/10.1016/S0961-9534(03)00084-9.

[185] N. Jand, V. Brandani, P.U. Foscolo, Thermodynamic limits and actual product yields and compositions in biomass gasification processes, Ind. Eng. Chem. Res. 45 (2006) 834–843. https://doi.org/10.1021/ie050824v.

[186] A.V. Bridgwater, The technical and economic feasibility of biomass gasification for power generation, Fuel. 74 (1995) 631–653. https://doi.org/10.1016/0016-2361(95)00001-L.

[187] a G. Barea, H. Thunman, Prediction of gas composition in biomass gasifiers., ... Congr. Energy .... (2007) 4–7. http://grupo.us.es/bioenergia/templates/jubilee/pdf/presentacion8-1.pdf.

[188] W. Gumz, Gas producers and blast furnaces : theory and methods of calculation / Wilhelm Gumz, Wiley ; Chapman & Hall, New York : London, 1950.

[189] A. Gómez-Barea, B. Leckner, Modeling of biomass gasification in fluidized bed, Prog. Energy Combust. Sci. 36 (2010) 444–509. https://doi.org/10.1016/j.pecs.2009.12.002.

[190] P. Kaushal, J. Abedi, N. Mahinpey, A comprehensive mathematical model for biomass gasification in a bubbling fluidized bed reactor, Fuel. 89 (2010) 3650–3661. https://doi.org/10.1016/j.fuel.2010.07.036.

[191] X. Bingyan, L. Zhengfen, Z.X.I. Guang, Kinetic study on biomass gasification, Sol. Energy. (1992) 199–204. https://doi.org/0038-092X/92.

[192] B. Hejazi, J.R. Grace, X. Bi, A. Mahecha-Botero, Kinetic Model of Steam Gasification of

Biomass in a Bubbling Fluidized Bed Reactor, Energy & Fuels. 31 (2017) 1702–1711. https://doi.org/10.1021/acs.energyfuels.6b03161.

[193] J.C. Wurzenberger, S. Wallner, H. Raupenstrauch, J.G. Khinast, Thermal conversion of biomass: Comprehensive reactor and particle modeling, AIChE J. 48 (2002) 2398–2411. https://doi.org/10.1002/aic.690481029.

[194] M.L. Boroson, J.B. Howard, J.P. Longwell, W.A. Peters, Product yields and kinetics from the vapor phase cracking of wood pyrolysis tars, AIChE J. 35 (1989) 120–128. https://doi.org/10.1002/aic.690350113.

[195] C. Dupont, T. Nocquet, J.A. Da Costa, C. Verne-Tournon, Kinetic modelling of steam gasification of various woody biomass chars: Influence of inorganic elements, Bioresour. Technol. 102 (2011) 9743–9748. https://doi.org/10.1016/j.biortech.2011.07.016.

[196] Y. Wang, C.M. Kinoshita, Kinetic model of biomass gasification, Sol. Energy. 51 (1993) 19–25. https://doi.org/10.1016/0038-092X(93)90037-O.

[197] R. Radmanesh, J. Cnaouki, C. Guy, Biomass gasification in a bubbling fluidized bed reactor: Experiments and modeling, AIChE J. (2006). https://doi.org/10.1002/aic.11020.

[198] M.B. Nikoo, N. Mahinpey, Simulation of biomass gasification in fluidized bed reactor using ASPEN PLUS, Biomass and Bioenergy. 32 (2008) 1245–1254. https://doi.org/10.1016/j.biombioe.2008.02.020.

[199] N.R. Mitta, S. Ferrer-Nadal, A.M. Lazovic, J.F. Parales, E. Velo, L. Puigjaner, Modelling and simulation of a tyre gasification plant for synthesis gas production, Comput. Aided Chem. Eng. 21 (2006) 1771–1776. https://doi.org/10.1016/S1570-7946(06)80304-4.

[200] N. Ramzan, A. Ashraf, S. Naveed, A. Malik, Simulation of hybrid biomass gasification using Aspen plus: A comparative performance analysis for food, municipal solid and poultry waste, Biomass and Bioenergy. 35 (2011) 3962–3969. https://doi.org/10.1016/j.biombioe.2011.06.005.

[201] N.A. Pambudi, T. Laukkanen, M. Syamsiro, I.M. Gandidi, Simulation of Jatropha curcas shell in gasifier for synthesis gas and hydrogen production, J. Energy Inst. 90 (2017) 672–679. https://doi.org/10.1016/j.joei.2016.07.010.

[202] A. Gagliano, F. Nocera, M. Bruno, G. Cardillo, Development of an Equilibrium-based Model of Gasification of Biomass by Aspen Plus, Energy Procedia. 111 (2017) 1010–1019. https://doi.org/10.1016/j.egypro.2017.03.264.

[203] L. Abdelouahed, O. Authier, G. Mauviel, J.P. Corriou, G. Verdier, A. Dufour, Detailed modeling of biomass gasification in dual fluidized bed reactors under aspen plus, Energy and Fuels. 26 (2012) 3840–3855. https://doi.org/10.1021/ef300411k.

[204] J.H. Pauls, N. Mahinpey, E. Mostafavi, Simulation of air-steam gasification of woody biomass in a bubbling fluidized bed using Aspen Plus: A comprehensive model including pyrolysis, hydrodynamics and tar production, Biomass and Bioenergy. 95 (2016) 157–166. https://doi.org/10.1016/j.biombioe.2016.10.002.

[205] N. Hanchate, S. Ramani, C.S. Mathpati, V.H. Dalvi, Biomass gasification using dual fluidized bed gasification systems: A review, J. Clean. Prod. 280 (2021) 123148. https://doi.org/10.1016/J.JCLEPRO.2020.123148.

[206] H. Thunman, M. Seemann, T. Berdugo Vilches, J. Maric, D. Pallares, H. Ström, G. Berndes, P. Knutsson, A. Larsson, C. Breitholtz, O. Santos, Advanced biofuel production via gasification – lessons learned from 200 man-years of research activity with Chalmers' research gasifier and the GoBiGas demonstration plant, Energy Sci. Eng. (2018). https://doi.org/10.1002/ese3.188.

[207] G. Gautam, S. Adhikari, S. Bhavnani, Estimation of biomass synthesis gas composition using equilibrium modeling, in: Energy and Fuels, 2010. https://doi.org/10.1021/ef901477c.

[208] K.D. Panopoulos, L.E. Fryda, J. Karl, S. Poulou, E. Kakaras, High temperature solid oxide fuel cell integrated with novel allothermal biomass gasification. Part I: Modelling and feasibility study, J. Power Sources. 159 (2006) 570–585. https://doi.org/10.1016/j.jpowsour.2005.12.024.

[209] G. Schuster, G. Löffler, K. Weigl, H. Hofbauer, Biomass steam gasification - An extensive parametric modeling study, Bioresour. Technol. 77 (2001) 71–79. https://doi.org/10.1016/S0960-8524(00)00115-2.

[210] W. Doherty, A. Reynolds, D. Kennedy, Aspen plus simulation of biomass gasification in a steam blown dual fluidised bed, Mater. Process Energy. (2013) 212–220.

[211] A. Alamia, S. Òsk Gardarsdòttir, A. Larsson, F. Normann, H. Thunman, Efficiency Comparison of Large-Scale Standalone, Centralized, and Distributed Thermochemical Biorefineries, Energy Technol. 5 (2017) 1435–1448. https://doi.org/10.1002/ente.201600719.

[212] R.P. Field, R. Brasington, Baseline flowsheet model for IGCC with carbon capture, Ind. Eng. Chem. Res. (2011). https://doi.org/10.1021/ie200288u.

[213] A.P. Watkinson, J.P. Lucas, C.J. Lim, A prediction of performance of commercial coal gasifiers, Fuel. 70 (1991) 519–527. https://doi.org/10.1016/0016-2361(91)90030-E.

[214] H.C. Frey, N. Akunuri, Probabilistic Modeling and Evaluation of the Performance, Emissions, and Cost of Texaco Gasifier-Based Integrated Gasification Combined Cycle Systems Using ASPEN, 2001.

[215] M. Bockelie, M. Denison, Z. Chen, C. Senior, A. Sarofim, Using Models To Select Operating Conditions for Gasifiers, (2003).

[216] E. Rubin, G. Booras, J. Davison, C. Ekstrom, M. Matuszewski, S. McCoy, C. Short, Toward a common method of cost estimation for co2 capture and storage at fossil fuel power plants, (2013) 1–36. http://cdn.globalccsinstitute.com/sites/default/files/publications/85761/toward-common-method-cost-estimation-ccs-fossil-fuel-power-plants-white-paper.pdf.

[217] A.W. Zimmermann, J. Wunderlich, L. Müller, G.A. Buchner, A. Marxen, S. Michailos, K. Armstrong, H. Naims, S. McCord, P. Styring, V. Sick, R. Schomäcker, Techno-Economic Assessment Guidelines for CO2 Utilization, Front. Energy Res. 8 (2020) 31. https://doi.org/10.3389/fenrg.2020.00005.

[218] R.K. Sinnott, G. Towler, Chemical Engineering Design 5th Edition, 2009. https://doi.org/10.1016/C2009-0-61216-2.

[219] M.S. Peters, K.D. Timmerhaus, R.E. West, Plant Design and Economics for Chemical Engineers 5th edition, 2003.

[220] G. Towler, R.K. Sinnott, Chemical Engineering Design - Principles, Practice and Economics of Plant and Process Design (2nd Edition), 2013.

[221] P. Christensen, L.R. Dysert, AACE International Recommended Practice No. 18R-97, (2005) 10. http://www.costengineering.eu/Downloads/articles/AACE_CLASSIFICATION_SYSTEM.pdf.

[222] R.K. Sinnott, Coulson and Richardson's Chemical Engineering, 2018. https://doi.org/10.1016/c2017-0-02843-4.

[223] F.G. Albrecht, D.H. König, N. Baucks, R.U. Dietrich, A standardized methodology for the techno-economic evaluation of alternative fuels – A case study, Fuel. 194 (2017) 511–526. https://doi.org/10.1016/j.fuel.2016.12.003.

[224] R. Petter, W.E. Tyner, L. Hu, S. Managi, J. Zarnikau, Technoeconomic and Policy Analysis for Corn Stover Biofuels, 2014.

[225] M. Lauer, Methodology guideline on techno economic assessment (TEA) , n.d.

[226] S.E. Tanzer, A. Ramírez, When are negative emissions negative emissions?, Energy Environ. Sci. 12 (2019) 1210–1218. https://doi.org/10.1039/c8ee03338b.

[227] N. Hill, R. Bramwell, E. Karagianni, L. Jones, J. Maccarthy, S. Hinton, C. Walker, 2020 Government greenhouse gas conversion factors for company reporting: Methodology Paper, London, 2020. www.nationalarchives.gov.uk/doc/open-government-licence/ (accessed February 18, 2021).

[228] Department for Business Energy and Industrial Strategy, Greenhouse gas reporting: conversion factors 2020, Dep. Business, Energy Ind. Strateg. (2020). https://www.gov.uk/government/publications/greenhouse-gas-reporting-conversion-factors-2020 (accessed January 22, 2021).

[229] IEA Bioenergy, Implementation of bio-CCS in biofuels production, IEA Bioenergy, 2018.

[230] T. Lockwood, A Compararitive Review of Next-generation Carbon Capture Technologies for Coal-fired Power Plant, in: Energy Procedia, 2017. https://doi.org/10.1016/j.egypro.2017.03.1850.

[231] Global CCS Institute, The Global Status of CCS, (2018) 84. www.globalccsinstitute.com.

[232] E. Institute, Hazard analysis for offshore carbon capture platforms and offshore pipelines, Hazard Anal. Offshore Carbon Capture Platforms Offshore Pipelines. Research R (2013).

[233] M. Anheden, U. Burchhardt, H. Ecke, R. Faber, O. Jidinger, R. Giering, H. Kass, S. Lysk, E. Ramström, J. Yan, Overview of operational experience and results from test activities in Vattenfall's 30 MWth oxyfuel pilot plant in Schwarze Pumpe, Energy Procedia. 4 (2011) 941–950. https://doi.org/10.1016/j.egypro.2011.01.140.

[234] J.S. Tumuluru, J.R. Hess, R.D. Boardman, C.T. Wright, T.L. Westover, Formulation, Pretreatment, and Densification Options to Improve Biomass Specifications for Co-Firing High Percentages with Coal, Https://Home.Liebertpub.Com/Ind. 8 (2012) 113–132. https://doi.org/10.1089/IND.2012.0004.

[235] R. Ray, S. Ferguson, Assessing the cost reduction potential and competitiveness of novel (next generation) UK carbon capture technology. Benchmarking State-of-the-art and Next Generation Technologies, Technical Report 13333-8820-RP-001, (2018).

[236] E.S. Rubin, International Journal of Greenhouse Gas Control Understanding the pitfalls of CCS cost estimates, Int. J. Greenh. Gas Control. 10 (2012) 181–190. https://doi.org/10.1016/j.ijggc.2012.06.004.

[237] J. Szuhanszki, O.F. Moguel, K. Finney, M. Akram, M. Pourkashanian, Biomass combustion under oxy-fuel and post combustion capture conditions at the PACT 250 kW air/oxy-fuel CTF, (n.d.).

[238] B. Dooley, Combustion characteristics of coal , biomass and their chars in air and oxy-fuel environments, (2017).

[239] Phyllis2 - Database for biomass and waste, (n.d.).

[240] BEIS, Electricity Generating Costs, (2016) 84. https://doi.org/267393///1/1 25 May 2010.

[241] M. Finkenrath, Cost and Performance of Carbon Dioxide Capture from Power Generation, 2011. http://www.environmentportal.in/files/costperf_ccs_powergen.pdf.

[242] OFX, Yearly Average Rates | OFX, Yrly. Aver. Rates. (2018) 1. https://www.ofx.com/en-

gb/forex-news/historical-exchange-rates/yearly-average-rates/.

[243] A.E.T.I. Insights, UNDERSTANDING VARIABILITY IN BIOMASS FEEDSTOCKS AND THE OPPORTUNITIES FOR PRE-PROCESSING An ETI Insights report, (n.d.). www.eti.co.uk.

[244] Department for Business Energy and Industrial Strategy, Greenhouse gas reporting: conversion factors 2018, Dep. Business, Energy Ind. Strateg. (2018) 1. https://doi.org/10.1007/s11434-008-0470-7.

[245] NEB - Canada's Energy Future 2017_ Energy Supply and Demand Projections to 2040 - Chapter 2, (n.d.).

[246] N. Traded, GUIDANCE ON ESTIMATING CARBON VALUES BEYOND 2050 : AN INTERIM APPROACH, (2020) 1–13.

[247] H.J. Herzog, the Economics of Co 2 Capture 1, MIT Energy Lab. (1998) 2–19.

[248] I. Renewable, E. Agency, Power Generation Costs in 2017, 2017.

[249] J. Ahrenfeldt, T.P. Thomsen, U. Henriksen, L.R. Clausen, Biomass gasification cogeneration - A review of state of the art technology and near future perspectives, Appl. Therm. Eng. 50 (2013) 1407–1417. https://doi.org/10.1016/j.applthermaleng.2011.12.040.

[250] N. Pour, P.A. Webley, P.J. Cook, Potential for using municipal solid waste as a resource for bioenergy with carbon capture and storage (BECCS), Int. J. Greenh. Gas Control. 68 (2018) 1–15. https://doi.org/10.1016/j.ijggc.2017.11.007.

[251] M. Rodrigues, A.P.C. Faaij, A. Walter, Techno-economic analysis of co-fired biomass integrated gasification / combined cycle systems with inclusion of economies of scale, 28 (2003) 1229–1258. https://doi.org/10.1016/S0360-5442(03)00088-4.

[252] Petrol and diesel prices since 2014 - wholesale and average pump - The RAC Media Centre, (n.d.).

[253] EU Emissions Trading System (EU ETS) _ Climate Action, (n.d.).

[254] British Columbia's Carbon Tax - Province of British Columbia, (n.d.).

[255] O. Effective, C. Rates, Effective Carbon Rates, (2018).

[256] Renewable incentives guide: towards a subsidy-free world? 6, (n.d.).

[257] P. Ibarra-Gonzalez, B.G. Rong, A review of the current state of biofuels production from lignocellulosic biomass using thermochemical conversion routes, Chinese J. Chem. Eng. 27 (2019) 1523–1535. https://doi.org/10.1016/j.cjche.2018.09.018.

[258] IEA, From 1 st- to 2nd-Generation Biofuel technologies, Paris, 2008. https://www.iea.org/reports/from-1st-to-2nd-generation-biofuel-technologies (accessed June 30, 2020).

[259] S.N. Naik, V. V. Goud, P.K. Rout, A.K. Dalai, Production of first and second generation biofuels: A comprehensive review, Renew. Sustain. Energy Rev. 14 (2010) 578–597. https://doi.org/10.1016/j.rser.2009.10.003.

[260] A. Demirbas, Competitive liquid biofuels from biomass, Appl. Energy. 88 (2011) 17–28. https://doi.org/10.1016/j.apenergy.2010.07.016.

[261] M. Stöcker, Biofuels and Biomass-To-Liquid Fuels in the Biorefinery: Catalytic Conversion of Lignocellulosic Biomass using Porous Materials, Angew. Chemie Int. Ed. 47 (2008) 9200–9211. https://doi.org/10.1002/anie.200801476.

[262] F. Trippe, M. Fröhling, F. Schultmann, R. Stahl, E. Henrich, Techno-economic assessment of gasification as a process step within biomass-to-liquid (BtL) fuel and chemicals production, Fuel Process. Technol. 92 (2011) 2169–2184. https://doi.org/10.1016/j.fuproc.2011.06.026.

[263] F. Trippe, M. Fröhling, F. Schultmann, R. Stahl, E. Henrich, A. Dalai, Comprehensive techno-economic assessment of dimethyl ether (DME) synthesis and Fischer-Tropsch synthesis as alternative process steps within biomass-to-liquid production, Fuel Process. Technol. 106 (2013) 577–586. https://doi.org/10.1016/j.fuproc.2012.09.029.

[264] I. Aspen Technology, Aspen Physical Property System 11.1 Physical Property Methods and Models, (2001). https://esupport.aspentech.com/S_Article?id=000062950 (accessed July 6, 2020).

[265] I. Aspen Technology, Aspen Plus 11.1 Getting Started Modeling Processes with Solids, (2001). https://esupport.aspentech.com/S_Article?id=000064733 (accessed July 6, 2020).

[266] J.R. Thome, Engineering Data Book III.pdf, 2004.

[267] E.E. Baruth, Water Treatment Plant Design, 1988. https://doi.org/10.1061/(ASCE)0733-9372(1988)114:6(1487).

[268] L. Creech, Waste wood processing rises by six per cent in 2019, Resour. Mag. (2020). https://resource.co/article/waste-wood-processing-rises-six-cent-2019 (accessed March 24, 2021).

[269] John Clegg Consulting Ltd, WOOD FIBRE AVAILABILITY & DEMAND IN BRITAIN 2013-2035, Edinburgh, 2016.

[270] S. Mani, L.G. Tabil, S. Sokhansanj, Grinding performance and physical properties of wheat and barley straws, corn stover and switchgrass, Biomass and Bioenergy. 27 (2004) 339–352. https://doi.org/10.1016/j.biombioe.2004.03.007.

[271] H. Ghassemi, R. Shahsavan-Markadeh, Effects of various operational parameters on biomass gasification process; A modified equilibrium model, Energy Convers. Manag. 79 (2014) 18–24. https://doi.org/10.1016/j.enconman.2013.12.007.

[272] R.F. Probstein, R.E. Hicks, Synthetic fuels, Dover Publications, 2006.

[273] Henrik Thunmann, GoBiGas demonstration – a vital step for a large-scale transition from fossil fuels to advanced biofuels and electrofuels, 2018.

[274] M. Asadullah, Biomass gasification gas cleaning for downstream applications: A comparative critical review, Renew. Sustain. Energy Rev. 40 (2014) 118–132. https://doi.org/10.1016/j.rser.2014.07.132.

[275] P.J. Woolcock, R.C. Brown, A review of cleaning technologies for biomass-derived syngas, Biomass and Bioenergy. 52 (2013) 54–84. https://doi.org/10.1016/j.biombioe.2013.02.036.

[276] S.D. Phillips, J.K. Tarud, M.J. Biddy, Gasoline from Wood via Integrated Gasification , Synthesis , and Methanol-to- Gasoline Technologies, Energy. (2011). https://doi.org/NREL/TP-5100-47594.

[277] H.-S. Song, D. Ramkrishna, S. Trinh, H. Wright, Operating Strategies for Fischer-Tropsch Reactors: A Model-Directed Study, 2004.

[278] M.N. Rosli, N. Aziz, Simulation of ethane steam cracking with severity evaluation, in: IOP Conf. Ser. Mater. Sci. Eng., 2016. https://doi.org/10.1088/1757-899X/162/1/012017.

[279] N. Schmitz, F. Homberg, J. Berje, J. Burger, H. Hasse, Chemical Equilibrium of the Synthesis of Poly(oxymethylene) Dimethyl Ethers from Formaldehyde and Methanol in Aqueous Solutions, (2015). https://doi.org/10.1021/acs.iecr.5b01148.

[280] Z.J. Ai, C.Y. Chung, I.L. Chien, Design and Control of Poly(Oxymethylene) Dimethyl Ethers Production Process Directly From Formaldehyde and Methanol in Aqueous Solutions, IFAC-PapersOnLine. 51 (2018) 578–583. https://doi.org/10.1016/j.ifacol.2018.09.362.

[281] V.E. Onyebuchi, A. Kolios, D.P. Hanak, C. Biliyok, V. Manovic, A systematic review of key challenges of CO2 transport via pipelines, Renew. Sustain. Energy Rev. 81 (2018) 2563–2583. https://doi.org/10.1016/j.rser.2017.06.064.

[282] I.S. Cole, P. Corrigan, S. Sim, N. Birbilis, Corrosion of pipelines used for CO 2 transport in CCS: Is it a real problem?, Int. J. Greenh. Gas Control. 5 (2011) 749–756. https://doi.org/10.1016/j.ijggc.2011.05.010.

[283] Company Salaries | Glassdoor, (2019). https://www.glassdoor.com/Salaries/index.htm.

[284] Payscale, PayScale - Salary Comparison, Salary Survey, Search Wages, Payscale. (2013). http://www.payscale.com/.

[285] S. Phillips, A. Aden, J. Jechura, D. Dayton, T. Eggeman, Thermochemical Ethanol via Direct Gasification and Mixed Alcohol Synthesis of Lignocellulosic Biomass. Technical Report NREL/TP-510-41168, NREL, Natl. Renew. Energy Lab. (2007) 125. http://www.nrel.gov/docs/fy07osti/41168.pdf.

[286] X. Zhang, A.O. Oyedun, A. Kumar, D. Oestreich, U. Arnold, J. Sauer, An optimized process design for oxymethylene ether production from woody-biomass-derived syngas, Biomass and Bioenergy. 90 (2016) 7–14. https://doi.org/10.1016/j.biombioe.2016.03.032.

[287] C.R. Vitasari, M. Jurascik, K.J. Ptasinski, Exergy analysis of biomass-to-synthetic natural gas (SNG) process via indirect gasification of various biomass feedstock, Energy. 36

(2011) 3825–3837. https://doi.org/10.1016/j.energy.2010.09.026.

[288] A. Brown, L. Waldheim, I. Landälv, J. Saddler, M. Ebadian, J.D. McMillan, A. Bonomi, B. Klein, Advanced Biofuels – Potential for Cost Reduction, (2020) 88.

[289] Department of Business Energy & Industrial Strategy, Greenhouse gas reporting: conversion factors 2019 - GOV.UK, Dep. Business, Energy Ind. Strateg. (2019). https://www.gov.uk/government/publications/greenhouse-gas-reporting-conversion-factors-2019 (accessed January 24, 2021).

[290] C. Charles, R. Bridle, T. Moerenhout, Biofuels—At What Cost? A review of costs and benefits of U.K. biofuel policies, 2013.

[291] Wholesale gas charts and indicators | Ofgem | Ofgem, (n.d.). https://www.ofgem.gov.uk/data-portal/all-charts/policy-area/gas-wholesale-markets.

[292] Bioenergy Insight, Generators of biomethane can claim RHI and RTFO payments | Bioenergy Insight Magazine, Bioenergy-News.Com. (2019). https://doi.org/RHI.

[293] Local authorities | ADBA | Anaerobic Digestion & Bioresources Association, (n.d.). http://adbioresources.org/about-ad/how-ad-benefits-everyone/local-authority-and-government/local-authorities.

[294] Ofgem, Non-Domestic RHI tariff table | Ofgem, (2020).

[295] T. Fout, A. Zoelle, D. Keairns, M. Turner, M. Woods, N. Kuehn, V. Shah, V. Chou, L. Pinkerton, Cost and Performance Baseline for Fossil Energy Plants Volume 1a: Bituminous Coal (PC) and Natural Gas to Electricity Revision 3, 2015. https://doi.org/DOE/NETL-2010/1397.

[296] C.-H. Huang, C.-S. Tan, A Review: CO 2 Utilization, Aerosol Air Qual. Res. 14 (2014) 480–499. https://doi.org/10.4209/aaqr.2013.10.0326.

[297] J. Amouroux, P. Siffert, J. Pierre Massué, S. Cavadias, B. Trujillo, K. Hashimoto, P. Rutberg, S. Dresvin, X. Wang, Carbon dioxide: A new material for energy storage, Prog. Nat. Sci. Mater. Int. 24 (2014) 295–304. https://doi.org/10.1016/j.pnsc.2014.06.006.

[298] P. Styring, Carbon dioxide utilisation: closing the carbon cycle, Elsevier, 2014.

[299] European Environment Agency, Cutting greenhouse gas emissions through circular economy actions in the buildings sector, (2020). https://doi.org/10.2800/675663.

[300] M. Lehtveer, S. Brynolf, M. Grahn, What Future for Electrofuels in Transport? Analysis of Cost Competitiveness in Global Climate Mitigation, Environ. Sci. Technol. 53 (2019) 1690–1697. https://doi.org/10.1021/acs.est.8b05243.

[301] O. Schmidt, A. Gambhir, I. Staffell, A. Hawkes, J. Nelson, S. Few, Future cost and performance of water electrolysis: An expert elicitation study, Int. J. Hydrogen Energy. 42 (2017) 30470–30492. https://doi.org/10.1016/j.ijhydene.2017.10.045.

[302] E. Commission, Horizon 2020 - Work Programme 2016 - 2017, 20. General Annexes: G. Technology readiness level (TRL), 2017. https://ec.europa.eu/research/participants/data/ref/h2020/other/wp/2016-2017/annexes/h2020-wp1617-annex-ga_en.pdf (accessed January 25, 2021).

[303] P. Schmidt, W. Weindorf, A. Roth, V. Batteiger, F. Riegel, Power-to-Liquids Potentials and Perspectives for the Future Supply of Renewable Aviation Fuel, Dessau-Roßlau, 2016. https://www.umweltbundesamt.de/en/publikationen/ (accessed January 25, 2021).

[304] S.M. Jarvis, S. Samsatli, Technologies and infrastructures underpinning future CO2 value chains: A comprehensive review and comparative analysis, Renew. Sustain. Energy Rev. 85 (2018) 46–68. https://doi.org/10.1016/j.rser.2018.01.007.

[305] R. Otten, The first industrial PtG plant – Audi e-gas as driver for the energy turnaround, (2014). http://www.cedec.com/files/default/8-2014-05-27-cedec-gas-day-reinhard-otten-audi-ag.pdf (accessed January 25, 2021).

[306] R. Otten, Push for the energy revolution | audi.com, (2018). https://www.audi.com/en/experience-audi/models-and-technology/alternative-drive-systems/energy-revolution.html (accessed January 25, 2021).

[307] A. Zimmermann, R. Schomäcker, E. Gençer, F. O'Sullivan, K. Armstrong, P. Styring, S. Michailos, OME Worked Example for the TEA Guidelines for CO 2 Utilization, 2019. https://doi.org/10.3998/2027.42/147468.

[308] A. Godula-Jopek, D. Stolten, Hydrogen Production: By Electrolysis, 2015.

https://doi.org/10.1002/9783527676507.

[309] A. Buttler, H. Spliethoff, Current status of water electrolysis for energy storage, grid balancing and sector coupling via power-to-gas and power-to-liquids: A review, Renew. Sustain. Energy Rev. 82 (2018) 2440–2454. https://doi.org/10.1016/j.rser.2017.09.003.

[310] K. Atsonios, K.D. Panopoulos, E. Kakaras, Investigation of technical and economic aspects for methanol production through CO2 hydrogenation, Int. J. Hydrogen Energy. 41 (2016) 2202–2214. https://doi.org/10.1016/j.ijhydene.2015.12.074.

[311] L. Bertuccioli, A. Chan, D. Hart, F. Lehner, B. Madden, E. Standen, Development of Water Electrolysis in the EU, 2014.

[312] Z.J. Ai, C.Y. Chung, I.L. Chien, Design and Control of Poly(Oxymethylene) Dimethyl Ethers Production Process Directly From Formaldehyde and Methanol in Aqueous Solutions, IFAC-PapersOnLine. 51 (2018) 578–583. https://doi.org/10.1016/j.ifacol.2018.09.362.

[313] W. Kuckshinrichs, T. Ketelaer, J.C. Koj, Economic analysis of improved alkaline water electrolysis, Front. Energy Res. 5 (2017). https://doi.org/10.3389/fenrg.2017.00001.

[314] P. Christensen, L.R. Dysert, AACE International Recommended Practice No. 18R-97, (2005) 10.

[315] C. Thomson, G.P. Harrison, Life cycle costs and carbon emissions of wind power Executive Summary, n.d.

[316] E. Charles, The Carbon Footprint of a Solar Panel, (n.d.). https://blog.spiritenergy.co.uk/homeowner/solar-carbon-footprint-calculator (accessed January 22, 2021).

[317] G. Heath, D. Sandor, Life Cycle Greenhouse Gas Emissions from Solar Photovoltaics , n.d. www.nrel.gov/harmonization (accessed January 22, 2021).

[318] N. Von Der Assen, J. Jung, A. Bardow, Life-cycle assessment of carbon dioxide capture and utilization: Avoiding the pitfalls, Energy Environ. Sci. 6 (2013) 2721–2734. https://doi.org/10.1039/c3ee41151f.

[319] M.M.J. de Jonge, J. Daemen, J.M. Loriaux, Z.J.N. Steinmann, M.A.J. Huijbregts, Life cycle

carbon efficiency of Direct Air Capture systems with strong hydroxide sorbents, Int. J. Greenh. Gas Control. 80 (2019) 25–31. https://doi.org/10.1016/j.ijggc.2018.11.011.

[320] K.S. Lackner, Capture of carbon dioxide from ambient air, Eur. Phys. J. Spec. Top. 176 (2009) 93–106. https://doi.org/10.1140/epjst/e2009-01150-3.

[321] N. McQueen, P. Psarras, H. Pilorgé, S. Liguori, J. He, M. Yuan, C.M. Woodall, K. Kian, L. Pierpoint, J. Jurewicz, J.M. Lucas, R. Jacobson, N. Deich, J. Wilcox, Cost Analysis of Direct Air Capture and Sequestration Coupled to Low-Carbon Thermal Energy in the United States, Environ. Sci. Technol. 54 (2020) 7542–7551. https://doi.org/10.1021/acs.est.0c00476.

[322] Er.C. Tan, M. Talmadge, A. Dutta, J. Hensley, J. Schaidle, M. Biddy, D. Humbird, L.J. Snowden-Swan, J. Ross, D. Sexton, R. Yap, J. Lukas, Process Design and Economics for the Conversion of Lignocellulosic Biomass to Hydrocarbons via Indirect Liquefaction, Natl. Renew. Energy Lab. Pacific Northwest Natl. Lab. (2015) 2.

[323] J.C. Meerman, M.M.J. Knoope, A. Ramírez, W.C. Turkenburg, A.P.C. Faaij, Technical and economic prospects of coal- and biomass-fired integrated gasification facilities equipped with CCS over time, Int. J. Greenh. Gas Control. 16 (2013) 311–323. https://doi.org/10.1016/j.ijggc.2013.01.051.

[324] R.M. Swanson, A. Platon, J.A. Satrio, R.C. Brown, Techno-economic analysis of biomass-to-liquids production based on gasification scenarios, ACS Natl. Meet. B. Abstr. (2009).

[325] J. Xu, G.F. Froment, Methane steam reforming, methanation and water-gas shift: I. Intrinsic kinetics, AIChE J. 35 (1989) 88–96. https://doi.org/10.1002/aic.690350109.

[326] B.Y. Yu, I.L. Chien, Design and economic evaluation of a coal-to-synthetic natural gas process, Ind. Eng. Chem. Res. 54 (2015) 2339–2352. https://doi.org/10.1021/ie503595r.

[327] A. Pavone, Mega Methanol Plants, Report No. 43D, Menlo Park, California, 2003.

[328] K.M. Vanden Bussche, G.F. Froment, A Steady-State Kinetic Model for Methanol Synthesis and the Water Gas Shift Reaction on a Commercial Cu/ZnO/Al 2 O 3 Catalyst, 1996.

[329] G.J. Millar, M. Collins, Industrial Production of Formaldehyde Using Polycrystalline

Silver Catalyst, Ind. Eng. Chem. Res. 56 (2017) 9247–9265. https://doi.org/10.1021/acs.iecr.7b02388.

[330] Politecnico di Milano - Alstom UK, CArbon-free Electricity by SEWGS: Advanced materials, Reactor-, and process design, 2008.

[331] J.S. Umbach, Online Pinch Analysis Tool, (2010). http://www.uic-che.org/pinch/index.php (accessed March 22, 2021).

Appendices

Appendix A: Supplementary Information for Chapter 4

A1 – Calculation of reference emission factors

Table A1: Scope 1 and Scope 3 emission factors and calorific value of sample biomass [244].

Biomass	Scope 1 (kg CO_2e/kWh)	Scope 3 (kg CO_2e/kWh)	Calorific value (MJ/kg)
Wood pellets	0.01500	0.03744	18.29
Grass/Straw	0.01314	0.01604	15.68

Calorific value of white wood pellets = 19.41 MJ/kg

Assuming a linear relationship between calorific value and emission factor:

Emission factor of white wood pellets =

$$\frac{19.41}{18.29} \times 0.0525 = 0.0557 \text{ kg } CO_2e/\text{kWh}$$

Calorific value of miscanthus = 18.27 MJ/kg

Emission factor of miscanthus =

$$\frac{18.27}{15.68} \times 0.02918 = 0.0340 \text{ kg } CO_2e/\text{kWh}$$

Calorific value of wheat straw = 17.82 MJ/kg

Emission factor of wheat straw =

$$\frac{17.82}{15.68} \times 0.02918 = 0.0332 \text{ kg } CO_2e/\text{kWh}$$

A2 – Syngas Composition from the Entrained Gasifier

The syngas compositions obtained from the gasifier model and fed into the IECM to complete the techno-economic analysis are presented in Table A1.

Table A1: Syngas composition of the various biomass used in pre-combustion capture.

Vol %	White wood pellet	Miscanthus	Wheat straw
CO	29.82	28.72	29.37
H_2	33.08	30.56	30.65
CH_4	9.23e-3	6.45e-3	6.90e-3
C_2H_6	1.42e-8	7.52e-9	8.58e-9
C_3H_8	5.77e-14	2.31e-14	2.81e-14
H_2S	5.23e-3	2.79e-2	4.93e-2
COS	2.09e-4	1.16e-3	2.09e-3
NH_3	3.22e-3	3.05e-3	3.35e-3
HCl	2.46e-3	3.42e-2	4.93e-2
CO_2	7.49	8.50	8.35
H_2O	24.87	27.05	26.08
N_2	0.76	0.86	1.04
Ar	3.96	4.23	4.40

A3 – Carbon pricing calculations

Table A2: Effect of carbon pricing as a negative emission incentive to BECCS on the LCOE (£/MWh).

	Technology	Base case (no carbon price)	Low case £25/tCO_2	Medium £75/ tCO_2	High £125/ t CO_2
Wood	PCC	200.0	175.0	124.0	73.9
	Oxy	224.0	199.0	149.0	99.0
	IGCC	190.0	172.0	136.0	99.0
Miscanthus	PCC	168.0	141.0	87.0	32.2
	Oxy	183.0	158.0	108.0	57.7
	IGCC	158.0	139.0	103.0	66.2
Straw	PCC	184.0	156.0	102.0	47.1
	Oxy	196.0	170.0	120.0	70.0
	IGCC	168.0	150.0	113.0	76.4
Natural gas	PCC	71.5	73.6	77.9	82.0

Appendix B: Supplementary Information for Chapter 5 and 6

Table B1: Major process equipment references and scaling factors.

Process unit	Base capacity	Base cost ($ million)	Base year	Scaling factor	References
Pretreatment	2200 dt/d	22.7	2007	0.77	[150,155]
Gasification (EFG)	2200 dt/d	67.8	2007	0.66	[150,155]
Gasification (DFB)	20 MW	4.3	2014	0.66	[156]
Electrolyser	1 MW	1.2	2015	0.85	[313]
Syngas cleaning	3823 t/d	33.5	2007	0.7	[150,155]
Primary cleaning	20 MW	3.48	2014	0.67	[156]
WGS & cracking	20 MW	3.44	2014	0.7	[156]
FT synthesis	2200 dt/d	49.4	2007	0.7	[150,155]
Methanation	20 MW	3.59	2014	0.7	[156]
Methanol synthesis	44.3 ton/d	3.5	2011	0.8	[322]
OMEx synthesis	1 Mio. t/yr	274	2014	0.65	[134]
Pressure swing adsorption	797.6 t/d	12.8	2015	0.7	[150,323]
Hydrocracking	378 t/d	33	2007	0.67	[150,155]
Upgrading unit	20 MW	0.73	2014	0.7	[156]
Power generation	35.9 MW	45.6	2015	0.75	[155]
Air separation	2903 t/d	24.3	2007	0.8	[150,155]
Centrifugal compression	500 kW	1.41	2010	0.6	[218]
Reciprocal compression	500 kW	0.55	2010	0.75	[218]
Cooling system	10000 l/s	5.33	2010	0.9	[218]

Table B2: Estimated labour costs for operating costs.

Position	Salary	Number	Total
Plant manager	£60,000	1	£60,000
Plant engineer	£40,000	2	£80,000
Maintenance supervisor	£30,000	1	£30,000
Lab manager	£38,000	1	£38,000
Shift supervisor	£26,000	5	£130,000
Lab technician	£22,000	4	£88,000
Maintenance technician	£29,000	8/12	£232,000/£348,000
Shift operators	£29,000	20/30	£580,000/£870,000
Yard employees	£20,000	12	£240,000
Clerks & secretaries	£20,000	3	£60,000
Total			£1,538,000/£1,944,000

Table B3: Operating and maintenance costs data [155,156,219,222,313].

Parameter	Value
Fixed costs	
Insurance, taxes & rent	2.5% fixed capital investment
Maintenance and repairs	2% fixed capital investment
Operating supplies	15% maintenance & repairs
Laboratory charges	10% operating labour
Overhead costs	50% operating labour
Variable costs	
Feedstock	£50/dry tonne
Ash disposal	£19/tonne
Wastewater treatment	£4.52/m^3
MEA	£1.92/tCO_2
WGS catalyst	£16/kg
FTS catalyst	£30/kg
Methanation catalyst	£0.02/GJ of SNG
Methanol catalyst	£18.8/kg
OMEx catalyst	£33.2/kg
Formaldehyde catalyst	£437/kg
Activated carbon	£10.4/kWh
Boiler feed water	£0.50/tonne
Cooling water	£0.023/tonne
Fired heat	£8.06/MWh
Electricity to grid	£58/MWh
Electricity from grid	£104/MWh
LO-CAT chemicals	£160/tonne S
Hydroprocessing	£3.63/barrel produced
PSA	£3.31/kg
CO_2 transportation and storage	£11/tCO_2
KOH	£1.87/kg
Nitrogen	£0.21/kg
Pentane	£364/Mtonne
CO_2 feed	£42/tonne
Deionised water	£1/tonne

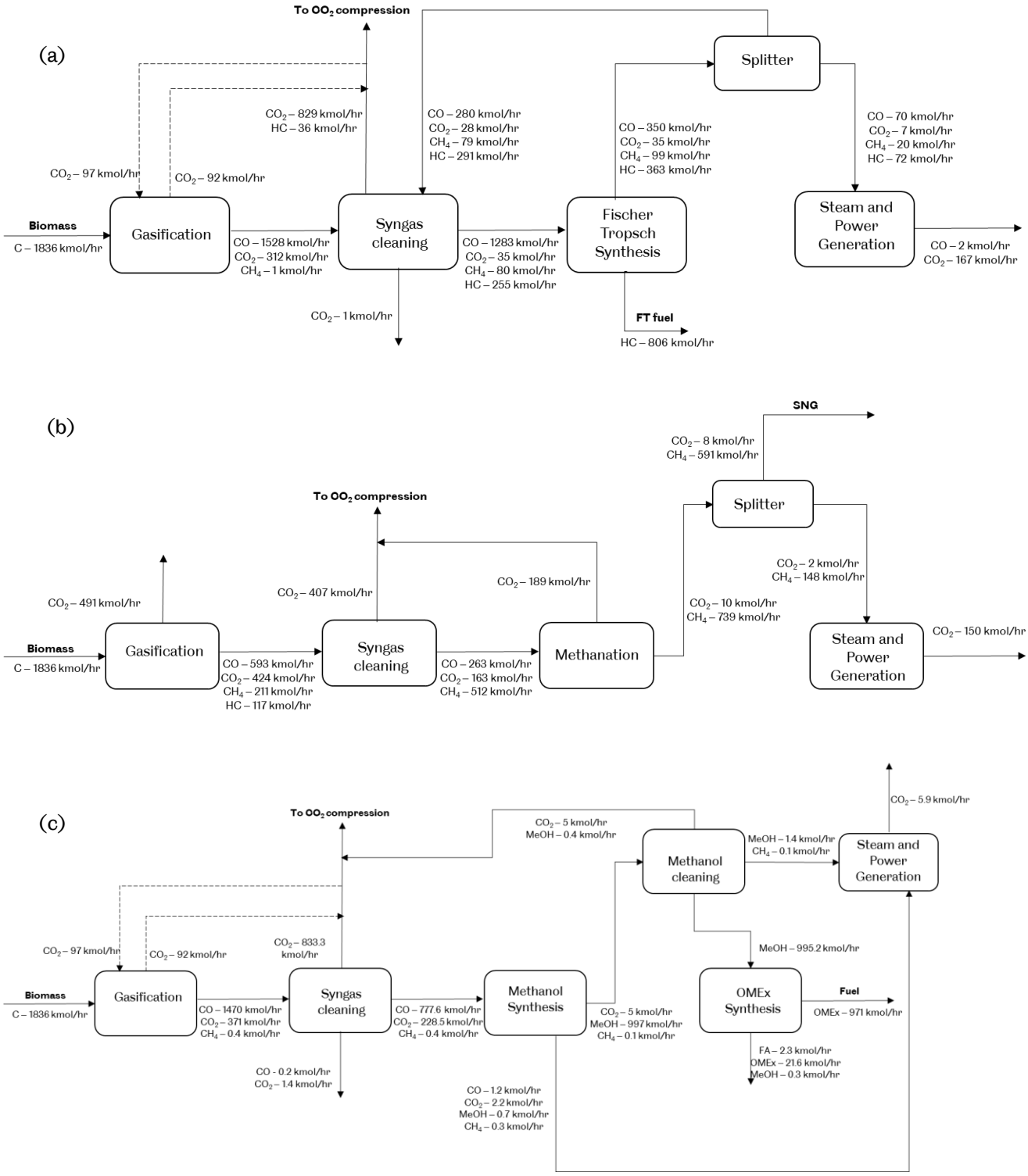

Figure C1: Carbon balance investigated for the production routes (a) Fischer-Tropsch synthesis, (b) Methanation and (c) Oxymethylene ether synthesis.

Appendix C: Supplementary Information for Chapter 6

C1 - Power requirements for electrofuel production

Table C1: Power requirements and generation for three electrofuel production routes.

Power requirement (MW)	FTS	SNG	OME	Remarks
USAGE				
Electrolyser	339.4	324.2	356.6	
AGR pumps	0.3	-	-	Scaled
Syngas booster compressor	1.07	15.1	7.88	Aspen
PSA compressor	0.24	-	-	Scaled
SNG compressor	-	1.43	-	Aspen
Naphtha pump	2.90E-04	-	-	Aspen
Diesel pump	6.20E-04	-	-	Aspen
MeOH synthesis compressors	-	-	0.03	Aspen
MeOH cleaning pumps	-	-	2.86E-03	Aspen
OMEx pump	-	-	3.10E-03	Aspen
Air compressor (OME synthesis)	-	-	1.56	Aspen
Hydroprocessing	1.40E-01	-	-	Aspen
ORC	-	0.3	-	
Water pumps (Steam generation)	0.01	0.02	0.03	Aspen
CO2 compression	0.00	0.00	0.11	Aspen
Refrigeration	1.79	0.00	0.03	Aspen
Total	343.0	358.3	366.4	
GENERATION				
Combined cycle / ORC	16.7	4.1	4.1	
NET ELECTRICITY	-327.3	-336.9	-362.1	

C2 - Environmental assessment calculations

Table C2: Legend key explanations

Legend key	Value
Background	Upstream - harvest and transport
CO_2 capture loss	CO_2 lost to the atmosphere due to reduced capture system efficiency
CO_2 from process	CO_2 vented to the atmosphere during fuel synthesis
CO_2 intake	CO_2 absorbed from the atmosphere to generate biomass
Wind electricity	CO_2 emissions associated with generating electricity from wind
PV electricity	CO_2 emissions associated with generating electricity from solar-PV in direct air capture
Fuel combustion	CO_2 emissions from combustion of final fuel

The energy output in chapter 6 is a mixture of both electricity generated at the CO_2 source and the fuel generated from captured CO_2. This is the case for both the biogenic sourced and non-biogenic sourced CO_2. In direct air capture, the energy output is all from the fuel generated. The energy output mixture is calculated based on the mole fraction of carbon in the resulting process e.g. If 50% of the carbon in biomass goes to fuel synthesis, the energy output is calculated as the sum of 50% of energy in fuel output and 50% of energy in electricity generated upstream. A calculation example is shown below:

In a biogenic sourced route, 43.4 MW of electricity is generated in the biomass powered plant. 87% of the CO_2 from this process is captured and goes to FT synthesis producing 89.9 MW of fuel. The total CO_2 equivalent emission is 12,583 kg/h.

To calculate the carbon intensity, the total energy output is calculated as:

Electricity generated from power plant (E) = 43.4 MW

Energy in fuel (F) = 89.9 MW

Fraction of carbon in biomass captured and sent to fuel synthesis (y) = 0.87

Total energy output = (y x F) + ((1 – y) x E)

$$= (0.87 \times 89.9) + (0.13 \times 43.37)$$

$= 83.9\ \text{MW}$

Overall CO_2 equivalent emissions =

$$\frac{12583}{83.9 \times 1000} = 0.15\ \text{kg}CO_2\text{e/MWh}$$

Appendix D: Additional Aspen Modelling and Simulation Information

D1 - Biomass preparation

The biomass preparation section covers the chopping, grinding and drying of biomass. The moisture in biomass is reduced to 10% using steam. The amount of steam required and the final moisture content are set by a calculator block. The moisture removed and the steam used in drying are separated from the biomass feed in an adiabatic flash unit.

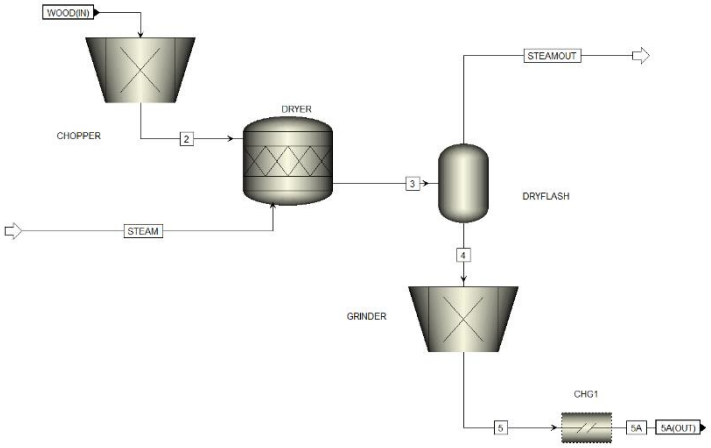

Figure D1: Aspen Plus flowsheet for biomass preparation.

D2 – Electrolysis

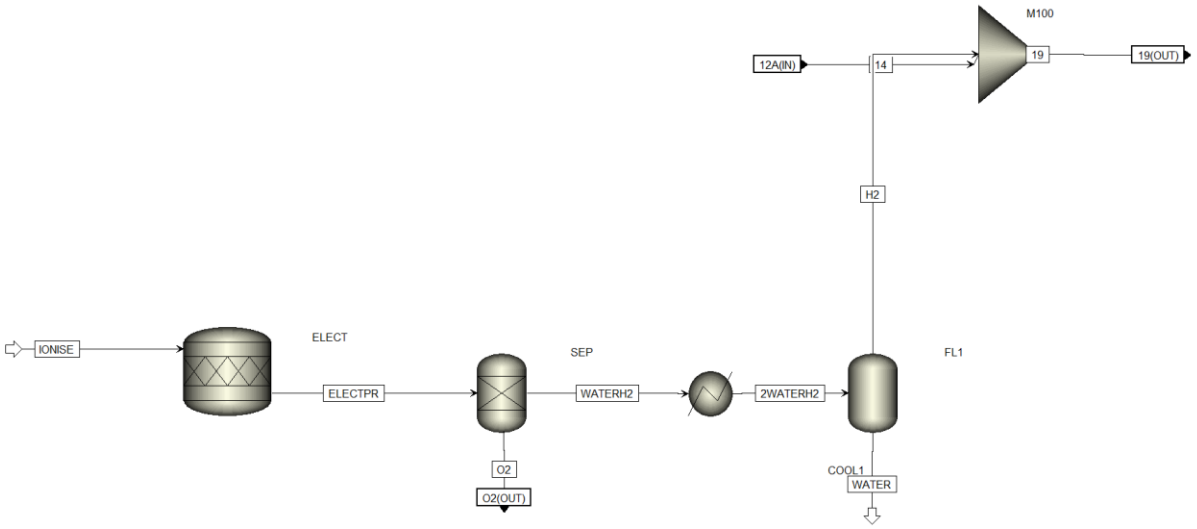

Figure D2: Aspen Plus flowsheet for electrolysis.

The electrolysis section is presented in Figure D2 and it covers alkaline water electrolysis to give a stream of H_2 that is mixed with CO_2 for electrofuel production. The water splitting

reaction is modelled in the stoichiometric reactor operating at 80 °C and 20 bar. Subsequently, a separator block is used to model the migration of hydrogen and hydroxyl ions to their respective electrodes for collection. The collected hydrogen is cooled before purification is a flash unit.

D3 - Syngas cleaning and conditioning

The syngas cleaning and conditioning section is presented in Figure D3. Wet scrubbing to remove impurities in the syngas is modelled as a flash unit using information from Field and Brasington [212]. The water flow is adjusted by a design specification to ensure the unit is in adiabatic mode and a calculator block sets the operating temperature to 5 °C below the dewpoint of the incoming stream. The sour water-gas shift reactor is modelled in one stage instead of the two stages in Field and Brasington [212] due to the requirements downstream. As the syngas is intended for fuel synthesis instead of power generation, one reactor is sufficient to adjust the ratio. A splitter is added after the scrubber to split the syngas into two streams. The ratio of the split is set by a design specification to ensure that the final mixed stream has the necessary H_2/CO ratio; this also helps to control the temperature of the exothermic WGS reaction, minimise the reactor size and the amount of catalyst required. The WGS reactor inlet stream is warmed up using the outlet stream to a temperature that is 15 °C above the dewpoint of the inlet stream. The WGS reactor is an adiabatic equilibrium reactor.

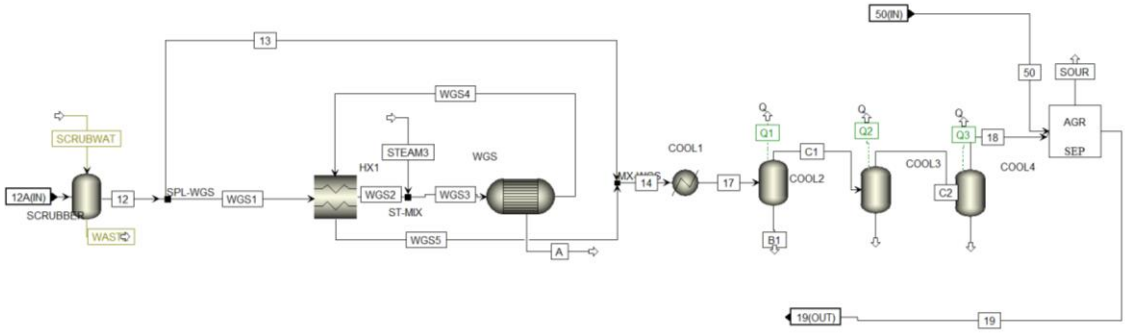

Figure D3: Aspen Plus flowsheet for syngas cleaning and conditioning.

After the WGS reactor, syngas is cooled in a series of adiabatic flash units at 100 °C, 60 °C and 39 °C. Water condensate in the syngas is removed at each stage.

D4 - Fischer Tropsch synthesis

The FTS reactor is modelled according to the work of Swanson et al. [155]. Detailed information including the equations used in the calculator block for FTS distribution of the products can be found in this document [324].

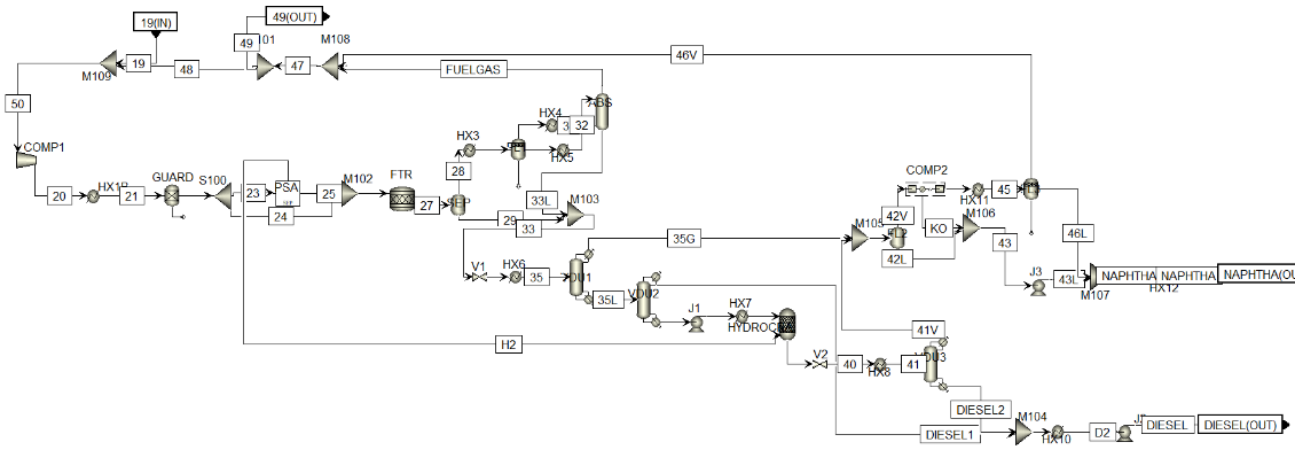

Figure D4: Aspen Plus flowsheet of FTS.

The fuel from the FTS reactor needs to undergo separation. An adiabatic two-phase flash unit is first used to separate the unconverted syngas from the products. The unconverted syngas is cooled and goes into an adiabatic three-phase flash for further product separation; the resulting streams are water, unconverted syngas and the lighter end of the FT-fuel. The lighter end of the FT-fuel and the unconverted syngas from the second flash unit are chilled and sent to an absorber to recover the rest of the FT-fuel from the unconverted syngas.

Table D1: Specification of vacuum distillation columns in FTS.

	VDU1	VDU2	VDU3
Purpose	Separate naphtha from diesel and wax	Separate diesel from wax	Separate cracked wax into naphtha and diesel
Number of stages	30	10	20
Reflux ratio	1.32	1.72	2.65
Bottoms rate (kmol/hr)	32.54	11.35	13.28

The FT-fuel from both the first flash unit and the absorber are combined in a mixer block for separation into naphtha and diesel in a series of distillation columns. The distillation columns to separate the FT-fuel into naphtha and diesel are modelled using RADRAC columns. The number of stages, reflux ratio and bottoms rate were first estimated using the DSTWU

columns. These first estimates were used in designing the RADFRAC columns and the bottoms rates were varied to achieve >99.5% recovery of the desired products. The results of the columns are shown in Table D1.

D5 - Methanation

The methanation synthesis section has been modelled according to the work of Alamia et al. [211]. The thermodynamic equilibrium methanation model used in this study was compared to a kinetic model. The kinetic model was developed using kinetics from Xu and Froment [325] and a Fortran subroutine from Yu [326]. The reactions considered in the kinetics are:

$$CH_4 + H_2O \rightarrow CO + 3H_2 \quad \text{(D1)}$$

$$CO + H_2O \rightarrow CO_2 + H_2 \quad \text{(D2)}$$

$$CH_4 + 2H_2O \rightarrow CO_2 + 4H_2 \quad \text{(D3)}$$

$$C_2H_6 + 2H_2O \rightarrow 2CO + 5H_2 \quad \text{(D4)}$$

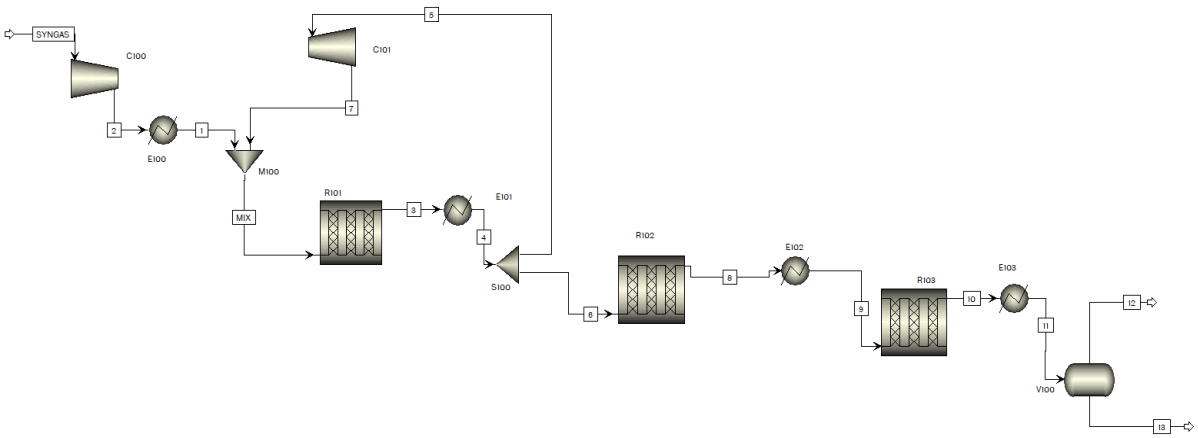

Figure D5: Aspen Plus kinetic model of methanation.

The results after three reactors are presented in Table D2. In the thermodynamic model, there is one more reactor and there is no recycling after the first reactor. Due to the similarities in both models and to reduce convergence time, the thermodynamic equilibrium model was used for this study.

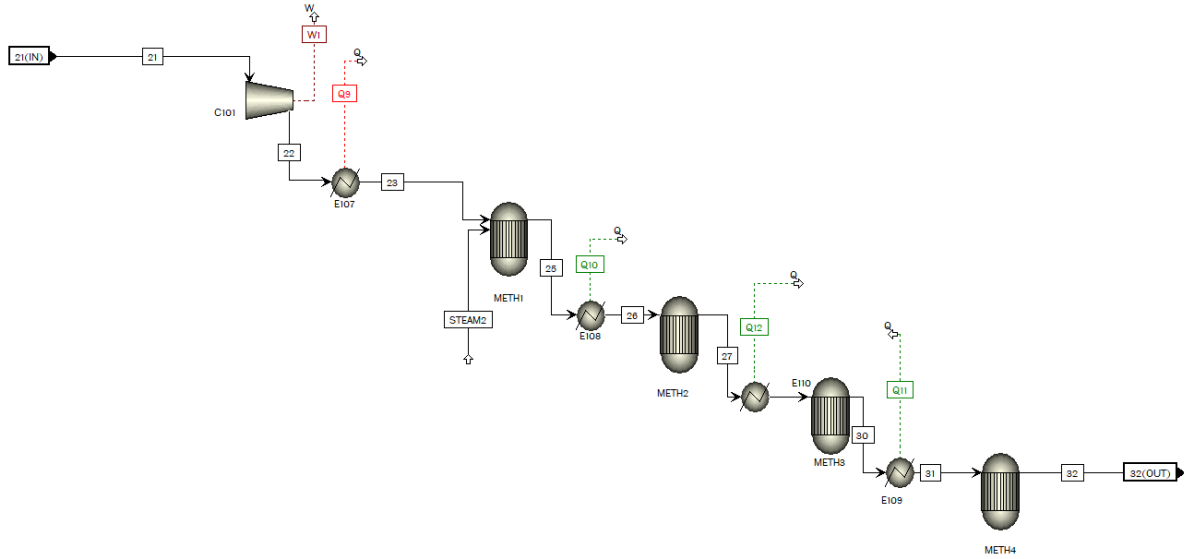

Figure D6: Aspen Plus thermodynamic model of methanation.

The methanation reactors are modelled as adiabatic reactors in series with interstage cooling. In the first reactor, steam is added to prevent the formation of carbon on the catalyst [211]. The amount of steam added is determined by a design specification. The streams in between are cooled to 200 °C and used to generate steam.

Table D2: Comparison of the percentage conversion after each reactor between the kinetic model and the thermodynamic equilibrium model for methanation.

		Kinetic	Thermodynamic
Reactor 1	CO	31.3%	29.8%
	CO_2	22.5%	21.0%
	H_2	52.2%	51.1%
Reactor 2	CO	82.7%	81.9%
	CO_2	24.8%	21.0%
	H_2	84.0%	81.7%
Reactor 3	CO	98.1%	97.6%
	CO_2	26.5%	21.5%
	H_2	96.7%	93.5%

D6 - OMEx synthesis

i. Methanol

The details for modelling methanol synthesis according to the ICI Synetix process are available in the document 'Aspen Plus Methanol Modelling Synthesis' found in the Aspen Plus database. The operating conditions are based on the SRI Process Economics Report 43D "Mega Methanol Plants" [327]. The model is based on reaction kinetics from Vanden Bussche and Froment [328]. The Aspen document describes the process in detail; it also presents the reaction kinetics and the model validation in detail. A kinetic model based on the details from the report was completed and a thermodynamic equilibrium model was derived from it to simplify the model and reduce the convergence time. The reactions considered in the kinetic model are:

$$CO + H_2O \leftrightarrow CO_2 + H_2 \quad \text{(D5)}$$

$$CO_2 + 3H_2 \leftrightarrow CH_3OH + H_2O \quad \text{(D6)}$$

$$2CO + 4H_2 \rightarrow C_2H_5OH + H_2O \quad \text{(D7)}$$

$$2CH_3OH \rightarrow C_2H_6O + H_2O \quad \text{(D8)}$$

Table D3: Comparison of the final stream from kinetic and thermodynamic methanol synthesis modelling

	Kinetic	Thermodynamic
CO (vol%)	0.007	0.005
CO_2 (vol%)	0.500	0.400
H_2 (vol%)	0.340	0.370
H_2O (vol%)	18.200	18.300
MeOH (vol%)	80.600	80.600

The temperature of the thermodynamic model was set at 250 °C, which is the exit temperature of the fourth reactor. In both models, a purge stream (stream 29), which 1.0% of the recycle was introduced to enable computation. The results of both models are compared in Table D3. The similarity in the results indicates the suitability of the thermodynamic equilibrium model for this study.

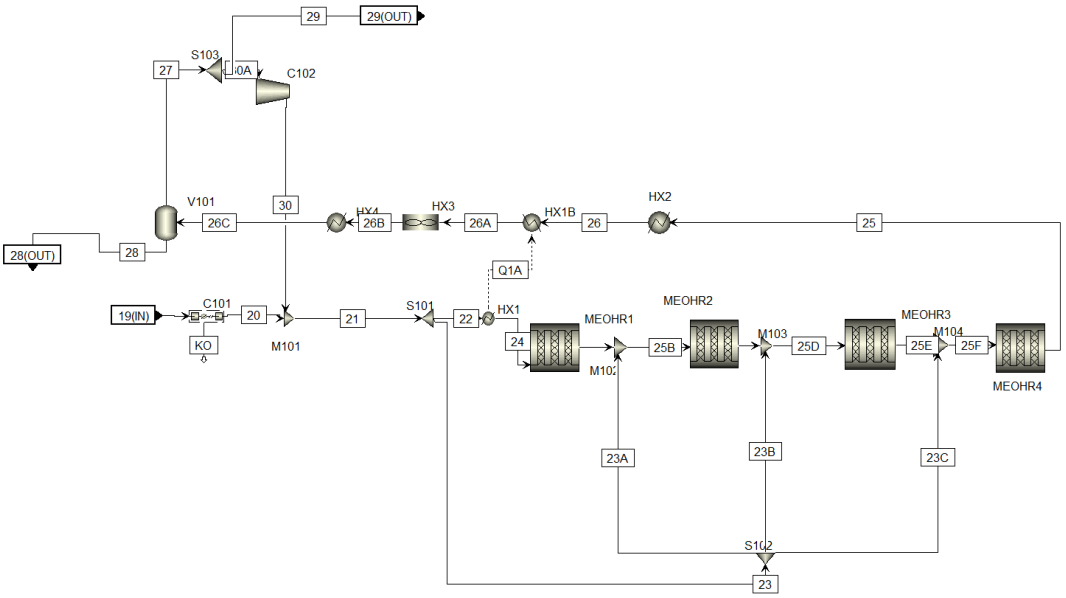

Figure D7: Aspen Plus kinetic model of methanol synthesis

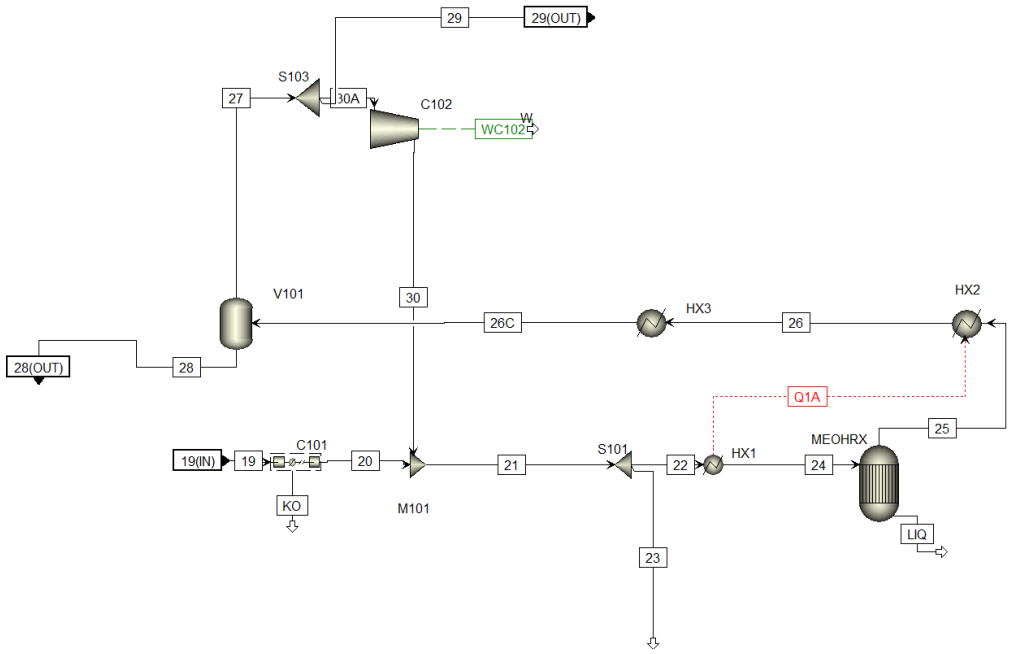

Figure D8: Aspen plus thermodynamic model of methanol synthesis.

ii. Formaldehyde synthesis

Formaldehyde synthesis is modelled in an adiabatic equilibrium reactor. In this reactor, methanol is dehydrated to formaldehyde. Before the reactor, a splitter removes a fraction of the methanol using a design specification to ensure that the methanol and formaldehyde going into OMEx synthesis have the same mass fraction as specified in Ai [312]. In the formaldehyde reactor, oxygen is added via air and the conversion of methanol to

formaldehyde is set at 87% which is a common conversion in formaldehyde synthesis over silver catalysts [329]. Due to the exothermic nature of the reaction, heat from the exit stream is recovered to generate steam for the plant. Absorption of formaldehyde using water is simulated using a common separator block. The quantity of water used in the process is set by a design specification to ensure 37%wt FA in the resulting stream as is the requirement for the OMEx synthesis in Zhang [286] and Ai [280].

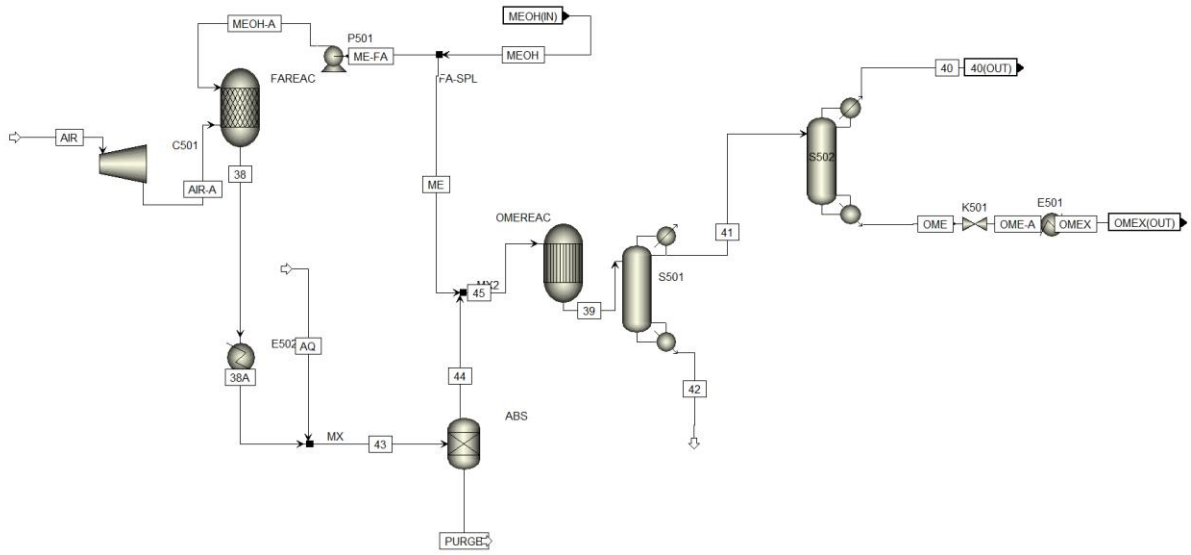

Figure D9: Aspen Plus flowsheet of OMEx synthesis from methanol

iii. OMEx synthesis

The OMEx synthesis was modelled based on previous experimental and modelling results available in literature. OMEx synthesis is modelled in an RYield reactor and the distribution of the products are calculated from the mass balance presented in the work of Ai [280].

Table D4: Distribution of OMEx products.

Product	Mass yield
OME_3	0.433825333
OME_4	0.007346855
OME_5	0.000001003
Methanol	0.000166213
Formaldehyde	0.001142909
H_2O	0.557517687

D7 - Power generation

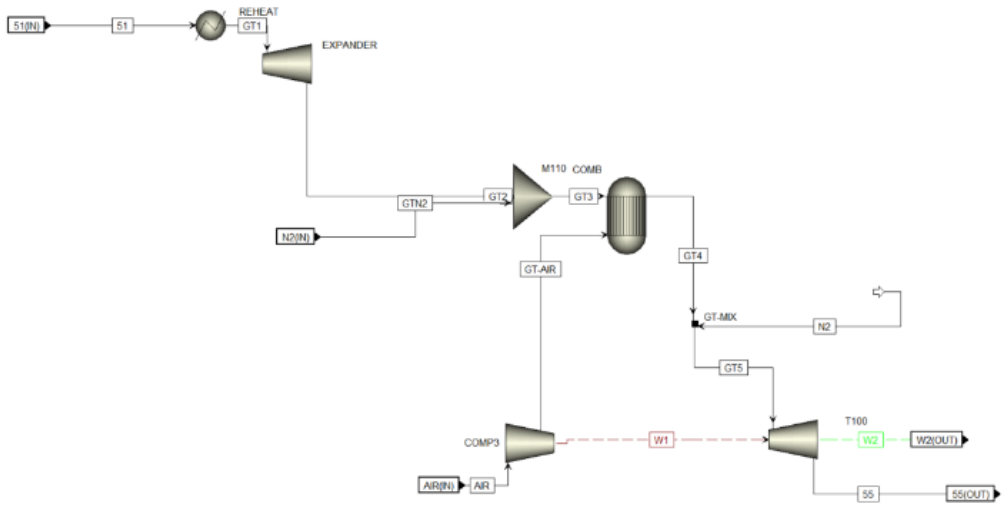

Figure D10: Aspen Plus model of the gas turbine.

Power is generated in a combined cycle to provide electricity to meet some of the plants demand. In FTS and OMEx synthesis, nitrogen from the air separation is added to syngas to achieve the 4.81 MJ/Nm^3 LHV based on the NETL report [295]. The flue gas stream before the gas turbine is mixed with either compressed air or nitrogen to cool the stream to an acceptable temperature (1370 °C) for the gas turbine. In methanation, there is no ASU so compressed air was used. In FTS and OMEx synthesis, the amount of nitrogen required for cooling was less than the leftover after nitrogen was used to dilute syngas, so only nitrogen was used. Where compressed air was used as the coolant, the compressed air was split into two; one part goes to the combustion chamber while the other part is used to cool down the flue gas. The amount of air required to achieve this temperature was calculated and added to the stoichiometric amount of air required for combustion and a 10% excess to ensure complete combustion. The combustion chamber is a RGibbs reactor operating adiabatically and the discharge pressure of the gas turbine was set at 1.05 bar.

In the steam cycle, power was generated from a medium-pressure turbine and a low-pressure turbine. The water inlet pressure varied between 8 bar and 15 bar and heated with the flue gas in a heat exchanger with a temperature approach of 10 °C. The discharge pressure of the medium-pressure turbine was set at 5 bar and exit stream was reheated with the flue gas stream before the low-pressure turbine. The discharge pressure of the low-pressure turbine was set 0.06 bar (1 psi) and the exit stream was sent to a condenser to bring the vapour fraction to 0 before recycling (not modelled) to the pump.

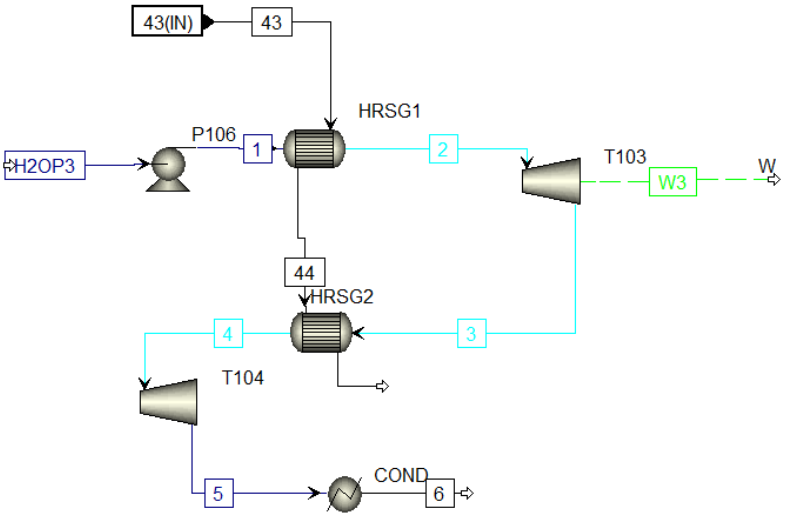

Figure D11: Aspen Plus model of the steam cycle.

D8 - CO_2 compression

The CO_2 removed in syngas cleaning requires compression for transport and storage in the CCS cases. Compression is achieved in two stages with interstage cooling and water removal. Water removal in between stages is modelled using a flash unit to represent a molecular sieve [330]. The amount of work required and cooling duty are determined by the mixer blocks.

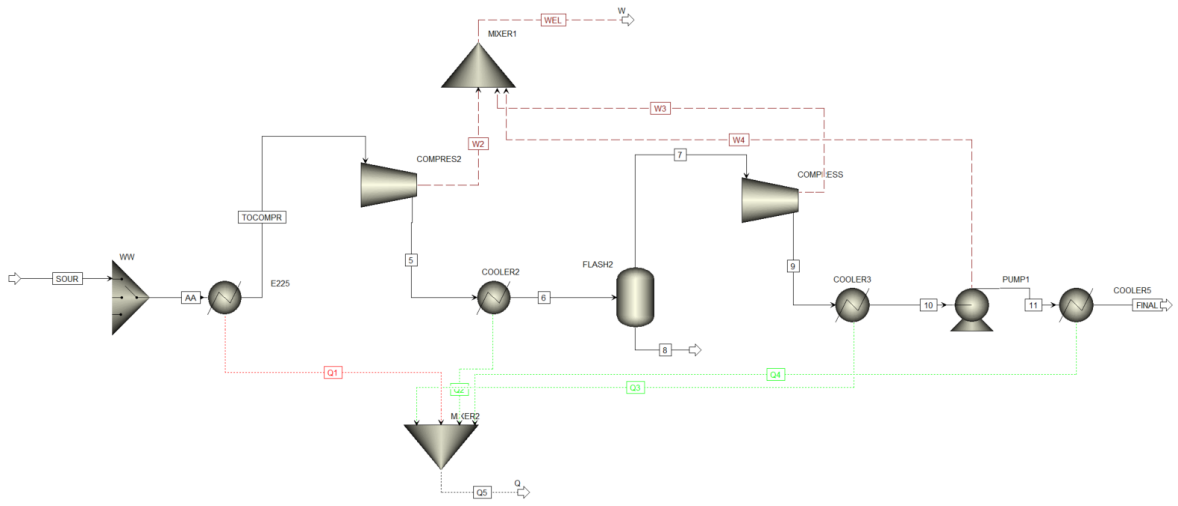

Figure D12: Aspen Plus flowsheet of CO_2 compression.

D9 - Heat Integration

Heat integration on each plant was completed in order to minimise the heating and cooling utilities using the Aspen Energy Analyser, an online pinch analysis tool [331]. The minimum temperature was set at 10 °C. Depending on the temperature range of the stream, heating utilities supplied were low pressure steam (2.3 bar), medium pressure steam (8.9 bar) and high-pressure steam (39.8 bar) while the cooling utilities were water and air.

Table D5: Results of heat integration.

	FTS		BioSNG		OMEx	
	Before	After	Before	After	Before	After
Heating Duty (MW)	49.81	20.51	40.92	0.00	78.67	51.30
Cooling Duty (MW)	29.44	0.135	103.13	62.25	72.25	44.88